Desarrollo y validación de los modelos de Barcelona para la predicción del riesgo de cáncer de próstata clínicamente significativo

Marina Triquell Llauradó

UAB
Universitat Autònoma de Barcelona

Desarrollo y validación de los modelos de Barcelona para la predicción del riesgo de cáncer de próstata clínicamente significativo

TESIS DOCTORAL

Programa de Doctorado en Cirugía y Ciencias Morfológicas
Departamento de Cirugía
Universitat Autònoma de Barcelona

Marina Triquell Llauradó

Directores

Dr. Juan Morote Robles

Dr. Enrique Trilla Herrera

Tutor

Dr. Juan Morote Robles

Barcelona, 2024

"Las preguntas más importantes de la vida son, en su mayoría, sólo problemas de probabilidad"

Laplace, *Théorie Analytique des Probabilités*, 1812.

AGRADECIMIENTOS

AGRAÏMENTS

Al Professor Juan Morote, tutor i co-director d'aquesta tesi, per tota la seva paciència i dedicació. Sense la seva empenta, constància i saviesa no hagués estat possible realitzar aquesta tesi.

Al Dr. Enrique Trilla, co-director d'aquesta tesi, per tot l'afecte i acollida rebuts durant els meus anys de residència a la Vall d'Hebron.

Als co-autors dels articles publicats, per la seva participació en el projecte.

Al Dr. José Placer, el meu tutor durant la residència, pel seu constant recolzament i exemple de professionalitat.

A la Cintia, el Juan, la Míriam, la Mercè, l'Aina, l'Enric, l'Adrià, l'Oriol, el Nico, l'Adriana i el Marc, perquè conèixer-vos va ser casualitat però estimar-vos una elecció. Al Jordi, per celebrar els meus èxits com si fossin seus.

A les meves amigues, la Cla, la Marina, la Patri i la Repiso, per haver-me acompanyat en les antigues etapes de la meva vida i seguir fent-ho en el present.

Als meus padrins, padrines, Padrinet i Padrineta per ser segons pares i educar-me amb amor.

Per últim, als meus pares, Maria José i Benet, per llaurar el camp on he pogut sembrar les meves llavors i ajudar a fer créixer els meus fruits. Gràcies per ser-hi sempre.

ACRÓNIMOS

5-ARI = inhibidores de la 5-alfa reductasa

AS = vigilancia activa

AUC = área bajo la curva

BCN-PM = modelo predictivo de Barcelona

BCN-RC = calculadora de riesgo de Barcelona

bpMRI = resonancia magnética biparamétrica

CI = intervalo de confianza

csPCa = cáncer de próstata clínicamente significativo

CUC = curva de utilidad clínica

DCE = coeficiente de difusión

DNA = ácido desoxirribonucleico

DRE = tacto rectal

DOI = *Digital Object Identifier*

DWI = imágenes en difusión

ERSPC = *European Randomized Study of Screening for Prostate Cancer*

GG = grupo de grado

GS = suma de Gleason

iPCa = cáncer de próstata insignificante

ISUP = *International Society of Urological Pathology*

mpMRI = resonancia magnética multiparamétrica

MRI = resonancia magnética

MRI-PM = modelo predictivo basado en la resonancia magnética y variables clínicas

PCa = cáncer de próstata

PCA3 = *Prostate Cancer Antigen* 3

PHI = *Prostate Health Index*

PI-RADS = *Prostate Imaging-Reporting and Data System*

PICO = *Participants, Intervention, Comparator, Outcomes*

PRISMA = *Preferred Reporting Items for Systematic Reviews and Meta-analyses*

PSA = antígeno prostático específico

PSAD = densidad de *PSA*

QUADAS = *Quality Assessment of Diagnostic Accuracy Studies*

RC = calculadora de riesgo

RNA = ácido ribonucleico

ROC = *receiver operating characteristic*

ROM = modelo organizado de riesgo

TRUS = ultrasonografía transrectal

WW = vigilancia expectante

ÍNDICE

RESUMEN

INTRODUCCIÓN

La detección precoz del cáncer de próstata clínicamente significativo (*csPCa*) reduce la mortalidad específica del cáncer de próstata (*PCa*). Por ello, el cribado del *PCa* actualmente se focaliza en el *csPCa*. No obstante, la sospecha del *PCa* se sigue estableciendo a partir de la elevación sérica del antígeno específico prostático (*PSA*) y/o un tacto rectal (*DRE*) sospechoso, y su diagnóstico sigue realizándose a través de la biopsia prostática. En los últimos años, se ha producido un cambio de paradigma gracias a la introducción de la resonancia magnética multiparamétrica *(mpMRI*) antes de la biopsia, que permite identificar lesiones sospechosas proporcionando el riesgo semicuantitativo de *csPCa* a través del *Prostate Imaging-Reporting and Data System* (*PI-RADS)*. Esta estrategia permite realizar biopsias dirigidas a través de la fusión de imágenes de *mpMRI* y ultrasonografía transrectal. La *mpMRI* posee un valor predictivo negativo elevado y por ello se recomienda evitar la biopsia prostática cuando no objetiva lesiones sospechosas, mientras que cuando existen lesiones *PI-RADS* $\geq$ *3* se recomienda realizar biopsias dirigidas complementadas por biopsias sistemáticas. A pesar de ello, existen escenarios inciertos en los que existe un elevado porcentaje de biopsias innecesarias y sobre-detección de *PCa* insignificante (*iPCa*). Actualmente, la *European Association of Urology* recomienda el uso de modelos predictivos de riesgo de *csPCa* para estratificar los hombres con sospecha de *PCa.* Estas herramientas tienen como objetivo reducir la demanda de *mpMRI*, biopsias prostáticas y evitar la sobre-detección de *iPCa.*

HIPÓTESIS

La predicción individualizada del riesgo de *csPCa* a través de una calculadora diseñada a partir de los modelos predictivos para ser utilizados antes

y después de la *MRI*, mejoran el diagnóstico precoz del *csPCa* reduciendo la demanda de *MRIs* y biopsias prostáticas innecesarias.

OBJETIVOS

El objetivo principal fue desarrollar una calculadora de riesgo (*RC*) de *csPCa* basada en dos nuevos modelos predictivos que incorporan variables clínicas disponibles en el momento de la sospecha de *PCa* para su uso antes y después de la *MRI*.

Objetivos secundarios:

1. Analizar, a través de una revisión sistemática de la literatura, la evidencia científica actual respecto a los modelos predictivos de *csPCa* basados en la *MRI* y sus *RCs*.

2. Desarrollar y validar externamente un nuevo modelo predictivo y su *RC*, basados en la *MRI* prostática y las variables clínicas disponibles en el momento de sospecha de *PCa,* para seleccionar candidatos a biopsia prostática.

3. Comparar el nuevo modelo predictivo basado en la *MRI* y variables clínicas con la densidad de *PSA* (*PSAD*) y con el modelo predictivo de Rotterdam-*MRI* para seleccionar candidatos a biopsia prostática.

4. Desarrollar y validar externamente un nuevo modelo predictivo y su *RC*, basados en variables clínicas disponibles en el momento de sospecha de *PCa,* para seleccionar candidatos a *MRI* prostática.

METODOLOGÍA

La memoria de esta tesis doctoral se presenta como un compendio de cinco publicaciones.

La primera publicación consistió en una revisión sistemática de la literatura de los modelos predictivos de *csPCa* basados en la *MRI (MRI-PMs)*. Se siguieron los criterios *PRISMA* (*Preferred Reporting Items for Systematic Reviews and Meta-analyses*). La elegibilidad de los estudios se basó en la estrategia *PICO* (*Participants, Intervention, Comparator, Outcomes*). Se utilizó *QUADAS-2* (*Quality Assessment of Diagnostic Accuracy Studies 2*) como herramienta de evaluación de calidad de los estudios.

Los modelos predictivos de Barcelona desarrollados para establecer el riesgo de *csPCa* antes de la *MRI* (*BCN PM*-1) y después *(BCN PM-2)*, fueron desarrollados a partir de una cohorte de 1,486 hombres con sospecha de *PCa* sometidos a *mpMRI* y biopsias prostáticas sistemáticas con o sin biopsias dirigidas en el Hospital Universitario Vall d'Hebron, entre 2016 y 2019. La cohorte de validación externa incluyó 946 hombres con sospecha de *PCa* seleccionados en dos instituciones del área metropolitana de Barcelona. Para determinar variables predictoras independientes de *csPCa* e incluirlas como variables clínicas de los modelos se empleó una regresión logística. Se analizó el peso de cada una de la variables y se construyeron los nomogramas correspondientes. La variable a predecir fue el *csPCa*, que se definió como grupo de grado 2 de la *International Society of Urologic Pathology*. Se diseñaron las correspondientes *RCs* a partir de los nomogramas construidos para ambos modelos, accesibles en la dirección *web*: https://mripcaprediction.shinyapps.io/MRIPCaPrediction/.

Se comparó el *BCN PM-2* con la *PSAD* y con el modelo de Rotterdam-*MRI*. Se realizaron curvas de calibración para analizar la correlación entre riesgos predichos y observados, el área bajo la curva (*AUC*) para analizar la capacidad discriminatoria de los modelos, curvas de decisión clínica para analizar el beneficio neto de los modelos frente a biopsiar a todos los participantes, y curvas de utilidad clínica para analizar la correlación entre biopsias evitadas y *csPCa* dejados de diagnosticar según el nivel de corte elegido.

Este proyecto fue aprobado por el comité ético del Hospital Universitario Vall d' Hebron (PRAG-317/2017). Todos los participantes firmaron el consentimiento informado.

RESULTADOS

En la revisión sistemática de la literatura se encontraron 723 registros y finalmente se seleccionaron 17 publicaciones. Como síntesis de la evidencia se verificó que las variables clínicas en combinación con la *MRI* mejoraron la predicción del *csPCa* de la *MRI*, incrementando el *AUC* entre 0.78 y 0.92. Solamente siete modelos tenían alguna validación externa y solamente uno disponía de una *RC* accesible *online*. La versión 2.0 del *PI-RADS* se utilizó en 10 *MRI-PMs*. Ninguno de los modelos analizó su rendimiento en las distintas categorías *PI-RADS*.

Las variables predictoras independientes comunes de los modelos predictivos de Barcelona desarrollados fueron edad (años), nivel sérico de *PSA* (ng/ml), *DRE* (normal *vs*. anormal), antecedentes familiares de *PCa* (no *vs*. familiares de primer grado) y tipo de biopsia (inicial *vs*. repetida). En el *BCN PM-2* se incluyó el volumen prostático obtenido a partir de la *MRI* (ml) y *PI-RADSv2.0* (1-5). En el *BCN PM-1* se incluyó el volumen prostático categorizado a partir del *DRE*

(próstata pequeña, mediana, grande). La incidencia de *csPCa* fue 36.9% en la cohorte de desarrollo y 40.8% en la cohorte de validación (p = 0.054). El *AUC* de la *MRI* establecida en 0.842 aumentó a 0.897 en el *BCN PM-2* (p < 0.001), y de 0.743 a 0.858 en la cohorte de validación (p < 0.001). Globalmente, seleccionando un umbral de riesgo del 15% se evitó el 40.1% de las biopsias de próstata y se dejó de detectar el 5.4% del *csPCa* en la cohorte de desarrollo. La utilidad clínica del modelo en *PI-RADS* 4 fue de 4% de biopsias evitadas dejando de detectar el 0.6% de *csPCa*, datos similares a *PI-RADS* 5, en cambio, en *PI-RADS* < 3 sugeriría biopsia solamente en 4.3% de los casos y se perderían solamente 6 casos de *csPCa*. En la validación externa, para una probabilidad estimada de *csPCa* del 20% la real fue del 25% aproximadamente.

Las *AUC* del *BCN PM*-1 fueron de 0.823 en la cohorte de desarrollo y de 0.837 en la cohorte de validación (p = 0.447). Seleccionando el umbral de riesgo del 5%, las *MRIs* evitadas fueron del 17.2% en la cohorte de desarrollo y del 22.3% en la cohorte de validación, dejando de detectar el 1.8% y el 2% de *csPCa*, respectivamente.

El *AUC* del *BCN PM-2* fue de 0.893 y de 0.764 para la *PSAD* (p < 0.001). El *BCN PM-2* mostró un beneficio neto frente a biopsiar a todos los hombres cuando la probabilidad de *csPCa* era mayor al 2%, mientras que la *PSAD* hizo lo mismo cuando la probabilidad de *csPCa* era mayor al 18%. El beneficio neto del *BCN PM-2* fue siempre superior a la *PSAD* en todas las categorías *PI-RADS* excepto en *PI-RADS* 5.

El rendimiento del *BCN PM*-2 con respecto al Rotterdam *MRI-PM* fue superior, mostrando *AUCs* de 0.856 y de 0.844, respectivamente (p = 0.116). *BCN PM*-2 también mostró mayor beneficio neto y utilidad clínica. Utilizando umbrales apropiados se necesitaron, respectivamente, el 75 y el 80% de las biopsias para

identificar el 50% de *csPCa* en hombres con *PI-RADS* <3, mientras que se evitó el 35 y el 21% de las biopsias, perdiendo el 10% de *csPCa* detectado en hombres con *PI-RADS* 3. El *BCN PM-2* evitó el 15% de las biopsias, perdiendo el 2% de *csPCa* en hombres con *PI-RADS* 4, mientras que Rotterdam *MRI-PM* evitó el 10%, perdiendo el 6%. Ninguno de los dos modelos evitó biopsias sin perder *csPCa* en hombres con *PI-RADS* 5.

CONCLUSIONES

1. Los modelos predictivos de *csPCa* basados en *MRI* y variables clínicas son el mejor método para seleccionar candidatos a biopsia prostática. Las *RCs* y la validación externa en la población en la que van a ser utilizadas son esenciales para la aplicación de los modelos predictivos en la práctica clínica diaria. En el momento de nuestra revisión sistemática de la literatura, el modelo Rotterdam-*MRI*, desarrollado con la versión *PI-RADS* 1.0, disponía de una *RC* accesible y ninguno de los publicados se había evaluado según la categoría *PI-RADS*. Estos resultados nos llevaron a desarrollar una *RC* actualizada y validada a en el área metropolitana de Barcelona.

2. El *BCN MRI-PM*, actualmente denominado *BCN PM-2*, consiguió evitar biopsias innecesarias con una tasa aceptable de *csPCa* no detectados. Se demostró que la utilidad clínica de los modelos predictivos varía en función de la categoría *PI-RADS*. Su validación externa mostró una buena calibración. La *RC* diseñada permite la selección del umbral de probabilidad de *csPCa,* novedad que facilitará la validación del modelo en otras poblaciones o diferentes *PI-RADS.*

3. El *BCN PM-2* fue más preciso y presentó mayor beneficio neto que la *PSAD* para seleccionar candidatos para biopsia prostática en global y para

todos los *PI-RADS*, con la excepción de varones con *PI-RADS* 5. El *BCN PM-2* mostró mayor beneficio neto para seleccionar candidatos a biopsia prostática que el Rotterdam *MRI-PM* globalmente, aunque ninguno de ellos fue útil para seleccionar individuos con *MRI* negativa o *PI-RADS* 5.

4. El *BCN PM-1*, mostró una buena calibración y consiguió reducir la demanda de *MRI* con una tasa aceptable de *csPCa* no detectados. Su *RC* diseñada permite la selección del umbral de probabilidad de *csPCa.*

5. En relación a nuestro objetivo principal, concluimos que los modelos predictivos de Barcelona y su *RC* permitieron mejorar el diagnóstico precoz del *csPCa*, optimizando la selección de candidatos a *MRI* y a biopsia prostática.

SUMMARY

INTRODUCTION

Early detection of clinically significant prostate cancer (*csPCa*) reduces prostate cancer (*PCa*)-specific mortality. Therefore, *PCa* screening currently focuses on *csPCa*. However, the suspicion of *PCa* is still established from elevated serum prostate-specific antigen (*PSA*) and/or a suspicious digital rectal examination (*DRE*), and its diagnosis is still made through prostate biopsy. Lately, a paradigm shift has occurred thanks to the introduction of multiparametric magnetic resonance imaging (*mpMRI*) before biopsy, which allows the identification of suspicious lesions and provides the semiquantitative risk of *csPCa* through the Prostate Imaging-Reporting and Data System (*PI-RADS*)**.** This strategy allows for targeted biopsies through the fusion of *mpMRI* images and transrectal ultrasonography. *mpMRI* has a high negative predictive value and is therefore recommended to avoid prostate biopsy when no lesions are observed, while when there are *PI-RADS* >3 lesions, targeted biopsies complemented by systematic biopsies are recommended. Despite this, there are uncertain scenarios with a high percentage of unnecessary biopsies and over-detection of insignificant *PCa* (*iPCa*). Currently, the European Association of Urology recommends using predictive models (*PMs*) for the risk of *csPCa* to stratify men suspected of *PCa*. These tools aim to reduce the demand for *mpMRI*, prostate biopsies, and avoid over-detection of *iPCa*.

HYPOTHESIS

The individualized prediction of the risk of *csPCa* through a calculator designed from predictive models to be used before and after *MRI*, improves the early diagnosis of *csPCa*, reducing the demand for *MRIs* and unnecessary prostate biopsies.

OBJECTIVES

The primary objective was to develop a risk calculator (*RC*) for *csPCa* based on two nobel predictive models that incorporate clinical variables available at the time of *PCa* suspicion for its use before and after *MRI*.

Secondary objectives:

1. To analyze, through a systematic review of the literature, the current scientific evidence regarding the *MRI*-based predictive models developed and their *RCs*.

2. To develop and externally validate a new predictive model and its *RC*, based on prostate *MRI* and clinical variables available at the time of suspicion of *PCa*, to select candidates for prostate biopsy.

3. To compare the new predictive model based on *MRI* and clinical variables with *PSA* density (*PSAD*) and Rotterdam-MRI predictive model to select candidates for prostate biopsy.

4. To develop and externally validate a new predictive model and its *RC*, based on clinical variables available at the time of suspicion of *PCa*, to select candidates for prostate *MRI*.

METHODOLOGY

This doctoral thesis is presented as a compendium of five publications. The first publication consisted of a systematic review of the literature on *csPCa* predictive models based on *MRI* (*MRI-PMs*). *PRISMA* (Preferred Reporting Items for Systematic Reviews and Meta-analyses) criteria were followed. The eligibility

of the studies was based on the *PICO* (Participants, Intervention, Comparator, Outcomes) strategy. *QUADAS*-2 (Quality Assessment of Diagnostic Accuracy Studies 2) was used as a quality assessment tool for the studies.

The Barcelona predictive models developed to establish the risk of *csPCa* before *mpMRI* (*BCN PM-1*) and after (*BCN PM-2*) were developed from a cohort of 1,486 men with suspected *PCa* undergoing *mpMRI* and targeted and/or systematic prostate biopsies at the Vall d'Hebron University Hospital between 2016 and 2019. The external validation cohort included 946 men with suspected *PCa* from two institutions in the metropolitan area of Barcelona. Logistic regression was used to determine independent predictive variables of *csPCa* and include them as clinical variables in the models. The weight of each variable was analyzed, and corresponding nomograms were constructed. The variable to be predicted was *csPCa*, defined as grade group 2 according to the International Society of UroPathology. Corresponding risk calculators were designed from the constructed nomograms for both models, accessible at the web address: https://mripcaprediction.shinyapps.io/MRIPCaPrediction/.

BCN PM-2 was compared with *PSAD* and the Rotterdam-*MRI* model. Statistically, calibration curves were used to analyze the correlation between predicted and observed risks, the area under the curve (*AUC*) to analyze the discriminatory capacity of the models, decision curve analysis to analyze the net benefit of the models compared to biopsying all participants, and clinical utility curves to analyze the correlation between avoided biopsies and missed *csPCa* diagnoses based on the chosen threshold level.

This project was approved by the ethics committee of the Vall d'Hebron University Hospital (PRAG-317/2017). All participants signed informed consent.

RESULTS

The systematic literature review found 723 records, and 17 publications were finally selected. As a synthesis of the evidence, it was verified that clinical variables combined with *MRI* improved *MRI* prediction, increasing the *AUC* from 0.78 to 0.92. Only seven models had some external validation, and only one had an accessible online risk calculator. The *PI-RADS* version 2.0 was used in 10 *MRI-PMs*. None of the models analyzed their performance in different *PI-RADS* categories.

The common independent predictive variables of the developed *BCN-PMs* were age (years), serum *PSA* level (ng/ml), *DRE* (normal *vs*. abnormal), family history of *PCa* (no *vs*. first-degree relatives), and type of biopsy (initial *vs*. repeat). In *BCN PM-2*, prostate volume obtained from *MRI* (ml) and *PI-RADSv2.0* (1-5) were included. In *BCN PM-1*, semiquantitative prostate volume obtained from *DRE* (small, medium, large prostate) was included. The incidence of *csPCa* was 36.9% in the development cohort and 40.8% in the validation cohort ($p = 0.054$). The *MRI*-established *AUC* of 0.842 increased to 0.897 in *BCN PM*-2 ($p < 0.001$), and from 0.743 to 0.858 in the validation cohort ($p < 0.001$). Selecting a 15% risk threshold avoided 40.1% of prostate biopsies and missed 5.4% of *csPCa* in the development cohort. In external validation, the model showed good calibration. The *AUCs* of *BCN PM-1* were 0.823 in the development cohort and 0.837 in the validation cohort ($p = 0.447$). Avoided *MRIs* were 17.2% in the development cohort and 22.3% in the validation cohort, missing 1.8% and 2% of *csPCa*, respectively.

The *AUC* of *BCN PM-2* was 0.893 and 0.764 for *PSAD* ($p < 0.001$). *BCN PM-2* showed a net benefit over biopsying all men when the probability of *csPCa* was greater than 2%, while *PSAD* did the same when the probability of csPCa was

greater than 18%. The net benefit of *BCN PM-2* was always superior to *PSAD* in all *PI-RADS* categories except *PI-RADS* 5.

The performance of *BCN PM-2* compared to the Rotterdam *MRI-PM* was superior, showing *AUCs* of 0.856 and 0.844, respectively (p = 0.116). *BCN PM-2* also showed greater net benefit and clinical utility. Using appropriate thresholds, 75% and 80% of biopsies were needed to identify 50% of *csPCa* in men with *PI-RADS* <3, while 35% and 21% of biopsies were avoided, missing 10% of detected *csPCa* in men with *PI-RADS* 3. *BCN PM-2* avoided 15% of biopsies, missing 2% of *csPCa* in men with *PI-RADS* 4, while Rotterdam *MRI-PM* avoided 10%, missing 6%. Neither model avoided biopsies without missing *csPCa* in men with *PI-RADS* 5.

CONCLUSIONS

1. Predictive models of *csPCa* based on MRI and clinical variables are the best method to select candidates for prostate biopsy. *RCs* and external validation in the population in which they will be used are essential for the application of predictive models in daily clinical practice. At the time of our systematic review of the literature, the Rotterdam-*MRI* model, developed with the *PI-RADS* 1.0 version, had an accessible *RC*, and none of the published models had been evaluated according to the *PI-RADS* category. These results led us to develop an updated *RC* validated in the metropolitan area of Barcelona.

2. The *BCN MRI-PM*, currently called *BCN PM-2*, managed to avoid unnecessary biopsies with an acceptable rate of undetected *csPCa*. For the first time in the literature, it was demonstrated that the clinical usefulness of predictive models varies depending on the *PI-RADS* category. Its

external validation showed good calibration. The designed *RC* allows the selection of the *csPCa* probability threshold, a novelty that will facilitate the validation of the model in other populations or different *PI-RADS*.

3. The *BCN PM-2* was more accurate and presented a greater net benefit than *PSAD* in selecting candidates for prostate biopsy overall and for all *PI-RADS* categories, except for men with *PI-RADS* 5. The *BCN PM-2* showed a greater overall net benefit for selecting candidates for prostate biopsy than the Rotterdam *MRI-PM*, although neither was useful for selecting individuals with a negative *MRI* or *PI-RADS* 5.

4. The *BCN PM*-1 showed good calibration and managed to reduce the demand for *mpMRI* with an acceptable rate of undetected *csPCa*. Its designed *RC* allows selection of *csPCa* probability threshold.

5. Regarding our main objective, we concluded that the predictive models of Barcelona and its *RC* allowed the improvement of early diagnosis of *csPCa*, optimizing the selection of candidates to *MRI* and prostate biopsy.

1. Introducción

1.1. EPIDEMIOLOGÍA Y ETIOLOGÍA DEL CÁNCER DE PRÓSTATA

El cáncer de próstata (*PCa*) es el segundo tumor maligno más frecuentemente diagnosticado en el mundo y fue la quinta causa de muerte en varones en el año 2020, en el que se diagnosticaron 1.4 millones de nuevos casos y fue la causa de 375.000 muertes (1). Según los estudios realizados en autopsias de hombres, la prevalencia del *PCa* es similar en diferentes poblaciones del mundo; sin embargo, entre países existe gran variabilidad, siendo ésta dependiente, entre otros factores, de que existan programas de cribado poblacional oportunista o estructurado (2).

En Canadá, Estados Unidos y Australia la incidencia de *PCa* se incrementó súbitamente a finales de la década de los ochenta y principios de los noventa como resultado del cribado poblacional oportunista con el antígeno prostático específico (*PSA*), que permitía la detección precoz del *PCa* antes de la aparición de síntomas (3). Con la adopción de la estrategia de cribado poblacional, el incremento en la incidencia de *PCa*, aunque de forma más tardía y gradual también se ha observado en Europa y algunos países de Centro América y Asia hasta su estabilización en los últimos cinco años (4). La mortalidad por *PCa* se está reduciendo los últimos años en los países más desarrollados gracias a las estrategias de cribado, que han permitido su detección en estadios precoces, y el progreso en las estrategias terapéuticas (5). La incidencia del *PCa* y su mortalidad en los 136 países analizados por Globocan en 2020, se muestra en los mapas de las **Figuras 1 y 2** respectivamente (1).

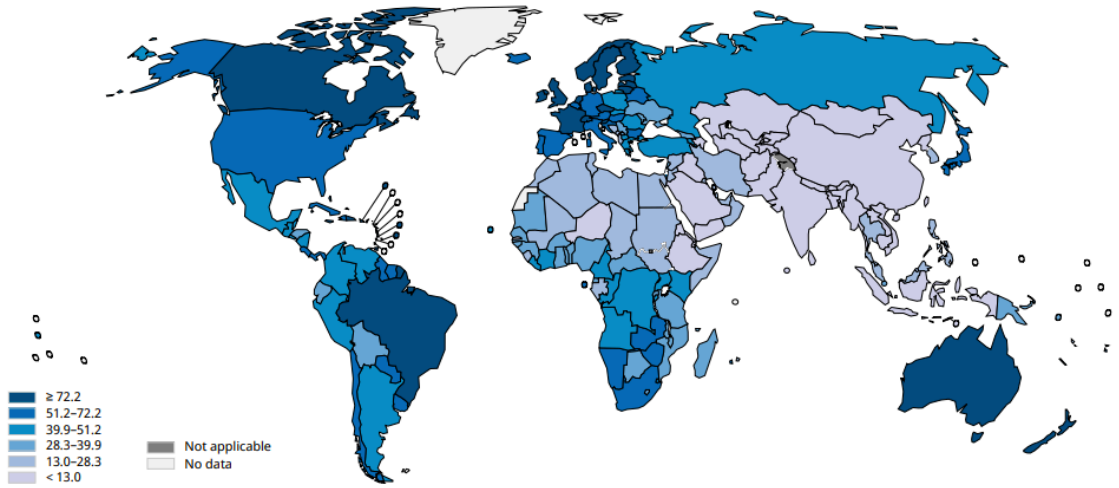

Figura 1 Incidencia de *PCa* estandarizada por edad en cada país, según Globocan en 2020 (1)

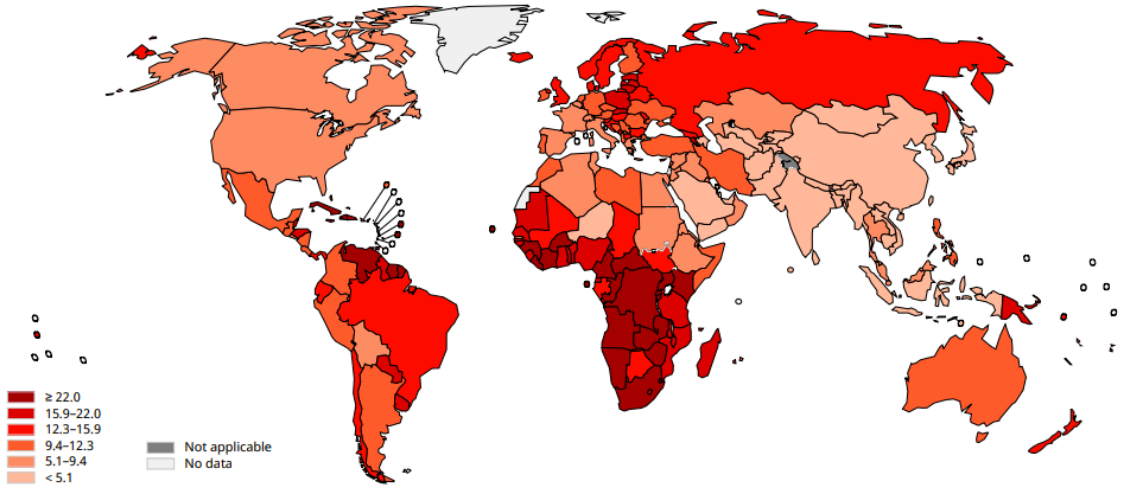

Figura 2 Tasa de mortalidad por *PCa* estandarizada por edad en cada país, según Globocan en 2020 (1)

La incidencia del *PCa* y su mortalidad varía sustancialmente. En Europa, la incidencia de *PCa* en los países escandinavos es la mayor del mundo, reduciéndose sustancialmente en los países mediterráneos, **Figura 3** (1).

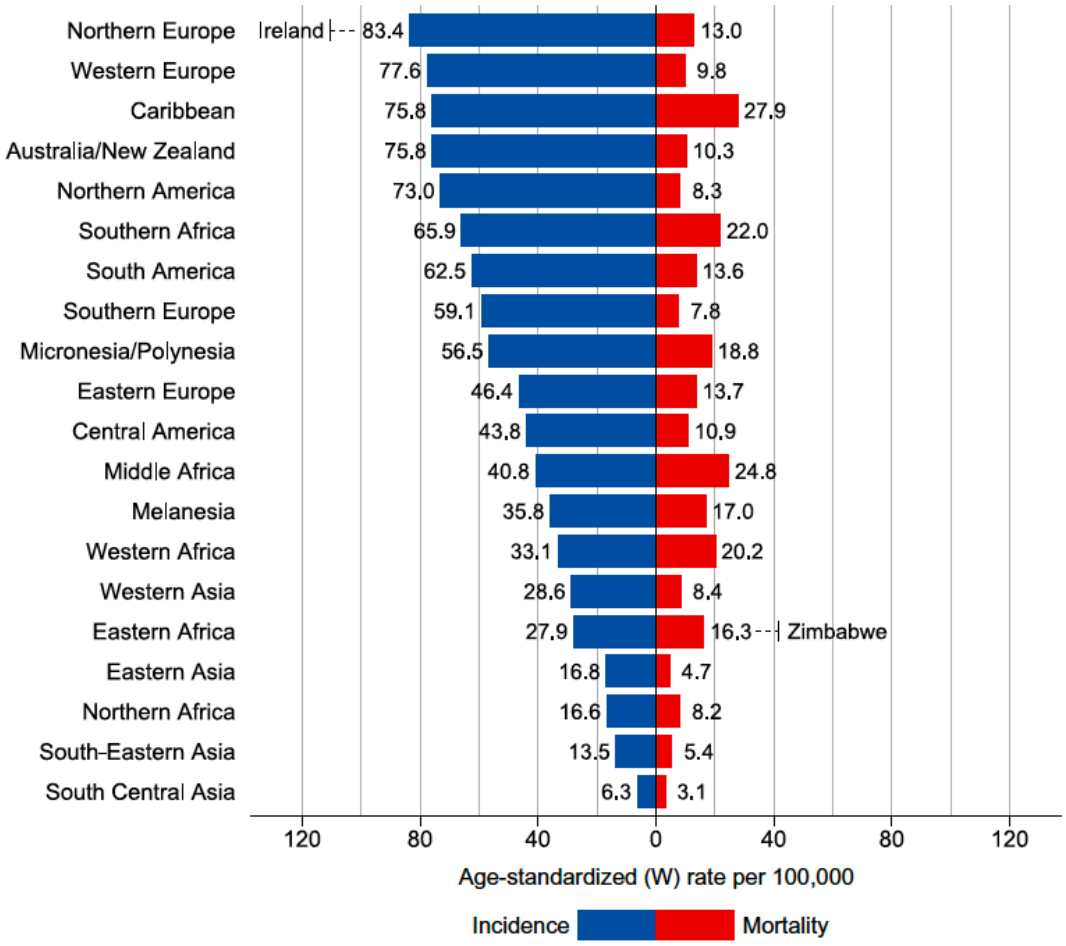

Figura *3* Incidencia y mortalidad por *PCa* estandarizada por edad *según Globocan en 2020* (1)

En España, según el informe la Sociedad Española de Oncología Médica, el *PCa* fue el tumor con mayor incidencia en varones, diagnosticándose 29.900 nuevos casos diagnosticados en 2022, ocupando la mortalidad específica el tercer lugar con 5.900 defunciones (6). La incidencia del *PCa* en Cataluña también ocupó el primer lugar en 2022 con 4.470 nuevos casos detectados (6).

El principal factor de riesgo para desarrollar *PCa* es la edad. En una revisión sistemática de estudios realizados en autopsias se reportó globalmente una prevalencia del *PCa* en el 5% de hombres con menos de 30 años y del 59% a partir de los 79 años (7). Otro factor de riesgo conocido es la asociación familiar, aunque solamente en una pequeña parte de los hombres diagnosticados de *PCa* se

identifica (8). Se ha observado que los hombres con antecedentes familiares de *PCa* tienen un riesgo relativo 2.3 superior al de la población sin antecedentes familiares, 3.4 veces mayor riesgo de diagnóstico precoz, 2.2 mayor riesgo de muerte específica y 2.3 mayor riesgo de tener un *PCa* clínicamente significativo (*csPCa*) (9). Numerosas mutaciones germinales de genes reparadores del ácido desoxirribonucleico (*DNA*) se han relacionado con el *PCa* hereditario (10). Las mutaciones germinales son mutaciones en el *DNA* que se transmiten de progenitores a hijos. Un estudio realizado en 1.328 pacientes con *PCa* identificó mutaciones del gen *BRCA2* en el 4.5%, del gen *CHEK2* en el 2.2%, del gen *ATM* en el 1.8%, y del gen *BRCA1* en el 1.1%. Los pacientes con suma de Gleason superior a 8 y con *PCa* metastásico se asociaron significativamente a una mayor incidencia de mutaciones de genes reparadores del *DNA* (11,12).

La información sobre la asociación entre el uso de los inhibidores de la 5-alfa reductasa (*5-ARI*) y el *PCa* es contradictoria. Algunos estudios han indicado que los *5-ARI* pueden disminuir el riesgo de desarrollar *PCa*, mientras que otros han informado de un mayor riesgo de *PCa* de alto grado (13–16). Por otro lado, los pacientes con hipogonadismo que reciben suplementos de testosterona no han mostrado mayor riesgo de *PCa* (17). Por el contrario, en 2018 se ha reportado que los hombres con bajas concentraciones séricas de testosterona libre tenían un riesgo inferior de desarrollar *PCa* (18).

Se ha identificado la etnicidad como un factor de riesgo de *PCa*, observándose en Estados Unidos una incidencia mayor en hombres afroamericanos que en los de origen caucásico (19). Los hombres chinos y japoneses tienen un riesgo menor de *PCa* que el de los hombres de los países occidentales. No obstante, se ha observado que los hombres chinos y japoneses emigrados a Estados Unidos ven aumentado su riesgo de *PCa,* similar al de los estadounidenses, a partir de la segunda generación (19). Existen otras factores ambientales como el grado de

insolación; sin embargo, ningún factor ambiental o dietético ha sido bien definido como factor de riesgo de *PCa* por lo que actualmente no existen recomendaciones específicas para la prevención del *PCa* (20).

1.2. SOSPECHA DE CÁNCER DE PRÓSTATA

La mayoría de los casos de *PCa* diagnosticados actualmente son asintomáticos. Por tanto, establecer una sospecha de *PCa* es importante para su detección precoz ya que reduce las tasas de diagnóstico en estadios avanzados y mortalidad (21). La sospecha de *PCa* se establece a través de la elevación del *PSA* en suero y/o la detección de un tacto rectal (*DRE*) anormal. No obstante, el diagnóstico definitivo del *PCa* se realiza a través de la biopsia prostática (22).

1.2.1. ANTÍGENO PROSTÁTICO ESPECÍFICO

El *PSA* es una proteasa tipo serina también conocida como kallicreína humana 3 y se describió por primera vez en 1975 (23,24). La proteína *PSA* es codificada por el gen *hKLK3* localizado en el cromosoma 19 (25). La expresión de este gen es mayoritariamente andrógeno-dependiente (26). El *PSA* se sintetiza en los ductos y acinos prostáticos y su función es romper la uniones entre semenogelina I y II para disolver el coágulo seminal (27).

El *PSA* como marcador tumoral del *PCa* ha revolucionado su diagnóstico precoz y se puede asociar al *DRE* como parte de su cribado. Es un marcador muy sensible pero poco específico ya que se eleva en otras condiciones como la hiperplasia benigna de próstata y la prostatitis (28). A pesar de no existir una estandarización para medir los niveles de *PSA*, la mayoría de los ensayos

comercializados establecen un *PSA* normal por debajo de 4 ng/ml (29). No obstante, varones con niveles considerados normales pueden presentar porcentajes bajos de *PCa*, **Tabla 1** (30). En caso de encontrar niveles de *PSA* en la zona gris, entre 4 y 10 ng/ml, se recomienda su repetición para confirmar la elevación.

Tabla 1 Riesgo de presentar *PCa* en función del nivel sérico de *PSA* (30)

Nivel de *PSA* (ng/ml)	**Riesgo de *PCa* (%)**	**Riesgo de *PCa* ISUP-*GG* ≥ 2 (%)**
0-0.5	6.6	0.8
0.6-1.0	10.1	1.0
1.1-2.0	17.0	2.0
2.1-3.0	23.9	4.6
3.1-4.0	26.9	6.7

PCa = cáncer de próstata, *PSA* = antígeno prostático específico, *ISUP-GG* = grupo de grado de la *International Society of Urological Pathology*

La periodicidad óptima del testeo con *PSA* no está bien establecida, aunque se ha propuesto una estrategia basada en el *PSA* inicial (31). Se propone posponer la próxima determinación de *PSA* ocho años a los hombres con ausencia de historia familiar de *PCa* que presentan un *PSA* inferior a 1 ng/ml a los 40 años de edad, o inferior a 2 ng/ml a los 60 años de edad, ya que su riesgo de progresión y muerte por *PCa* es muy bajo (32). Para el resto de hombres, considerados en riesgo de *PCa*, se ha propuesto repetir la determinación sérica de *PSA* con una cadencia bianual (33).

El cociente entre el *PSA* total y su fracción libre se ha propuesto como marcador para incrementar la especificidad del *PSA* y discriminar entre *PCa* e hiperplasia

benigna de próstata (34). En cuanto a la sensibilidad y especificidad del porcentaje de *PSA* libre para el diagnóstico del *PCa*, se sitúan en el 70 y 50 %, respectivamente cuando el rango de *PSA* total oscila entre 4 y 10 ng/ml, sin tener un valor clínico relevante cuando el *PSA* total es superior a 10 ng/ml (35). La utilidad del porcentaje de *PSA* libre ha retomado recientemente sentido en el contexto de algunos de los nuevos marcadores tumorales basados en modelos predictivos (36).

En 2012, la *US Preventive Services Task Force* se posicionó en contra del cribado con *PSA*, destacando la falta de beneficio en la reducción de la mortalidad cáncer específica y los perjuicios basados en el excesivo número de biopsias prostáticas innecesarias y sobredetección de *PCa* insignificante (*iPCa*), impulsando la recomendación en contra del testeo con *PSA* (37). Esta estrategia fue también adoptada un año después por las guías americanas de *PCa* (31). Esta recomendación derivó en un aumento de diagnósticos de *PCa* avanzado y su mortalidad, que se había reducido en los veinte años previos desde de la introducción del cribado con *PSA* (38,39). A raíz de esta evolución, la *US Preventive Services Task Force* emitió un nuevo comunicado en 2017 en el que recomendaba el cribado con *PSA* a varones con edades comprendidas entre los 55 y 69 años en una decisión compartida entre médico y paciente después de explicarle potenciales beneficios y riesgos del cribado (40). En el ámbito europeo, según el informe emitido por el *European Union Council* hay evidencia sólida de que el cribado de *PCa* mediante *PSA* reduce la mortalidad específica por *PCa* (41). Aunque el sobrediagnóstico y sobretratamiento del *iPCa* son problemas importantes del cribado del *PCa*, el uso de un límite superior de edad y la recomendación de la resonancia magnética nuclear como método complementario al cribado con *PSA*, tema que ahondaremos más adelante, puede reducir significativamente el sobrediagnóstico y mejorar la relación entre beneficios y daños del cribado (41).

1.2.2. TACTO RECTAL

El binomio *DRE* y *PSA* ha sido utilizado clásicamente para el diagnóstico del *PCa* (42). El uso del *DRE* como única exploración en centros de atención primaria tiene una sensibilidad y especificad por debajo del 60% (43). El *PSA* como marcador es superior al *DRE*. En una serie de 6.630 pacientes, un 18% de los *PCa* fueron detectados únicamente a través del *DRE* mientras un 45% fueron detectados exclusivamente a través del *PSA*. No obstante, el uso de la combinación de ambos fue superior en la detección de *PCa* (42). La combinación de *PSA* elevado y *DRE* sospechoso también se ha relacionado con mayor detección de *PCa* de alto grado (Gleason *score* > 7) (44).

Actualmente el *DRE* se utiliza para el estadiaje clínico del *PCa* siendo un fuerte predictor de enfermedad avanzada (45). Se considera un *DRE* patológico a partir de cT2a, siendo a partir de cT3a sospechoso de afectación extracapsular (46).

1.2.3. RESONANCIA MAGNÉTICA NUCLEAR PÉLVICA

La estrategia de realización de biopsias prostáticas sistemáticas para diagnosticar el *PCa* en varones con un *PSA* elevado y/o un *DRE* anormal ha comportado un número elevado de *csPCa* no detectados, además de una sobre-detección de *iPCa* (47). A lo largo de los años, se han analizado varias técnicas para incrementar el rendimiento de las biopsias sistemáticas de próstata como la ultrasonografía transrectal (*TRUS*), aunque no ha resultado útil para la identificación de lesiones sospechosas de *PCa* (48).

La resonancia magnética multiparamétrica (*mpMRI*) pélvica combina la imagen morfológica proporcionada por las secuencias potenciadas T1 y T2 con la imagen

funcional y fisiológica proporcionada por las imágenes potenciadas de difusión (*DWI*) y el coeficiente de difusión aparente (*DCE*). Estas herramientas permiten la detección y localización de zonas sospechosas de *csPCa* hacia las que se pueden realizar biopsias dirigidas (49). En un meta-análisis se ha observado que la sensibilidad y la especificad globales de la *mpMRI* para detectar *PCa* con *ISUP-GG* igual o superior a 2 fue de 91 y 37% respectivamente (50). Para los *ISUP-GG* igual o superiores a 3 se observó una sensibilidad de 95% y especificidad de 35%,. Además, la capacidad de detección de *PCa* fue inferior en el caso de lesiones pequeñas y con grado *ISUP-GG* 1 (49). Por tanto, la *mpMRI* no es capaz de detectar todos grados *ISUP-GG* por igual.

La probabilidad de *csPCa* según las lesiones prostáticas identificadas en la *mpMRI* se estandarizó por primera vez a través de la clasificación de Likert en 2011 y un año después según la clasificación de *PI-RADS* (*Prostate Imaging-Reporting and Data System*), que ha sido actualizada recientemente y sustituida por la versión 2.0 y posteriormente por la versión 2.1 (51–53)

La clasificación *PI-RADS*, la más ampliamente utilizada en la actualidad, consiste en una escala de 5 puntos que establece la probabilidad de que una lesión corresponda a un *csPCa* según sus características anatómicas y funcionales de la imagen (54). En la **Tabla 2** se describe la probabilidad de *csPCa* según las categorías de *PI-RADS* v2.1.

Tabla 2 Probabilidad de *csPCa* según la categoría *PI-RADS* (54)

Categoría de *PI-RADS*	**Probabilidad de *csPCa***
PI-RADS 1	Muy baja
PI-RADS 2	Baja
PI-RADS 3	Intermedia
PI-RADS 4	Alta
PI-RADS 5	Muy alta

csPCa = cáncer de próstata clínicamente significativo, *PI-RADS* = *Prostate Imaging-Reporting and Data System*

Se ha estudiado el papel de las biopsias dirigidas en ausencia de biopsias sistemáticas. Varios meta-análisis han determinado que la tasa de detección de lesiones con *ISUP-GG* 2 o superior es mayor en caso de realizar biopsias dirigidas frente a las biopsias sistemáticas en hombres sometidos a biopsia inicial y especialmente en aquellos con biopsia previa negativa (50,55,56). Contrariamente, se ha observado en varios estudios que la tasa de detección de *iPCa* (*ISUP-GG* 1) disminuye (56–58). Por tanto, las biopsias dirigidas podrían evitar las biopsias sistemáticas, además de disminuir el sobrediagnóstico de cáncer de *iPCa*.

Respecto al valor añadido de las biopsias dirigidas a las biopsias sistemáticas, se ha observado que la tasa de detección de *csPCa* aumenta alrededor de un 20% en el caso de biopsias iniciales y hasta en un 40% en caso de biopsias repetidas. Omitir la biopsia sistemática puede, no obstante, condicionar la pérdida de detección del 16% de *csPCa* en caso de hombres sometidos a su primera biopsia y del 10% en el caso de biopsias de repetición (56). Las guías de *PCa* recomiendan, en varones sometidos a primera biopsia y lesiones *PI-RADS* 3 o superior, realizar

biopsias dirigidas a las zonas de sospecha y biopsia sistemática, mientras que en casos de *PI-RADS* ≤ 2 se podría evitar la biopsia, excepto casos con alto riesgo (59). Por lo anteriormente expuesto, las guías recomiendan en pacientes sin biopsia previa y lesiones *PIRADS* 3 o superior realizar biopsias sistemáticas y dirigidas, reservando biopsias únicamente dirigidas en casos biopsiados previamente (60). En el caso de una *MRI* negativa, debido a su alto valor predictivo negativo, se podría evitar la biopsia (59).

Debido a la elevada demanda de exámenes de *MRI*, algunos centros con alta experiencia han sustituido la *mpMRI* por la *MRI* biparamétrica (*bpMRI*), que no incluye la secuencia *DCE,* reduciéndose el coste y el tiempo de la prueba (61). Existen algunos meta-análisis que han demostrado que la adición del *DCE* no mejora la detección de *csPCa* comparado con las secuencias *T2* y *DWI* (62,63). Sin embargo, otro estudio ha sugerido contrario (64). Por lo tanto, la eficacia de la utilidad de la *bpMRI* no puede generalizarse. Hoy en día existe la necesidad de estandarizar y evaluar la reproducibilidad del informe de lesiones sospechosas mediante *bpMRI* (65).

1.3. DIAGNÓSTICO DEL CÁNCER DE PRÓSTATA

1.3.1. BIOPSIA PROSTÁTICA

El diagnóstico definitivo del *PCa* se basa en el estudio histopatológico. El patrón de Gleason, establecido en 1974 por Donald Gleason, presenta cinco grados en función de la desestructuración de la arquitectura de las glándulas prostáticas (66). En 2005 se estableció que la suma de Gleason (*GS*) se estima a partir del patrón más frecuente (patrón primario) y el menos frecuente (patrón

secundario). Si solamente existe un patrón se debe de duplicar para obtener la *GS* (67). Se ha constatado que este sistema de gradación es un buen predictor del pronóstico de la enfermedad, independientemente del tratamiento que se realice. Una *GS* 6 o inferior es indicativo de *iPCa*; sin embargo, una *GS* 8 o superior se asocia a enfermedad agresiva y mayor probabilidad de diseminación metastásica (68). Los subtipos histológicos del *PCa* deberían ser también reportados, como el carcinoma intraductal, el patrón cribiforme, o el patrón neuroendocrino, ya que su presencia confiere un peor pronóstico (69,70). La *ISUP*, en 2014 y 2019, acordó a limitar la clasificación del *PCa* a los *ISUP-GG* entre 1 y 5 (**Tabla 3**) (71,72).

Tabla 3 Puntuación de Gleason y correspondencia con los grados de la ISUP 2019 (72)

Puntuación de Gleason	***ISUP-GG***
2-6	1
7 (3+4)	2
7 (4+3)	3
8 (4+4 o 3+5 o 5+3)	4
9-10 (4+5 o 5+4 o 5+5)	5

ISUP = International Society of Urological Pathology, GG = grupo de grado

La biopsia prostática se realiza mediante aguja gruesa con la que se obtienen los cilindros prostáticos. Como se ha mencionado, existen las biopsias sistemáticas o randomizadas, tomadas con ayuda de la *TRUS* y las biopsias dirigidas a lesiones sospechosas identificadas en la *MRI* (60). Las biopsias sistemáticas deben ubicarse en la zona periférica más lateral de ambos lóbulos prostáticos. Se recomienda obtener 12 cilindros prostáticos (6 por lóbulo) (73). El número de cilindros prostáticos obtenido en cada lesión con biopsia dirigida se recomienda que oscile entre 3 y 5, aunque el nivel de evidencia de esta recomendación es moderado (74).

Las biopsias dirigidas a las lesiones identificadas en la *MRI* pueden ser realizadas de manera cognitiva, utilizando algún *software* de fusión entre las imágenes de *MRI* con las de la *TRUS* o *in-bore* de forma guiada in situ mediante un transductor transrectal de *MRI*. La técnica *in-bore* es inasumible debido al elevado tiempo de utilización del equipo de *MRI* aunque sus resultados parecen ser los mejores (75). Respecto a las técnicas cognitiva y con utilización de *software* no se ha demostrado una superioridad de una frente a otra, al menos a través de la vía transrectal (76,77).

El abordaje de la biopsia prostática se puede realizar través del recto o del periné. La vía transperineal parece alcanzar mayor sensibilidad por el *csPCa* que la vía transrectal. Un meta-análisis publicado en 2019 ha reportado una sensibilidad del 86% para la vía transperineal y del 73% para la vía transrectal, siendo el beneficio especialmente importante en caso de las lesiones localizadas en la zona fibrosa anterior prostática (78). Actualmente, se recomienda la vía transperineal para realizar las biopsias prostáticas con el objetivo de reducir la tasa de complicaciones sépticas de la vía transrectal, potencialmente graves a pesar de la profilaxis antibiótica (79–81).

1.3.2. Definición de cáncer de próstata clínicamente significativo

El interés por diagnosticar el *csPCa* se inicia hace unas cuantas décadas, desde que se identificó la elevada prevalencia de *PCa* en autopsias de individuos que nunca habían desarrollado síntomas por esta neoplasia hecho que puso de manifiesto la existencia del *iPCa* (82). Las investigaciones anatomopatológicas realizadas en especímenes de prostatectomía radical han demostrado que los

ISUP-GG 1 causan solamente un 0.3% de extensión extraprostática y un 3.5% de recidivas bioquímicas, además de nula invasión de las vesículas seminales o de los ganglios linfáticos. De hecho, la mayoría de los estudios consideran un *ISUP-GG* igual o superior a 2 y un volumen tumoral superior a 0.5 cc como definición de *csPCa* en especímenes quirúrgicos (83–85).

En cuanto a los aspectos anatomopatológicos en la biopsia prostática, Ahmed *et al.* propusieron dos definiciones para el *csPCa* basadas en dos parámetros de carga de enfermedad obtenidos en la biopsia perineal por mapeo. El primer parámetro fue la longitud de cilindro total afectada con valores de ≥ 10 mm y ≥ 6 mm, dependiendo de las preferencias individuales, comorbilidades, edad y esperanza de vida. El segundo parámetro consistió en dos umbrales de volumen de lesión medidos utilizando la longitud máxima en un solo cilindro de ≥ 6 mm y ≥ 4 mm. Combinaron estos umbrales de carga tumoral con el patrón 4 de Gleason dominante y no dominante para obtener dos definiciones de *csPCa*. Estas dos definiciones son *GS* ≥ 3 + 4 con longitud máxima de cilindro afectado ≥ 4 mm y una longitud total afectada ≥ 6 mm y la siguiente definición la describe como *GS* ≥ 4 + 3 con longitud máxima de cilindro afectado ≥ 6 mm y una longitud total afectada ≥ 10 mm. No obstante, la mayor limitación de estas definiciones de *csPCa* en la biopsia prostática fue no ser contrastada con los especímenes de prostatectomía (86). En 2016, Epstein *et al*. propone una definición *de iPCa* que consiste en presencia de *GS* = 3+3 afectando a dos o menos cilindros en una proporción menor al 50% en cada uno, y una densidad de *PSA* menor a 0.15 ng/dl/cc, suponiendo un riesgo mínimo de *csPCa* en especímenes de prostatectomía radical (87). Estos criterios fueron clasificados como categoría de "muy bajo riesgo" según la guías de la *National Comprehensive Cancer Network* (88). Actualmente, la investigación está dirigida en ampliar estos criterios por lo que varios grupos proponen criterios más laxos como la presencia de *PCa* con menos del 10% de patrón 4 de Gleason (89–91).

A través del conocimiento de la alta prevalencia del *iPCa*, surgió la necesidad de evitar los efectos adversos del tratamiento activo, fundamentalmente, cirugía y radioterapia, introduciéndose el término vigilancia activa (*AS*) (92). Los criterios para implementar la *AS* se suelen superponer en muchas ocasiones a la definición de *iPCa* (93). En la **Tabla 4** se recogen diferentes criterios clínicos y anatomopatológicos de entrada en *AS* publicados por diferentes grupos de trabajo.

Tabla 4 Criterios clínicos y anatomopatológicos de para implementar vigilancia activa según diferentes estudios

Institución	**Estadio clínico**	***PSA* (ng/dl)**	**Gleason**	***PSAD* (ng/dl/ cc)**	**Num. Cil. Pos.**	**% afectación**
RM (94)	T1/T2	< 15	< 65y ; ≤ 6 ≥ 65 ; ≤ 3+4 = 7	-	≤ 50 %	-
UoTSB (95)	T1/T2b ≥ 70 años ; ≤ T2c	≤ 10 ≥ 70 años ; ≤ 15	6 ≥ 70años ; ≤ 3+4	-	-	-
UCSF (96)	T1/T2a	<10	≤ 6	-	≤ 33%	-
UoTPM (97)	≤ T2a	≤ 10	≤ 6	-	≤ 3	≤ 50
PRIAS (98)	T1/T2	≤ 10	≤ 6	< 0.2	≤ 2	-
UM (99)	T1/T2	≤ 15	≤ 6	-	≤ 2	≤ 50
JH (100)	T1c	≤ 15	≤ 6	< 0.15	≤ 2	≤ 50
MSKCC (101)	T1/T2a	< 10	≤ 6		≤ 3	≤ 50

PSA = antígeno prostático específico, *PSAD* = densidad de PSA, Num. Cil. Pos. = Número de cilindros positivos, *RM* = Royal Marsden, *UoTSB* = University of Toronto- Sunnybrook, *UCSF* = University of California San Francisco, *UoTPM* = Princess Margaret Cancer Centre, *PRIAS* = Prostate Cancer Research International Active Surveillance, *UM* = University of Miami, *JH* = Johns Hopkins, *MSKCC* = Memorial Sloan Kettering Cancer Centre

La *AS* define un manejo conservador del *PCa* con la posibilidad de implementar un tratamiento curativo en el momento que se aprecie una progresión en pacientes con *PCa* localizado de bajo riesgo y con una esperanza de vida superior a 10 años (102). En contraposición, el denominado *watchful waiting* (*WW*) o vigilancia expectante, hace referencia a un manejo conservador del *PCa* localizado en pacientes que no se consideran candidatos a recibir tratamiento curativo y que serían observados esperando a la aparición de síntomas y consecuente realización de tratamientos paliativos (103). El seguimiento de los pacientes en *WW* se realiza según sea su posibilidad en función de dolencias intercurrentes, al contrario que la *VA* en la que existe un control específico, riguroso y protocolizado (92).

El estudio ProtecT incluyó 1.643 pacientes con *PCa* localizado que fueron aleatorizados a tratamiento activo con prostatectomía radical, radioterapia y *AS*. El 60% de los pacientes incluidos en este estudio presentaron *PCa* de bajo riesgo con un *PSA* inferior a 10 ng/ml en el 90% de los casos, un *ISUP-GG* 1 en el 77% y un *DRE* normal en el 76%. El resto de pacientes presentaron mayormente *PCa* de riesgo intermedio (104). El hallazgo clave del estudio fue que la supervivencia cáncer específica a 10 años de los pacientes sometidos a AS fue del 98.8% frente al 99% observados en los dos brazos de tratamiento activo. Sin embargo, las tasas de diseminación metastásica fueron del 6% y del 2.6%, respectivamente (104). Para refinar los datos reportados en el estudio ProtecT, se han analizado las diferencias clínico-patológicas entre la población que progresó y la que presentó enfermedad estable a 10 años de seguimiento. La edad, el nivel sérico de *PSA*, el *ISUP-GG*, el estadio clínico, el número de cilindros positivos, la longitud máxima de afectación tumoral y la presencia de invasión perineural fueron predictores de la supervivencia libre de progresión (105). También es importante destacar que el seguimiento de los pacientes en *AS* se basó en un protocolo no estandarizado, basado mayormente en determinaciones de *PSA* (105).

El estudio DETECTIVE ha pretendido homogeneizar los criterios de seguimiento durante la *AS*. Sin embargo, actualmente no es posible definir un protocolo basado en alta evidencia sobre la monitorización y los criterios de abandono de la *AS* para realizar un tratamiento curativo. No obstante, se recomienda determinar el *PSA* sérico cada 6 meses y realizar un *DRE* anualmente, además de una *mpMRI* en algún momento del seguimiento, sin especificar si su realización debería ser periódica o estar en relación a algún cambio en la evaluación clínica. Se consensua repetir la biopsia si hay un cambio en la *mpMRI*, es decir aumento en la puntuación de *PI-RADS*, volumen de la lesión o estadio radiológico, detección de un *DRE* patológico o progresión del *PSA* (102).

1.4. MÉTODOS PARA MEJORAR LA SELECCIÓN DE CANDIDATOS A BIOPSIA PROSTÁTICA

Actualmente la selección de candidatos para realizar una biopsia prostática en los hombres con sospecha de *PCa* se basa en la información de la *MRI*. No obstante, siguen existiendo escenarios inciertos como el *PI-RADS* 3 en el que la probabilidad de *csPCa* no supera el 20% y además existe una sobredetección de *iPCa* que puede llegar al 50% (106). Con el objetivo de mejorar la selección de candidatos para la biopsia prostática se ha recomendado utilizar la densidad de *PSA*, nuevos marcadores del *PCa*, y modelos predictivos.

1.4.1. DENSIDAD DE PSA

La densidad de *PSA* (*PSAD*) es la cantidad de *PSA* en suero por cada centímetro cúbico de próstata. La *PSAD* fue introducida por Benson *et al.* (107)

en 1992 como una herramienta para incrementar la especificidad del *PSA* y poder diferenciar hombres portadores de *PCa* de aquellos con una hiperplasia benigna de próstata, especialmente en la llamada zona gris del *PSA* definida por un incremento moderado entre 4 y 10 ng/ml (108). Cuanto más elevada es la *PSAD* mayor es la probabilidad de que exista *csPCa* (109). Algunos estudios han sugerido un punto de corte de 0.15 ng/ml/cc como mejor predictor de *csPCa*, existiendo por el contario una baja probabilidad cuando la *PSAD* está por debajo de 0.09 ng/ml/cc (110,111).

Se ha observado que el valor predictivo negativo de la *MRI* para detectar *csPCa* aumenta desde el 84.4 al 90.4% cuando la *PSAD* es inferior a 0.15 ng/ml/cc (112,113). Un reciente meta-análisis sugiere que el riesgo de *csPCa* oscila entre el 27 y 40% en hombres con una *PSAD* superior a 0.15-0.2 ng/ml/cc aunque la *MRI* sea negativa (114). Nuestro grupo ha demostrado que el comportamiento de la *PSAD* en relación con el *PI-RADS* para detectar precozmente el *csPCa* es dinámico, de manera que el nivel de corte más eficaz se va aumentado a medida que lo hace el *PI-RADS*. En consecuencia, parece una variable clínica interesante para incorporar en los modelos predictivos (115). El cálculo de la *PSAD* requiere de una adecuada estimación del volumen prostático, de manera que habitualmente se ha recomendado realizar la *TRUS* para su cálculo a través de la fórmula del elipsoide. Actualmente, la realización de una *TRUS* con el único objetivo de calcular el volumen prostático ha caído en desuso, aunque la mayoría de las publicaciones acerca de la *PSAD* se han realizado con el volumen prostático estimado en la *TRUS* realizada durante la biopsia prostática (116). Ese fue el motivo por el cual se propuso la estimación del volumen prostático a través del *DRE* para ser utilizado en modelos predictivos de riesgo de *PCa* para su uso antes de la *MRI* (117). Sin embargo, la eficacia de la *PSAD* estimada a partir del *DRE* es menor que la obtenida a partir del volumen prostático estimado a partir de la *MRI* (118).

Actualmente existe un resurgimiento en la utilización de la *PSAD* debido al reporte habitual del volumen prostático en los informes de la *MRI* de próstata. No obstante, y ya que tanto el *PSA* como el volumen prostático son variables predictoras independientes del *csPCa*, la propia *PSAD* o ambas variables por separado se incorporan habitualmente en los modelos predictivos más eficaces (119).

1.4.2. NUEVOS MARCADORES TUMORALES

Prostate Health Index (*PHI*) es un prueba sérica que combina *PSA* libre, *PSA* total y la isoforma *p2PSA*. La determinación de *PHI* ha demostrado ser más específica en la detección de *csPCa* que el porcentaje de *PSA* libre en hombres sometidos a su primera biopsia (120). El *4K score test* es otra prueba sérica que cuantifica *PSA* total, libre e intacto, además de la peptidasa *kallikrein-like* 2, en combinación con la edad, *DRE* y tipo de biopsia (inicial o repetida). Una revisión sistemática que incluyó más de 10.000 pacientes mostró una área bajo la curva (*AUC*) para 4K por encima de 0.80 en la discriminación del *csPCa* (121). Varios estudios prospectivos con *PHI* o *4Kscore test* han demostrado mayor eficacia que el porcentaje de *PSA* libre en la detección del *csPCa* (122). Sin embargo, un estudio ha demostrado que ambos son comparables en su capacidad de predicción de *csPCa* en biopsias iniciales (123). Proclarix es una nueva prueba sérica que combina la determinación de trombospondina-1, catepsina D, *PSA* total y libre, además de la edad. Ésta proporciona el riesgo de *csPCa*, siendo de especial interés en el caso de hombres con *PI-RADS* 3 (36). Proclarix también se ha relacionado con la agresividad del *csPCa*, siendo su predicción superior en el caso de *PCa* avanzado y con alto *ISUP-GG* (124).

El *Prostate Cancer Antigen 3* (*PCA3*) es un gen que trascribe un ácido ribonucleico (*RNA*) mensajero no codificante largo que se sobre-expresa en el tejido prostático tumoral y se puede detectar en orina después del masaje prostático. *PCA3* establece la relación entre su *RNA* mensajero y el del *PSA* (125). Varios estudios indican que *PCA3 score* es más preciso que el *PSA* total y el porcentaje de *PSA* libre para la detección de *PCa* en hombres con biopsia previa negativa (126,127). Aun así, debido a que actualmente es de mayor interés la detección del *csPCa* su utilidad es incierta (125). *SelectMDx* es también un marcador urinario basado en el *RNA* mensajero de los genes HOXC6 y *DLX1* que se encuentran sobre-expresados en el *PCa*, siendo poco específico para el *csPCa* (128). Se ha comparado su utilidad frente a la *MRI* siendo la última mejor respecto al número de *csPCa* detectados y las biopsias evitadas (129). También se ha observado que la combinación de *SelectMDX* con la *MRI* incrementa la sobredetección de *iPCa* (129). Otro marcador urinario como el *TMPRSS3-ERG* ha mostrado mayor eficacia que *PSA* total con una especificidad del 93% y un valor predictivo del 94% para la detección de *PCa* (130). La combinación del *PCA3* y el TMPRSS2-ERG podría mejorar la detección de *csPCa* (131). Aunque su utilidad parece prometedora, el valor añadido de estos biomarcadores en la era de la *MRI* se encuentra cuestionada (132).

La realidad de los marcadores de *PCa* modernos es su coste elevado, la necesidad de nuevas obtenciones de muestras para su determinación y la competitividad de los modelos predictivos. La mayoría de los marcadores mencionados incorporan variables clínicas siendo en realidad modelos predictivos que incorporan los marcadores tumorales, y en algún caso no se ha comprobado su mayor eficacia frente a las propias variables clínicas que incorporan (132).

1.4.3. MODELOS PREDICTIVOS

Los modelos predictivos son herramientas utilizadas para predecir el riesgo de un determinado evento a partir de variables predictoras independientes históricas (133). El desarrollo de un modelo predictivo se basa en primer lugar en la recopilación de datos históricos relacionados con el evento que se desea predecir. Estas bases de datos deben incluir las posibles variables predictoras y las variables objetivo. Los datos siempre requieren de una depuración para evitar valores erróneos, de un manejo apropiado de los valores perdidos y también requieren realizar las recodificaciones oportunas de determinadas variables. En segundo lugar, deben identificarse las variables predictoras independientes del modelo a partir de una regresión logística binaria, y como tercer paso, se procede a la construcción del modelo predictivo. La generación de probabilidades y la estimación de la razón de probabilidades y de sus intervalos de confianza (*CI*) para cada variable permiten definir su peso en el contexto del modelo (134). La calibración de un modelo define la concordancia entre valores predichos y observados. Posteriormente, el modelo debe ser validado internamente en una muestra independiente (133). La eficacia del modelo se evalúa a través de su capacidad discriminatoria del evento mediante la estimación del área bajo la curva *ROC (receiver operating characteristic)*, que establece una relación entre su sensibilidad y especificidad. También es posible realizar validaciones cruzadas u otras técnicas de validación para obtener estimaciones más precisas del rendimiento de un modelo en datos no confirmados (135). Una vez que se ha construido y validado internamente un modelo predictivo ya puede realizar predicciones sobre nuevos datos habitualmente a través de la construcción de los nomogramas correspondientes (**Figura 4**). Sin embargo, su cálculo es tedioso y lento, de manera que hacen difícil la utilización de los modelos predictivos en la práctica clínica. El desarrollo de aplicaciones *web* o para *smartphone* ha sido definitivo para construir calculadoras de riesgo y acercar la utilización de los modelos predictivos a la clínica diaria (136).

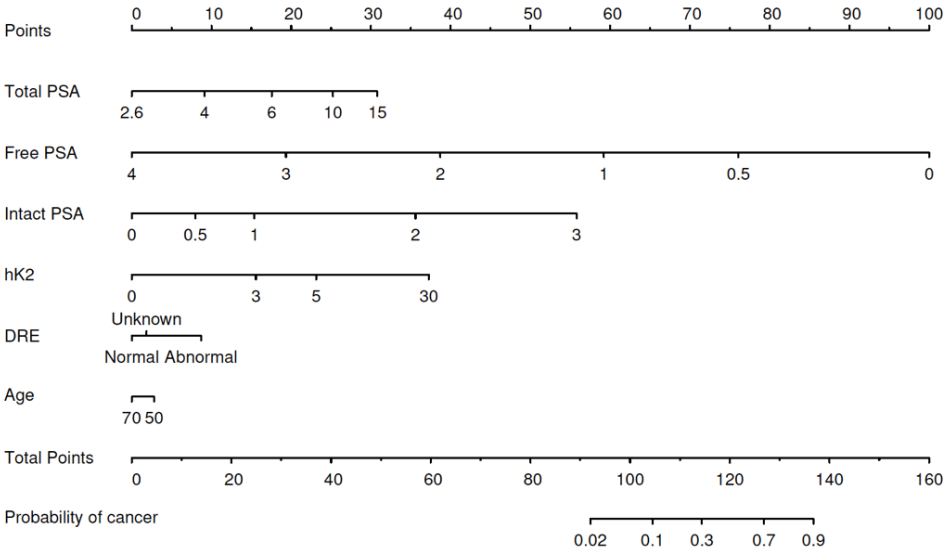

Figura 4 Nomograma para calcular el riesgo de *PCa* en la biopsia. Todos los marcadores se expresan en ng/ml excepto la kallikreina humana 2 que se expresa en 10 pg/ml. *tPSA = PSA* total; *fPSA =PSA* libre; *iPSA =PSA* intacto (137)

Es importante conocer que los modelos predictivos desarrollados no van a predecir con exactitud lo que ocurra en poblaciones distintas a la población de desarrollo, y de manera especial con una prevalencia de evento distinta (138). La elección y rendimiento de un modelo predictivo dependen en gran medida de la representatividad de sus variables predictoras en la población diana y de manera especial de la prevalencia del evento a predecir (135). Por ello, son necesarias las validaciones externas en las poblaciones donde se van a implementar los modelos desarrollados, y efectuar las oportunas recalibraciones y ajustes de los valores de corte del propio modelo para asegurar la exactitud de las predicciones (135).

Existen múltiples modelos predictivos de *csPCa*, pero en muy pocos se han desarrollado calculadoras de riesgo, siendo la más prestigiosa la calculadora de Rotterdam (www.prostatecancer-riskcalculator.com), desarrollada inicialmente

a partir de la sección de Rotterdam del *European Randomized Study of Screening for Prostate Cancer* (*ERSPC)*. El *ERSPC* fue publicado en 2009, reportando una disminución relativa de la mortalidad específica por *PCa* del 30% en el brazo de hombres sometidos a cribado con *PSA* (139). Poco después, la sección de Rotterdam se convierte en el referente que cuestiona el verdadero riesgo-beneficio del cribado del *PCa* solo con *PSA* y aboga por la utilización de otros factores predictores para seleccionar candidatos apropiados para la biopsia prostática (140). Roobol *et al*. desarrollaron un modelo predictivo de riesgo de *PCa* y *PCa* de alto grado basado en factores predictores independientes a través de regresión logística. Este modelo incluyó el volumen prostático medido por *TRUS*, la detección de áreas hipoecoicas en la *TRUS* y el *DRE* (141). Años más tarde, el modelo incorporó la información de la *mpMRI* a través del *PI-RADS* v.1, convirtiéndose en uno de los modelos más utilizados en el mundo y que se ha validado externamente en varias poblaciones (142). Otro modelo predictivo bastante utilizado en la práctica clínica es el desarrollado a partir del *Prostate Cancer Prevention Trial*, el cual utiliza como variables para predecir el riesgo de *PCa* la edad, el *PSA*, el volumen prostático y la existencia de biopsias previas negativas (143). Varios grupos han desarrollado modelos predictivos que utilizan variables clínicas (144–147). Otros modelos han incorporado biomarcadores como el *Stockholm-3, SelectMDx, 4K score o PHI* (148–151).

La introducción de la *mpMRI* ha cambiado el paradigma de la detección precoz del *csPCa* y actualmente la mayoría de los modelos incorporan el *PI-RADS* como la variable predictora de mayor peso (152). Ya que la estrategia actual de detección precoz del *PCa* es evitar la sobredetección de *iPCa*, los modelos más recientes tienden a predecir solamente el riego de *csPCa* y no del *CaP* en general (119).

La recomendación actual de la *European Association of Urology* para implementar el cribado del *PCa* en los países de la Unión Europea es estratificar los varones con sospecha de *PCa*, basándose inicialmente en la determinación sérica de *PSA* superior a 3.0 ng/ml para reducir la demanda de *MRI,* y una vez realizada ésta última, una nueva estratificación permitiría seleccionar los candidatos a biopsia prostática (153,154). La *European Association of Urology* posiciona los modelos predictivos que utilizan variables clínicas como el método más eficiente para estratificar los varones con sospecha de *PCa*, tanto para reducir la demanda de *MRI* como de biopsias prostáticas (154). Por tanto, es necesario generar ambos tipos de modelos predictivos, para el uso justo después de la sospecha de *PCa* y para después de la *MRI*. En cuanto a las posibles variables predictoras independientes del primer modelo pueden tenerse en cuenta la edad, los antecedentes familiares de primer grado de *PCa*, el tipo de biopsia prostática (inicial *versus* repetida) y *DRE* (normal *versus* sospechoso). Puesto que el volumen prostático es una variable predictora del *csPCa* de gran peso (155) y justo después de la sospecha de *PCa* habitualmente no se conoce, la posibilidad de categorizar el volumen prostático a través del *DRE* ya fue propuesta Robool *et al*. e incorporado en el modelo *ERSPC*-Rotterdam (117). Robool *et al*. propusieron el cálculo del volumen prostático a partir del volumen mediano encontrado en próstatas pequeñas, medianas y grandes, y establecieron unos intervalos de volumen prostático inferiores a 30 cc, entre 31 y 60 cc y superiores a 60 cc (156). En cuanto a la variables clínicas predictoras de *csPCa* después de la *MRI* podrían ser las mismas que las utilizadas en el modelo justo después de la sospecha de *PCa*, pero con el volumen prostático estimado a partir de la *MRI* y el *PI-RADS*.

2. JUSTIFICACIÓN DEL PROYECTO

El *PCa* es el tumor maligno más frecuentemente diagnosticado entre los varones de nuestro entorno (1). La determinación sérica de *PSA* y el *DRE* siguen siendo los elementos fundamentales para establecer la sospecha de *PCa* y su diagnóstico se realiza través de la biopsia prostática (22). La estrategia clásica de diagnóstico precoz del *PCa*, basada en la biopsia sistemática en varones con sospecha de *PCa,* presenta una baja especificidad y ha derivado en un número excesivo de biopsias prostáticas innecesarias y la sobredetección de *iPCa* (157). El *ERSPC*, el estudio europeo más notorio de cribado del *PCa*, puso de manifiesto una reducción del 30% en la mortalidad específica por *PCa* en el grupo de hombres sometido a cribado con *PSA* a partir del séptimo año de seguimiento (139), tasa que se ha mantenido por encima del 20% a los 22 años de seguimiento (158). La evidencia reportada por el *ERSPC* también ha producido un cambio de paradigma en el cribado del *PCa*, enfocado ahora hacia el *csPCa.* Este cambio ha sido posible gracias a la introducción y rápida generalización de la *MRI* prostática (106). La *MRI* permite reducir el número de biopsias prostáticas gracias a su elevado valor predictivo negativo, y además permite realizar biopsias dirigidas a las lesiones sospechosas de *csPCa* incrementando la sensibilidad proporcionada por las biopsias sistemáticas (159) .

A raíz de este avance, en marzo de 2022, el *European Council of Cancer Screening* ha recomendado a los países de la Unión Europea la implantación de programas de *screening* de *PCa* a través de la determinación sérica de *PSA* y la *MRI* prostática (41). Por su parte, la *European Association of Urology*, actualmente recomienda la estratificación de los hombres con sospecha de *PCa* con el objetivo de racionalizar la demanda de *MRI* y las biopsias prostáticas (153,154).

La *MRI* prostática permite detectar lesiones sospechosas de *csPCa*, cuyo riesgo se estima semi-cuantitativamente a través del *PI-RADS*, actualmente en su versión

2.1 (54). La indicación de biopsia prostática se establece cuando el *PI-RADS* es mayor o igual a 3, ya que el valor predictivo negativo de la *MRI* cuando se utiliza el *PI-RADS* 2.1 oscila entre 96% (95% *CI*: 91-100) y 98% (91-99) para *PI-RADS* 1 y 2 respectivamente. El valor predictivo positivo del *PI-RADS* 3 es del 20%, el del *PI-RADS* 4 del 52%, y el del *PI-RADS* 5 del 89% (160). En este contexto, el escenario de la biopsia prostática ha cambiado, de manera que actualmente se realizan biopsias dirigidas a las lesiones sospechosas, si bien se complementan por la clásica biopsia sistemática ya que un pequeño porcentaje de *csPCa* se diagnostica solamente en este tipo de biopsia (56). En este nuevo escenario para el diagnóstico precoz del *csPCa* siguen existiendo reductos de incerteza como el *PI-RADS* 3, en el que solamente un 20% de biopsias detecta *csPCa* y existe una sobredetección de *iPCa* que llega al 50% (161). En estas circunstancias desafiantes se ha recomendado utilizar herramientas como la *PSAD*, nuevos marcadores tumorales y modelos predictivos de *csPCa* (162). Los modelos predictivos de *csPCa* son especialmente atractivos siempre que asocien una calculadora de riesgo accesible para su uso habitual y rápido. Además, no tienen coste adicional cuando añaden otras variables clínicas independientes al *PI-RADS*, que se ha convertido en la variable predictora independiente de mayor peso (119).

En el momento de plantear nuestro proyecto de tesis doctoral, marzo de 2021, tan solo el modelo predictivo de *ERSPC*-Rotterdam disponía de una calculadora de riesgo con fácil acceso *web* y *app* para teléfonos inteligentes (142). Este modelo, aun siendo pionero, había sido adaptado en 2019 en una población de 918 varones con sospecha de *PCa* en un estudio multicéntrico de cuatro hospitales holandeses y otro alemán. El procedimiento diagnóstico que se utilizó incorporó las biopsias dirigidas a lesiones *PI-RADS* $\geq$ 3 y/o biopsias sistemáticas, que se realizaron también en varones con *PI-RADS* < 3. El *PI-RADS* utilizado en el desarrollo del modelo fue la versión 1, y además utilizó la edad (>50 y <75 años),

PSA sérico (>0.4 y < 50 ng/ml), *DRE* (normal *vs* sospechoso), volumen prostático basado en la *TRUS* (>10 y <110 cc), y tipo de biopsia (inicial *vs* repetida) (142).

La posibilidad de desarrollar y validar modelos predictivos actualizados para estratificar los pacientes en riesgo de *csPCa* antes y después de la *mpMRI*, basados en la población de nuestro entorno, y de incorporar el *PI-RADS* v.2.0, la edad, el *PSA* sérico, y el volumen prostático sin límites, además del antecedente familiar de *PCa*, el tipo de biopsia (inicial o repetida) y el *DRE*, nos motivó a plantear nuestro proyecto de tesis doctoral, basado en el desarrollo y validación de los modelos predictivos de Barcelona y sus calculadoras asociadas.

3. HIPÓTESIS

La predicción individualizada del riesgo de *csPCa* a través de una calculadora de riesgo diseñada a partir de los modelos predictivos de Barcelona para ser utilizados antes y después de la *MRI,* mejoran el diagnóstico precoz del *csPCa* reduciendo la demanda de *MRIs* y biopsias prostáticas innecesarias.

4. OBJETIVOS

Objetivo primario:

Desarrollar una calculadora de riesgo (*RC*) de *csPCa* basada en dos nuevos modelos predictivos que incorporan variables clínicas disponibles en el momento de la sospecha de *PCa* para su uso antes y después de la *MRI*.

Objetivos secundarios:

1. Analizar, a través de una revisión sistemática de la literatura, la evidencia científica actual acerca de los modelos predictivos de riesgo de *PCa* basados en la *MRI* desarrollados y sus *RC*.

2. Desarrollar y validar externamente un nuevo modelo predictivo y su *RC*, basados en la *MRI* prostática y las variables clínicas independientes disponibles en el momento de sospecha de *PCa*, para seleccionar eficazmente los candidatos a biopsia prostática.

3. Comparar el nuevo modelo predictivo basado en la *MRI* y variables clínicas con la *PSAD* y el prestigioso modelo predictivo de Rotterdam-*MRI,* para seleccionar eficazmente los candidatos a biopsia prostática.

4. Desarrollar y validar externamente un nuevo modelo predictivo y su *RC*, basado en variables clínicas disponibles en el momento de sospecha de *PCa,* para seleccionar apropiadamente los candidatos a *MRI* prostática.

5. COMPENDIO DE PUBLICACIONES

5.1. PUBLICACIÓN 1

Título: Magnetic Resonance Imaging-Based Predictive Models for Clinically Significant Prostate Cancer: A Systematic Review

Revista: Cancers

Año de publicación: 2022

Volumen: 14

Páginas: 4747

DOI: https://doi.org/10.3390/cancers14194747

Autores: Marina Triquell, Miriam Campistol, Ana Celma, Lucas Regis, Mercè Cuadras, Jacques Planas, Enrique Trilla y Juan Morote

Factor de impacto: 4.5 (2023)

Cuartil: Q1 (Oncología)

cancers

MDPI

Systematic Review

Magnetic Resonance Imaging-Based Predictive Models for Clinically Significant Prostate Cancer: A Systematic Review

Marina Triquell [1,2,*], Miriam Campistol [1,2], Ana Celma [1,2], Lucas Regis [1,2], Mercè Cuadras [1,2], Jacques Planas [1,2], Enrique Trilla [1,2,†] and Juan Morote [1,2,†]

[1] Department of Urology, Vall d'Hebron University Hospital, 08035 Barcelona, Spain
[2] Department of Surgery, Univesirtat Autònoma de Barcelona, 08193 Barcelona, Spain
* Correspondence: mtriquell@vhebron.net
† These authors contribute equally to this work.

Simple Summary: Magnetic resonance imaging (MRI) has allowed the early detection of PCa to evolve towards clinically significant PCa (csPCa), decreasing unnecessary prostate biopsies and overdetection of insignificant tumours. MRI identifies suspicious lesions of csPCa, predicting the semi-quantitative risk through the prostate imaging report and data system (PI-RADS), and enables guided biopsies, increasing the sensitivity of csPCa. Predictive models that individualise the risk of csPCa have also evolved adding PI-RADS score (MRI-PMs), improving the selection of candidates for prostate biopsy beyond the PI-RADS category. During the last five years, many MRI-PMs have been developed. Our objective is to analyse the current developed MRI-PMs and define their clinical usefulness through a systematic review. We have found high heterogeneity between MRI technique, PI-RADS versions, biopsy schemes and approaches, and csPCa definitions. MRI-PMs outperform the selection of candidates for prostate biopsy beyond MRI alone and PMs based on clinical predictors. However, few developed MRI-PMs are externally validated or have available risk calculators (RCs), which constitute the appropriate requirements used in routine clinical practice.

Abstract: MRI can identify suspicious lesions, providing the semi-quantitative risk of csPCa through the Prostate Imaging-Report and Data System (PI-RADS). Predictive models of clinical variables that individualise the risk of csPCa have been developed by adding PI-RADS score (MRI-PMs). Our objective is to analyse the current developed MRI-PMs and define their clinical usefulness. A systematic review was performed after a literature search performed by two independent investigators in PubMed, Cochrane, and Web of Science databases, with the Medical Subjects Headings (MESH): predictive model, nomogram, risk model, magnetic resonance imaging, PI-RADS, prostate cancer, and prostate biopsy. This review was made following the Preferred Reporting Items for Systematic Reviews and Meta-analyses (PRISMA) criteria and studied eligibility based on the Participants, Intervention, Comparator, and Outcomes (PICO) strategy. Among 723 initial identified registers, 18 studies were finally selected. Warp analysis of selected studies was performed with the Quality Assessment of Diagnostic Accuracy Studies (QUADAS-2) tool. Clinical predictors in addition to the PI-RADS score in developed MRI-PMs were age, PCa family history, digital rectal examination, biopsy status (initial vs. repeat), ethnicity, serum PSA, prostate volume measured by MRI, or calculated PSA density. All MRI-PMs improved the prediction of csPCa made by clinical predictors or imaging alone and achieved most areas under the curve between 0.78 and 0.92. Among 18 developed MRI-PMs, 7 had any external validation, and two RCs were available. The updated PI-RADS version 2 was exclusively used in 11 MRI-PMs. The performance of MRI-PMs according to PI-RADS was only analysed in a single study. We conclude that MRI-PMs improve the selection of candidates for prostate biopsy beyond the PI-RADS category. However, few developed MRI-PMs meet the appropriate requirements in routine clinical practice.

Keywords: prostate cancer; magnetic resonance imaging; predictive model; risk calculator

Citation: Triquell, M.; Campistol, M.; Celma, A.; Regis, L.; Cuadras, M.; Planas, J.; Trilla, E.; Morote, J. Magnetic Resonance Imaging-Based Predictive Models for Clinically Significant Prostate Cancer: A Systematic Review. *Cancers* **2022**, *14*, 4747. https://doi.org/10.3390/cancers14194747

Academic Editors: Giorgio Treglia and Ursula Maria Vogl

Received: 23 August 2022
Accepted: 23 September 2022
Published: 29 September 2022

1. Introduction

Prostate cancer (PCa) suspicion, based on elevated serum prostate-specific antigen (PSA) and/or abnormal digital rectal examination (DRE), followed by systematic prostate biopsy, has been the classic strategy for early detection of PCa [1]. However, this strategy has led to a high rate of unnecessary prostate biopsies and overdetection of insignificant PCa (iPCa) [2]. Currently, early detection of PCa has evolved towards the detection of clinically significant PCa (csPCa), which is usually defined in prostate biopsies as the International Society of Uro-Pathology (ISUP) grade group (GG) 2 or higher [3]. However, other existing definitions of csPCa based on tumour burden and PSA density (PSAD) in addition to ISUP GG may correlate better with the histopathological findings of surgical specimens [4].

Most relevant progress in the early detection of csPCa has come from pre-biopsy multiparametric magnetic resonance imaging (mpMRI), which can identify suspicious lesions, providing the semi-quantitative risk of csPCa through the Prostate Imaging-Report and Data System (PI-RADS) [5]. Additionally, guided biopsies of suspicious lesions identified in mpMRI increase the sensitivity of csPCa reached with systematic biopsies [6,7]. The negative predictive value of mpMRI for csPCa reaches up to 95% [8]; therefore, a prostate biopsy is usually avoided in men with PI-RADS <3 [9] However, the positive predictive value of mpMRI ranges from 15 to 20% in men with PI-RADS 3, between 50–60% in those with PI-RADS 4, and between 85–95% in men with PI-RADS 5 [10]. Consequently, there are uncertain scenarios in which modern markers, PSAD, and predictive models based on MRI findings and clinical predictors (MRI-PMs) are re-commended for improving the selection of candidates for prostate biopsy [11–13].

Predictive models (PMs) are the only tool providing the individual risk of csPCa. These PMs have usually been presented through nomograms [14]; however, the cumbersome and time-consuming use of nomograms makes designing user-friendly web and smartphone available risk calculators (RCs) essential to facilitating the daily use of PMs [15–17]. In addition, PMs need external validation in the populations where they will be used to know if predictions are accurate. From the spread of pre-biopsy MRI, many MRI-PMs have been developed; however, the heterogenicity of development cohorts, diffe-rences between MRI scanners and PI-RADS versions used, variability of prostate biopsy schemes and approaches, and different csPCa definitions, in addition to external validations and availability of RCs, justify a systematic review. This systematic review analyses the current developed MRI-PMs and defines their clinical usefulness.

2. Evidence Acquisition

2.1. Search Strategy

Two independent reviewers (M.T. and J.M.) searched the literature to retrieve all relevant studies published before 31 March 2022. This search was conducted in PubMed, Cochrane, and Web of Science databases, using the Medical Subject Headings (MeSH): nomogram, risk model, magnetic resonance imaging, PI-RADS, prostate cancer, and prostate biopsy. The Preferred Reporting Items for Systematic Reviews and Meta-analyses (PRISMA) criteria [18] were followed. Disagreements were resolved through discussion between reviewers. This systematic review was registered in PROSPERO (International prospective register of systematic reviews), with the ID number CRD42022345848.

2.2. Eligible Criteria

The study eligibility was based on the Participants, Intervention, Comparator, and Outcomes (PICO) strategy [19]. The inclusion criteria were (1) the population at risk of PCa due to abnormal DRE or elevated serum PSA; (2) MRI identification of suspicious lesions and the performance of guided and systematic biopsies; (3) a comparison between PMs based on clinical parameters alone and MRI; (4) the outcome of csPCa. The search criteria were limited to articles written in English. Review articles, meta-analyses, conference abstracts, and letters were excluded.

2.3. Study Selection

The flow diagram of study selection is illustrated in Figure 1. Among 723 registers initially identified, 302 were duplicated. The retrieved study abstracts were screened and selected by exclusion and inclusion criteria, with 267 excluded. Of the 154 remaining stu-dies, 136 were excluded after full-text screening because the outcomes were not the pre-diction of csPCa before a prostate biopsy, or a PM was not developed. Finally, 18 studies fulfilled the eligibility criteria.

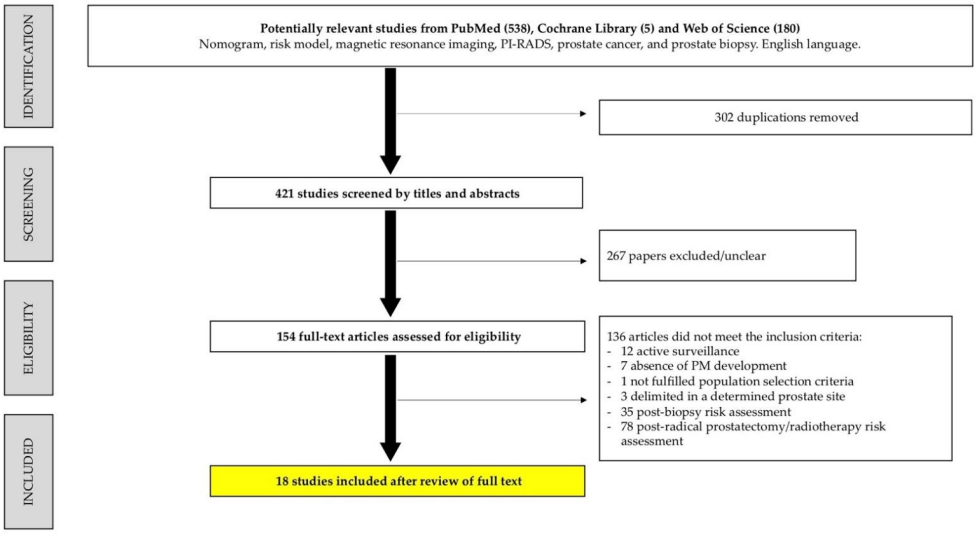

Figure 1. Flow chart of systematic review according to the PRISMA criteria.

2.4. Quality Assessment

Quality Assessment of Diagnostic Accuracy Studies 2 (QUADAS-2) was used as an evidence-based quality assessment tool [20]. QUADAS-2 comprised four domains: patient selection, index test, reference standard, and flow and timing. The risk of bias in each study was evaluated by two independent reviewers as low, high, or unclear. The QUADAS-2 results are summarised in Figure 2, suggesting an overall low risk of bias.

(A)

Authors, [Ref.]	Patient selection	Index test	Reference Standard	Flow and Timing
Fang et al, 2016	Low	Low	Low	Low
Kim et al, 2016	Low	Unclear	High	Low
Bjurlin et al, 2017	Low	High	High	Low
Lee et al, 2017	Low	Low	Low	Low
Niu et al, 2017	Low	High	Low	Low
Radtke et al, 2017	Low	Unclear	Low	Low
Truong et al, 2017	Low	Low	Low	Low
van Leeuwen et al, 2017	Low	Low	Low	Low
Alberts et al, 2018	Low	Low	Low	High
Huang et al, 2018	Low	Unclear	Low	Low
Mehralivand et al, 2018	Low	Low	Low	Low
Boesen et al, 2019	Low	Low	Low	Low
Borque et al, 2019	Low	Unclear	Low	Low
Chen et al, 2020	Low	Low	Low	Low
Noh et al, 2020	Low	High	High	Low
Sakaguchi et al, 2021	Low	Low	Low	Low
Kinnaird et al, 2022	Low	Low	Low	Low
Morote et al. 2022	Low	Low	Low	Low

Figure 2. *Cont.*

(B)

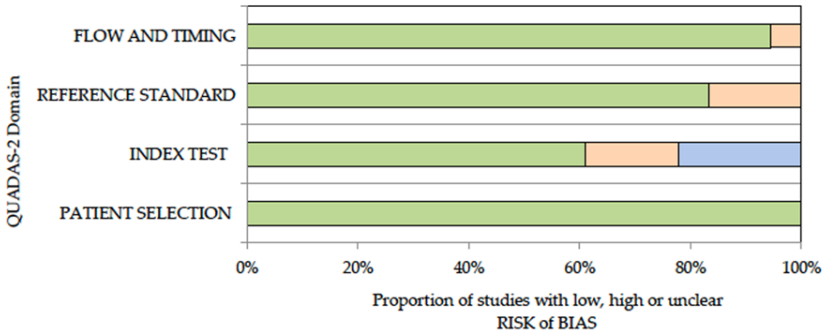

Figure 2. Analysis of bias risks (low, unclear, high) of analysed studies according to each bias. domain (**A**), and proportion of studies according to each domain (**B**) [15–17,21–36].

3. Synthesis of the Evid

The characteristics of development cohorts of each MRI-PM regarding size, prostate biopsy status (initial vs. repeat), MRI characteristics and reporting methods, prostate biopsy scheme and approach, types of guided biopsies, and the definition of csPCa are summarised in Table 1. The logistic regression analysis among the selected candidate clinical predictors of csPCa, in addition to the MRI report, was the only method used to generate all MRI-PMs. The independent clinical predictors of csPCa were included in each MRI- PM and are presented in Table 2. The csPCa discrimination ability of MRI-PMs was analysed using areas under the receiver operating characteristic curves (AUROCs). The net benefit over biopsy of all the men or other predictors as baseline models of clinical predictors or MRI alone were examined through decision curve analysis (DCAs). The clinical utility was explored with clinical utility curves (CUCs) as a representation of avoided biopsies and missed csPCa in a continuous evolution of thresholds for csPCa risk.

Table 1. Biopsy status and size of development cohorts, characteristics of pre-biopsy MRI, prostate biopsy approaches and types of systematic and guided biopsies, and csPCa definitions.

Authors, Year [Ref.]	Biopsy Status	MRI/T	PI-RADS Version	Biopsy Approach	Systematic Biopsy	Guided Biopsy	Type of GB	csPCa Definition
Fang et al., 2016 [21]	984/0	mp/1.5–3	1	TR	12	NA/≥3	NA	GS ≥ 3+4
Kim et al., 2016 [22]	185/154	mp/3	1–2	TR	12	NA/≥4	Cog/Soft	GS ≥ 3+4
Bjurlin et al., 2017 [23]	288/171	mp/3	1	TR	12	1–4/≥3	Soft	GS ≥ 3+4
Lee et al., 2017 [24]	484/131	bp/1.5	1	TP	24–40 *	2–4/≥3	Cog	GS≥7 or MCCL≥ 6 mm
Niu et al., 2017 [25]	151/0	mp/3	2	TR	12	1/≥3	Cog	GS ≥ 3+4
Radtke et al., 2017 [26]	670/489	mp/3	1	TP	24 *	2–4/≥2	Soft	GS ≥ 3+4
Truong et al., 2017 [27]	0/285	mp/3	2	TR	12–24 *	2/≥3	Soft	GS ≥ 3+4
van Leeuwen et al., 2017 [28]	344/49	mp/1.5–3	1	TP	30 *	2/≥3	Soft/Cog	GS≥ 7/> 5% G4 or MLCL≥ 20%/7 mm
Alberts et al., 2018 [29]	504/457	mp-bp/3	1–2	TR	12	NA/≥3	In bore/Cog/Soft	GS ≥ 3+4
Huang et al., 2018 [30]	0/231	mp/1.5–3	2	TR	12	2/≥4	NA	GS ≥ 3+4
Mehralivand et al., 2018 [31]	179/221	mp/NA	2	TR	12	2/≥3	Soft	GS ≥ 3+4
Boesen et al., 2019 [32]	876/0	bp/3	2	TR	10	2/≥3	Cog	GG ≥ 2
Borque et al., 2019 [15]	163/183	mp/3	2	TR	12	2/≥3	Cog	GG ≥ 2
Chen et al., 2020 [33]	316	mp/NA	2	NA	NA	NA	NA	GS ≥ 3+4
Noh et al., 2020 [34]	215/85	bp/3	2	TP	24–20 *	2–10/≥3	Cog	GS ≥ 3+4
Sakaguchi et al., 2021 [35]	773/0	bp/1.5–3	2	TR	8–14	2–4/≥3	Cog	GG3 or MCCL≥ 6 mm
Kinnaird et al., 2022 [17]	1449/905	mp/3	2	TR	12	2–3/≥3	Cog	GG ≥ 2
Morote et al. 2022 [16]	1098/388	mp/3	2	TR	12	2–4/≥3	Cog	GG ≥ 2

Ref. = reference; Biopsy status = number of biopsy naïve men/number of repeat biopsy; MRI = magnetic resonance imaging (mp = multiparametric, bp = biparametric/T = Tesla); Biopsy approach = TR (Transrectal), TP (Transperineal); Systematic biopsy = number of cores (* template); Guided biopsy = guided biopsy (Soft: software, Cog: cognitive); GB = guided biopsy; csPCa = clinically prostate cancer; GS = Gleason score; GG = grade group; MCCL = maximal core cancer length; NA = not available.

Table 2. Clinical predictors included in developed MRI-PMs for clinically significant prostate cancer.

Authors, [Ref.]	Age	PCa FH	DRE	Biopsy Status	Ethnicity	PSA	PSAD	PV
Fang et al., 2016 [21]	Y	N	Y	N	N	Y	N	Y
Kim et al., 2016 [22]	Y	Y	Y	Y	Y	Y	N	N
Bjurlin et al., 2017 [23]	Y	N	N	N	N	N	Y	N
Lee et al., 2017 [24]	Y	N	N	Y	N	N	Y	N
Niu et al., 2017 [25]	Y	N	N	N	N	N	Y	N
Radtke et al., 2017 [26]	Y	N	Y	N	N	Y	N	Y
Truong et al., 2017 [27]	Y	N	N	N	N	Y	N	Y
van Leeuwen et al., 2017 [28]	Y	N	Y	N	N	Y	N	Y
Alberts et al., 2018 [29]	Y	N	Y	N	N	Y	N	Y
Huang et al., 2018 [30]	Y	N	Y	N	N	Y	N	Y
Mehralivand et al., 2018 [31]	N	N	Y	Y	Y	Y	N	N
Boesen et al., 2019 [32]	Y	N	Y	N	N	N	Y	N
Borque et al., 2019 [15]	Y	N	Y	Y	N	N	Y	N
Chen et al., 2020 [33]	N	N	N	N	N	Y	N	Y
Noh et al., 2020 [34]	Y	N	N	N	N	N	Y	N
Sakaguchi et al., 2021 [35]	Y	N	N	N	N	Y	N	Y
Kinnaird et al., 2022 [17]	Y	N	Y	Y	Y	Y	Y	Y
Morote et al. 2022 [16]	Y	Y	Y	Y	N	Y	N	Y

Y = yes; N = no; PCaFH = prostate cancer family history; DRE = digital rectal examination; PSA = prostate-specific antigen; PSAD = PSA density; PV = prostate volume.

In addition, the specificity corresponded to 95% sensitivity of each MRI-PM and avoided prostate biopsies are summarised in Table 3. Below we review the most significant characteristics and findings of developed MRI-PMs regarding the year of publication.

Table 3. Clinical usefulness of developed MRI-PMs.

Authors, [Ref.]	n	Repeat Biopsy	csPCa	Sen.	Spe.	Avoided Biopsies	Cut-Off	AUROC	DCA	CUC
Fang et al., 2016 [21]	894	0	24.4	95	38	19.8	30	0.87	5	NA
Kim et al., 2016 [22]	339	35.4	34.0	95	20	15.1	NA	0.78	NA	NA
Bjurlin et al., 2017 [23]	288	0	33.6	95	56	42.2	NA	0.91	NA	NA
Bjurlin et al., 2017 [23]	171	100	18.1	95	40	33.9	NA	0.86	NA	NA
Lee et al., 2017 [24]	615	21.3	38.5	97.5	54.8	34.6	30	0.92	NA	NA
Niu et al., 2017 [25]	151	0	21.0	87.3	78.4	64.9	36	0.85	NA	NA
Radtke et al., 2017 [26]	660	0	NA	95	35	NA	NA	0.83	16	NA
Radtke et al., 2017 [26]	335	100	NA	95	25.5	NA	NA	0.81	12	NA
Truong et al., 2017 [27]	285	100	38.9	94.7	57.5	36.5	40	0.83	1	NA
van Leeuwen et al., 2017 [28]	393	12.5	37.9	93.9	NA	34.4	12.5	0.88	4	NA
Alberts et al., 2018 [29]	504	0	42.0	92	NA	24.0	15	0.84	10	NA
Alberts et al., 2018 [29]	504	100	29.0	95	NA	41.0	15	0.85	5	NA
Huang et al., 2018 [30]	231	100	25.5	95	63	48.0	21	0.92	10	NA
Mehralivand et al., 2018 [31]	400	55.2	48.3	96	54	30.0	15	0.84	10	NA
Boesen et al., 2019 [32]	876	0	40.0	96	60	38.0	15	0.89	5	NA
Borque et al., 2019 [15]	346	53.0	32.6	95	51	30.0	10	0.88	0.88	Y
Chen et al., 2020 [33]	257	NA	59.2	95	40	19.0	NA	0.84	NA	NA
Noh et al., 2020 [34]	300	28.3	34.0	95	52	30.1	10	0.86	10	NA
Sakaguchi et al., 2021 [35]	773	0	44.3	95	73	43.0	15	0.86	5	NA
Kinnaird et al., 2022 [17]	1885	62.0	40.0	95	32	21.2	NA	0.84	NA	NA
Morote et al. 2022 [16]	1486	26.1	36.9	95	56	40.0	15	0.90	12	Y

n = number of men; RB = percentage of repeat biopsies; csPCa = percentage of clinically significant prostate cancer; Sen = sensitivity; Spe = specificity; Repeat biopsy = percentage; Sen. = percent sensitivity; Esp. = percent specificity; Avoided biopsies = percentage; AUROC = area under Receiver operating characteristic curve; DCA = decision curve analysis; CUC = clinical utility curve; NA = not available.

In 2016, Fang et al. [21] developed the first MRI-PM. They recruited 984 biopsy-naïve men from a single centre in Pekin, China, in whom guided and 12-core systematic biopsies were performed by transrectal approach after multiparametric MRI (mpMRI) between 2011 and 2013. The CsPCa (GS ≥ 3+4) detection was 24.4%. Age, DRE, serum PSA, and prostate volume (PV) assessed from the transrectal ultrasound (TRUS) just before prostate biopsy, were the clinical predictors, in addition to the retrospective review of PI-RADS v1 as grade 0 (PI-RADS 1 and 2), grade 1 (PI-RADS 3), and grade 3 (PI-RADS 4 and 5). The AUROC of MRI-PM compared to that of the baseline model of clinical predictors were 0.87 and 0.85, respectively (p = 0.001). DCAs suggested the net benefit of MRI-PM over MRI and biopsy of all men from the risk threshold of 5%. At 95% sensitivity, the specificity was 38%, and the percentage of avoided biopsies was 19.8%. This model was not externally validated, and no RC was designed. Also in 2016, Kim et al. [22] incorporated MRI into the Prostate Cancer Prevention Trial RC (PCPT-RC). The MRI-PM was developed in 339 suspected PCa men (185 biopsy-naïve and 154 men subjected to repeat biopsy) from St. Louis, US, in whom 34% csPCa (GS ≥ 3+4) was detected after transrectal cognitive or -guided biopsies and 12-core systematic biopsy carried out between 2012 and 2015. MRI-PM improved the discrimination ability of the PCPT-RC of csPCa but not significantly; the AUROCs were 0.78 and 0.74, respectively (p = 0.06). At 95% sensitivity, the specificity was 20% and the rate of avoided biopsies was 15.1%. This MRI-PM was not externally validated and the current available PCPT-RC v.2.0 does not incorporate the MRI findings.

In 2017, six MRI-PMs were developed. Bjurlin et al. [23] developed two MRI-PM for csPCa (GS ≥ 3+4) regarding the biopsy status of 464 suspected PCa men, 288 biopsy-naïve and 171 with prior negative prostate biopsy. Prebiopsy mpMRI and 1 to 4-core software-guided biopsies and/or 12-core systematic biopsy carried out by transrectal approach were performed between 2012 and 2014, in New York, US. The rates of csPCa detection were 33.6% and 18.1%, respectively. The MRI-PM included age, PSAD, and PI-RADS v1 score for the mpMRI report as predictors. The AUROCs for csPCa detection were 0.91 in biopsy- naïve men and 0.86 in those with previous negative biopsies; 42% and 34% of prostate biopsies were avoided in these groups, missing 5% of csPCa. These models were not externally validated, and RC was not designed. Lee et al. [24] developed an MRI-PM including age, biopsy status, PSAD, and biparametric MRI (bpMRI) as predictors of csPCa (GS ≥ 7 or maximal core cancer length > 6 mm) in a cohort of 615 suspected. PCa men (21.3% with prior negative prostate biopsy) subjected to transperineal template biopsy (24–40 cores) and 2- to 5-core cognitive-guided biopsies in Essex, UK, between 2012 and 2015. The rate of detected csPCa was 38.5%. The AUROC of MRI improved from 0.87 to 0.92. With the 30% csPCa risk threshold, 34.6% of prostate biopsies were avoided, and 2.5% of csPCa were missed. No external validations were made, and no RC was designed. Niu et al. [25] developed an MRI-PM for csPCa (GS ≥ 3+4) among 151 biopsy-naïve men with serum PSA between 4 and 10 ng/mL. After mpMRI, a transrectal 1 or more-core cognitive-guided biopsy of suspicious lesions and/or a 12-core systematic biopsy were performed between 2014 and 2015 in Chengdu, China. The detection rate of csPCa was 21%, and the predictors of the model were age, PSAD, and PI-RADS v2. The AUROC of MRI increased from 0.76 to 0.85 when the model included the age and PSAD. The MRI-PM with 87.3% sensitivity obtained from the 36% csPCa threshold avoided 64.9% of prostate biopsies. The model was internally validated in a subsequent series of 74 men in the same centre; however, it was not externally validated, and no RC was designed. Radtke et al. [26] developed two MRI-PMs of csPCa (GS ≥ 3+4) after sharing the same clinical predictors used by the Rotterdam RC-3 and RC-4 among 1159 consecutive suspected PCa men subjected to mpMRI reported by PI-RADS v1, and transperineal 24-core template biopsies and 2 to 4 additional cognitive-guided biopsies to suspicious lesions, between 2012 and 2015, in Heidelberg, Germany. The rates of detected csPCa were not provided; however, the model developed from 660 biopsy-naïve men reached an AUC of 0.83 compared to the 0.81 obtained from 335 men with previous negative prostate biopsy. Both models presented a net benefit over mpMRI from 16 and 12% risk of csPCa, respectively. Additionally, their specificities were

35% and 25.5%, respectively, at 95% sensitivity. The rates of avoided biopsies and missed csPCa were not provided. These models have not been externally validated and no RC has been designed. Truong et al. [27] developed an MRI-PM in 285 men with suspected PCa and at least one previous negative biopsy from two institutions in Rochester, NY, and Birmingham, Alabama, US. Pre-biopsy mpMRI and 12- to 24-core transrectal biopsies and 2-core software-guided biopsies to suspicious lesions were performed, and 38.9% of csPCa (GS $\geq$ 3+4) was detected. The predictors shared in the model were age, serum PSA, PV, and PI-RADS v2. The AUROC to discriminate csPCa was 0.83; with a 40% threshold, 36.5% of prostate biopsies were avoided while missing 6.3% of csPCa. The model exhibited a net benefit over MRI from the 3% risk threshold. External validation of the Truong's MRI-PM was carried out by Bjurlin et al. [36] in a cohort of 104 men with previous negative prostate biopsy in whom csPCa was detected in 49%. The AUROCs were 0.77 and 0.80, respectively. In the validation cohort, 55% of prostate biopsies were avoided missing 7% of csPCa. RC has not been designed. Finally, van Leeuwen et al. [28] also reported their MRI-PM in 2017. The model was developed in 393 suspected PCa men in whom pre-biopsy mpMRI and transperineal 30-core template prostate biopsy with 2 additional-core software or cognitive-guided biopsies of each suspicious lesion were performed between 2012 and 2014 in Sidney, Australia. The model included age, DRE, serum PSA, PV, and PI-RADS v1 as predictors, and the rate of detected csPCa (GS $\geq$ 7 and >5% of G 4, and maximal core cancer length $\geq$ 20% or 7 mm) was 37.9%. The baseline model with clinical predictors presented an AUROC of 0.80, increasing to 0.88 when the MRI was shared ($p < 0.001$). A threshold of 12.5% of csPCa avoided 34.3% of prostate biopsies while missing 6.1% of csPCa. The MRI-PM exhibited a net benefit over MRI and biopsy of all men from the csPCa risk of 3%. This model was externally validated in a cohort of 198 men, from another hospital in Sidney, with an AUROC of 0.86. No RC was designed.

In 2018, Huang et al. [30] developed an MRI-PM including age, serum PSA, DRE, PV measured from TRUS, and mpMRI reported by PI-RADS v2 in 231 suspected PCa men after an initial negative prostate biopsy performed between 2007 and 2017, in whom 2-core guided biopsies to suspicious lesions and/or 12-core systematic biopsies were carried out by transrectal approach in Beijing, China. The detection rate of csPCa (GS $\geq$ 3+4) was 25.5%. The AUROC of MRI-PM increased to 0.92 from the 0.88 of the baseline model of clinical predictors. DCA showed a net benefit of MRI-PM over the baseline model from the csPCa risk threshold of 10%. At 95% sensitivity of the MRI-PM, the specificity was 63%, and 48% of prostate biopsies were avoided. No external validation of this MRI-PM was made, and RC was not designed. Also in 2018, Mehralivand et al. [31] developed an MRI-PM in 400 suspected PCa, 55.2% of them with previous negative prostate biopsy. After mpMRI transrectal 2-core software-guided biopsy and/or 12-core systematic biopsy were performed between 2015 and 2016 in Bethesda, US. The rate of detected csPCa (GS $\geq$ 3+4) was 48.3%. The MRI-PM, including DRE, biopsy status, ethnicity, PSA, and PI-RADS v2, exhibited an AUROC of 0.84 compared to 0.72 of the baseline model without MRI ($p < 0.001$). At 96% sensitivity of the MRI-PM, the specificity was 54%, and 30% of prostate biopsies were avoided. DCA showed the net benefit of MRI-PM over the baseline model and MRI alone from the 10% risk threshold of csPCa. This MRI-PM was externally validated in 251 men from two institutions in Chicago, IL and Birmingham, AL, where the incidence of csPCa was 41.6 and 36%, respectively. No RC was designed.

In 2019, Boesen et al. [32] developed a PM of csPCa (GG $\geq$ 2) including bpMRI, reported by PI-RADS v2 and stratified as negative (score 1–2), equivocal (score 3), and po- sitive (score 4–5), in addition to age, DRE, and PSAD, in 876 biopsy-naïve men from Herlev, Denmark. Suspected PCa men over 75 years or PSA serum levels behind 50 ng/mL were excluded. These men were subjected to transrectal 2-core cognitive-guided biopsies for each suspicious lesion and/or 10-core systematic biopsies between 2015 and 2017. The AUROC of 0.85, obtained from the baseline model with clinical predictors, increased to 0.89 when the MRI was shared ($p < 0.001$). The net benefit of MRI-PM over MRI alone, baseline model, and biopsy of all men were observed from a 5% risk of csPCa. At 96% sensitivity,

the MRI-PM presented a specificity of 60%, and 38% of prostate biopsies were avoided. No external validation was performed, and no RC was designed. Alberts et al. [29] adjusted the Rotterdam RC-3 and RC-4 to a multi-centre population of 961 suspected PCa men, 504 biopsy-naïve and 457 men with prior negative biopsy, in whom csPCa (GS $\geq$ 3+4) was detected in 42% and 29% respectively. These two models incorporated prebiopsy MRI, mostly multiparametric and reported by PI-RADS v1. Transrectal cognitive, software, or in bore-guided biopsies and/or 12-core systematic biopsies were performed, between 2012 and 2017, in Düsseldorf and four Dutch cities. The Rotterdam RC-3 improved its AUROC from 0.76 to 0.84 when the MRI was shared, while the RC-4 improved from 0.74 to 0.85. DCAs showed a net benefit of MRI-PM over RC-3 and RC-4 from the respective 10% and 4% csPCa risk thresholds. At 92% sensitivity, 24% of prostate biopsies were avoided in biopsy-naïve men, and at 96% sensitivity, 41% of prostate biopsies were avoided in men with prior negative prostate biopsy. Both MRI-PMs have been incorporated into the current Rotterdam MRI-RC, which has been externally validated in populations from China, Italy, and the UK [37–39]. Finally, Borque-Fernando et al. [15] developed an MRI-PM to predict csPCa (GG $\geq$ 2) in 346 men with suspected PCa, 52.8% with prior negative prostate biopsy in whom transrectal 2-core cognitive-guided biopsies to suspicious lesions and/or 12-core systematic biopsy were performed between 2015 and 2016 in Barcelona, Spain. The rate of detected csPCa was 32.6%. Age, DRE, PSAD, biopsy status, and PI-RADS v2 were the individual predictors of csPCa included in the model. The AUROC of MRI-PM was 0.88, and CUCs showed at 10% csPCa risk threshold that 30% of prostate biopsies were avoided, while 95% of csPCa were de-tected. This model was not externally validated, and no RC is available.

In 2020, Chen et al. [33] developed an MRI-PM to discriminate between low-grade PCa (GS $\leq$ 6) and high-grade (GS $\geq$ 3+4) among 257 newly diagnosed PCa between 2017 and 2019 in Wuhan, China. PCa was diagnosed after prebiopsy mpMRI and no referred type and approach of prostate biopsy. The rate of high-grade PCa was 59.2%. This PM shared serum PSA, PV, and PI-RADS v.2. The AUROC was 0.84, and the sensitivity and specificity of the greatest discriminative threshold were 79.4% and 77.6%, respectively. A median serum PSA of 51 ng/mL was noted in this development cohort. The corresponding sensitivity at 95% specificity of the model was 40%, and 19% of overdetection of low-grade PCa would be avoided. The net benefit of this MRI-PM developed was not analysed, and external validation of the designed nomogram was carried out on 57 patients in Xiangyang, China. The sensitivity to predict high-grade PCa in this validation cohort was 80%, the specificity was 77%, and the correlation between the prediction threshold and high-grade PCa was 57%. Noh et al. [34], also in 2020, developed an MRI-PM to predict csPCa (GS $\geq$ 3+4), sharing age, PSAD and bpMRI reported with PI-RADS v2 in 300 suspected PCa men, with 28.3% having a previous negative prostate biopsy, from Seoul, Korea. These men were subjected to transperineal up to 10-core software-guided prostate biopsies to PI-RADS $\geq$ 3 lesions and/or from 14 to 20-core template-prostate biopsy between 2017 and 2019. The csPCa detection rate was 34%. The AUROC of the MRI-PM model was 0.86 compared to 0.79 of the clinical predictors model. The MRI-PM resulted in a net benefit over MRI and the clinical predictors model from a 10% csPCa threshold. The 95% sensitivity threshold provided 52% specificity and avoided 30% of prostate biopsies. External validation of this MRI-PM has not been done, and no RC has been designed.

In 2021, Sakaguchi et al. [35] developed an MRI-PM in 773 biopsy-naïve men with suspected PCa recruited in a single centre in Tokyo, Japan. Pre-biopsy bpMRI was reported with PI-RADS v.2, and 2- to 4-core guided-cognitive biopsies and/or from 8- to 14-core systematic biopsies were carried out through a transrectal approach. The MRI-PM shared age, serum PSA, and PV as clinical predictors of csPCa, defined as GS $\geq$ 4+3 or maximum cancer core length $\geq$ 6 mm, and 44.3% of csPCa was detected. The AUROC of MRI alone (0.82) increased to 0.86 when MRI and clinical predictors were combined. DCAs showed a net benefit for MRI-PM over MRI from the csPCa risk threshold of 35%. At 95% sensitivity,

the MRI-PM presented 73% specificity, and 43% of prostate biopsies were avoided. This model was not externally validated, and no RC was designed.

Finally, in 2022 two new MRI-PMs have been reported. Kinnaird et al. [17] developed an MRI-PM in 2354 men with suspected PCa in whom mpMRI was reported by PI-RADS v2 and 2- to 3-core cognitive-guided biopsies and/or 12-core systematic biopsy by transrectal approach were performed between 2009 and 2019 in two centres in Los Angeles and New York, US. The rate of csPCa detected was 40%. The authors divided the po- pulation into five groups, and one of them was randomly selected for internal validation. The developed MRI-PM shared the clinical predictors, including age, DRE, biopsy status, ethnicity, serum PSA, PSAD, and PV. The AUROC of MRI-PM (0.84) outperformed that of MRI alone (0.76). DCAs evaluating the net benefit were not provided. At 95% sensiti-vity, the specificity of the MRI-PM was 56%, and 40% of prostate biopsies were avoided. External validation of this model has not been performed, and a designed RC is not currently available. Last, Morote et al. [16] designed the Barcelona RC from an MRI-PM developed in 1486 men with PSA > 3 ng/mL or abnormal DRE. The developed model was externally validated in a cohort of 946 men belonging to two centres in the same metropolitan area. The rate of csPCa, defined when GG $\geq$ 2, in the development cohort was 36.9% and 40.8% in the validation cohort. The developed model shared the independent predictors of age, PCa family history, biopsy status, DRE, serum PSA, PV, and PI-RADS v2. Prostate biopsies were performed by transrectal approach with two to four-core cognitive-guided biopsies to suspicious lesions and/or twelve-core systematic biopsy. The AUROC of MRI-PM increased that of MRI from 0.84 to 0.90 (p = 0.01) in development cohort and from 0.74 to 0.86 in validation cohort ($p < 0.001$). At the 15% csPCa threshold, 40.1% of overall biopsies would be avoided, and 95.7% of csPCa would be detected in the development cohort, while the specificity was 39.9% and 89.5% would be avoided in the validation cohort. This MRI-PM was analysed according to the PI-RADS categories for the first time. The authors concluded after this analysis that the clinical utility and net benefit of the Barcelona MRI-PM in entire developed and validation cohorts did not represent the true usefulness of the model regarding PI-RADS categories. The model's performance was low for men with PI-RADS >3, especially those with PI-RADS 5. The performance and clinical utility were greater in men with PI-RADS <3; in those men with PI-RADS 3, 61.9% and 62.3% of prostate biopsies would be avoidable in development and validation cohorts while 28.2% and 14% of the csPCa would be missed. In men with negative mpMRI (PI-RADS < 3), 4.3% and 6.5% of biopsies showed that 33.3% and 18.2% of existing csPCa would be detected in development and validation cohorts, respectively.

Many previous studies have compared baseline PMs based on clinical predictors, MRI alone, and the MRI-PM [17,21,22,26,28,29,32,34]. Other studies have compared the MRI-PM with MRI alone [15,17,25,26,32–35]. AUROCs for MRI setting alone, PM based only in clinical predictors and MRI-PMs are collected in Table 4. Net benefit was often represented by DCAs [15–17,26–33,35]. Some studies analysed the performance of MRI-PM from selected thresholds [24,28,29,32] while few studies reported CUCs, which represent the continuous probabilities of avoided prostate biopsies and missed csPCa regarding the continuous risk threshold of csPCa [15,16]. Only a single developed MRI-PM was analysed according to each PI-RADS category [16].

Table 4. AUROCs for MRI setting alone, PM based only in clinical predictors and MRI-based PMs.

		AUROC for csPCa	
Authors, Year [Ref.]	**MRI Setting Alone**	**Clinical Predictors Predictive Model**	**MRI-Based Predictive Model**
Fang et al., 2016 [21]	NA	BN: 0.85 PNPB: NA Both status: NA	BN: 0.872 PNPB: NA Both status: NA

Table 4. *Cont.*

	AUROC for csPCa		
Authors, Year [Ref.]	**MRI Setting Alone**	**Clinical Predictors Predictive Model**	**MRI-Based Predictive Model**
Kim et al., 2016 [22]	NA	BN: 0.60 PNPB: 0.63 Both status: 0.60	BN: 0.72 PNPB: 0.61 Both status: 0.69
Bjurlin et al., 2017 [23]	NA	NA	BN: 0.84 PNPB: 0.87 Both status: NA
Lee et al., 2017 [24]	NA	NA	BN: NA PNPB: NA Both status: 0.92
Niu et al., 2017 [25]	BN: 0.76 PNPB: NA Both status: NA	NA	BN: 0.85 PNPB: NA Both status: NA
Radtke et al., 2017 [26]	BN: 0.76 PNPB: 0.78 Both status: NA	BN: 0.81 PNPB: 0.66 Both status: NA	BN: 0.83 PNPB: 0.81 Both status: NA
Truong et al., 2017 [27]	NA	NA	NA
van Leeuwen et al., 2017 [28]	NA	BN: NA PNPB: NA Both status: 0.797	BN: NA PNPB: NA Both status: 0.897
Alberts et al., 2018 [29]	NA	BN: 0.76 PNPB: 0.74 Both status: NA	BN: 0.84 PNPB: 0.85 Both status: NA
Huang et al., 2018 [30]	NA	NA	BN: NA PNPB: 0.927 Both status: NA
Mehralivand et al., 2018 [31]	NA	BN: NA PNPB: NA Both status: 0.72	BN: NA PNPB: NA Both status: 0.84
Boesen et al., 2019 [32]	BN: 0.83 PNPB: NA Both status: NA	BN: 0.85 PNPB: NA Both status: NA	BN: 0.89 PNPB: NA Both status: NA
Borque et al., 2019 [15]	NA	NA	BN: NA PNPB: NA Both status: 0.856
Chen et al., 2020 [33]	0.869	NA	0.84
Noh et al., 2020 [34]	BN: 0.801 PNPB: NA Both status: NA	BN: 0.795 PNPB: NA Both status: NA	BN: 0.861 PNPB: NA Both status: NA
Sakaguchi et al., 2021 [35]	BN: 0.822 PNPB: NA Both status: NA	NA	BN: 0.862 PNPB: NA Both status: NA
Kinnaird et al., 2022 [17]	BN: NA PNPB: NA Both status: 0.760	BN: NA PNPB: NA Both status: 0.707	BN: NA PNPB: NA Both status: 0.843
Morote et al. 2022 [17]	BN: NA PNPB: NA Both status: 0.842	NA	BN: NA PNPB: NA Both status: 0.987

AUROC = area under Receiver operating characteristic curve; csPCa = clinically significant prostate cancer; MRI = magnetic resonance imaging, BN = biopsy-naïve, PNPB = previous negative prostate biopsy, NA = not available.

4. Discussion

Predictive models are the only tools providing the individualised risk of csPCa of men with suspected PCa [40]. These models have evolved and currently share MRI findings, mainly reported through PI-RADS v2, and independent clinical predictors helping clinicians improve the selection of candidates for prostate biopsy. This strategy can reduce

unnecessary prostate biopsies in uncertain scenarios beyond avoiding those in negative MRIs (PI-RADS < 3), while missing acceptable rates of csPCa according to the incidence in PI-RADS categories and its aggressiveness [13]. Almost all current MRI-PMs analysed in this systematic review have shown increased discrimination ability for csPCa than baseline models based on clinical predictors without MRI [28,31] and MRI alone [34,35].

Considerations of MRI characteristics are important since it is the weightiest predictor of csPCa [41]. Both 1.5 and 3 Tesla MRIs have been used for developing the reported MRI-PMs; however, the most recently developed models used a 3 Tesla MRI. The acquisition protocol of mpMRI included T2-weighted imaging (T2W), diffusion-weighted imaging (DWI) and dynamic contrast-enhanced (DCE) imaging [42]. In contrast, bpMRI, which avoids dynamic contrast-enhanced (DCE) imaging, is a cheaper and faster procedure than mpMRI while maintaining high diagnostic accuracy [43–45]; these were incorporated in MRI-PMs developed in high volume centres with experienced radiologists [24,32,34,35], even though comparison data between both MRI techniques in PMs is still missing. Update PI-RADS version 2 were used exclusively in eleven of the eighteen developed MRI-PMs [15–17,25,27,30–32,34,35,37]. A recent meta-analysis found higher pooled sensitivity of PI-RADSv2 over PI-RADSv1, but with similar pooled specificity [46]. In an external validation of the Radtke's MRI-PM based on PI-RADSv1 improved performance was observed when PI-RADSv1 was replaced by PI-RADSv2 [47]. However, consistent data analysing the influence of the PI-RADS version on MRI-PMs performance is lacking.

Clinical predictors incorporated in developed MRI-PMs are those with significant and independent weight to predict csPCa in logistic regression analysis [48]. Although PSA has known limitations it is still the mainstay for establishing PCa suspicion [49] and all MRI-PMs include serum PSA alone or in combination with prostate volume as PSAD [15,17,23–25,32,34]. In two of the analysed MRI-PMs [21,32], men with serum PSA levels above 50 ng/mL were excluded from the development cohort. Due to the low specificity of serum PSA between 4 and 10 ng/mL [50], Niu et al. developed an MRI-PM in patients with serum PSA in the "grey zone" in whom it could not predict csPCa. Contrarily, MRI-PM predicted csPCa efficiently in this uncertain scenario. [25]. PSAD has gained prominence since the spread of MRI, which provides the assessment of PV without additional cost and avoids the annoying and time-consuming training of urologists for transrectal ultrasonography (TRUS) [41]. Moreover, PV estimated volume by MRI either measured by ellipsoid or bullet formula has been shown to be the most accurate method compared to TRUS and DRE [51]. PSAD is the most powerful predictor of csPCa after the PI-RADS score [52]. PSAD has shown its dynamic behaviour across the PI-RADS categories, which improves its efficacy after selecting the appropriate threshold in each PI-RADS [12]. Age is related to a higher incidence and aggressiveness of PCa [53]. The Rotterdam MRI-RC and the MRI-PM developed by Boesen et al. restricted the age from 50 to 74 years, limiting clinical practice [32]. Although DRE is questioned due to the modest incremental gain of csPCa detection in men with low serum PSA [54], abnormal DRE is associated with increased detection of higher-grade tumours [55]. DRE has been commonly incorporated in developed MRI-PMs [15–17,21,22,26,28–32]. However, Niu et al. [25] and Truong et al. [27] did not include DRE in their MRI-PMs because it did not result in an independent predictor of csPCa in their logistic regression analysis. In the remaining MRI-PMs, DRE was not reported or not included in logistic regression analyses [23,24,34,35,37]. Ethnicity was only included as a predictor in three MRI-PMs [17,22,31]. In some developed MRI-PMs, ethnicity was not considered [15,23,24,26,29]; in others, it was not included as a predictor due to the low heterogenicity of race distribution, e.g. cohorts based in Asian [21,25,30,34] or Caucasian [28,32] populations. Kinnaird et al. [17] noted that Asian ethnicity predicted a reduced risk of csPCa in the American population, and this observation is consistent with the available literature [56]. Black men have been shown to have a poorer PCa prognosis and a higher risk of recurrence than white men [57]. However, a recent multiple-cohort study have seen no differences of PCa specific mortality in Black population after the adjustment of nonbiological differences [58]. Previous negative prostate biopsy is a

common occurrence in csPCa early detection. Four MRI-PMs have been developed only with biopsy-naïve men [21,25,32,35]. MRI-PMs based only on one type of biopsy status restricts their usefulness in everyday practice [21,25,27,30,32,34,35].

The biopsy scheme influence csPCa detection rate and its heterogenicity was observed in this systematic review. Between 8 to 14-core systematic prostate biopsy associated to 1 to 4-core guided biopsies was reported in nine developed MRI-PMs [15–17,23,25,30–32,35]. Some MRI-PMs did not provide information about the number of cores in guided biopsies [21,22,29]. 24- to 40-cores template biopsies and 2- to 4-core guided biopsies were reported in three developed MRI-PMs [24,26,28]; last, in one developed MRI-PM, the biopsy scheme was not reported [30], although in one it was previously described [34]. All biopsy approaches were transrectal except those using template biopsies, which used the transperineal approach [24,28,34]. Currently, studies comparing the influence of biopsy schemes on the efficacy of developed MRI-PM are lacking. Since 2021, the European Association of Urology PCa guidelines has highly recommended performing prostate biopsies using a transperineal approach due to the lower risk of infectious complications [59]. Therefore, MRI-PMs developed with biopsy schemes using the transrectal approach should be validated with the same schemes but carried out through a transperineal approach. A recent meta-analysis exhibited 86% csPCa detection rate when a transperineal approach was used against 73% when a transrectal approach [60]. The possibility of targeting biopsies to suspicious lesions detected in MRI increases the sensitivity of prostate biopsy to detect csPCa [10]. However, the Cochrane metanalysis noted the complementarity between guided and systematic biopsies [7]. All developed MRI-PMs incorporated cohorts of men in whom a cognitive approach (visual fusion between MRI and TRUS images) or software approach (MRI-TRUS fusion image with software) were performed. In one study, both types of guided biopsies and in-bore guided biopsies were performed [29]. Eight studies used exclusively cognitive guided biopsies [15–17,24,25,32,34,35], four only used software-guided biopsies [23,26,27,31] and two studies used both types of guided biopsies [22,28]. Based on the current knowledge, there is no clear benefit of software-guided biopsies over cognitive-guided biopsies, especially when experienced practitioners [61]. A recent meta-analysis regarding guided biopsies has shown similar csPCa detection rates for cognitive-guided biopsies, software-guided biopsies, and in bore-guided biopsies [62].

The definition of csPCa as the main outcome of MRI-PMs also has changed in developed MRI-PMs. In four MRI-PMs an ISUP-GG $\geq$ 2 was the used definition [15–17,32]. In eleven MRI-PMs Gleason grade 3+4 or higher was used [21–23,25–27,29–31,33,34]. Three MRI-PMs used definitions based on Gleason grade 3+4 and higher than 6–7 mm cancer core extension [24,28,35]. To our knowledge, no MRI-PM has been developed with the recommendation of the 2019 Consensus Conference on Grading Prostatic Carcinoma, which considers with poor prognosis the GG 2 tumours with cribriform differentiation or intraductal carcinoma [63]. Today, the Rotterdam RCs consider csPCa when GG > 2 or GG = 2 with cribriform differentiation or intraductal carcinoma, which was applied to RC-3 and RC-4 but not to the Rotterdam MRI-RC [39].

All included MRI-PMs use as a reference standard the histopathological findings of csPCa in the prostate biopsies. Liu et al. [64] developed a model with PI-RADSv2, PSA and PSAD for the prediction of PCa and csPCa for low and high-risk groups. In this study, histopathological findings of PCa were obtained from prostate biopsy but also from the whole prostate gland, including transurethral resection of the prostate, transurethral enucleation of the prostate and radical prostatectomy. Limitations of a PM based on a cohort of patients whose pathological specimens were obtained by a surgical approach are the exclusion of patients who underwent radiotherapy, active surveillance, watchful waiting, metastatic patients or refusal of standard of care. However, strengths could be the presence of the histology of the whole prostate gland, as prostate a biopsy may downgrade prostate cancer [65].

External validations are the key point for the extensive use of MRI-PMs in the development population. However, external validations that guarantee accurate predictions

have been made in less than half of developed MRI-PMs [16,27–29,31,33,34]. The significant difficulty of external validations of predictive models is the difference between development incidence and validation cohorts. Predictive models will overestimate csPCa likelihood when the incidence decreases and underestimate csPCa risk when the incidence increases [66]. An adjusted selection of threshold probability of csPCa might be required to sidestep this limitation [67]. Mehralivand et al. [31] validated their model in a cohort of 251 men from two independent centres. Despite a difference of about 10% in csPCa incidence between the development and validation cohort, the AUROCs were similar; however, after adjusting the probability threshold of csPCa to 20%, 38% of prostate biopsies were saved while missing 11% of csPCa. Pullen et al. [68] compared the external validation of three MRI-PMs in a cohort of 307 men. The AUROCs of the three models were similar; however, after adjusting their risk threshold, better calibration and net benefit of the Rotterdam MRI-RC were observed in biopsy-naïve men over the other two models with a worse balance between saved prostate biopsies and missed csPCa. Saba et al. [69] validated and compared three MRI-PMs [26,28,31], the Rotterdam MRI-RC [29] and the Prostate Biopsy Collaborative Group (PBCG)-RC [70] in 468 suspected PCa men, 31% with previous negative prostate biopsy, in whom transperineal 39 to 42-core template biopsy with additional 2 to 3-core software or cognitive-guided biopsies were performed between 2014 and 2018 in Zürich, Switzerland. The finding of any Gleason pattern 4 in prostate biopsy was considered csPCa. The authors concluded that MRI-PMs outperformed those models without MRI. However, the clinical net benefit was only observed when the risk threshold was not greater than 15%.

Risk calculators (RCs) are essential for the routine use of MRI-PMs because they avoid the cumbersome and time-consuming use of nomograms [38]. However, only three MRI-RCs were designed [15–17], and two of them are available [15,16]. The prestigious Rotterdam MRI-RC was validated by De Nunzio et al. [38] in a multi-centre study on 580 suspected PCa men from 12 Italian centres. Recalibration was necessary to obtain a net benefit between 20% and 80% csPCa probability threshold. More recently, Remmers et al. validated the Rotterdam MRI-RC in the PRECISION Trial population that only included biopsy-naïve men. Recalibration and adjustment of the csPCa probability threshold were also necessary to reach appropriate performance, which avoided 28% of prostate biopsies while missing 10% of csPCa when the 10% risk threshold for csPCa was used [39]. The Barcelona RC was designed from a developed MRI-PM using the same variables as the Rotterdam MRI-RC and PCa family history [16]. This new MRI-PM was produced in almost 1500 suspected PCa men in whom a 3 Tesla pre-biopsy mpMRI reported with PI-RADSv2 and the recommended by the EAU PCa guidelines scheme of guided and systematic prostate biopsy. The definition of csPCa was the same as the Rotterdam MRI-RC, as was the biopsy scheme and approach [29]. The Barcelona MRI-PM was externally validated in almost 1000 men from the same metropolitan area. The Barcelona RC was designed with the new option of selecting the threshold of csPCa risk, which offers the possibility of facilitating further external validations [16]. The Barcelona MRI-PM and RC were analysed according to the PI-RADS categories; their behaviour showed how the performance in the overall population did not reflect the performance in each PI-RADS category. Therefore, this analysis has shown the scenarios where the MRI-PM is helpful and what the optimal threshold to be used in each PI-RADS category based on the acceptable rate of missing csPCa is, according to its incidence and aggressiveness of detected tumours [16].

To summarise the synthesis of generated evidence from this systematic review, we note that MRI-PMs are the best way to individualise the risk of csPCa among men with suspected PCa. However, available MRI-RCs are essential to predict the individual csPCa risk in routine practice. Although the overall risk of bias of selected articles for this review was low, developed MRI-PMs are heterogeneous regarding the characteristics of development cohorts, the characteristics of MRIs scanners and reporting methods, the clinical predictors included in the models, the types of prostate biopsy schemes and approaches, and the definitions of csPCa. Few external validations were carried out, and recalibrations of the

model and adjustment of csPCa risk threshold were necessary when accurate predictions were made. The analysis of MRI-PMs regarding PI-RADS categories seems reasonable because clinical usefulness in overall populations does not represent the true utility in each PI-RADS. However, this analysis has only been carried out in a single MRI-PM, and, incredibly, only two RCs are currently available.

There is an emerging need for tools to improve the radiologist interpretation of MRI. Radiomics, known as the conversion of digital images into mineable high-dimensional data, which has gradually become a research focus in recent years [71]. uture developments envisage a comparison between radiomics performance and the radiologist eye [72]. There are existing algorithms that can detect suspicious lesions missed by the radiologist [73] and to distinguish accurately clinically significant lesions from indolent lesions and normal tissue in MRI [73,74]. These innovative tools identify histological grades of aggressiveness in suspicious lesions by a pixel-level label for the whole-mount histopathology, which can overstep the limitation of PMs based on biopsy histopathology. Moreover, other radiomic models have been proved to improve some aspects of the performance of PI-RADS v2 in predicting of csPCa [75–77]. Deep learning techniques might also make a difference in everyday clinical practice being used for prostate gland segmentation, increasing its speed and reducing error for suspicious lesion identification [78]. Mentioned strategies might help to improve csPCa detection by assisting guided targeted biopsies, reducing unnecessary biopsies while not missing csPCa. Radiomics will improve the future prediction of PI-RADS, and genomics will enhance the definition of csPCa [79]. The integration of big data from radiogenomics and clinical predictors using artificial intelligence algorithms will improve the prediction true csPCa. Because differences in csPCa incidence will persist among populations with suspected PCa, external validations of the generated MRI-PMs will be unresolved unless a federated network is implanted [79]. Recent appearance of this artificial intelligence algorithms create a need for validation tools such as ProstateX and the new Prostate Image: Cancer AI (PI-CAI) training (https://pi-cai.grand-challenge.org/) (accessed on 27 September 2022). This available dataset provides clinical information that could also be used for AI-based PM development. The continuous update of an MRI-RC by machine learning algorithms and feedback through the new diagnosed cases will provide the models with the evolution of attended populations, the current diagnostic approaches, and csPCa definition refinements to maintain the effectiveness of csPCa predictions [80].

5. Conclusions

MRI-PMs are the current way to individualise the risk of csPCa and improve the selection of candidates for prostate biopsy. Available RCs are essential to facilitate the routine use of MRI-PMs. External validations are needed to assure accurate predictions of csPCa in any population where a developed MRI-PM is to be accomplished. Among the recently developed MRI-PMs, few meet the appropriate requirements used in routine clinical practice. In addition, only a single MRI-PM has been analysed according to the PI-RADS categories, which seems essential to define the scenarios of clinical usefulness and the appropriate csPCa risk thresholds. Future MRI-PMs should incorporate improved methods of prediction through radiomics, better definition of csPCa through genomics, and the integration of bigdata and the generation of artificial intelligence algorithm. The key point of external validations should be resolved through the integration and feedback of generated algorithms in federated networks.

Author Contributions: Conceptualization, M.T. and J.M.; methodology, M.T. and J.M.; formal analysis, M.T., J.M.; data curation, M.T., M.C. (Miriam Campistol), A.C., L.R., M.C. (Mercè Cuadras), J.P., E.T. and J.M.; writing—original draft preparation, M.T. and J.M.; writing—review and editing, M.T., J.M., M.C. (Miriam Campistol) and E.T.; supervision, J.M. and E.T.; project administration, J.M.; funding acquisition, J.M. All authors have read and agreed to the published version of the manuscript.

Funding: This research was funded by the Instituto de Salud Carlos III (ESP), grant number PI20/01666.

Institutional Review Board Statement: Ethical review and approval were waived for this study since is based only on bibliographic research.

Informed Consent Statement: Patient consent was waived for this study since is based only on bibliographic research.

Conflicts of Interest: The authors declare no conflict of interest.

References

1. Mottet, N.; van den Bergh, R.C.N.; Briers, E.; Van den Broeck, T.; Cumberbatch, M.G.; De Santis, M.; Fanti, S.; Fossati, N.; Gandaglia, G.; Gillessen, S.; et al. EAU-EANM-ESTRO-ESUR-SIOG Guidelines on Prostate Cancer—2020 Update. Part 1: Screening, Diagnosis, and Local Treatment with Curative Intent. *Eur. Urol.* **2021**, *79*, 243–262. [CrossRef] [PubMed]
2. Drazer, M.W.; Huo, D.; Eggener, S.E. National Prostate Cancer Screening Rates after the 2012 US Preventive Services Task Force Recommendation Discouraging Prostate-Specific Antigen-Based Screening. *J. Clin. Oncol.* **2015**, *33*, 2416–2423. [CrossRef]
3. Epstein, J.I.; Egevad, L.; Amin, M.B.; Delahunt, B.; Srigley, J.R.; Humphrey, P.A. The 2014 International Society of Urological Pathology (ISUP) Consensus Conference on Gleason Grading of Prostatic Carcinoma Definition of Grading Patterns and Proposal for a New Grading System. *Am. J. Surg. Pathol.* **2016**, *40*, 244–252. [CrossRef] [PubMed]
4. Matoso, A.; Epstein, J.I. Defining Clinically Significant Prostate Cancer on the Basis of Pathological Findings. *Histopathology* **2019**, *74*, 135–145. [CrossRef] [PubMed]
5. Weinreb, J.C.; Barentsz, J.O.; Choyke, P.L.; Cornud, F.; Haider, M.A.; Macura, K.J.; Margolis, D.; Schnall, M.D.; Shtern, F.; Tempany, C.M.; et al. PI-RADS Prostate Imaging—Reporting and Data System: 2015, Version 2. *Eur. Urol.* **2016**, *69*, 16–40. [CrossRef]
6. Schoots, I.G.; Padhani, A.R.; Rouvière, O.; Barentsz, J.O.; Richenberg, J. Analysis of Magnetic Resonance Imaging-Directed Biopsy Strategies for Changing the Paradigm of Prostate Cancer Diagnosis. *Eur. Urol. Oncol.* **2020**, *3*, 32–41. [CrossRef]
7. Drost, F.J.H.; Osses, D.; Nieboer, D.; Bangma, C.H.; Steyerberg, E.W.; Roobol, M.J.; Schoots, I.G. Prostate Magnetic Resonance Imaging, with or Without Magnetic Resonance Imaging-Targeted Biopsy, and Systematic Biopsy for Detecting Prostate Cancer: A Cochrane Systematic Review and Meta-Analysis. *Eur. Urol.* **2020**, *77*, 78–94. [CrossRef]
8. Sathianathen, N.J.; Omer, A.; Harriss, E.; Davies, L.; Kasivisvanathan, V.; Punwani, S.; Moore, C.M.; Kastner, C.; Barrett, T.; Van Den Bergh, R.C.; et al. Negative Predictive Value of Multiparametric Magnetic Resonance Imaging in the Detection of Clinically Significant Prostate Cancer in the Prostate Imaging Reporting and Data System Era: A Systematic Review and Meta-Analysis. *Eur. Urol.* **2020**, *78*, 402–414. [CrossRef]
9. Moldovan, P.C.; Van den Broeck, T.; Sylvester, R.; Marconi, L.; Bellmunt, J.; van den Bergh, R.C.N.; Bolla, M.; Briers, E.; Cumberbatch, M.G.; Fossati, N.; et al. What Is the Negative Predictive Value of Multiparametric Magnetic Resonance Imaging in Excluding Prostate Cancer at Biopsy? A Systematic Review and Meta-Analysis from the European Association of Urology Prostate Cancer Guidelines Panel. *Eur. Urol.* **2017**, *72*, 250–266. [CrossRef]
10. Mazzone, E.; Stabile, A.; Pellegrino, F.; Basile, G.; Cignoli, D.; Cirulli, G.O.; Sorce, G.; Barletta, F.; Scuderi, S.; Bravi, C.A.; et al. Positive Predictive Value of Prostate Imaging Reporting and Data System Version 2 for the Detection of Clinically Significant Prostate Cancer: A Systematic Review and Meta-Analysis. *Eur. Urol. Oncol.* **2021**, *4*, 697–713. [CrossRef]
11. Becerra, M.F.; Atluri, V.S.; Bhattu, A.S.; Punnen, S. Serum and Urine Biomarkers for Detecting Clinically Significant Prostate Cancer. *Urol. Oncol. Semin. Orig. Investig.* **2021**, *39*, 686–690. [CrossRef] [PubMed]
12. Morote, J.; Celma, A.; Diaz, F.; Regis, L.; Roche, S.; Mast, R.; Semidey, M.E.; de Torres, I.M.; Planas, J.; Trilla, E. Prostatic-Specific Antigen Density Behavior According to Multiparametric Magnetic Resonance Imaging Result. *Urol. Oncol. Semin. Orig. Investig.* **2020**, *38*, 410–417. [CrossRef] [PubMed]
13. Schoots, I.G.; Roobol, M.J. Multivariate Risk Prediction Tools Including MRI for Individualized Biopsy Decision in Prostate Cancer Diagnosis: Current Status and Future Directions. *World J. Urol.* **2020**, *38*, 517–529. [CrossRef]
14. Stephenson, A.J.; Kattan, M.W. Nomograms for Prostate Cancer. *BJU Int.* **2006**, *98*, 39–46. [CrossRef]
15. Borque-Fernando, Á.; Esteban, L.M.; Celma, A.; Roche, S.; Planas, J.; Regis, L.; de Torres, I.; Semidey, M.E.; Trilla, E.; Morote, J. How to Implement Magnetic Resonance Imaging before Prostate Biopsy in Clinical Practice: Nomograms for Saving Biopsies. *World J. Urol.* **2020**, *38*, 1481–1491. [CrossRef] [PubMed]
16. Morote, J.; Borque-Fernando, A.; Triquell, M.; Celma, A.; Regis, L.; Escobar, M.; Mast, R.; de Torres, I.M.; Semidey, M.E.; Abascal, J.M.; et al. The Barcelona Predictive Model of Clinically Significant Prostate Cancer. *Cancers* **2022**, *14*, 1589. [CrossRef] [PubMed]
17. Kinnaird, A.; Brisbane, W.; Kwan, L.; Priester, A.; Chuang, R.; Barsa, D.E.; Delfin, M.; Sisk, A.; Margolis, D.; Felker, E.; et al. A Prostate Cancer Risk Calculator (PCRC-MRI): Use of Clinical and Magnetic Resonance Imaging Data to Predict Biopsy Outcome in North American Men. *Can. Urol. Assoc. J.* **2021**, *16*, 161–166. [CrossRef]
18. Shamseer, L.; Moher, D.; Clarke, M.; Ghersi, D.; Liberati, A.; Petticrew, M.; Shekelle, P.; Stewart, L.A.; Altman, D.G.; Booth, A.; et al. Preferred Reporting Items for Systematic Review and Meta-Analysis Protocols (Prisma-p) 2015: Elaboration and Explanation. *BMJ* **2015**, *349*, 1–25. [CrossRef]
19. Huang, X.; Lin, J.; Demner-Fushman, D. Evaluation of PICO as a Knowledge Representation for Clinical Questions. *AMIA Annu. Symp. Proc./AMIA Symp.* **2006**, 359–363.

20. Reitsma, J.B.; Leeflang, M.M.G.; Sterne, J.A.C.; Bossuyt, P.M.M.; Whiting, P.F.; Rutjes, A.W.S.S.; Westwood, M.E.; Mallet, S.; Deeks, J.J.; Reitsma, J.B.; et al. QUADAS-2: A Revised Tool for the Quality Assessment of Diagnostic Accuracy Studies. *Ann. Intern. Med.* **2011**, *155*, 529–536.
21. Fang, D.; Zhao, C.; Ren, D.; Yu, W.; Wang, R.; Wang, H.; Li, X.; Yin, W.; Yu, X.; Yang, K.; et al. Could Magnetic Resonance Imaging Help to Identify the Presence of Prostate Cancer Before Initial Biopsy? The Development of Nomogram Predicting the Outcomes of Prostate Biopsy in the Chinese Population. *Ann. Surg. Oncol.* **2016**, *23*, 4284–4292. [CrossRef] [PubMed]
22. Kim, E.H.; Weaver, J.K.; Shetty, A.S.; Vetter, J.M.; Andriole, G.L.; Strope, S.A. Magnetic Resonance Imaging Provides Added Value to the Prostate Cancer Prevention Trial Risk Calculator for Patients With Estimated Risk of High-Grade Prostate Cancer Less Than or Equal to 10%. *Urology* **2017**, *102*, 183–189. [CrossRef] [PubMed]
23. Bjurlin, M.A.; Rosenkrantz, A.B.; Sarkar, S.; Lepor, H.; Huang, W.C.; Huang, R.; Venkataraman, R.; Taneja, S.S. Prediction of Prostate Cancer Risk Among Men Undergoing Combined MRI-Targeted and Systematic Biopsy Using Novel Pre-Biopsy Nomograms That Incorporate MRI Findings. *Urology* **2018**, *112*, 112–120. [CrossRef] [PubMed]
24. Lee, S.M.; Liyanage, S.H.; Wulaningsih, W.; Wolfe, K.; Carr, T.; Younis, C.; van Hemelrijck, M.; Popert, R.; Acher, P. Toward an MRI-Based Nomogram for the Prediction of Transperineal Prostate Biopsy Outcome: A Physician and Patient Decision Tool. *Urol. Oncol. Semin. Orig. Investig.* **2017**, *35*, 664.e11–664.e18. [CrossRef] [PubMed]
25. Niu, X.K.; Li, J.; Das, S.K.; Xiong, Y.; Yang, C.B.; Peng, T. Developing a Nomogram Based on Multiparametric Magnetic Resonance Imaging for Forecasting High-Grade Prostate Cancer to Reduce Unnecessary Biopsies within the Prostate-Specific Antigen Gray Zone. *BMC Med. Imaging* **2017**, *17*, 1–9. [CrossRef]
26. Radtke, J.P.; Wiesenfarth, M.; Kesch, C.; Freitag, M.T.; Alt, C.D.; Celik, K.; Distler, F.; Roth, W.; Wieczorek, K.; Stock, C.; et al. Combined Clinical Parameters and Multiparametric Magnetic Resonance Imaging for Advanced Risk Modeling of Prostate Cancer—Patient-Tailored Risk Stratification Can Reduce Unnecessary Biopsies. *Eur. Urol.* **2017**, *72*, 888–896. [CrossRef]
27. Truong, M.; Wang, B.; Gordetsky, J.B.; Nix, J.W.; Frye, T.P.; Messing, E.M.; Thomas, J.V.; Feng, C.; Rais-Bahrami, S. Multi-Institutional Nomogram Predicting Benign Prostate Pathology on Magnetic Resonance/Ultrasound Fusion Biopsy in Men with a Prior Negative 12-Core Systematic Biopsy. *Cancer* **2018**, *124*, 278–285. [CrossRef]
28. Van Leeuwen, P.J.; Hayen, A.; Thompson, J.E.; Moses, D.; Shnier, R.; Böhm, M.; Abuodha, M.; Haynes, A.M.; Ting, F.; Barentsz, J.; et al. A Multiparametric Magnetic Resonance Imaging-Based Risk Model to Determine the Risk of Significant Prostate Cancer Prior to Biopsy. *BJU Int.* **2017**, *120*, 774–781. [CrossRef]
29. Alberts, A.R.; Roobol, M.J.; Verbeek, J.F.M.; Schoots, I.G.; Chiu, P.K.; Osses, D.F.; Tijsterman, J.D.; Beerlage, H.P.; Mannaerts, C.K.; Schimmöller, L.; et al. Prediction of High-Grade Prostate Cancer Following Multiparametric Magnetic Resonance Imaging: Improving the Rotterdam European Randomized Study of Screening for Prostate Cancer Risk Calculators. *Eur. Urol.* **2019**, *75*, 310–318. [CrossRef]
30. Huang, C.; Song, G.; Wang, H.; Ji, G.; Li, J.; Chen, Y.; Fan, Y.; Fang, D.; Xiong, G.; Xin, Z.; et al. MultiParametric Magnetic Resonance Imaging-Based Nomogram for Predicting Prostate Cancer and Clinically Significant Prostate Cancer in Men Undergoing Repeat Prostate Biopsy. *Biomed. Res. Int.* **2018**, *2018*. [CrossRef]
31. Mehralivand, S.; Shih, J.H.; Rais-Bahrami, S.; Oto, A.; Bednarova, S.; Nix, J.W.; Thomas, J.V.; Gordetsky, J.B.; Gaur, S.; Harmon, S.A.; et al. A Magnetic Resonance Imaging–Based Prediction Model for Prostate Biopsy Risk Stratification. *JAMA Oncol.* **2018**, *4*, 678–685. [CrossRef] [PubMed]
32. Boesen, L.; Thomsen, F.B.; Nørgaard, N.; Løgager, V.; Balslev, I.; Bisbjerg, R.; Thomsen, H.S.; Jakobsen, H. A Predictive Model Based on Biparametric Magnetic Resonance Imaging and Clinical Parameters for Improved Risk Assessment and Selection of Biopsy-Naïve Men for Prostate Biopsies. *Prostate Cancer Prostatic Dis.* **2019**, *22*, 609–616. [CrossRef] [PubMed]
33. Chen, S.; Yang, Y.; Peng, T.; Yu, X.; Deng, H.; Guo, Z. The Prediction Value of PI-RADS v2 Score in High-Grade Prostate Cancer: A Multicenter Retrospective Study. *Int. J. Med. Sci.* **2020**, *17*, 1366–1374. [CrossRef] [PubMed]
34. Noh, T.I.; Hyun, C.W.; Kang, H.E.; Jin, H.J.; Tae, J.H.; Shim, J.S.; Kang, S.G.; Sung, D.J.; Cheon, J.; Lee, J.G.; et al. A Predictive Model Based on Bi-Parametric Magnetic Resonance Imaging and Clinical Parameters for Clinically Significant Prostate Cancer in the Korean Population. *Cancer Res. Treat.* **2021**, *53*, 1148–1155. [CrossRef]
35. Sakaguchi, K.; Hayashida, M.; Tanaka, N.; Oka, S.; Urakami, S. A Risk Model for Detecting Clinically Significant Prostate Cancer Based on Bi-Parametric Magnetic Resonance Imaging in a Japanese Cohort. *Sci. Rep.* **2021**, *11*, 18829. [CrossRef]
36. Bjurlin, M.A.; Renson, A.; Rais-Bahrami, S.; Truong, M.; Rosenkrantz, A.B.; Huang, R.; Taneja, S.S. Predicting Benign Prostate Pathology on Magnetic Resonance Imaging/Ultrasound Fusion Biopsy in Men with a Prior Negative 12-Core Systematic Biopsy: External Validation of a Prognostic Nomogram. *Eur. Urol. Focus.* **2019**, *5*, 815–822. [CrossRef]
37. Chen, R.; Verbeek, J.F.M.; Yang, Y.; Song, Z.; Sun, Y.; Roobol, M.J. Comparing the Prediction of Prostate Biopsy Outcome Using the Chinese Prostate Cancer Consortium (CPCC) Risk Calculator and the Asian Adapted Rotterdam European Randomized Study of Screening for Prostate Cancer (ERSPC) Risk Calculator in Chinese and Europ. *World J. Urol.* **2021**, *39*, 73–80. [CrossRef]
38. De Nunzio, C.; Lombardo, R.; Baldassarri, V.; Cindolo, L.; Bertolo, R.; Minervini, A.; Sessa, F.; Muto, G.; Bove, P.; Vittori, M.; et al. Rotterdam Mobile Phone App Including MRI Data for the Prediction of Prostate Cancer: A Multicenter External Validation. *Eur. J. Surg. Oncol.* **2021**, *47*, 2640–2645. [CrossRef]
39. Remmers, S.; Kasivisvanathan, V.; Verbeek, J.F.M.; Moore, C.M.; Roobol, M.J. Reducing Biopsies and Magnetic Resonance Imaging Scans During the Diagnostic Pathway of Prostate Cancer: Applying the Rotterdam Prostate Cancer Risk Calculator to the PRECISION Trial Data. *Eur. Urol. Open Sci.* **2022**, *36*, 1–8. [CrossRef]

40. Louie, K.S.; Seigneurin, A.; Cathcart, P.; Sasieni, P. Do Prostate Cancer Risk Models Improve the Predictive Accuracy of PSA Screening? A Meta-Analysis. *Ann. Oncol.* **2015**, *26*, 848–864. [CrossRef]
41. Ahmed, H.U.; El-Shater Bosaily, A.; Brown, L.C.; Gabe, R.; Kaplan, R.; Parmar, M.K.; Collaco-Moraes, Y.; Ward, K.; Hindley, R.G.; Freeman, A.; et al. Diagnostic Accuracy of Multi-Parametric MRI and TRUS Biopsy in Prostate Cancer (PROMIS): A Paired Validating Confirmatory Study. *Lancet* **2017**, *389*, 815–822. [CrossRef]
42. Bjurlin, M.A.; Carroll, P.R.; Eggener, S.; Fulgham, P.F.; Margolis, D.J.; Pinto, P.A.; Rosenkrantz, A.B.; Rubenstein, J.N.; Rukstalis, D.B.; Taneja, S.S.; et al. Update of the Standard Operating Procedure on the Use of Multiparametric Magnetic Resonance Imaging for the Diagnosis, Staging and Management of Prostate Cancer. *J. Urol.* **2020**, *203*, 706–712. [CrossRef] [PubMed]
43. Sherrer, R.L.; Glaser, Z.A.; Gordetsky, J.B.; Nix, J.W.; Porter, K.K.; Rais-Bahrami, S. Comparison of Biparametric MRI to Full Multiparametric MRI for Detection of Clinically Significant Prostate Cancer. *Prostate Cancer Prostatic Dis.* **2019**, *22*, 331–336. [CrossRef] [PubMed]
44. Porter, K.K.; King, A.; Galgano, S.J.; Sherrer, R.L.; Gordetsky, J.B.; Rais-Bahrami, S. Financial Implications of Biparametric Prostate MRI. *Prostate Cancer Prostatic Dis.* **2020**, *23*, 88–93. [CrossRef] [PubMed]
45. Tamada, T.; Kido, A.; Yamamoto, A.; Takeuchi, M.; Miyaji, Y.; Moriya, T.; Sone, T. Comparison of Biparametric and Multiparametric MRI for Clinically Significant Prostate Cancer Detection With PI-RADS Version 2.1. *J. Magn. Reson. Imaging* **2021**, *53*, 283–291. [CrossRef] [PubMed]
46. Woo, S.; Suh, C.H.; Kim, S.Y.; Cho, J.Y.; Kim, S.H. Diagnostic Performance of Prostate Imaging Reporting and Data System Version 2 for Detection of Prostate Cancer: A Systematic Review and Diagnostic Meta-Analysis. *Eur. Urol.* **2017**, *72*, 177–188. [CrossRef]
47. Radtke, J.P.; Giganti, F.; Wiesenfarth, M.; Stabile, A.; Marenco, J.; Orczyk, C.; Kasivisvanathan, V.; Nyarangi-Dix, J.N.; Schütz, V.; Dieffenbacher, S.; et al. Prediction of Significant Prostate Cancer in Biopsy-Naïve Men: Validation of a Novel Risk Model Combining MRI and Clinical Parameters and Comparison to an ERSPC Risk Calculator and PI-RADS. *PLoS ONE* **2019**, *14*, e0221350. [CrossRef]
48. Osses, D.F.; Roobol, M.J.; Schoots, I.G. Prediction Medicine: Biomarkers, Risk Calculators and Magnetic Resonance Imaging as Risk Stratification Tools in Prostate Cancer Diagnosis. *Int. J. Mol. Sci.* **2019**, *20*, 1637. [CrossRef]
49. Ilic, D.; Djulbegovic, M.; Jung, J.H.; Hwang, E.C.; Zhou, Q.; Cleves, A.; Agoritsas, T.; Dahm, P. Prostate Cancer Screening with Prostate-Specific Antigen (PSA) Test: A Systematic Review and Meta-Analysis. *BMJ* **2018**, *362*, k3519. [CrossRef]
50. Vickers, A.J.; Cronin, A.M.; Roobol, M.J.; Hugosson, J.; Jones, J.S.; Clinic, C.; Kattan, M.W.; Klein, E.; Hamdy, F.; Neal, D.; et al. Cancer Risk: The Prostate Biopsy Collaborative Group. *Clin. Cancer Res.* **2011**, *16*, 4374–4381. [CrossRef]
51. Massanova, M.; Robertson, S.; Barone, B.; Dutto, L.; Caputo, V.F.; Bhatt, J.R.; Ahmad, I.; Bada, M.; Obeidallah, A.; Crocetto, F. The Comparison of Imaging and Clinical Methods to Estimate Prostate Volume: A Single-Centre Retrospective Study. *Urol. Int.* **2021**, *105*, 804–810. [CrossRef] [PubMed]
52. Nordström, T.; Akre, O.; Aly, M.; Grönberg, H.; Eklund, M. Prostate-Specific Antigen (PSA) Density in the Diagnostic Algorithm of Prostate Cancer. *Prostate Cancer Prostatic Dis.* **2018**, *21*, 57–63. [CrossRef] [PubMed]
53. Boyle, H.J.; Alibhai, S.; Decoster, L.; Efstathiou, E.; Fizazi, K.; Mottet, N.; Oudard, S.; Payne, H.; Prentice, M.; Puts, M.; et al. Updated Recommendations of the International Society of Geriatric Oncology on Prostate Cancer Management in Older Patients. *Eur. J. Cancer* **2019**, *116*, 116–136. [CrossRef] [PubMed]
54. Cui, T.; Kovell, R.C.; Terlecki, R.P. Is It Time to Abandon the Digital Rectal Examination? Lessons from the PLCO Cancer Screening Trial and Peer-Reviewed Literature. *Curr. Med. Res. Opin.* **2016**, *32*, 1663–1669. [CrossRef] [PubMed]
55. Okotie, O.T.; Roehl, K.A.; Han, M.; Loeb, S.; Gashti, S.N.; Catalona, W.J. Characteristics of Prostate Cancer Detected by Digital Rectal Examination Only. *Urology* **2007**, *70*, 1117–1120. [CrossRef]
56. Gandaglia, G.; Leni, R.; Bray, F.; Fleshner, N.; Freedland, S.J.; Kibel, A.; Stattin, P.; Van Poppel, H.; La Vecchia, C. Epidemiology and Prevention of Prostate Cancer. *Eur. Urol. Oncol.* **2021**, *4*, 877–892. [CrossRef]
57. Evans, S.; Metcalfe, C.; Ibrahim, F.; Persad, R.; Ben-Shlomo, Y. Investigating Black-White Differences in Prostate Cancer Prognosis: A Systematic Review and Meta-Analysis. *Int. J. Cancer* **2008**, *123*, 430–435. [CrossRef]
58. Dess, R.T.; Hartman, H.E.; Mahal, B.A.; Soni, P.D.; Jackson, W.C.; Cooperberg, M.R.; Amling, C.L.; Aronson, W.J.; Kane, C.J.; Terris, M.K.; et al. Association of Black Race with Prostate Cancer-Specific and Other-Cause Mortality. *JAMA Oncol.* **2019**, *5*, 975–983. [CrossRef]
59. Pradere, B.; Veeratterapillay, R.; Dimitropoulos, K.; Yuan, Y.; Omar, M.I.; MacLennan, S.; Cai, T.; Bruyère, F.; Bartoletti, R.; Köves, B.; et al. Nonantibiotic Strategies for the Prevention of Infectious Complications Following Prostate Biopsy: A Systematic Review and Meta-Analysis. *J. Urol.* **2021**, *205*, 653–663. [CrossRef]
60. Tu, X.; Liu, Z.; Chang, T.; Qiu, S.; Xu, H.; Bao, Y.; Yang, L.; Wei, Q. Transperineal Magnetic Resonance Imaging–Targeted Biopsy May Perform Better Than Transrectal Route in the Detection of Clinically Significant Prostate Cancer: Systematic Review and Meta-Analysis. *Clin. Genitourin. Cancer* **2019**, *17*, e860–e870. [CrossRef]
61. Khoo, C.C.; Eldred-Evans, D.; Peters, M.; van Son, M.; van Rossum, P.S.N.; Connor, M.J.; Hosking-Jervis, F.; Tanaka, M.B.; Reddy, D.; Bass, E.; et al. A Comparison of Prostate Cancer Detection between Visual Estimation (Cognitive Registration) and Image Fusion (Software Registration) Targeted Transperineal Prostate Biopsy. *J. Urol.* **2021**, *205*, 1075–1081. [CrossRef] [PubMed]

62. Bass, E.J.; Pantovic, A.; Connor, M.; Gabe, R.; Padhani, A.R.; Rockall, A.; Sokhi, H.; Tam, H.; Winkler, M.; Ahmed, H.U. A Systematic Review and Meta-Analysis of the Diagnostic Accuracy of Biparametric Prostate MRI for Prostate Cancer in Men at Risk. *Prostate Cancer Prostatic Dis.* **2021**, *24*, 596–611. [CrossRef] [PubMed]
63. JLH van Leenders, G.; van der Kwast, T.H.; Grignon, D.J.; Evans, A.J.; Kristiansen, G.; Kweldam, C.F.; Litjens, G.; McKenney, J.K.; Melamed, J.; Mottet, N.; et al. The 2019 International Society of Urological Pathology (ISUP) Consensus Conference on Grading of Prostatic Carcinoma. *Am. J. Surg. Pathol.* **2020**, *44*, 87–99. [CrossRef]
64. Liu, C.; Liu, S.L.; Wang, Z.X.; Yu, K.; Feng, C.X.; Ke, Z.; Wang, L.; Zeng, X.Y. Using the Prostate Imaging Reporting and Data System Version 2 (PI-RIDS v2) to Detect Prostate Cancer Can Prevent Unnecessary Biopsies and Invasive Treatment. *Asian. J. Androl.* **2018**, *20*, 459–464. [CrossRef] [PubMed]
65. Andras, I.; Cata, E.D.; Serban, A.; Kadula, P.; Telecan, T.; Buzoianu, M.; Bungardean, M.; Stanca, D.V.; Coman, I.; Crisan, N. Combined Systematic and Mri-Us Fusion Prostate Biopsy Has the Highest Grading Accuracy When Compared to Final Pathology. *Medicina* **2021**, *57*, 519. [CrossRef] [PubMed]
66. Wynants, L.; Van Smeden, M.; McLernon, D.J.; Timmerman, D.; Steyerberg, E.W.; Van Calster, B. Three Myths about Risk Thresholds for Prediction Models. *BMC Med.* **2019**, *17*, 192. [CrossRef] [PubMed]
67. Vickers, A.J.; Van Calster, B.; Steyerberg, E.W. Net Benefit Approaches to the Evaluation of Prediction Models, Molecular Markers, and Diagnostic Tests. *BMJ* **2016**, *352*, 3–7. [CrossRef]
68. Püllen, L.; Radtke, J.P.; Wiesenfarth, M.; Roobol, M.J.; Verbeek, J.F.M.; Wetter, A.; Guberina, N.; Pandey, A.; Hüttenbrink, C.; Tschirdewahn, S.; et al. External Validation of Novel Magnetic Resonance Imaging-Based Models for Prostate Cancer Prediction. *BJU Int.* **2020**, *125*, 407–416. [CrossRef]
69. Saba, K.; Wettstein, M.S.; Lieger, L.; Hötker, A.M.; Donati, O.F.; Moch, H.; Ankerst, D.P.; Poyet, C.; Sulser, T.; Eberli, D.; et al. External Validation and Comparison of Prostate Cancer Risk Calculators Incorporating Multiparametric Magnetic Resonance Imaging for Prediction of Clinically Significant Prostate Cancer. *J. Urol.* **2020**, *203*, 719–726. [CrossRef]
70. Ankerst, D.P.; Straubinger, J.; Selig, K.; Guerrios, L.; De Hoedt, A.; Hernandez, J.; Liss, M.A.; Leach, R.J.; Freedland, S.J.; Kattan, M.W.; et al. A Contemporary Prostate Biopsy Risk Calculator Based on Multiple Heterogeneous Cohorts. *Eur. Urol.* **2018**, *74*, 197–203. [CrossRef]
71. Gillies, R.J.; Kinahan, P.E.; Hricak, H. Radiomics: Images Are More than Pictures, They Are Data. *Radiology* **2016**, *278*, 563–577. [CrossRef] [PubMed]
72. Ferro, M.; de Cobelli, O.; Musi, G.; del Giudice, F.; Carrieri, G.; Busetto, G.M.; Falagario, U.G.; Sciarra, A.; Maggi, M.; Crocetto, F.; et al. Radiomics in Prostate Cancer: An up-to-Date Review. *Ther. Adv. Urol.* **2022**, 14. [CrossRef] [PubMed]
73. Seetharaman, A.; Bhattacharya, I.; Chen, L.C.; Kunder, C.A.; Shao, W.; Soerensen, S.J.C.; Wang, J.B.; Teslovich, N.C.; Fan, R.E.; Ghanouni, P.; et al. Automated Detection of Aggressive and Indolent Prostate Cancer on Magnetic Resonance Imaging. *Med. Phys.* **2021**, *48*, 2960–2972. [CrossRef] [PubMed]
74. Bhattacharya, I.; Seetharaman, A.; Kunder, C.; Shao, W.; Chen, L.C.; Soerensen, S.J.C.; Wang, J.B.; Teslovich, N.C.; Fan, R.E.; Ghanouni, P.; et al. Selective Identification and Localization of Indolent and Aggressive Prostate Cancers via CorrSigNIA: An MRI-Pathology Correlation and Deep Learning Framework: CorrSigNIA: An MRI-Pathology Correlation and Deep Learning Framework. *Med. Image Anal.* **2022**, *75*, 102288. [CrossRef] [PubMed]
75. Hou, Y.; Bao, M.L.; Wu, C.J.; Zhang, J.; Zhang, Y.D.; Shi, H. bin A Radiomics Machine Learning-Based Redefining Score Robustly Identifies Clinically Significant Prostate Cancer in Equivocal PI-RADS Score 3 Lesions. *Abdom. Radiol.* **2020**, *45*, 4223–4234. [CrossRef]
76. Brancato, V.; Aiello, M.; Basso, L.; Monti, S.; Palumbo, L.; di Costanzo, G.; Salvatore, M.; Ragozzino, A.; Cavaliere, C. Evaluation of a Multiparametric MRI Radiomic-Based Approach for Stratification of Equivocal PI-RADS 3 and Upgraded PI-RADS 4 Prostatic Lesions. *Sci. Rep.* **2021**, *11*, 643. [CrossRef]
77. Wang, J.; Wu, C.J.; Bao, M.L.; Zhang, J.; Wang, X.N.; Zhang, Y.D. Machine Learning-Based Analysis of MR Radiomics Can Help to Improve the Diagnostic Performance of PI-RADS v2 in Clinically Relevant Prostate Cancer. *Eur. Radiol.* **2017**, *27*, 4082–4090. [CrossRef]
78. Soerensen, S.J.C.; Fan, R.E.; Seetharaman, A.; Chen, L.; Shao, W.; Bhattacharya, I.; Kim, Y.H.; Sood, R.; Borre, M.; Chung, B.I.; et al. Deep Learning Improves Speed and Accuracy of Prostate Gland Segmentations on Magnetic Resonance Imaging for Targeted Biopsy. *J. Urol.* **2021**, *206*, 604–612. [CrossRef]
79. Ferro, M.; de Cobelli, O.; Vartolomei, M.D.; Lucarelli, G.; Crocetto, F.; Barone, B.; Sciarra, A.; Del Giudice, F.; Muto, M.; Maggi, M.; et al. Prostate Cancer Radiogenomics—From Imaging to Molecular Characterization. *Int. J. Mol. Sci.* **2021**, *22*, 9971. [CrossRef]
80. Zhang, Y.; Chen, W.; Yue, X.; Shen, J.; Gao, C.; Pang, P.; Cui, F.; Xu, M. Development of a Novel, Multi-Parametric, MRI-Based Radiomic Nomogram for Differentiating Between Clinically Significant and Insignificant Prostate Cancer. *Front. Oncol.* **2020**, *10*, 888. [CrossRef]

5.2. PUBLICACIÓN 2

Título: The Barcelona Predictive Model of Clinically Significant Prostate Cancer

Revista: Cancers

Año de publicación: 2022

Volumen: 14

Páginas: 1589

DOI: https://doi.org/10.3390/cancers14061589

Autores: Juan Morote, Angel Borque-Fernando, Marina Triquell, Anna Celma, Lucas Regis, Manel Escobar, Richard Mast, Inés M. de Torres, María E. Semidey, José M. Abascal, Carles Solà, Pol Servian, Daniel Salvador, Anna Santamaría, Jacques Planas, Luis M. Esteban y Enrique Trilla

Factor de impacto: 4.5 (2023)

Cuartil: Q1 (Oncología)

cancers

MDPI

Article

The Barcelona Predictive Model of Clinically Significant Prostate Cancer

Juan Morote [1,2,*,†], Angel Borque-Fernando [3,†], Marina Triquell [1,2], Anna Celma [1,2], Lucas Regis [1,2], Manel Escobar [4], Richard Mast [4], Inés M. de Torres [5,6], María E. Semidey [5,6], José M. Abascal [7], Carles Sola [7], Pol Servian [8], Daniel Salvador [8], Anna Santamaría [9], Jacques Planas [1], Luis M. Esteban [10,‡] and Enrique Trilla [1,2,‡]

[1] Department of Urology, Vall d'Hebron Hospital, 08035 Barcelona, Spain; mtriquell@vhebron.net (M.T.); acelma@vhebron.net (A.C.); lregis@vhebron.net (L.R.); jplanas@vhebron.net (J.P.); etrilla@vhebron.net (E.T.)
[2] Department of Surgery, Universitat Autònoma de Barcelona, 08193 Barcelona, Spain
[3] Department of Urology, Hospital Universitario Miguel Servet, IIS-Aragon, 50009 Zaragoza, Spain; aborque@comz.org
[4] Department of Radiology, Vall d'Hebron Hospital, 08035 Barcelona, Spain; mescobar@vhebon.net (M.E.); rmast@vhebron.net (R.M.)
[5] Department of Pathology, Vall d'Hebron Hospital, 08035 Barcelona, Spain; itorres@vhebron.net (I.M.d.T.); mesemidey@vehbron.net (M.E.S.)
[6] Department of Morphological Sciences, Universitat Autònoma de Barcelona, 08193 Barcelona, Spain
[7] Department of Urology, Parc de Salut Mar, 08003 Barcelona, Spain; jmabascalj@gmail.com (J.M.A.); csolamarques@psmar.cat (C.S.)
[8] Department of Urology, Hospital Germans Trias I Pujol, 08916 Badalona, Spain; p.serviangermanstrias@gencat.cat (P.S.); dsalvadorhidalgo@gmail.com (D.S.)
[9] Urology Research Group, Vall d'Hebron Research Institute, 08035 Barcelona, Spain; anna.santamaria@vhir.org
[10] Department of Applied Mathematics, Escuela Universitaria Politécnica La Almunia, Universidad de Zaragoza, 50100 Zaragoza, Spain; lmeste@unizar.es
* Correspondence: jmorote@vhebron.net; Tel.: +34-9327-46009
† These authors contribute equally as co-first authors.
‡ These authors contribute equally as co-last authors.

Simple Summary: Magnetic-resonance-imaging-based predictive models (MRI-PMs) improve the MRI prediction of clinically significant prostate cancer (csPCa) in prostate biopsies. Risk calculators (RC) provide easy individual assessment of csPCa likelihood. MRI-PMs have been analysed in overall populations of men suspected to have PCa, but they have never been analysed according to the prostate imaging-report and data system (PI-RADS) categories. Therefore, the true clinical usefulness of MRI-PMs regarding the specific PI-RADS categories is unknown.

Abstract: A new and externally validated MRI-PM for csPCa was developed in the metropolitan area of Barcelona, and a web-RC designed with the new option of selecting the csPCa probability threshold. The development cohort comprised 1486 men scheduled to undergo a 3-tesla multiparametric MRI (mpMRI) and guided and/or systematic biopsies in one academic institution of Barcelona. The external validation cohort comprised 946 men in whom the same diagnostic approach was carried out as in the development cohort, in two other academic institutions of the same metropolitan area. CsPCa was detected in 36.9% of men in the development cohort and 40.8% in the external validation cohort ($p = 0.054$). The area under the curve of mpMRI increased from 0.842 to 0.897 in the developed MRI-PM ($p < 0.001$), and from 0.743 to 0.858 in the external validation cohort ($p < 0.001$). A selected 15% threshold avoided 40.1% of prostate biopsies and missed 5.4% of the 36.9% csPCa detected in the development cohort. In men with PI-RADS <3, 4.3% would be biopsied and 32.3% of all existing 4.2% of csPCa would be detected. In men with PI-RADS 3, 62% of prostate biopsies would be avoided and 28% of all existing 12.4% of csPCa would be undetected. In men with PI-RADS 4, 4% of prostate biopsies would be avoided and 0.6% of all existing 43.1% of csPCa would be undetected. In men with PI-RADS 5, 0.6% of prostate biopsies would be avoided and none of the existing 42.0% of csPCa would be undetected. The Barcelona MRI-PM presented good performance on the overall population; however, its clinical usefulness varied regarding the PI-RADS category. The selection of csPCa

check for updates

Citation: Morote, J.; Borque-Fernando, A.; Triquell, M.; Celma, A.; Regis, L.; Escobar, M.; Mast, R.; de Torres, I.M.; Semidey, M.E.; Abascal, J.M.; et al. The Barcelona Predictive Model of Clinically Significant Prostate Cancer. *Cancers* **2022**, *14*, 1589. https://doi.org/10.3390/cancers14061589

Academic Editors: Ana Faustino, Paula A. Oliveira and Lúcio Lara Santos

Received: 24 February 2022
Accepted: 16 March 2022
Published: 21 March 2022

Publisher's Note: MDPI stays neutral with regard to jurisdictional claims in published maps and institutional affiliations.

probability thresholds in the designed RC may facilitate external validation and outperformance of MRI-PMs in specific PI-RADS categories.

Keywords: clinically significant prostate cancer; magnetic resonance imaging; predictive model; risk calculator

1. Introduction

Prostate cancer (PCa) suspicion is established from prostate-specific antigen (PSA) serum elevation and/or abnormal digital rectal examination (DRE), while its diagnosis is confirmed with a prostate biopsy [1]. The classic approach based on systematic biopsies results in high rates of unnecessary biopsies and overdetection of insignificant PCa (iPCa) [2]. The detection of clinically significant prostate cancer (csPCa) has improved with the use of magnetic resonance imaging (MRI) and guided biopsies [3,4]. However, that approach can improve by emploting the proper selection of prostate biopsy candidates after MRI [5,6]. For this purpose, PSA density (PSAD) [7], MRI-based predictive models (MRI-PMs) [8], and modern markers [9] have been recommended. MRI-PMs share Prostate Imaging-Report and Data System (PI-RADS) scores and additional independent predictors as PSAD [8–10]. External validation is always required before implementing any predictive model in new population [11,12]. To date, at least fifteen MRI-PMs have been developed [11–25]. In 10 of them, MRI results were reported using the latest PI-RADS versions 2.0–2.1 [11,13,19–25]; 5 of them had any external validation [20–22,24,25]; and none had any associated web or smartphone risk calculator (RC). In addition, the performance of MRI-PMs regarding the PI-RADS categories has never been analysed.

Our main objective was to design a new web-RC for csPCa likelihood, derived from a developed MRI-PM in the metropolitan area of Barcelona, Spain. The RC calculator will provide the novel option of selecting the csPCa probability threshold to facilitate future external validations and outperformances in specific PI-RADS categories. The specific objectives were: i. to develop the Barcelona MRI-PM; ii. to externally validate the developed model in a representative cohort of the Barcelona metropolitan area; iii. to design a friendly and free available web-RC with the PCa probability threshold selection allowed; and iv. to analyse the MRI-PM performance regarding PI-RADS categories in the development and external validation cohorts.

2. Materials and Methods

2.1. Development Cohort

The development cohort was formed of 1987 men with suspected PCa who had serum PSA > 3 ng/mL and/or abnormal DRE and were referred to our early PCa detection program from the primary care system. All men were scheduled for pre-biopsy multiparametric MRI (mpMRI), and thereafter, underwent guided and/or systematic biopsies from 1 to 4 weeks later, between 1 January 2016 and 31 December 2019, in one academic institution (VHH) of the metropolitan area of Barcelona, Spain. Data were collected in a prospective database according to the standards of reporting for MRI-targeted biopsy studies (START) [26]. Written consent was provided by all participants, and the institutional review board approved the project (PR/AG-317/2017). Men excluded from the study were: those undergoing 5-alpha reductase inhibitors for symptomatic benign prostatic hyperplasia; those with a previous PCa diagnosis; those with previous findings of atypical small acinar proliferation or prostate-intraepithelial neoplasia with atypia; and those with an incomplete data set. Additionally, 183 men were also excluded because mpMRI was not carried out due to technical reasons (56 due to claustrophobia, 32 due to a heart pacemaker, and 95 due to any metal prosthesis). The final development cohort comprised 1486 men (Figure 1).

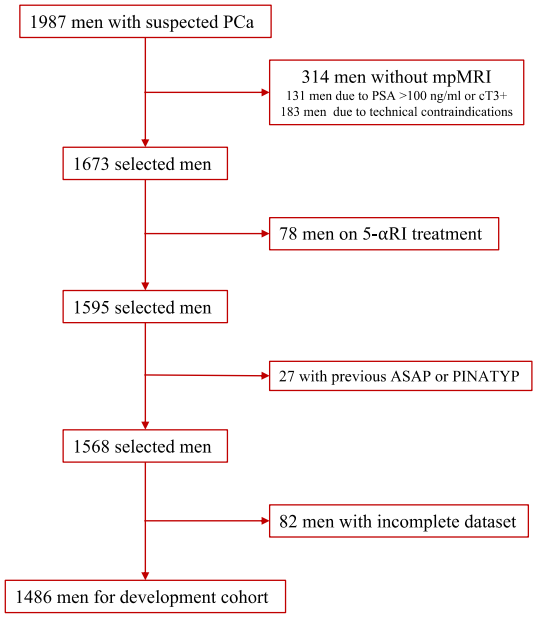

Figure 1. Flow chart of development cohort creation: inclusion and exclusion criteria.

2.2. External Validation Cohort

The external validation cohort comprised 946 men with suspected PCa who were retrospectively selected in two other academic institutions (PSM and GTIPH) and were representative of the metropolitan area of Barcelona, Spain. The criteria of PCa suspicion, the period of recruitment, and the diagnostic approach were the same as in the development cohort.

2.3. MRI Technique and Evaluation

MRI scans were acquired using a 3-tesla scanner with a standard surface phased-array coil. Magneto Trio (Siemens Corp., Erlangen, Germany) equipment was used for the development cohort and Diamond Select Achieva 3.0-TX (Phillips Corp., Eindoven, The Netherlands) and Nova Dual (Phillips Corp., Eindoven, The Netherlands) were used for the external validation cohorts. The acquisition protocol included T2-weighted imaging (T2W), diffusion-weighted imaging (DWI) and dynamic contrast-enhanced (DCE) imaging, according to the guidelines of the European Society of Urogenital Radiology. Two expert radiologists in each institution analysed images using the PI-RADSv.2.0, and in cases with multiple PI-RADS category lesions, the highest PI-RADS was selected for the model [27]. Prostate volume was assessed using MRI in all three institutions.

2.4. Prostate Biopsy Procedure

All men underwent a 2- to 4-core transrectal ultrasound (TRUS), cognitive-fusion guided biopsies for all PI-RADS > 3 lesions, and a 12-core TRUS systematic biopsy. Men with PI-RADS < 3 underwent a 12-core TRUS systematic biopsy. All biopsies were performed by one experienced urologist in each institution using the BK Focus 400 ultrasound scanner (BK Medical Inc., Herlev, Denmark) for the development cohort, and the Siemens Acuson 150 (Siemens Inc., Erlangen, Germany) and the Sonolite Antares (Siemens Inc., Erlangen, Germany) for the external validation cohort.

2.5. Pathologic Analysis and csPCa Definition

Biopsy samples were sent separately to local pathology departments, where two expert uro-pathologists analysed them, assigning them an International Society of Uro-Pathology (ISUP) grade group when PCa was detected. csPCa was defined when ISUP grade > 2 was founded [28].

2.6. Development of MRI-PM

The independent ability to predict csPCa of PI-RADSv.2.0 (1–5), age (years), ethnicity (Caucasian vs. others), serum PSA level (ng/mL), prostate volume (mL), DRE (normal vs. abnormal), PCa family history (no vs. first-degree relatives), and biopsy type (initial vs. repeat) was explored. PSAD was not directly included as a predictor because of the need for previous calculation, and due to having an area under the curve for csPCa detection of 0.892 and 0.897 when serum PSA and prostate volume were the predictors (data not shown).

2.7. Endpoint Measurements for the Performance Analysis of MRIPM

CsPCa detection rates and avoidable prostate biopsy rates.

2.8. Statistical Analysis

Descriptive statistics for the development and external validation cohorts were analysed and compared with the Chi-square and Mann–Whitney U tests. Binary logistic stepwise regression analysis of csPCa candidate predictors was performed for the model development. Continuous variables were modelled as linear or nonlinear predictors using restricted cubic splines. Calibration of the predictive model was assessed in both cohorts. Discrimination power was determined using the receiver operating characteristic (ROC) curve and the area under the curve (AUC), and clinical utility was determined using the clinical utility curve (CUC), which explored the potential rates of missed csPCa detection and avoidable prostate biopsies. The net benefit of the mpMRI- and MRI-based predictive model over biopsying all men was evaluated with a decision curve analysis (DCA). AUCs and specificities for 90% sensitivity to csPCa of the MRI and MRI-based predictive model in the development and external validation cohorts were compared with the DeLong and Chi-square tests, respectively. After selecting the threshold with 95% sensitivity to csPCa, the overall performances of the MRI and MRI-based predictive model were compared, and a sub-analysis—after stratifying by PI-RADS < 3, 3, 4 and 5—was performed. Sensitivity, specificity, positive and negative predictive values, and accuracy of rates of avoidable biopsies and potentially undetected csPCa were analysed. For the external validation, transparent reporting of a multivariable prediction model for individual prognosis or diagnosis (TRIPOD) statements were followed. Statistical analyses were computed using R programming language v.4.0.3 (The R Foundation for Statistical Computing, Vienna, Austria) and SPSS v.24 (IBM, statistical package for the social sciences, San Francisco, CA, USA).

3. Results

3.1. Characteristics of Development and External Validation Cohorts

The characteristics of development and external validation cohorts are summarised in Table 1. We noted a lower significant age and higher serum PSA in the development cohort than in the external validation cohort ($p < 0.001$). We also noted higher abnormal DRE, PCa family history, and repeat prostate biopsy rates in the external validation cohort ($p < 0.001$). The prostate volume was similar in both cohorts ($p = 0.559$). The Caucasian race was predominant in both cohorts ($p = 0.738$). Different case-mixes of PI-RADS categories existed between both cohorts ($p < 0.001$). We noted no significant increase in csPCa in the external validation cohort ($p = 0.054$), and a significant increase in iPCa ($p < 0.001$). The overall detection rate of csPCa was 36.9% in the development cohort, and regarding PI-RADS categories, 4.1% of men had PI-RADS < 3, 15.3% of men had PI-RADS 3, 52.4% of men had PI-RADS 4, and 83.4% of men had PI-RADS 5. The overall detection rate of csPCa was 40.8% in the external validation cohort, and regarding PI-RADS categories, 10.9% of

men had PI-RADS < 3, 20.4% of men had PI-RADS 3, 51.9% of men had PI-RADS 4, and 84.0% of men had PI-RADS 5.

Table 1. Characteristics of men suspected to have PCa in development and external validation cohorts and comparisons between them.

Characteristic	Development Cohort	External Validation Cohort	*p* Value
Number of men	1486	946	-
Caucasian race, *n* (%)	1465 (98.6)	931 (98.4)	0.738
Median age at biopsy (IQR), years	69 (62–74)	67 (61–72)	<0.001
Median serum PSA (IQR), ng/mL	6.0 (4.4–9.2)	7.4 (5.5–10.9)	<0.001
Abnormal DRE, *n* (%)	329 (22.1)	283 (29.9)	<0.001
PCa family history, *n* (%)	127 (8.5)	34 (3.6)	<0.001
Median prostate volume (IQR), mL	55 (40–76)	55 (40–78)	0.559
Prior negative prostate biopsy, *n* (%)	388 (26.1)	293 (31.0)	0.010
PI-RADS v.2.0, *n* (%)			
1	242 (16.3)	185 (19.6)	
2	73 (4.9)	50 (5.3)	
3	444 (29.9)	201 (21.2)	<0.001
4	450 (30.3)	391 (41.3)	
5	277 (18.6)	119 (12.6)	
PCa detection, *n* (%)	693 (46.6)	521 (55.1)	<0.001
csPCa detection, *n* (%)	548 (36.9)	386 (40.8)	0.054
iPCa detection, *n* (%)	145 (9.8)	135 (14.3)	<0.001

IQR = interquartile range; *n* = number; PSA = prostate-specific antigen; DRE = digital rectal examination; PI-RADS = Prostate Imaging-Reporting and Data System; PCa = prostate cancer; csPCa = clinically significant PCa; iPCa = insignificant PCa.

3.2. MRI-Based Predictive Model Development and Performance

Logistic regression analysis showed age, serum PSA, DRE, prostate volume, PCa family history, type of biopsy, and PI-RADSv2.0 as independent predictors of csPCa (Table 2), and a forest plot ranking the odds ratios is presented in Figure S1.

Table 2. Logistic regression analysis of independent significant predictors of csPCa in prostate biopsies.

Predictor	Odds Ratio (95% CI)	*p* Value
Age at prostate biopsy, ref. prior year	1.056 (1.036–1.077)	<0.001
Serum PSA, ref. prior ng/mL	1.085 (1.056–1.114)	<0.001
DRE, ref. normal.	1.730 (1.195–2.503)	0.004
Prostate volume, ref. prior mL	0.970 (0.964–0.977)	<0.001
Family history of PCa, ref. no	1.788 (1.066–3.002)	0.028
Biopsy type, ref. initial	0.668 (0.478–0.934)	0.018
PI-RADS v.2.0 score, 2 to ref. 1	3.311 (1.008–10.879)	0.048
3 to ref. 1	6.551 (2.740–15.661)	<0.001
4 to ref. 1	32.088 (13.660–75.377)	<0.001
5 to ref. 1	75.673 (30.738–186.311)	<0.001

CI = confidence interval; PSA = prostate-specific antigen; DRE = digital rectal examination; PI-RADSv.2 = Prostate Imaging-Reporting and Data System v.2.; ref. = referenced to.

The ROC curves of mpMRI and MRI-PM in the development cohort are presented in Figure 2A. MRI-PM exhibited a net benefit of mpMRI over biopsying all men within the threshold, with a csPCa probability of 2%. MpMRI also exhibited a net benefit over biopsying all men (Figure 2B).

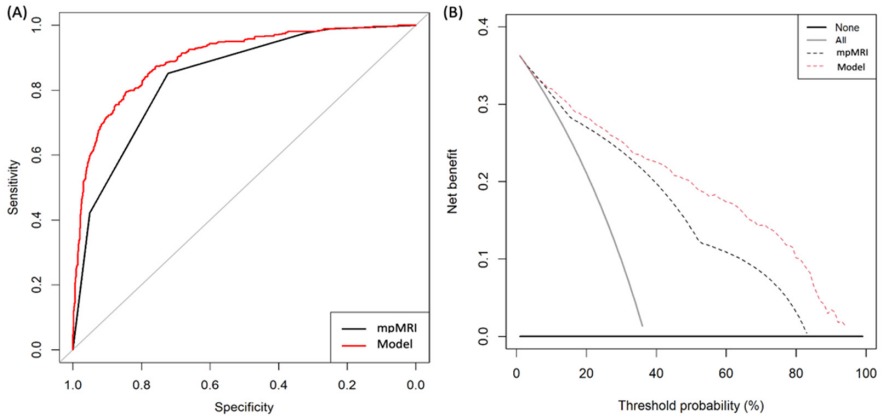

Figure 2. ROC curves showing the efficiency of MRI and MRI-PM in the development cohort (**A**). DCAs evaluating the net benefit of MRI and MRI-PM over biopsying all men belonging to the development cohort (**B**).

The AUC of the mpMRI increased from 0.842 (95% CI: 0.822–0.861) to 0.902 (95% CI: 0.880–0.914) of MRI-PM in the development cohort ($p = 0.011$). The efficacies of the mpMRI-PM were higher than those of mpMRI ($p < 0.001$) at 85%, 90%, and 95% sensitivities. At 90% sensitivity, the specificity of mpMRI was 56.8% (95% CI: 53.6–60.0) and that of MRI-PM was 69.5% (95% CI: 66.4–72.4; $p < 0.001$) (Table 3 (A)).

Table 3. Efficacy of mpMRI and MRI-based predictive model analysed from the AUCs and specificities corresponding to the 85%, 90% and 95% sensitivity thresholds for csPCa, in development cohort (A) and external validation cohort (B).

Predictor	Development Cohort (A)				External Validation Cohort (B)			
	AUC (95% CI)	Specificities According to Sensitivity			AUC (95% CI)	Specificities According to Sensitivity		
		85%	90%	95%		85%	90%	95%
mpMRI	0.842 (0.822–0.861)	72.4 (69.4–75.2%)	56.8 (53.6–60.0)	40.7 (37.5–43.9)	0.743 (0.711–0.776)	45.5 (41.3–49.7)	41.3 (32.9–48.3)	14.3 (11.6–17.5)
MRI-PM	0.897 (0.880–0.914)	78.1% (75.3–80.7)	69.5 (66.4–72.4)	55.7 (52.5–58.9)	0.858 (0.833–0.883)	67.7 (63.6–71.5)	52.3 (48.1–56.5)	32.3 (28.5–36.4)
p Value	=0.011	$p = 0.005$	<0.001	<0.001	<0.001	<0.001	<0.001	<0.001

mpMRI = multiparametric magnetic resonance imaging; MRI-PM = MRI-based predictive model; AUC = area under the curve; CI = confidence interval.

The MRI-PM derived nomogram is presented in Figure 3, and its calibration curve is presented in Figure S2A.

CUCs showing the rate of avoidable biopsies and the corresponding rate of potentially missed csPCa, regarding the continuous csPCa probability threshold, are presented in Figure 4.

Details of avoidable biopsies and the corresponding risk of missing csPCa detection, regarding the probability threshold for a development cohort of 1000 men with suspected PCa, are displayed with absolute values in Table S1 (A), and relative values in Table S2 (A). The 15% threshold was selected due to its 95% csPCa sensitivity, which corresponded with a 40% rate of avoidable biopsies. In PI-RADS 5, all csPCas would be correctly classified, and 0.5% of biopsies would be avoided. In PI-RADS 4, 0.6% of csPCas would be missed, and 4% of biopsies would be avoided. In PI-RADS 3, 28.2% of csPCa would be missed, and 61.9% of biopsies would be avoided. Finally, in PI-RADS < 3, an MRI-based predictive model would suggest biopsy in 4.3% of cases, and 33.3% of extremely infrequent csPCa in this scenario (4.2%) would be detected (Table 4 (A)). The discrimination ability of the

MRI-based predictive model regarding PI-RADS categories is shown in Figure S3A, and its net benefits over biopsying all men regarding PI-RADS are presented in Figure S4A.

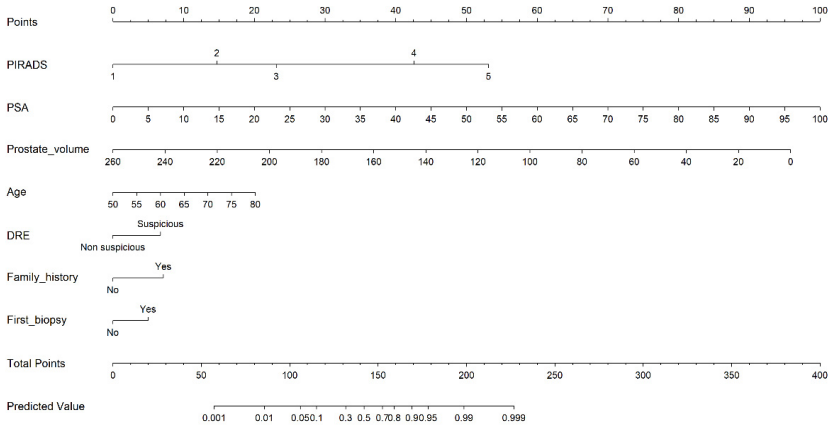

Figure 3. Nomogram derived from the developed MRI-PM model of csPCa in prostate biopsies.

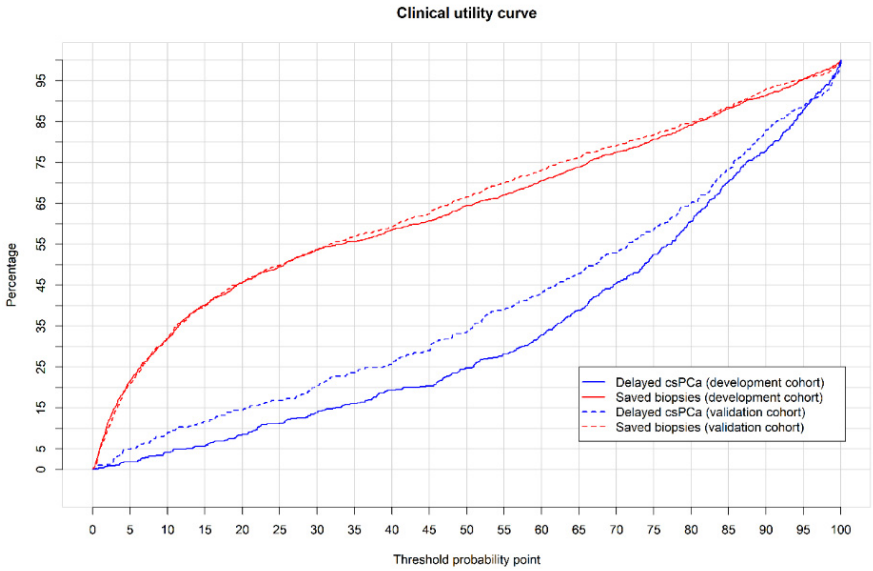

Figure 4. CUCs showing the rates of avoided biopsies (red lines) and corresponding missed csPCa (blue lines) regarding the continuous threshold of csPCa probability using MRI-PMs in development cohort (continuous lines) and external validation cohorts (interrupted lines).

3.3. External Validation of MRI-PM and Its Performance

The calibration curve of the MRI-PM shows how the nomogram slightly underestimated csPCa occurrence in the external validation cohort. For instance, for a 20% csPCa probability provided by the model (X axis), the real incidence is approximately 25%; thus, the model underestimates real csPCa occurrence. The intercept (0.261) and slope (0.815) show this disagreement, which is probably due to a 4% higher csPCa incidence (40.8 vs. 36.9%) in the cohort (Figure S2B).

Table 4. Clinical utility of MRI-based predictive model in terms of avoidable prostate biopsies and potentially missed csPCa in a 1000-sample-size development cohort (A) and external validation cohort (B), using the 15% threshold and regarding PI-RADS categories.

PI-RADS	Development Cohort (A)		External Validation Cohort (B)	
	Missed csPCa	Avoidable Biopsies	Missed csPCa	Avoidable Biopsies
1–2, *n* (%)	6/9 (66.7)	203/212 (95.7)	36/44 (81.8)	232/248 (93.5)
3, *n* (%)	13/46 (28.2)	185/299 (61.9)	6/43 (14.0)	134/212 (63.2)
4, *n* (%)	1/159 (0.6)	12/303 (4.0)	4/215 (1.9)	30/413 (7.3%)
5, *n* (%)	0/155 (0)	1/186 (0.5)	1/106 (0.9)	3/126 (2.4)
All, *n* (%)	20/369 (5.4)	401/1000 (40.1)	47/408 (11.5)	399/1000 (39.9)

The ROC curves of MRI-PM in the external validation cohort and development cohort are presented in Figure 5A and DCA, showing the net benefit of MRI-PM in both the external validation cohort and the development cohort (presented in Figure 5B, respectively). The AUC of mpMRI in the external validation cohort was 0.743 (95% CI: 0.711–0.776) compared to 0.842 (95% CI: 0.822–0.861) in the development cohort ($p < 0.001$). The AUC of MRI-PM in the external validation cohort was 0.858 (95% CI: 0.833–0.883) while it was 0.897 (95% CI: 0.880–0.914) in the development cohort ($p = 0.009$) (Table 3 (A) and (B)). At 90% sensitivity for csPCa, the specificity of MRI-PM decreased from 52.3% to 41.3% in the external validation cohort ($p < 0.001$) (Table 3 (B)).

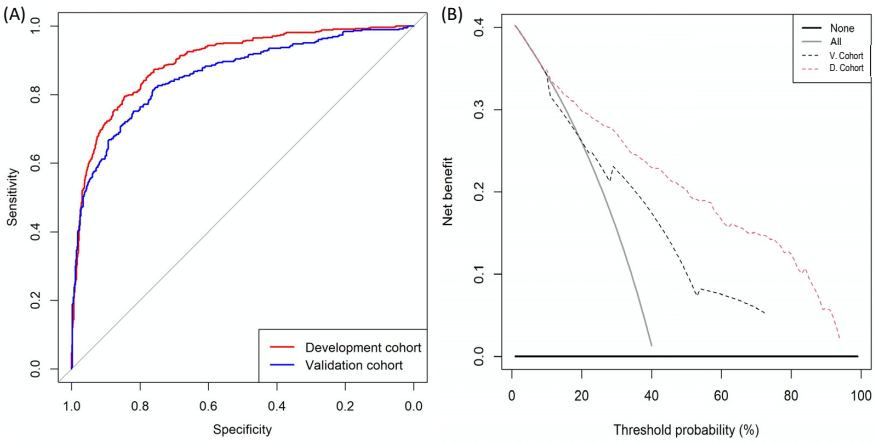

Figure 5. (**A**) ROC curves showing the efficacy of MRI-PM in development cohort and external validation cohort; (**B**) DCAs analysing the net benefit of MRI-PM in development (red interrupted line) and external validation (blue interrupted line) cohort over biopsying all men (continuous grey line).

The CUCs of MRI-PMs in the external validation cohort are presented in Figure 4, where those in the development cohort are also presented. Details of avoided prostate biopsies regarding the csPCa probability thresholds, and the corresponding risk of non-detected csPCa for an external validation cohort of 1000 men, are displayed with absolute and relative values in Tables S1 (B) and S2 (B). At the 15% threshold, MRI-PM avoided 39.9% of prostate biopsies and missed 11.5% of csPCas. In PI-RADS 5, 2.4% of prostate biopsies would be avoided and 0.9% of csPCa would be missed. In PI-RADS 4, 7.3% of prostate biopsies would be avoided and 18.6% of csPCa would be missed. In PI-RADS 3, 63.2% of prostate biopsies would be avoided and 14% of csPCas would be missed. Finally, in men with PI-RADS < 3, MRI-PM would suggest biopsying 6.5% of them, detecting 18.2% of existing csPCa (Table 4 (B)). The discrimination ability of MRI-PM regarding PI-RADS categories is shown in the ROC curves in Figure S4A, and the net benefits over biopsying all men regarding PI-RADS categories are presented in the DCA in Figure S4B.

3.4. Web-RC Design

The validated nomogram was implemented in a web-diagnostic tool using RStudio v.1.2.5001 (RStudio Team, 2015; RStudio: Integrated Development for RStudio, Inc., Boston, MA, USA; URL: http://www.rstudio.com/; accessed on 12 April 2020) and the shiny library. The designed RC incorporates the novel option of selecting the csPCa probability threshold, and it is freely available at https://mripcaprediction.shinyapps.io/MRIPCaPrediction/ (accessed on 23 November 2020).

4. Discussion

Early detection of csPCa can improve even after the spread of MRI and guided biopsies. The proper individualised selection of candidates for prostate biopsy is the current challenge [6]. The most recent MRI-PMs include the latest versions of PI-RADS as well as the prostate volume derived from MRI [11,19,20,24]. Our model was developed from PI-RADS v2.0, which was always reported from 3-tesla mpMRI. The clinical independent predictors finally included in the developed MRI-PM, without a limited range, were the age, serum PSA, and prostate volume. We aimed to design an RC covering real clinical practice in contrast with others that limit the range of these predictors [12]. Ethnicity was not part of our developed model, since it was not an independent predictor of csPCa, perhaps because only one race was prevalent in both the development and external validation cohorts, in contrast to others [16]. PSAD, which is the most powerful predictor of csPCa after PI-RADS, has undergone increased use following the spread of MRI, providing the most accurate measurement of prostate volume without the additional cost [5,6,10]. Furthermore, PSAD appears to be an ideal predictor of csPCa for MRI-PM sharing due to its dynamic behavior across PI-RADS categories [7]. PSAD can be directly incorporated into models as a ratio [11,16,17,19,23,24], or indirectly through the serum PSA and the prostate volume, which also are independent predictors of csPCa [12,13,15,18,21,25]. Due to the observation of similar odds ratios of the two ways of expressing PSAD, we used serum PSA and prostate volume to avoid any calculation before the introduction of data into the RC. PSAD has been compared with some MRI-PMs, showing good performances compared to those MRI-PMs with inadequate calibration in the external validation cohorts [29]. We also included in our MRI-PM the type of biopsy (initial or repeat), since it was also an independent predictor and it provided greater clinical applicability than MRI-PM developed exclusively in biopsy-naïve men [20,21] or in men with previous negative biopsies [13,19,23,24].

External validation of developed model is a key point. It was carried out in a cohort selected in two representative institutions of the same metropolitan area where the MRI-PM was developed, using the same criteria of suspected PCa and the same diagnostic approach to csPCa. Even so, a non-significant 4-percentage-point difference in csPCa incidence of 36.9% vs. 40.8% was observed. This was stressful for the developed model, although its ability to discriminate csPCa remained accurate in the external validation cohort only, with minimal underestimation. We selected the 15% probability threshold of csPCa from development cohort due to its 95% sensitivity and avoidance of 40% of prostate biopsies. The same threshold provided a chance of avoiding 39.9% of biopsies with an 11.5% lack of csPCa detection in the external validation cohort. The clinical utility and net benefit of developed MRI-PMs over biopsying all men with PI-RADS > 3 was low in both the development and external validation cohorts. The avoidable biopsies would be 4% in PI-RADS 4 and 0.5% in PI-RADS 5 in the development cohort, and 7.3% and 2.4%, respectively, in the external validation cohort. CsPCa would be undetected in 0.6% and 0%, and 1.9% and 0.9%, respectively, in the development and external validation cohorts. The performance and net benefit in men with PI-RADS < 3 was better. In men with PI-RADS 3, 61.9% and 62.3% of prostate biopsies would be avoided in the development and external validation cohorts, respectively, while 28.2% and 14% of the few existing csPCas would be undetected. Finally, in men with normal mpMRIs (PI-RADS < 3), 4.3% and 6.5% would be biopsied, respectively, in the developed and external validation cohorts, detecting 33.3% and 18.2% of existing csPCa, respectively. In these low and intermediate PI-RADS categories, the

absolute number of undetected csPCa is low due to the limited number of existing csPCa that did not reach rates higher than 5–10% of all detected csPCa.

External validations in populations where predictive models are going to be used are essential, and accessible and friendly RC are needed to avoid the cumbersome and time-consuming use of nomograms [11,12]. A novelty of our designed RC is the option to select the csPCa probability threshold for the overall population or according to the PI-RADS categories. The threshold can be adapted to the overall csPCa incidence of external validation populations [30]. In addition, the threshold selection can also improve the usefulness of the model in specific PI-RADS categories. For example, if we find it unacceptable that 28% of existing csPCa in men with PI-RADS 3 are not detected, we can select the csPCa probability threshold of 7%, which results in 11% of csPCa missing; however, it will result in 26% avoided prostate biopsies instead of 62%. This is the first time that the behavior of any MRI-PM for csPCa has been analysed according to the PI-RADS categories. This analysis shows that the usefulness of MRI-PM is limited in men with PI-RADS >3, and especially in men with PI-RADS 5, in whom the biopsy must be always. High PI-RADS categories exhibit high rates of csPCa; therefore, loosing small rates of csPCa, in addition to their greater aggressiveness, is dangerous [27,31–35].

We developed a new MRI-PM for csPCa and externally validated it, initially in the same metropolitan area. An accessible and friendly RC was designed for its easy and widespread use. The novelty of selecting the csPCa probability threshold may be helpful in new external validations and to modulate the desired sensitivity to csPCa in each PI-RADS category. Rather than limitations, we believe that local reporting by experienced radiologists following PI-RADS v.2 [27]; local experienced pathologists reporting ISUP grades [28]; and local experienced urologist performing biopsies according to the recommended EAU scheme [1] are strengths, because they represent real-life early detection of csPCa. We believe a true limitation of our MRI-PM is the prediction of csPCa made in prostate biopsies, which do not represent the true pathology in whole prostate gland [36]. Our model cannot be implemented in populations where ethnicity predicts different risk of csPCa. The applicability of our developed predictive model in other contemporary populations is unknown and should be evaluated in future studies; these include non-academic populations or in referred populations for prostate biopsy centers with a different case-mix of PI-RADS and csPCa incidence. Performing guided biopsies using a cognitive-fusion technique does not seem to be a limitation, since all men in the development and validation cohorts underwent the same technique, and no difference with the software fusion-guided technique has been found [37]. Further validations in cohorts in which other biopsy schemes and fusion techniques are used are needed. Finally, genomics must report a deeper understanding of PCa aggressiveness, and will help to improve the current csPCa definition. Thus, in the near future, radiomics will be able to predict the newly redefined csPCa [38].

5. Conclusions

A new MRI-PM for csPCa was developed to improve and individualise the selection of candidates for prostate biopsy in the metropolitan area of Barcelona, Spain. An associated web-RC incorporates the option to select the csPCa probability threshold, which may improve further external validations and outperformances in specific PI-RADS categories. The developed MRI-PM was able to detect 95% of existing csPCa, avoiding 40% of prostate biopsies in our overall population. However, the analysis regarding PI-RADS categories shows that the developed MRI-PM outperforms in PI-RADS < 3.

Supplementary Materials: The following supporting information can be downloaded at: https://www.mdpi.com/article/10.3390/cancers14061589/s1, Figure S1: Forest plot of the odds ratios of independent predictors of csPCa in the development cohort; Figure S2: Calibration curve of MRI-PM in development cohort (A) and external validation cohort (B); Table S1: Estimation, in a 1000-case development cohort (A) and external validation cohort (B), of absolute missed csPCa and avoided biopsies for different thresholds and PI-RADS v.2.0 categories; Table S2: Estimation, in a 1000-case development cohort (A) and validation cohort (B), of relative values of missed csPCa and avoided

biopsies for different thresholds and PI-RADS categories; Figure S3: Boxplots of the likelihoods of csPCa in men overall and regarding PI-RADS categories in development cohort (A) and external validation cohort (B); Figure S4: DCAs showing the net benefit of generated mpMRI-based predictive model over biopsying all men, according to the PI-RADS categories <3 (upper left), 3 (upper right), 4 (lower left), and 5 (lower right) in the development cohort (A), and the validation cohort (B).

Author Contributions: Conceptualization, J.M., A.B.-F. and L.M.E.; methodology, J.M., A.B.-F. and L.M.E.; software, L.M.E.; validation, L.M.E.; formal analysis, L.M.E.; investigation, J.M., A.B.-F. and L.M.E.; resources, J.M.; data curation, M.T., A.C., L.R., M.E., R.M., I.M.d.T., M.E.S., J.M.A., C.S., P.S., D.S., A.S. and J.P.; writing—original draft preparation, J.M.; writing—review and editing, J.M., A.B.-F. and L.M.E.; supervision, E.T.; project administration, J.M.; funding acquisition, J.M. All authors have read and agreed to the published version of the manuscript.

Funding: This research was funded by the Instituto de Salud Carlos III (ESP), grant number PI20/01666.

Institutional Review Board Statement: The study was conducted in accordance with the Declaration of Helsinki and approved by the Institutional Review of the Vall d´Hebron Hospital Campus (PR/AG-317/2017, approved on 28 August 2017).

Informed Consent Statement: Informed consent was obtained from all subjects involved in the study.

Data Availability Statement: The data presented in this study are available on request from the corresponding author.

Conflicts of Interest: The authors declare no conflict of interest.

References

1. Mottet, N.; van den Bergh, R.C.N.; Briesrs, E.; Briers, E.; Van den Broeck, T.; Cumberbatch, M.G.; De Santis, M.; Fanti, S.; Fossati, N.; Gandaglia, G.; et al. EAU-EANM-ESTRO-ESUR-SIOG Guidelines on Prostate Cancer-2020 Update. Part 1: Screening, Diagnosis, and Local Treatment with Curative Intent. *Eur. Urol.* **2021**, *79*, 243–262. [CrossRef] [PubMed]
2. Drazer, M.W.; Huo, D.; Eggener, S.E. National Prostate Cancer Screening Rates After the 2012 US Preventive Services Task Force Recommendation Discouraging Prostate-Specific Antigen-Based Screening. *J. Clin. Oncol.* **2015**, *33*, 2416–2423. [CrossRef] [PubMed]
3. Ahmed, H.U.; El-Shater Bosaily, A.; Brown, L.C.; Gabe, R.; Kaplan, R.; Parmar, M.K.; Collaco-Moraes, Y.; Ward, K.; Hindley, R.G.; Freeman, A.; et al. Diagnostic accuracy of multi-parametric MRI and TRUSbiopsy in prostate cancer (PROMIS): A paired validating confirmatory study. *Lancet* **2017**, *389*, 815–822. [CrossRef]
4. Schoots, I.G.; Padhani, A.R.; Rouvière, O.; Barentsz, J.O.; Richenberg, J. Analysis of Magnetic Resonance Imaging-directed Biopsy Strategies for Changing the Paradigm of Prostate Cancer Diagnosis. *Eur. Urol. Oncol.* **2020**, *3*, 32–41. [CrossRef]
5. Van Poppel, H.; Roobol, M.J.; Chapple, C.R.; Catto, J.W.F.; N'Dow, J.; Sønksen, J.; Stenzl, A.; Wirth, M. Prostate-specific Antigen Testing as Part of a Risk-Adapted Early Detection Strategy for Prostate Cancer: European Association of Urology Position and Recommendations for 2021. *Eur. Urol.* **2021**, *80*, 703–711. [CrossRef]
6. Van Poppel, H.; Hogenhout, R.; Albers, P.; van den Bergh, R.C.N.; Barentsz, J.O.; Roobol, M.J. A European Model for an Organised Risk-stratified Early Detection Programme for Prostate Cancer. *Eur. Urol. Oncol.* **2021**, *4*, 731–739. [CrossRef]
7. Morote, J.; Celma, A.; Diaz, F.; Regis, L.; Roche, S.; Mast, R.; Semidey, M.E.; de Torres, I.M.; Planas, J.; Trilla, E. Prostatic-specific antigen density behavior according to multiparametric magnetic resonance imaging result. *Urol. Oncol.* **2020**, *38*, 410–417. [CrossRef]
8. Schoots, I.G.; Roobol, M.J. Multivariate risk prediction tools including MRI for individualized biopsy decision in prostate cancer diagnosis: Current status and future directions. *World J. Urol.* **2020**, *38*, 517–529. [CrossRef]
9. Becerra, M.F.; Atluri, V.S.; Bhattu, A.S.; Punnen, S. Serum and urine biomarkers for detecting clinically significant prostate cancer. *Urol. Oncol.* **2021**, *39*, 686–690. [CrossRef]
10. Dianat, S.S.; Rancier Ruiz, R.M.; Bonekamp, D.; Carter, H.B.; Macura, K.J. Prostate volumetric assessment by magnetic resonance imaging and transrectal ultrasound: Impact of variation in calculated prostate-specific antigen density on patient eligibility for active surveillance program. *J. Comput. Assist. Tomogr.* **2013**, *37*, 589–595. [CrossRef]
11. Borque-Fernando, A.; Esteban, L.M.; Celma, A.; Regis, L.; de Torres, I.M.; Semidey, M.E.; Trilla, E.; Morote, J. How to implement magnetic resonance imaging before prostate biopsy in clinical practice: Nomograms for saving biopsies. *World J. Urol.* **2019**, *38*, 1481–1491. [CrossRef] [PubMed]
12. Alberts, A.R.; Roobol, M.J.; Verbeek, J.F.M.; Schoots, I.G.; Chiu, P.K.; Osses, D.F.; Tijsterman, J.D.; Beerlage, H.P.; Mannaerts, C.K.; Schimmöller, L.; et al. Prediction of High-grade Prostate Cancer Following Multiparametric Magnetic Resonance Imaging: Improving the Rotterdam European Randomized Study of Screening for Prostate Cancer Risk Calculators. *Eur. Urol.* **2019**, *75*, 310–318. [CrossRef] [PubMed]

13. Fang, D.; Zhao, C.; Ren, D.; Yu, W.; Wang, R.; Wang, H.; Li, X.; Yin, W.; Yu, X.; Yang, K.; et al. Could Magnetic Resonance Imaging Help to Identify the Presence of Prostate Cancer Before Initial Biopsy? The Development of Nomogram Predicting the Outcomes of Prostate Biopsy in the Chinese Population. *Ann. Surg. Oncol.* **2016**, *23*, 4284–4292. [CrossRef] [PubMed]
14. Kim, E.H.; Weaver, J.K.; Shetty, A.S.; Vetter, J.M.; Andriole, G.L.; Strope, S.A. Magnetic Resonance Imaging Provides Added Value to the Prostate Cancer Prevention Trial Risk Calculator for Patients With Estimated Risk of High-grade Prostate Cancer Less Than or Equal to 10. *Urology* **2017**, *102*, 183–189. [CrossRef]
15. Radtke, J.P.; Wiesenfarth, M.; Kesch, C.; Freitag, M.T.; Alt, C.D.; Celik, K.; Distler, F.; Roth, W.; Wieczorek, K.; Stock, C.; et al. Combined Clinical Parameters and Multiparametric Magnetic Resonance Imaging for Advanced Risk Modeling of Prostate Cancer-Patient-tailored Risk Stratification Can Reduce Unnecessary Biopsies. *Eur. Urol.* **2017**, *72*, 888–896. [CrossRef]
16. Bjurlin, M.A.; Rosenkrantz, A.B.; Sarkar, S.; Lepor, H.; Huang, W.C.; Huang, R.; Venkataraman, R.; Taneja, S. Prediction of Prostate Cancer Risk Among Men Undergoing Combined MRI-targeted and Systematic Biopsy Using Novel Pre-biopsy Nomograms That Incorporate MRI Findings. *Urology* **2018**, *112*, 112–120. [CrossRef]
17. Lee, S.M.; Liyanage, S.H.; Wulaningsih, W.; Wolfe, K.; Carr, T.; Younis, C.; Van Hemelrijck, M.; Popert, R.; Acher, P. Toward an MRI-based nomogram for the prediction of transperineal prostate biopsy outcome: A physician and patient decision tool. *Urol. Oncol.* **2017**, *35*, 66411–66418. [CrossRef]
18. Van Leeuwen, P.J.; Hayen, A.; Thompson, J.E.; James, E.; Moses, D.; Shnier, R.; Böhm, M.; Abuodha, M.; Haynes, A.M.; Ting, F.; et al. Multiparametric magnetic resonance imaging-based risk model to determine the risk of significant prostate cancer prior to biopsy. *BJU Int.* **2017**, *120*, 774–781. [CrossRef]
19. Niu, X.K.; Li, J.; Das, S.K.; Yang, C.B.; Peng, T. Developing a nomogram based on multiparametric magnetic resonance imaging for forecasting high-grade prostate cancer to reduce unnecessary biopsies within the prostate-specific antigen gray zone. *BMC Med. Imaging* **2017**, *17*, 11. [CrossRef]
20. Truong, M.; Wang, B.; Gordetsky, J.B.; Nix, J.W.; Frye, T.P.; Messing, E.M.; Thomas, J.V.; Feng, C.; Rais-Bahrami, S. Multi-institutional nomogram predicting benign prostate pathology on magnetic resonance/ultrasound fusion biopsy in men with a prior negative 12-core systematic biopsy. *Cancer* **2018**, *124*, 278–285. [CrossRef]
21. Huang, C.; Song, G.; Wang, H.; Li, J.; Chen, Y.; Fan, Y.; Fang, D.; Xiong, G.; Xin, Z.; Zhou, L. Multiparametric Magnetic Resonance Imaging-Based Nomogram for Predicting Prostate Cancer and Clinically Significant Prostate Cancer in Men Undergoing Repeat Prostate Biopsy. *Biomed. Res. Int.* **2018**, 6368309. [CrossRef]
22. Mehralivand, S.; Shih, J.H.; Rais-Bahrami, S.; Oto, A.; Bednarova, S.; Nix, J.W.; Thomas, J.V.; Gordetsky, J.B.; Gaur, S.; Harmon, S.A.; et al. A Magnetic Resonance Imaging-Based Prediction Model for Prosate Biopsy Risk Stratification. *JAMA Oncol.* **2018**, *4*, 678–685. [CrossRef] [PubMed]
23. Boesen, L.; Thomsen, F.B.; Nørgaard, N.; Løgager, V.; Balslev, I.; Bisbjerg, R.; Thomsen, H.S.; Jakobsen, H. A predictive model based on biparametric magnetic resonance imaging and clinical parameters for improved risk assessment and selection of biopsy-naïve men for prostate biopsies. *Prostate Cancer Prostatic Dis.* **2019**, *2*, 311–319. [CrossRef] [PubMed]
24. Noh, T.I.; Hyun, C.W.; Kang, H.E.; Jin, H.J.; Tae, J.H.; Shim, J.S.; Kang, S.G.; Sung, D.J.; Cheon, J.; Lee, J.G.; et al. A Predictive Model Based on Bi-parametric Magnetic Resonance Imaging and Clinical Parameters for Clinically Significant Prostate Cancer in the Korean Population. *Cancer Res. Treat.* **2021**, *53*, 1148–1155. [CrossRef]
25. Chen, I.A.; Chu, C.H.; Lin, J.T.; Tsai, J.Y.; Yu, C.C.; Sridhar, A.N.; Sooriakumaran, P.; Loureiro, R.C.V.; Chand, M. Prostate Cancer Risk Calculator Apps in a Taiwanese Population Cohort: Validation Study. *J. Med. Internet Res.* **2020**, *22*, e16322. [CrossRef]
26. Bossuyt, P.M.; Reitsma, J.B.; Bruns, D.E.; Korevaar, D.A.; STARD Group. STARD 2015: An updated list of essential items for reporting diagnostic accuracy studies. *BMJ* **2015**, *351*, h5527. [CrossRef] [PubMed]
27. Weinreb, J.C.; Barentsz, J.O.; Choyke, P.L.; Choyke, P.L.; Cornud, F.; Haider, M.A.; Macura, K.J.; Margolis, D.; Schnall, M.D.; Shtern, F.; et al. PI-RADS Prostate Imaging—Reporting and Data System: 2015, Version 2. *Eur. Urol.* **2016**, *69*, 16–40. [CrossRef]
28. Epstein, J.I.; Egevad, L.; Amin, M.B.; Delahunt, B.; Srigley, J.R.; Humphrey, P.A.; Grading Committee. The 2014 International Society of Urological Pathology (ISUP) Consensus Conference on Gleason Grading of Prostatic Carcinoma: Definition of Grading Patterns and Proposal for a New Grading System. *Am. J. Surg. Pathol.* **2016**, *40*, 244–252. [CrossRef]
29. Deniffel, D.; Healy, G.M.; Dong, X.; Ghai, S.; Salinas-Miranda, E.; Fleshner, N.; Hamilton, R.; Kulkarni, G.; Toi, A.; van der Kwast, T.; et al. Avoiding Unnecessary Biopsy: MRI-based Risk Models versus a PI-RADS and PSA Density Strategy for Clinically Significant Prostate Cancer. *Radiology* **2021**, *300*, 369–379. [CrossRef]
30. Remmers, A.; Kasivisvanathan, V.; Verbeek, J.; Moore, C.M.; Roobol, M.J.; ERSPC Rotterdam Study Group and PRECISION Investigators Group. Reducing Biopsies and Magnetic Resonance Imaging Scans During the Diagnostic Pathway of Prostate Cancer: Applying the Rotterdam Prostate Cancer Risk Calculator to the PRECISION Trial Data. *Eur. Urol. Open Sci.* **2022**, *36*, 1–8. [CrossRef]
31. Mazzone, E.; Stabile, A.; Pellegrino, F.; Basile, G.; Cignoli, D.; Cirulli, G.O.; Sorce, G.; Barletta, F.; Scuderi, S.; Bravi, C.A.; et al. Positive Predictive Value of Prostate Imaging Reporting and DataSystem Version 2 for the Detection of Clinically Significant Prostate Cancer: A Systematic Review and Meta-analysis. *Eur. Urol. Oncol.* **2020**, *4*, 697–713. [CrossRef] [PubMed]
32. Schoots, I.G. MRI in early prostate cancer detection: How to manage indeterminate or equivocal PI-RADS 3lesions. *Transl. Urol.* **2018**, *7*, 70–82. [CrossRef] [PubMed]
33. Osses, D.F.; Roobol, M.J.; Schoots, I.G. Prediction Medicine: Biomarkers, Risk Calculators and Magnetic Resonance Imaging as Risk Stratification Tools in Prostate Cancer Diagnosis. *Int. J. Mol. Sci.* **2019**, *20*, 1637. [CrossRef] [PubMed]

34. Abreu-Gomez, J.; Wu, M.; McInnes, M.D.F.; Thornhill, R.E.; Flood, T.A.; Schieda, N. Shape Analysis of Peripheral Zone Observations on Prostate DWI: Correlation to Histopathology Outcomes After Radical Prostatectomy. *AJR. Am. J. Roentgenol.* **2020**, *214*, 1239–1247. [CrossRef]
35. Boschheidgen, M.; Schimmöller, L.; Arsov, C.; Ziayee, F.; Morawitz, J.; Valentin, B.; Radke, K.L.; Giessing, M.; Esposito, I.; Albers, P.; et al. MRI grading for the prediction of prostate cancer aggressiveness. *Eur. Radiol.* **2021**, *32*, 2351–2359. [CrossRef] [PubMed]
36. Rapisarda, S.; Bada, M.; Crocetto, F.; Barone, B.; Arcaniolo, D.; Polara, A.; Imbimbo, C.; Grosso, G. The role of multiparametric resonance and biopsy in prostate cancer detection: Comparison with definitive histological report after laparoscopic/robotic radical prostatectomy. *Abdom. Radiol.* **2020**, *45*, 4178–4184. [CrossRef] [PubMed]
37. Khoo, C.; Eldred-Evans, D.; Peters, M.; van Son, M.; van Rossum, P.S.N.; Connor, M.J.; Hosking-Jervis, F.; Tanaka, M.B.; Reddy, D.; Bass, E.; et al. Comparison of Prostate Cancer Detection between Visual Estimation (Cognitive Registration) and Image Fusion (Software Registration) Targeted Transperineal Prostate Biopsy. *J. Urol.* **2021**, *205*, 1075–10781. [CrossRef] [PubMed]
38. Ferro, M.; de Cobelli, O.; Vartolomei, M.D.; Lucarelli, G.; Crocetto, F.; Barone, B.; Sciarra, A.; Del Giudice, F.; Muto, M.; Maggi, M.; et al. Prostate Cancer Radiogenomics-From Imaging to Molecular Characterization. *Int. J. Mol. Sci.* **2021**, *22*, 9971. [CrossRef]

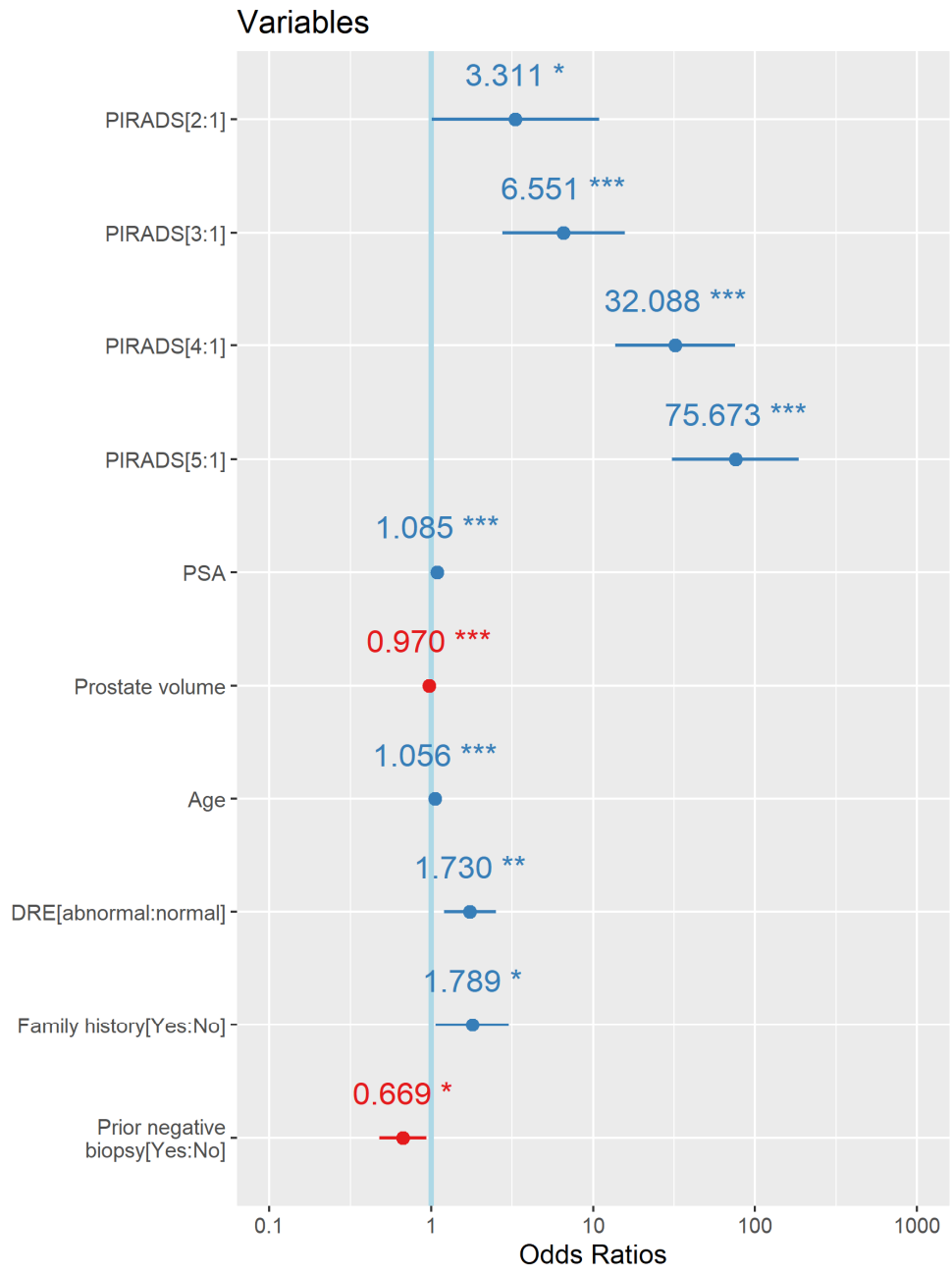

Figure S1. Forest plot of the odds ratios of independent predictors of csPCa included in the development cohort. PI-RADS = Prostate Imaging-Reporting and Data System; PSA = prostate-specific antigen; DRE = digital rectal examination; *p = 0.05, **p = 0.01, ***p < 0.001

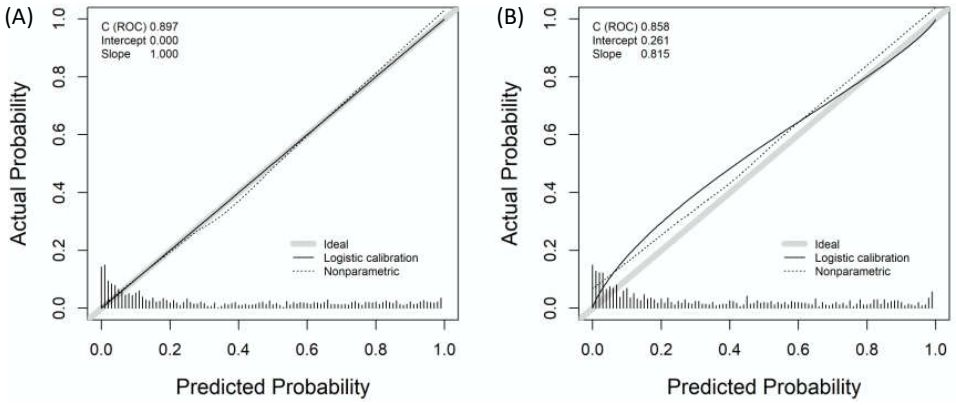

Figure S2. Calibration curve of MRI-PM in development cohort (**A**), and external validation cohort (**B**).

Table S1. Estimation, in a 1000 cases development (A) and external validation (B) cohorts of absolute missed csPCa and avoided biopsies for different thresholds and PI-RADS categories.

Series	DEVELOPMENT COHORT (A)										VALIDATION COHORT (B)									
Group	PIRADS 1-2		PIRADS 3		PIRADS 4		PIRADS 5		Global cohort		PIRADS 1-2		PIRADS 3		PIRADS 4		PIRADS 5		Global cohort	
Cases	*csPC* 9	*total* 212	*csPC* 46	*total* 299	*csPC* 159	*total* 303	*csPC* 155	*total* 186	*csPC* 369	*total* 1000	*csPC* 44	*total* 248	*csPC* 43	*total* 212	*csPC* 215	*total* 413	*csPC* 106	*total* 126	*csPC* 408	*total* 999
Cut-off point	Missed csPC (n)	Avoided Bx (n)	Missed csPC (n)	Avoided Bx (n)	Missed csPC (n)	Avoided Bx (n)	Missed csPC (n)	Avoided Bx (n)	Missed csPC (n)	Avoided Bx (n)	Missed csPC (n)	Avoided Bx (n)	Missed csPC (n)	Avoided Bx (n)	Missed csPC (n)	Avoided Bx (n)	Missed csPC (n)	Avoided Bx (n)	Missed csPC (n)	Avoided Bx (n)
0	0	0	0	0	0	0	0	0	0	0	0	0	0	0	0	0	0	0	0	0
1	1	47	0	9	0	0	0	0	1	56	3	45	0	6	0	0	1	1	4	52
2	3	99	0	15	0	1	0	0	3	115	4	86	0	11	0	0	1	2	5	99
3	3	131	0	20	0	1	0	0	3	152	10	119	1	18	0	2	1	2	12	141
4	5	151	1	33	0	1	0	0	6	185	14	151	2	26	1	5	1	2	18	184
5	5	164	1	51	0	1	0	0	6	216	15	162	3	37	1	7	1	2	20	208
6	5	174	1	64	0	3	0	0	6	241	18	181	3	44	1	7	1	2	23	234
7	5	182	5	79	0	3	0	0	10	264	20	191	4	57	1	8	1	2	26	258
8	5	187	7	92	0	3	0	0	12	282	23	202	4	71	1	13	1	2	29	288
9	5	192	7	106	0	4	0	0	12	302	26	207	4	78	1	14	1	2	32	301
10	5	194	9	118	1	7	0	0	15	319	30	216	4	89	1	16	1	2	36	323
11	5	196	11	136	1	8	0	1	17	341	32	224	5	101	1	18	1	3	39	346
12	5	199	11	153	1	11	0	1	17	364	33	225	6	111	2	20	1	3	42	359
13	6	201	11	167	1	11	0	1	18	380	34	226	6	123	2	25	1	3	43	377
14	6	202	13	177	1	11	0	1	20	391	35	228	6	131	3	26	1	3	45	388
15	6	203	13	185	1	12	0	1	20	401	36	232	6	134	4	30	1	3	47	399
16	7	205	15	196	1	13	1	1	24	415	36	234	8	142	4	37	1	3	49	416
17	7	206	16	202	2	15	1	1	26	424	38	236	10	146	4	42	1	3	53	427
18	7	206	16	208	3	17	1	2	27	433	39	239	13	151	4	47	1	3	57	440
19	7	207	16	216	3	22	1	2	27	447	40	240	14	155	4	52	1	3	59	450
20	7	207	20	223	3	25	1	2	31	457	40	240	14	159	4	55	1	3	59	457
21	7	207	21	229	4	26	1	3	33	465	40	240	16	164	5	61	1	3	62	468
22	7	208	24	236	4	29	1	3	36	476	40	240	16	167	6	64	1	3	63	474
23	7	209	27	241	5	31	1	3	40	484	40	241	18	173	7	70	1	3	66	487
24	7	209	27	242	5	34	1	3	40	488	40	241	19	177	8	74	1	3	68	495
25	7	209	28	248	5	36	1	3	41	496	40	242	19	177	8	77	1	3	68	499
26	7	209	31	258	5	39	1	3	44	509	41	243	19	177	10	85	1	3	71	508
27	7	209	31	261	6	44	1	3	45	517	41	244	19	180	10	87	1	3	71	514
28	8	210	31	263	6	46	1	3	46	522	41	244	20	183	13	94	1	3	75	524
29	8	210	32	266	7	50	1	3	48	529	41	244	21	185	15	98	1	3	78	530
30	8	210	33	268	9	57	1	3	51	538	41	244	23	188	17	100	1	3	82	535
31	8	211	35	271	9	59	1	3	53	544	41	244	29	193	17	104	1	3	88	544
32	8	211	36	272	9	61	1	3	54	547	42	245	31	196	19	109	1	3	93	553
33	8	211	36	273	11	63	1	3	56	550	42	245	31	199	19	111	1	3	93	558
34	8	211	37	277	12	65	1	3	58	556	42	245	31	199	21	115	1	4	95	563
35	8	211	37	277	13	66	1	3	59	557	42	245	32	200	21	118	1	4	96	567
36	8	211	38	279	13	67	1	3	60	560	42	246	34	202	23	123	1	4	100	575
37	8	211	40	281	13	71	1	3	62	566	42	246	34	202	24	126	1	4	101	578
38	8	211	41	283	16	74	1	3	66	571	42	246	34	202	24	130	1	4	101	582
39	8	211	43	285	17	79	1	3	69	578	42	246	34	202	25	135	1	4	102	587
40	8	211	43	285	19	86	1	3	71	585	42	246	36	204	26	137	1	5	105	592
41	8	211	43	285	20	90	1	3	72	589	42	246	38	206	30	145	1	5	111	602
42	8	211	43	285	22	93	1	4	74	593	42	246	38	207	33	152	1	5	114	610
43	8	211	43	286	22	98	1	4	74	599	43	247	38	207	34	158	1	5	116	617
44	8	211	43	287	22	101	1	4	74	603	43	247	38	207	34	160	1	5	116	619
45	8	211	43	288	23	104	1	4	75	607	43	247	38	207	36	164	1	5	118	623
46	8	211	43	289	26	109	1	4	78	613	43	247	39	208	44	178	1	5	127	638
47	8	211	43	289	28	114	3	6	82	620	43	247	39	208	45	182	1	6	128	643
48	8	211	43	289	32	123	3	6	86	629	43	247	39	208	47	187	2	7	131	649
49	8	211	43	289	34	129	3	6	88	635	44	248	39	208	50	196	2	7	135	659

50	8	211	43	289	36	137	4	7	91	644	44	248	39	208	52	202	2	7	137	665
51	8	211	43	289	39	142	4	7	94	649	44	248	39	208	59	209	2	7	144	672
52	8	211	43	290	43	147	5	7	99	655	44	248	39	208	63	216	2	7	148	679
53	8	211	44	291	44	150	5	7	101	659	44	248	39	208	69	223	2	8	154	687
54	8	211	44	291	44	151	5	7	101	660	44	248	39	208	71	226	3	10	157	692
55	8	211	44	293	48	159	5	7	105	670	44	248	39	208	72	232	4	12	159	700
56	8	211	44	293	49	164	5	8	106	676	44	248	39	208	74	237	4	12	161	705
57	8	211	44	293	53	170	5	9	110	683	44	248	39	208	77	243	5	13	165	712
58	8	211	44	294	55	175	5	9	112	689	44	248	39	208	79	247	5	13	167	716
59	8	211	44	294	59	180	5	12	116	697	44	248	39	208	84	255	6	14	173	725
60	8	211	44	295	63	186	5	12	120	704	44	248	39	208	87	262	6	14	176	732
61	8	211	45	296	66	190	7	15	126	712	44	248	40	209	89	266	7	16	180	739
62	8	211	45	296	70	194	7	15	130	716	44	248	41	210	92	272	7	16	184	746
63	8	211	45	296	73	199	9	20	135	726	44	248	41	210	93	275	10	19	188	752
64	8	211	46	297	77	204	9	21	140	733	44	248	41	210	97	280	10	19	192	757
65	8	211	46	297	79	209	10	22	143	739	44	248	41	210	99	282	11	21	195	761
66	8	211	46	297	83	215	10	24	147	747	44	248	41	210	107	294	11	21	203	773
67	8	211	46	297	91	224	11	26	156	758	44	248	41	210	107	295	12	22	204	775
68	8	211	46	297	94	229	11	26	159	763	44	248	41	210	113	301	13	23	211	782
69	8	211	46	297	97	232	12	28	163	768	44	248	41	210	115	303	14	25	214	786
70	8	211	46	297	100	236	14	30	168	774	44	248	41	210	116	307	14	25	215	790
71	8	211	46	297	104	240	14	31	172	779	44	248	41	210	121	312	14	25	220	795
72	8	211	46	297	106	244	15	32	175	784	44	248	41	210	126	317	15	27	226	802
73	8	211	46	298	108	248	15	32	177	789	44	248	41	210	129	320	16	29	230	807
74	8	211	46	298	114	253	18	35	186	797	44	248	41	210	134	326	17	30	236	814
75	8	211	46	298	120	260	20	38	194	807	44	248	41	210	136	329	17	30	238	817
76	8	211	46	298	122	264	23	40	199	813	44	248	41	210	140	334	20	34	245	826
77	8	211	46	298	124	266	24	42	202	817	44	248	41	210	142	336	20	34	247	828
78	8	211	46	298	128	271	28	46	210	826	44	248	41	210	144	338	23	37	252	833
79	8	211	46	298	132	275	30	49	216	833	44	248	42	211	150	346	25	39	261	844
80	8	211	46	298	135	279	34	53	223	841	44	248	42	211	153	349	26	40	265	848
81	8	211	46	298	138	282	40	59	232	850	44	248	42	211	155	351	27	42	268	852
82	8	211	46	298	140	284	43	62	237	855	44	248	42	211	161	356	27	42	274	857
83	8	211	46	298	141	285	50	69	245	863	44	248	42	211	166	362	32	48	284	869
84	8	211	46	298	143	287	55	77	252	873	44	248	42	211	174	370	33	50	293	879
85	8	211	46	298	145	289	61	83	260	881	44	248	42	211	177	372	36	53	299	884
86	8	211	46	298	146	290	66	89	266	888	44	248	42	211	178	373	44	62	308	894
87	8	211	46	298	147	291	74	98	275	898	44	248	42	211	180	376	48	66	314	901
88	8	211	46	298	148	292	77	102	279	903	44	248	42	211	182	378	54	72	322	909
89	8	211	46	298	148	292	81	106	283	907	44	248	42	211	184	382	59	78	329	919
90	8	211	46	298	149	293	84	111	287	913	44	248	42	211	188	386	63	84	337	929
91	9	212	46	298	150	294	90	118	295	922	44	248	42	211	191	389	68	88	345	936
92	9	212	46	298	150	294	96	123	301	927	44	248	42	211	192	390	70	90	348	939
93	9	212	46	298	150	294	102	129	307	933	44	248	42	211	192	390	75	95	353	944
94	9	212	46	298	151	295	109	137	315	942	44	248	42	211	195	392	77	97	358	948
95	9	212	46	298	152	296	117	147	324	953	44	248	42	211	196	393	79	99	361	951
96	9	212	46	298	153	297	124	155	332	962	44	248	42	211	198	395	85	105	369	959
97	9	212	46	298	153	297	132	162	340	969	44	248	42	211	199	396	87	107	372	962
98	9	212	46	299	154	298	138	168	347	977	44	248	42	211	202	400	88	108	376	967
99	9	212	46	299	156	300	144	175	355	986	44	248	42	211	208	406	94	114	388	979
100	9	212	46	299	159	303	155	186	369	1000	44	248	43	212	215	413	106	126	408	999

Table S2. Estimation, in a 1000 cases development (A) and external validation (B) cohorts of relative values of missed csPCa and avoided biopsies for different thresholds and PI-RAD categories.

Series	DEVELOPMENT COHORT										VALIDATION COHORT									
Group	PIRADS 1-2		PIRADS 3		PIRADS 4		PIRADS 5		Global cohort		PIRADS 1-2		PIRADS 3		PIRADS 4		PIRADS 5		Global cohort	
Cases	*csPC* 9	*total* 212	*csPC* 46	*total* 299	*csPC* 159	*total* 303	*csPC* 155	*total* 186	*csPC* 369	*total* 1000	*csPC* 44	*total* 248	*csPC* 43	*total* 212	*csPC* 215	*total* 413	*csPC* 106	*total* 126	*csPC* 408	*total* 999
Cut-off point	Missed csPC (%)	Avoided Bx (%)	Missed csPC (%)	Avoided Bx (%)	Missed csPC (%)	Avoided Bx (%)	Missed csPC (%)	Avoided Bx (%)	Missed csPC (%)	Avoided Bx (%)	Missed csPC (%)	Avoided Bx (%)	Missed csPC (%)	Avoided Bx (%)	Missed csPC (%)	Avoided Bx (%)	Missed csPC (%)	Avoided Bx (%)	Missed csPC (%)	Avoided Bx (%)
0	0	0	0	0	0	0	0	0	**0**	**0**	0	0	0	0	0	0	0	0	**0**	**0**
1	11	22	0	3	0	0	0	0	**0**	**6**	7	18	0	3	0	0	1	1	**1**	**5**
2	33	47	0	5	0	0	0	0	**1**	**12**	9	35	0	5	0	0	1	2	**1**	**10**
3	33	62	0	7	0	0	0	0	**1**	**15**	23	48	2	8	0	0	1	2	**3**	**14**
4	56	71	2	11	0	0	0	0	**2**	**19**	32	61	5	12	0	1	1	2	**4**	**18**
5	56	77	2	17	0	0	0	0	**2**	**22**	34	65	7	17	0	2	1	2	**5**	**21**
6	56	82	2	21	0	1	0	0	**2**	**24**	41	73	7	21	0	2	1	2	**6**	**23**
7	56	86	11	26	0	1	0	0	**3**	**26**	45	77	9	27	0	2	1	2	**6**	**26**
8	56	88	15	31	0	1	0	0	**3**	**28**	52	81	9	33	0	3	1	2	**7**	**29**
9	56	91	15	35	0	1	0	0	**3**	**30**	59	83	9	37	0	3	1	2	**8**	**30**
10	56	92	20	39	1	2	0	0	**4**	**32**	68	87	9	42	0	4	1	2	**9**	**32**
11	56	92	24	45	1	3	0	1	**5**	**34**	73	90	12	48	0	4	1	2	**10**	**35**
12	56	94	24	51	1	4	0	1	**5**	**36**	75	91	14	52	1	5	1	2	**10**	**36**
13	67	95	24	56	1	4	0	1	**5**	**38**	77	91	14	58	1	6	1	2	**11**	**38**
14	67	95	28	59	1	4	0	1	**5**	**39**	80	92	14	62	1	6	1	2	**11**	**39**
15	67	96	28	62	1	4	0	1	**5**	**40**	82	94	14	63	2	7	1	2	**12**	**40**
16	78	97	33	66	1	4	1	1	**7**	**42**	82	94	19	67	2	9	1	2	**12**	**42**
17	78	97	35	68	1	5	1	1	**7**	**42**	86	95	23	69	2	10	1	2	**13**	**43**
18	78	97	35	70	2	6	1	1	**7**	**43**	89	96	30	71	2	11	1	2	**14**	**44**
19	78	98	35	72	2	7	1	1	**7**	**45**	91	97	33	73	2	13	1	2	**14**	**45**
20	78	98	43	75	2	8	1	1	**8**	**46**	91	97	33	75	2	13	1	2	**14**	**46**
21	78	98	46	77	3	9	1	2	**9**	**47**	91	97	37	77	2	15	1	2	**15**	**47**
22	78	98	52	79	3	10	1	2	**10**	**48**	91	97	37	79	3	15	1	2	**15**	**47**
23	78	99	59	81	3	10	1	2	**11**	**48**	91	97	42	82	3	17	1	2	**16**	**49**
24	78	99	59	81	3	11	1	2	**11**	**49**	91	97	44	83	4	18	1	2	**17**	**50**
25	78	99	61	83	3	12	1	2	**11**	**50**	91	98	44	83	4	19	1	2	**17**	**50**
26	78	99	67	86	3	13	1	2	**12**	**51**	93	98	44	83	5	21	1	2	**17**	**51**
27	78	99	67	87	4	15	1	2	**12**	**52**	93	98	44	85	5	21	1	2	**17**	**51**
28	89	99	67	88	4	15	1	2	**12**	**52**	93	98	47	86	6	23	1	2	**18**	**52**
29	89	99	70	89	4	17	1	2	**13**	**53**	93	98	49	87	7	24	1	2	**19**	**53**
30	89	99	72	90	6	19	1	2	**14**	**54**	93	98	53	89	8	24	1	2	**20**	**54**
31	89	100	76	91	6	19	1	2	**14**	**54**	93	98	67	91	8	25	1	2	**22**	**54**
32	89	100	78	91	6	20	1	2	**15**	**55**	95	99	72	92	9	26	1	2	**23**	**55**
33	89	100	78	91	7	21	1	2	**15**	**55**	95	99	72	94	9	27	1	2	**23**	**56**
34	89	100	80	93	8	21	1	2	**16**	**56**	95	99	72	94	10	28	1	3	**23**	**56**
35	89	100	80	93	8	22	1	2	**16**	**56**	95	99	74	94	10	29	1	3	**24**	**57**
36	89	100	83	93	8	22	1	2	**16**	**56**	95	99	79	95	11	30	1	3	**25**	**58**
37	89	100	87	94	8	23	1	2	**17**	**57**	95	99	79	95	11	31	1	3	**25**	**58**
38	89	100	89	95	10	24	1	2	**18**	**57**	95	99	79	95	11	31	1	3	**25**	**58**
39	89	100	93	95	11	26	1	2	**19**	**58**	95	99	79	95	12	33	1	3	**25**	**59**
40	89	100	93	95	12	28	1	2	**19**	**59**	95	99	84	96	12	33	1	4	**26**	**59**
41	89	100	93	95	13	30	1	2	**20**	**59**	95	99	88	97	14	35	1	4	**27**	**60**
42	89	100	93	95	14	31	1	2	**20**	**59**	95	99	88	98	15	37	1	4	**28**	**61**
43	89	100	93	96	14	32	1	2	**20**	**60**	98	100	88	98	16	38	1	4	**28**	**62**
44	89	100	93	96	14	33	1	2	**20**	**60**	98	100	88	98	16	39	1	4	**28**	**62**
45	89	100	93	96	14	34	1	2	**20**	**61**	98	100	88	98	17	40	1	4	**29**	**62**
46	89	100	93	97	16	36	1	2	**21**	**61**	98	100	91	98	20	43	1	4	**31**	**64**
47	89	100	93	97	18	38	2	3	**22**	**62**	98	100	91	98	21	44	1	5	**31**	**64**
48	89	100	93	97	20	41	2	3	**23**	**63**	98	100	91	98	22	45	2	6	**32**	**65**
49	89	100	93	97	21	43	2	3	**24**	**64**	100	100	91	98	23	47	2	6	**33**	**66**

50	89	100	93	97	23	45	3	4	**25**	**64**	100	100	91	98	24	49	2	6	**34**	**67**
51	89	100	93	97	25	47	3	4	**25**	**65**	100	100	91	98	27	51	2	6	**35**	**67**
52	89	100	93	97	27	49	3	4	**27**	**66**	100	100	91	98	29	52	2	6	**36**	**68**
53	89	100	96	97	28	50	3	4	**27**	**66**	100	100	91	98	32	54	2	6	**38**	**69**
54	89	100	96	97	28	50	3	4	**27**	**66**	100	100	91	98	33	55	3	8	**38**	**69**
55	89	100	96	98	30	52	3	4	**28**	**67**	100	100	91	98	33	56	4	10	**39**	**70**
56	89	100	96	98	31	54	3	4	**29**	**68**	100	100	91	98	34	57	4	10	**39**	**71**
57	89	100	96	98	33	56	3	5	**30**	**68**	100	100	91	98	36	59	5	10	**40**	**71**
58	89	100	96	98	35	58	3	5	**30**	**69**	100	100	91	98	37	60	5	10	**41**	**72**
59	89	100	96	98	37	59	3	6	**31**	**70**	100	100	91	98	39	62	6	11	**42**	**73**
60	89	100	96	99	40	61	3	6	**33**	**70**	100	100	91	98	40	63	6	11	**43**	**73**
61	89	100	98	99	42	63	5	8	**34**	**71**	100	100	93	99	41	64	7	13	**44**	**74**
62	89	100	98	99	44	64	5	8	**35**	**72**	100	100	95	99	43	66	7	13	**45**	**75**
63	89	100	98	99	46	66	6	11	**37**	**73**	100	100	95	99	43	67	9	15	**46**	**75**
64	89	100	100	99	48	67	6	11	**38**	**73**	100	100	95	99	45	68	9	15	**47**	**76**
65	89	100	100	99	50	69	6	12	**39**	**74**	100	100	95	99	46	68	10	17	**48**	**76**
66	89	100	100	99	52	71	6	13	**40**	**75**	100	100	95	99	50	71	10	17	**50**	**77**
67	89	100	100	99	57	74	7	14	**42**	**76**	100	100	95	99	50	71	11	17	**50**	**78**
68	89	100	100	99	59	76	7	14	**43**	**76**	100	100	95	99	53	73	12	18	**52**	**78**
69	89	100	100	99	61	77	8	15	**44**	**77**	100	100	95	99	53	73	13	20	**52**	**79**
70	89	100	100	99	63	78	9	16	**46**	**77**	100	100	95	99	54	74	13	20	**53**	**79**
71	89	100	100	99	65	79	9	17	**47**	**78**	100	100	95	99	56	76	13	20	**54**	**80**
72	89	100	100	99	67	81	10	17	**47**	**78**	100	100	95	99	59	77	14	21	**55**	**80**
73	89	100	100	100	68	82	10	17	**48**	**79**	100	100	95	99	60	77	15	23	**56**	**81**
74	89	100	100	100	72	83	12	19	**50**	**80**	100	100	95	99	62	79	16	24	**58**	**81**
75	89	100	100	100	75	86	13	20	**53**	**81**	100	100	95	99	63	80	16	24	**58**	**82**
76	89	100	100	100	77	87	15	22	**54**	**81**	100	100	95	99	65	81	19	27	**60**	**83**
77	89	100	100	100	78	88	15	23	**55**	**82**	100	100	95	99	66	81	19	27	**61**	**83**
78	89	100	100	100	81	89	18	25	**57**	**83**	100	100	95	99	67	82	22	29	**62**	**83**
79	89	100	100	100	83	91	19	26	**59**	**83**	100	100	98	100	70	84	24	31	**64**	**84**
80	89	100	100	100	85	92	22	28	**60**	**84**	100	100	98	100	71	85	25	32	**65**	**85**
81	89	100	100	100	87	93	26	32	**63**	**85**	100	100	98	100	72	85	25	33	**66**	**85**
82	89	100	100	100	88	94	28	33	**64**	**86**	100	100	98	100	75	86	25	33	**67**	**86**
83	89	100	100	100	89	94	32	37	**66**	**86**	100	100	98	100	77	88	30	38	**70**	**87**
84	89	100	100	100	90	95	35	41	**68**	**87**	100	100	98	100	81	90	31	40	**72**	**88**
85	89	100	100	100	91	95	39	45	**70**	**88**	100	100	98	100	82	90	34	42	**73**	**88**
86	89	100	100	100	92	96	43	48	**72**	**89**	100	100	98	100	83	90	42	49	**75**	**89**
87	89	100	100	100	92	96	48	53	**75**	**90**	100	100	98	100	84	91	45	52	**77**	**90**
88	89	100	100	100	93	96	50	55	**76**	**90**	100	100	98	100	85	92	51	57	**79**	**91**
89	89	100	100	100	93	96	52	57	**77**	**91**	100	100	98	100	86	92	56	62	**81**	**92**
90	89	100	100	100	94	97	54	60	**78**	**91**	100	100	98	100	87	93	59	67	**83**	**93**
91	100	100	100	100	94	97	58	63	**80**	**92**	100	100	98	100	89	94	64	70	**85**	**94**
92	100	100	100	100	94	97	62	66	**82**	**93**	100	100	98	100	89	94	66	71	**85**	**94**
93	100	100	100	100	94	97	66	69	**83**	**93**	100	100	98	100	89	94	71	75	**87**	**94**
94	100	100	100	100	95	97	70	74	**85**	**94**	100	100	98	100	91	95	73	77	**88**	**95**
95	100	100	100	100	96	98	75	79	**88**	**95**	100	100	98	100	91	95	75	79	**88**	**95**
96	100	100	100	100	96	98	80	83	**90**	**96**	100	100	98	100	92	96	80	83	**90**	**96**
97	100	100	100	100	96	98	85	87	**92**	**97**	100	100	98	100	93	96	82	85	**91**	**96**
98	100	100	100	100	97	98	89	90	**94**	**98**	100	100	98	100	94	97	83	86	**92**	**97**
99	100	100	100	100	98	99	93	94	**96**	**99**	100	100	98	100	97	98	89	90	**95**	**98**
100	100	100	100	100	100	100	100	100	**100**	**100**	100	100	100	100	100	100	100	100	**100**	**100**

(**A**)

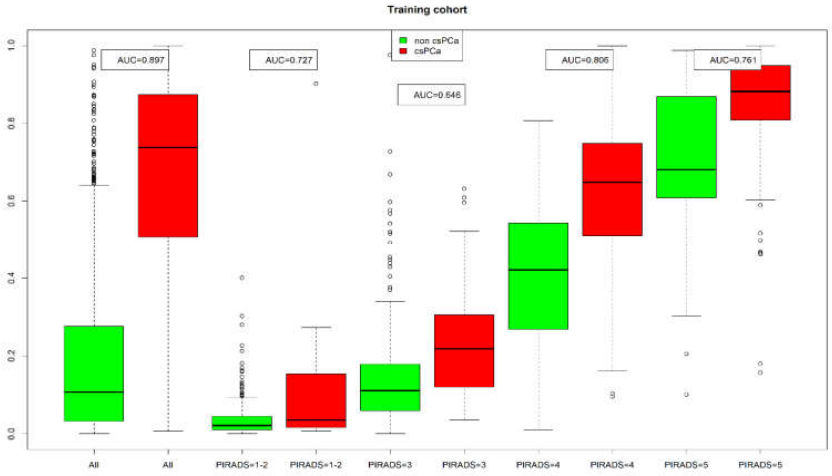

(**B**)

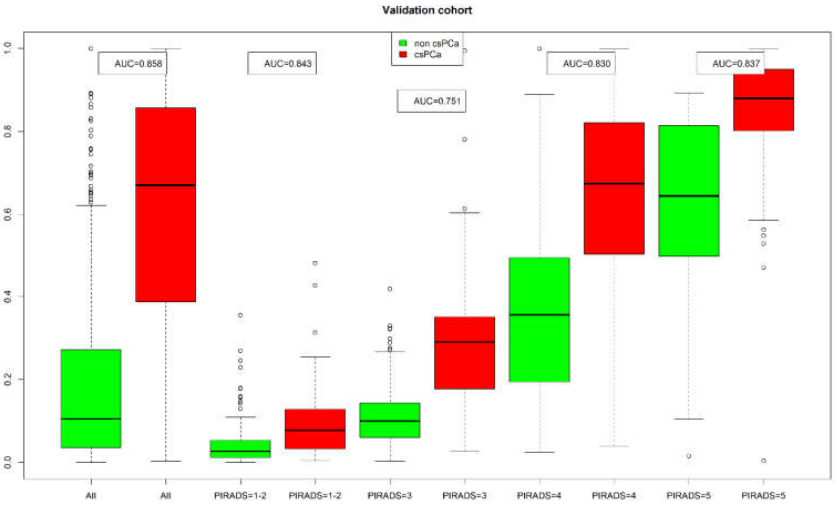

Figure S3. Boxplots of the likelihoods of csPCa in overall men and regarding PI-RADS categories in development cohort (**A**) and external validation cohort (**B**).

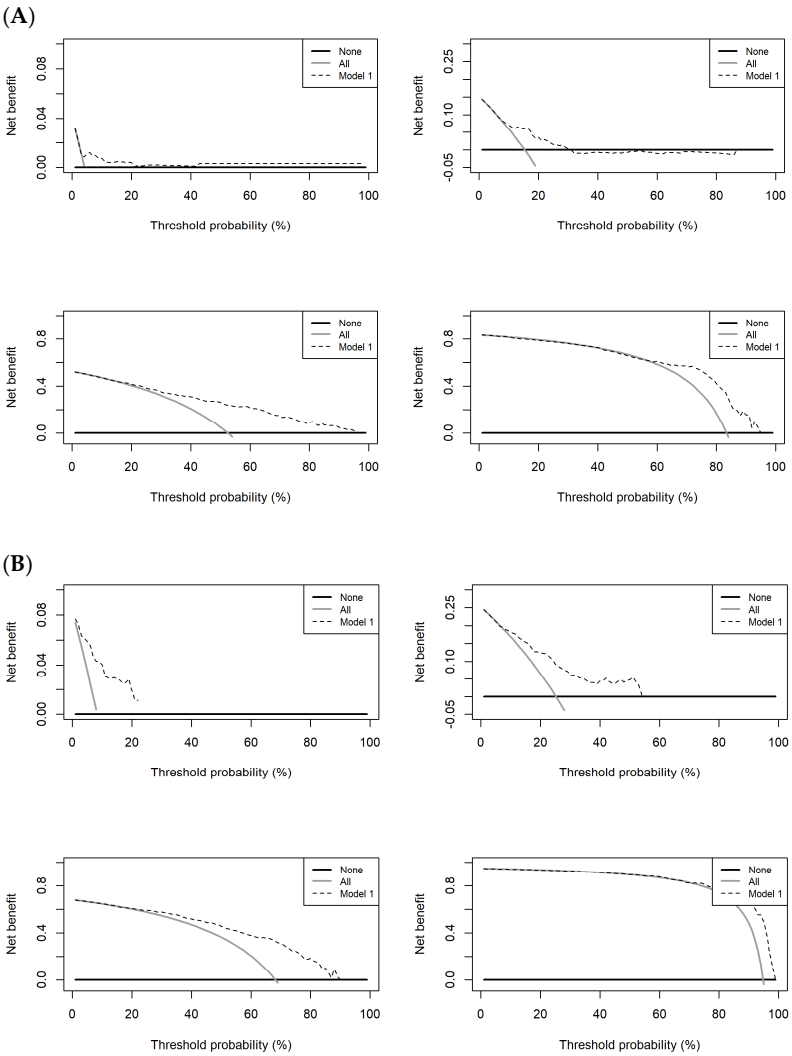

Figure S4. DCA showing the net benefit of MRI-PM biopsying all men according to the PI-RADS categories <3 (upper left), 3 (upper right), 4 (lower left), and 5 (lower right) in development cohort (**A**) and external validation cohort (**B**).

5.3. PUBLICACIÓN 3

Título: Comparative Analysis of PSA Density and an MRI-Based Predictive Model to Improve the Selection of Candidates for Prostate Biopsy

Revista: Cancers

Año de publicación: 2022

Volumen: 14

Páginas: 2374

DOI: https://doi.org/10.3390/cancers14102374

Autores: Juan Morote, Angel Borque-Fernando, Marina Triquell, Anna Celma, Lucas Regis, Richard Mast, Inés M. de Torres, María E. Semidey, José M. Abascal, Pol Servian, Anna Santamaría, Jacques Planas, Luis M. Esteban y Enrique Trilla

Factor de impacto: 4.5 (2023)

Cuartil: Q1 (Oncología)

cancers

MDPI

Article

Comparative Analysis of PSA Density and an MRI-Based Predictive Model to Improve the Selection of Candidates for Prostate Biopsy

Juan Morote [1,2,*,†], Angel Borque-Fernando [3,†], Marina Triquell [1], Anna Celma [1], Lucas Regis [1], Richard Mast [4], Inés M. de Torres [5,6], María E. Semidey [5,6], José M. Abascal [7], Pol Servian [8], Anna Santamaría [9], Jacques Planas [1], Luis M. Esteban [10,‡] and Enrique Trilla [1,2,‡]

1 Department of Urology, Vall d'Hebron Hospital, 08035 Barcelona, Spain; mtriquell@vhebron.net (M.T.); acelma@vhebron.net (A.C.); lregis@vhebron.net (L.R.); jplanas@vhebron.net (J.P.); etrilla@vhebron.net (E.T.)
2 Department of Surgery, Universitat Autònoma de Barcelona, 08193 Barcelona, Spain
3 Department of Urology, Hospital Miguel Servet, IIS-Aragon, 50009 Zaragoza, Spain; aborque@comz.org
4 Department of Radiology, Vall d'Hebron Hospital, 08035 Barcelona, Spain; rmast@vhebron.net
5 Department of Pathology, Vall d´Hebron Hospital, 08035 Barcelona, Spain; itorres@vhebron.net (I.M.d.T.); mesemidey@vhebron.net (M.E.S.)
6 Department of Morphological Sciences, Universitat Autònoma de Barcelona, 08193 Barcelona, Spain
7 Department of Urology, Parc de Salut Mar, Universitat Pompeu Fabra, 08003 Barcelona, Spain; jmabascalj@gmail.com
8 Department of Urology, Hospital Germans Trias i Pujol, 08035 Badalona, Spain; pservian.germantrias@gencat.cat
9 Vall d´Hebron Research Institute, 08035 Barcelona, Spain; anna.santamaria@vhir.org
10 Department of Applied Mathematics, Escuela Universitaria Politécnica La Almunia, Universidad de Zaragoza, 50100 Zaragoza, Spain; lmeste@unizar.es
* Correspondence: jmorote@vhebron.net; Tel.: +34-932746009
† These authors contribute equally as co-first authors.
‡ These authors contribute equally as co-last authors.

Citation: Morote, J.; Borque-Fernando, A.; Triquell, M.; Celma, A.; Regis, L.; Mast, R.; de Torres, I.M.; Semidey, M.E.; Abascal, J.M.; Servian, P.; et al. Comparative Analysis of PSA Density and an MRI-Based Predictive Model to Improve the Selection of Candidates for Prostate Biopsy. *Cancers* **2022**, *14*, 2374. https://doi.org/10.3390/cancers14102374

Academic Editor: David Wong

Received: 6 April 2022
Accepted: 9 May 2022
Published: 11 May 2022

Publisher's Note: MDPI stays neutral with regard to jurisdictional claims in published maps and institutional affiliations.

Simple Summary: Magnetic resonance imaging (MRI)-associated prostate-specific antigen density (mPSAD) and MRI predictive models have been proposed for improving the selection of candidates for prostate biopsy among men with suspected prostate cancer (PCa). While the calculation of mPSAD only requires a simple division, the individual risk assessment of PCa using the available risk calculators is also a swift process. We aim to compare the clinical usefulness of mPSAD and an MRI predictive model that utilises the same predictors as the recently developed and externally validated Barcelona MRI predictive model (MRI-PMbdex).

Abstract: This study is a head-to-head comparison between mPSAD and MRI-PMbdex. The MRI-PMbdex was created from 2432 men with suspected PCa; this cohort comprised the development and external validation cohorts of the Barcelona MRI predictive model. Pre-biopsy 3-Tesla multiparametric MRI (mpMRI) and 2 to 4-core transrectal ultrasound (TRUS)-guided biopsies for suspicious lesions and/or 12-core TRUS systematic biopsies were scheduled. Clinically significant PCa (csPCa), defined as Gleason-based Grade Group 2 or higher, was detected in 934 men (38.4%). The area under the curve was 0.893 (95% confidence interval [CI]: 0.880–0.906) for MRI-PMbdex and 0.764 (95% CI: 0.774–0.783) for mPSAD, with $p < 0.001$. MRI-PMbdex showed net benefit over biopsy in all men when the probability of csPCa was greater than 2%, while mPSAD did the same when the probability of csPCa was greater than 18%. Thresholds of 13.5% for MRI-PMbdex and 0.628 ng/mL^2 for mPSAD had 95% sensitivity for csPCa and presented 51.1% specificity for MRI-PMbdex and 19.6% specificity for mPSAD, with $p < 0.001$. MRI-PMbdex exhibited net benefit over mPSAD in men with prostate imaging report and data system (PI-RADS) <4, while neither exhibited any benefit in men with PI-RADS 5. Hence, we can conclude that MRI-PMbdex is more accurate than mPSAD for the proper selection of candidates for prostate biopsy among men with suspected PCa, with the

exception of men with a PI-RAD S 5 score, for whom neither tool exhibited clinical guidance to determine the need for biopsy.

Keywords: prostate-specific antigen density; predictive model; clinically significant prostate cancer

1. Introduction

Early detection of clinically significant prostate cancer (csPCa) decreases the specific mortality of PCa [1]. The classic approach of PCa detection based on systematic biopsies after PCa suspicion, has been disapproved due to the high rates of unnecessary biopsies and the over detection of insignificant tumours (iPCa) [2–5]. While PCa suspicion continues to be based on serum prostate-specific antigen (PSA) elevation or abnormal digital rectal examination (DRE), the detection of csPCa has improved since the introduction of multiparametric magnetic resonance imaging (mpMRI) and guided biopsies [6,7]. Nevertheless, there remain uncertain scenarios in which a high rate of unnecessary biopsies and over detection of iPCa occur [8,9]. The current high negative predictive value of mpMRI enables clinicians to avoid systematic biopsies in men with prostate imaging report and data system (PI-RADS) <3; however, this approach may fail to detect 5–20% of existing csPCa in men with a negative mpMRI [10–12]. Contrarily, clinicians usually recommend prostate biopsy for men with PI-RADS > 3, as csPCa is usually detected approximately at a rate of 50–60% for men with PI-RADS 4, and up to 95% for men with PI-RADS 5 [13–15]. PI-RADS 3 remains the most uncertain scenario, in which csPCa usually does not reach 20% and in which more than 50% of the biopsied lesions reflect iPCa [9,15]. Prostate-specific antigen density (PSAD), MRI-based predictive models (MRI-PM), and modern markers are currently recommended for improving the selection of candidates for prostate biopsy [6,7,16].

PSAD is a classic tool that improves the specificity of serum PSA [17]. However, PSAD can be strengthened by pre-biopsy MRI (mPSAD), which yields a more accurate prostate volume at no additional cost [18]. mPSAD has been analysed in overall populations of men to enhance the detection of csPCa in relation to the PI-RADS score [19–22]. MRI-PMs are also effective tools. However, few MRI-PMs have been developed from the latest versions of PI-RADS; furthermore, external validation should be performed before their use. Easily accessible risk calculators (RCs) are essential for avoiding nomograms, which are cumbersome and time-consuming [23–37]. Recently, the Barcelona MRI-PM was developed from the following independent predictors: PI-RADS score v.2.0, age, serum PSA, DRE, PCa family history, type of biopsy (initial vs. repeat), and MRI-derived prostate volume. External validation was carried out in the same metropolitan area, and a web-RC is freely available at https://mripcaprediction.shinyapps.io/
MRIPCaPrediction/ (accessed on 5 March 2022). For the first time, the performance of an MRI-PM has been analysed with regard to PI-RADS categories, showing a net benefit over biopsy for all men in each PI-RADS < 4. The designed RC also incorporates the novel option of selecting the csPCa probability threshold [38], which may facilitate further external validation [15] and improve the model's performance in specific PI-RADS categories [39]. Furthermore, modern markers can also be helpful; however, they are expensive and require the procurement of new samples of blood or urine, usually after prostate massage [40]. Four-Kallikrein test (4K) [41–45], the Prostate Health Index (PHI) [46–48], SelectMDx [49–52], Proclarix [52,53], and the combination of multiple markers have improved the prognostic performance of mpMRI [30].

This study aims to compare the clinical usefulness of mPSAD and MRI-PMbdex for the proper selection of candidates for prostate biopsy in a sizable, multicentre population of men with suspected PCa, according to PI-RADS categories.

2. Materials and Methods

2.1. Design, Setting and Participants

A head-to-head comparison of mPSAD and MRI-PMbdex was designed from a multicentre trial conducted in the metropolitan area of Barcelona. The trial involved 2432 men with suspected PCa due to a serum PSA > 3.0 ng/mL or an abnormal DRE. MRI-PMbdex was created from the development cohort of 1486 men studied at Vall d'Hebron Hospital (VHH) and the external validation cohort of 946 men from Parc de Salut Mar (PSM) as well as Hospital Germans Trias i Pujol (GTiPH). This study was conducted between January 1, 2006, and 31 December 2019 [38]. Pre-biopsy 3-Tesla mpMRI and guided or systematic prostate biopsies were always performed. Men undergoing 5-α reductase inhibitor treatment due to symptomatic benign prostatic hyperplasia, having a previous diagnosis of PCa, exhibiting isolated atypical small acinar proliferation, and exhibiting high-grade prostatic intraepithelial neoplasia with atypia were excluded. Furthermore, written consent for prostate biopsy was obtained from all participants, and the project was approved by the institutional review board of VHH (PRAG-317/2017).

2.2. Intervention

The development of MRI-PMbdex and the individual generation of csPCa likelihood was expressed as percentages ranging from 0 to 100%. mPSAD (ng/mL^2) was calculated from the pre-biopsy serum PSA and the prostate volume reported in the pre-biopsy MRI, and individual generation of csPCa likelihood was expressed as percentages ranging from 0 to 100%.

2.3. MRI Technique and Evaluation

Magnetic resonance scans were acquired on 3-Tesla scanners with a standard surface phased-array coil. Magnetom Trio (Siemens Corp., Erlangen, Germany) equipment was used in VHH, Diamond Select Achieva (Phillips Corp., Eindoven, Nederland) in PSM, and Nova Dual (Phillips Corp., Eindoven, Nederland) in GTiPH. The acquisition protocol included T2-weighted imaging (T2W), diffusion-weighted imaging (DWI), and dynamic contrast-enhanced (DCE) imaging, in accordance with the European Society of Urogenital Radiology guidelines [54]. In each institution, an expert radiologist, with over five years of experience and over 300 mpMRI reported per year, analysed the images and reported them according to PI-RADS v2.0, using a 5-point likelihood scale for csPCa [55]. Complex cases were reviewed by two expert radiologists.

2.4. Prostate Biopsy Procedure

All men from the participant institutions underwent 2 to 4-core mpMRI-TRUS cognitive fusion-guided biopsies of suspicious lesions and 12-core TRUS systematic biopsies when the PI-RADS reported in the pre-biopsy mpMRI was 3 or higher, while 12-core TRUS systematic biopsies were performed when the PI-RADS was lower than 3 [56]. In each institution, the biopsies were performed by an experienced urologist, with over five years of experience and who had performed over 300 biopsies per year, using a BK Focus 400 ultrasound scanner (BK Medical Inc. Herlev, Denmark) in VHH, Siemens Acuson 150 (Siemens Inc., Erlangen, Germany) in PSM, and a Sonolite Antares (Siemens Inc., Erlangen, Germany) in GTiPH.

2.5. Pathologic Analysis and csPCa Definition

The biopsy samples were sent separately to each pathology department, where an expert uro-pathologist analysed the biopsy specimens and, after identifying the PCa, reported the International Society of Uro-Pathology (ISUP) Gleason-based Grade Group (GG) [57]. Complex cases were analysed by two expert uro-pathologists. Any ISUP-GGG ≥ 2 was defined as csPCa.

2.6. Endpoint Measurements

The endpoint measurements were the rates of detected csPCa and missed csPCa, in addition to the frequency of avoided prostate biopsies and iPCa.

2.7. Statistical Analysis

The reporting recommendations for tumour marker prognostic studies (REMARK) [58] and the update of standards for reporting diagnostic accuracy studies (STARD 2015) [59] were followed. Medians and interquartile ranges (25–75 percentiles) were used to describe the quantitative variables, and rates were used to describe the qualitative variables. The MRI-PMbdex individual likelihoods of csPCa were generated from the logistical regression analysis performed from the included independent predictors of the Barcelona MRI-PM [38]. The mPSAD individual likelihoods of csPCa were generated from the logistic regression analysis performed from the following independent predictors: PI-RADS score and mPSAD. The chi-square and Mann–Whitney tests were used to find associations between the variables. Receiver operating characteristic curves (ROC) and areas under the curve (AUC) were used to analyse the efficacy of mPSAD and MRI-PMbdex for csPCa detection; the DeLong test was conducted to compare the AUCs [60,61]. Furthermore, decision curve analysis (DCA) was used to discern the net benefits of mPSAD and MRI-PMbdex over performing biopsies in all men [62]. The thresholds of mPSAD and MRI-PMbdex were selected from the 95% sensitivity for csPCa, and the specificities were analysed and compared. The performances were analysed based on sensitivity, specificity, negative and positive predictive values, accuracy, avoidable biopsies, and potentially missed csPCa. In addition, odds ratios and 95% confidence intervals (CI) were assessed. Tests with two-sided $p < 0.05$ were considered statistically significant. The statistical analyses were computed using the R programming language v.4.0.3 (The R Foundation for Statistical Computing, Vienna, Austria), and SPSS v.25 (IBM, Statistical Package for Social Sciences, San Francisco, CA, USA) was used.

3. Results

3.1. Characteristics of the Study Population

The characteristics of the entire population are summarised in Table 1. A median age of 68 years, serum PSA of 6.5 ng/mL, and prostate volume of 55 cm3 can be observed. The DRE was abnormal in 25% of the men; 28% were scheduled to repeat prostate biopsies, and 6.6% had PCa family history. PCa was diagnosed in 1214 men (49.9%), csPCa in 934 men (38.4%), and iPCa in 280 men (11.5%).

Table 1. Characteristics of study population.

Characteristic	Measurement
Number of cases	2432
Median age, years (IQR)	68 (62–73)
Median total PSA, ng/mL (IQR)	6.5 (4.7–10.0)
Abnormal DRE, *n* (%)	612 (25.2)
Median prostate volume, ml (IQR)	55 (40–77)
Median PSA density, ng/mL^2 (IQR)	0.12 (0.08–0.20)
Repeat biopsy, *n* (%)	681 (28.0)
Family history of PCa, *n* (%)	161 (6.6%)
PI-RADS, *n* (%)	
1–2	550 (22.6)
3	645 (26.5)
4	841 (34.6)
5	396 (16.3)

Overall PCa detection, *n* (%)	1214 (49.9)
csPCa detection, *n* (%)	934 (38.4)
iPCa detection, *n* (%)	280 (11.5)

The characteristics of the men according to PI-RADS categories as well as comparisons between each pair of consecutive PI-RADS are presented in Table 2. All characteristics showed differences regarding all PI-RADS categories ($p < 0.001$), with the exception of PCa family history, which showed a non-significant trend that ranged from 4.7% in men with PI-RADS 1 to 8.3% in men with PI-RADS 5 ($p = 0.287$). On comparing the characteristics of men with PI-RADS 1 and those with PI-RADS 2, it was found that only the frequency of repeat biopsies was significantly higher among the latter (19.4% vs. 34.1%; $p < 0.001$); all other characteristics were similar between the two categories. Between PI-RADS 2 and PI-RADS 3, the frequency of PCa detection increased from 20.3% to 30.5% ($p = 0.028$), while the frequency of csPCa and iPCa exhibited no significant increase. Men with PI-RADS 4 were significantly older than those with PI-RADS 3, had a higher PSA and mPSAD, had a lower prostate volume, and exhibited an abnormal DRE more often. The frequency of repeat biopsies, PCa family history, and iPCa detection was similar in both PI-RADS 3 and PI-RADS 4 categories; however, a significant increase in csPCa frequency was observed ($p < 0.001$). Moreover, in PI-RADS 5 compared with PI-RADS 4, the frequency of repeat biopsies and iPCa was low, while the frequency of csPCa and overall PCa increased significantly ($p < 0.001$). The frequency of repeat biopsies as well as iPCa also decreased, while the frequency of all PCa and csPCa increased significantly ($p < 0.001$).

Table 2. Characteristics of study population according to the PI-RADS category

Characteristic	PI-RADS 1	*p* Value	PI-RADS 2	*p* Value	PI-RADS 3	*p* Value	PI-RADS 4	*p* Value	PI-RADS 5
Number of cases	427	-	123	-	645	-	841	-	396
Median age, years (IQR)	66 (60–72)	=0.633	66 (60–71)	=0.901	66 (60–71)	<0.001	69 (63–74)	<0.001	72 (66–76)
Median total PSA, ng/mL (IQR)	6.2 (4.5–8.7)	=0.323	5.8 (4.4–8.4)	=0.644	6.0 (4.4–8.4)	<0.001	6.6 (4.8–9.5)	<0.001	9.4 (5.8–18.0)
Abnormal DRE, *n* (%)	59 (13.8)	=0.818	18 (14.6)	=0.497	80 (12.4)	<0.001	216 (25.7)	<0.001	239 (60.4)
Median PV, mL (IQR)	63 (43–90)	=0.666	60 (45–84)	=0.833	63 (45–82)	<0.001	50 (37–74)	<0.001	46 (35–60)
Median PSAD, ng/mL^2 (IQR)	0.10 (0.07–0.15)	=0.960	0.11 (0.07–0.15)	=0.797	0.10 (0.07–0.15)	<0.001	0.13 (0.08–0.20)	<0.001	0.21 (0.13–0.37)
Repeat biopsy, *n* (%)	83 (19.4)	<0.001	42 (34.1)	=0.631	206 (31.9)	=0.860	271 (32.3)	<0.001	78 (19.7)
Family history of PCa, *n* (%)	20 (4.7)	=0.649	7 (5.7)	=0.733	42 (6.5)	=0.702	59 (7.0)	=0.410	33 (8.3)
Overall PCa detection, *n* (%)	97 (22.7)	=0.574	25 (20.3)	=0.028	194 (30.5)	<0.001	548 (65.2)	<0.001	350 (88.4)
csPCa detection, *n* (%)	42 (9.8)	=0.865	13 (10.6)	=0.081	109 (16.9)	<0.001	439 (52.2)	<0.001	331 (83.6)
iPCa detection, *n* (%)	55 (12.9)	=0.351	12 (9.8)	=0.295	85 (13.2)	=0.902	109 (13.0)	<0.001	19 (4.8)

3.2. Performance of mPSAD and MRI-PMbdex in the Entire Population

The efficacy of MRI-PMbdex in detecting csPCa was higher than that of mPSAD. The AUC was 0.893 (95% CI: 0.880–0.906) for MRI-PMbdex and 0.763 (95% CI: 0.774–0.783) for mPSAD, with $p < 0.001$ (Figure 1A). The MRI-PMbdex exhibited net benefit over mPSAD and over biopsy of all men from a csPCa probability threshold of 2%, while mPSAD exhibited net benefit over biopsy of all men from a csPCa probability threshold of 18% (Figure 1B).

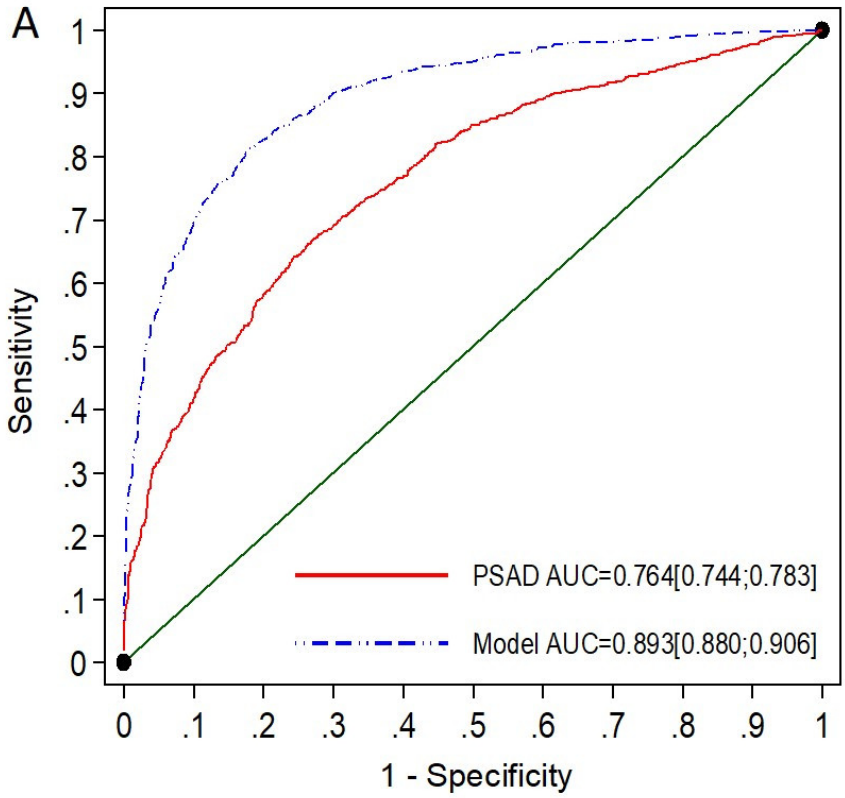
A
Sensitivity
1
.9
.8
.7
.6
.5
.4
.3
.2
.1
0
0
.1
.2
.3
.4
.5
.6
.7
.8
.9
1
1 - Specificity
PSAD AUC=0.764[0.744;0.783]
Model AUC=0.893[0.880;0.906]

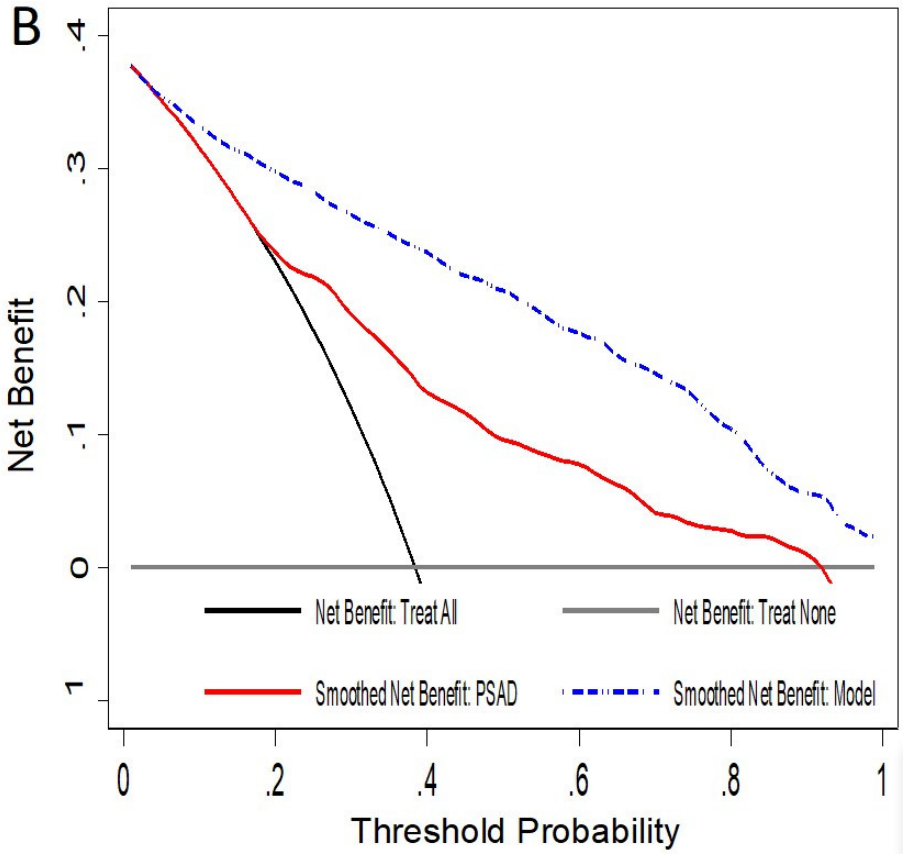

Figure 1. The ROC curves and AUCs show the efficacy of mPSAD (PSAD in the graphic) and MRI-PMbdex (model in the graphic) in detecting csPCa (**A**). The DCAs show the net benefit of mPSAD and MRI-PMbdex compared to performing biopsies on all men according to the csPCa probability threshold (**B**).

The thresholds of MRI-PMbdex and mPSAD with 95% sensitivity for csPCa were 13.5% and 0.628 ng/mL^2, respectively, and their corresponding specificities were 51.1% and 19.6%, respectively, with $p < 0.001$ (Table 3). MRI-PMbdex and mPSAD were able to avoid 33.4% and 14.0% of prostate biopsies, respectively, while missing 5% of csPCa ($p < 0.001$). In relation to the aggressiveness of missed csPCa, both mPSAD and MRI-PMbdex missed 2.4% of PCa with ISUP-GG ≥ 3 (22/934). Furthermore, mPSAD missed 1% of csPCa with ISUP-GG ≥ 4 (9/934), while MRI-PMbdex did not miss any of them.

Table 3. Performance of mPSAD and MRI-PMbdex, with respective thresholds of 0.628 ng/mL^2 and 13.5%, in the entire study population and grade groups of detected tumours.

Parameter	mPSAD	MRI-PMbdex
Sensitivity	887/934 (95.0)	887/934 (95.0)
Specificity	294/2091 (19.6)	765/1498 (51.1)
Negative predictive value	294/341 (86.2)	765/812 (94.2)
Positive predictive value	887/2091 (42.4)	887/1620 (54.8)
Accuracy	1181/2432 (48.6)	1652/2432 (67.9)
Avoided biopsies	341/2432 (14.0)	812/2432 (33.4)
Missed csPCa	47/934 (5%)	47/934 (5%)
Odds ratios (95% CI)	4.61 (3.35–6.35)	19.70 (14.44–26.86)

p Value	<0.001	<0.001
GG 2	25	25
GG 3	13	22
GG 4	8	0
GG 5	1	0

3.3. Performance of mPSAD and MRI-PMbdex According to the PI-RADS Categories

Among the 550 men with negative mpMRI (PI-RADS < 3), the MRI-PMbdex exhibited an AUC of 0.824 (95% CI: 0.756–0.892), while mPSAD exhibited an AUC of 0.685 (95% CI: 0.610–0.761), with $p < 0.001$ (Figure 2A). MRI-PMbdex showed net benefit over mPSAD in detecting csPCa (Figure 2B).

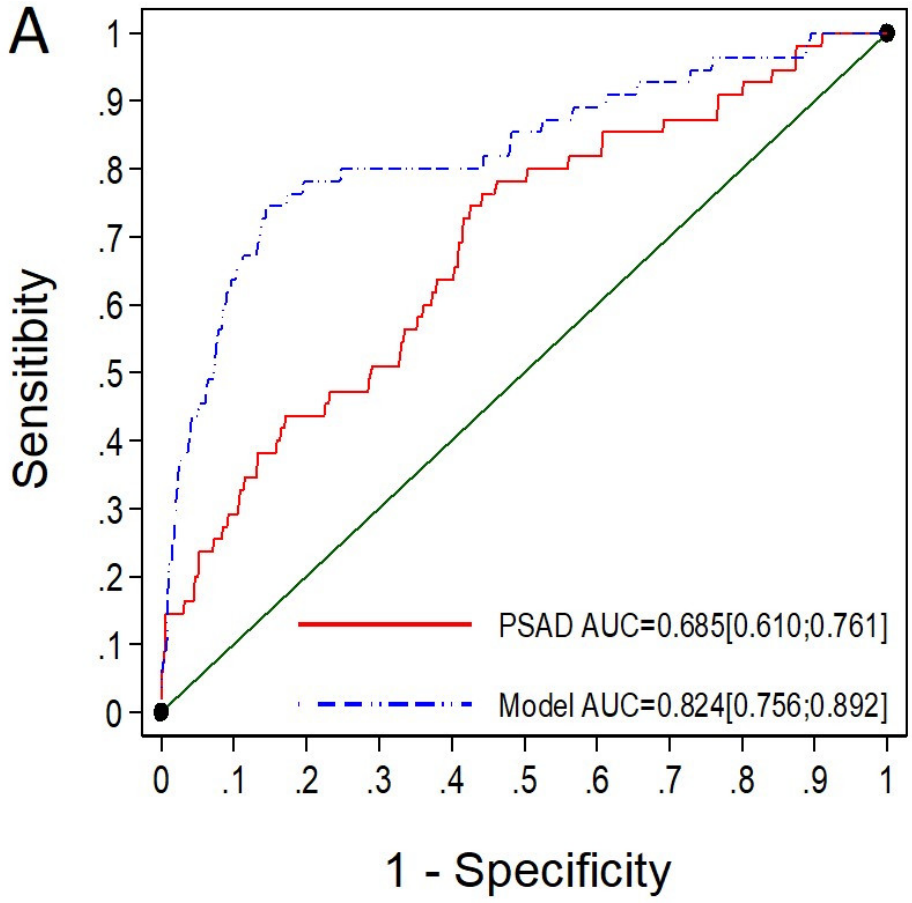

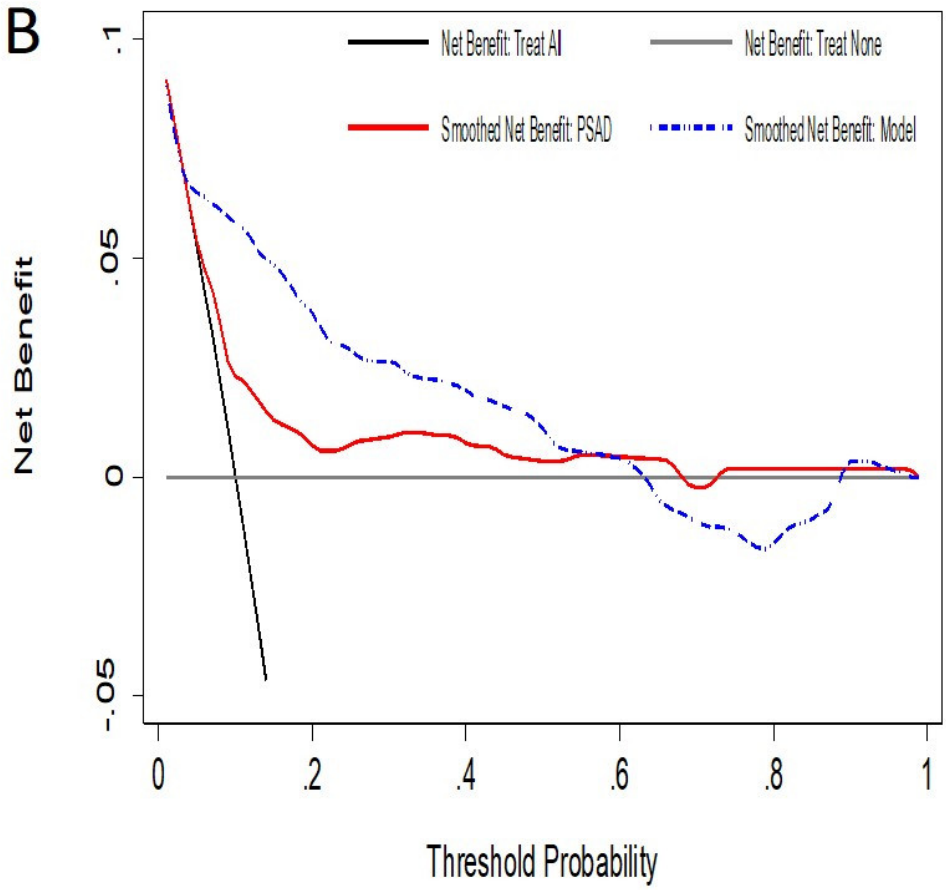

Figure 2. The ROC curves and AUCs show the efficacy of mPSAD (PSAD in the graphic) and MRI-PMbdex (model in the graphic) in detecting csPCa in men with PI-RADS < 3 (**A**). The DCAs showing the net benefit of mPSAD and MRI-PMbdex over performing biopsies on all men according to the csPCa probability threshold (**B**).

The selected thresholds of MRI-PMbdex and mPSAD provided sensitivities of 67.3% and 90.9% as well as specificities of 87.7% and 21.4%, respectively, in men with PI-RADS < 3. The MRI-PMbdex avoided 82.2% of prostate biopsies, whereas mPSAD avoided 20.2%. However, the probabilities of missed csPCa were 32.7% and 9.1%, for MRI-PMbdex and mPSAD, respectively. MRI-PMbdex did not detect 0.9% of PCa with ISUP-GG = 3 (5/55), while mPSAD did not detect 0.2% (1/55) (Table 4).

Table 4. Performance of mPSAD and MRI-PMbdex, with respective thresholds of 0.628 ng/mL^2 and 13.5%, in men with PI-RADS < 3.

Parameter	mPSAD	MRI-PMbdex
Sensitivity	50/55 (90.9)	37/55 (67.3)
Specificity	106/495 (21.4)	434/495 (87.7)
Negative predictive value	106/111 (95.5)	434/452 (96.0)
Positive predictive value	50/439 (11.4)	37/98 (67.3)
Accuracy	156/550 (28.4)	471/550 (85.6)
Avoided biopsies	111/550 (20.2)	452/550 (82.2)

Missed csPCa	5/55 (9.1)	18/55 (32.7)
Odds ratio (95% CI)	2.27 (1.06–7.00)	14.62 (7.84–27, 29)
p Value	=0.033	<0.001
GG 2	4	13
GG 3	1	5
GG 4	0	0
GG 5	0	0

Among the 645 men with PI-RADS 3, MRI-PMbdex exhibited an AUC of 0.768 (95% CI: 0.717–0.819), while mPSAD exhibited an AUC of 0.696 (95% CI: 0.641–0.750), with $p < 0.001$ (Figure 3A). Thus, MRI-PMbdex showed net benefit over mPSAD from the 18% csPCa probability threshold (Figure 3B).

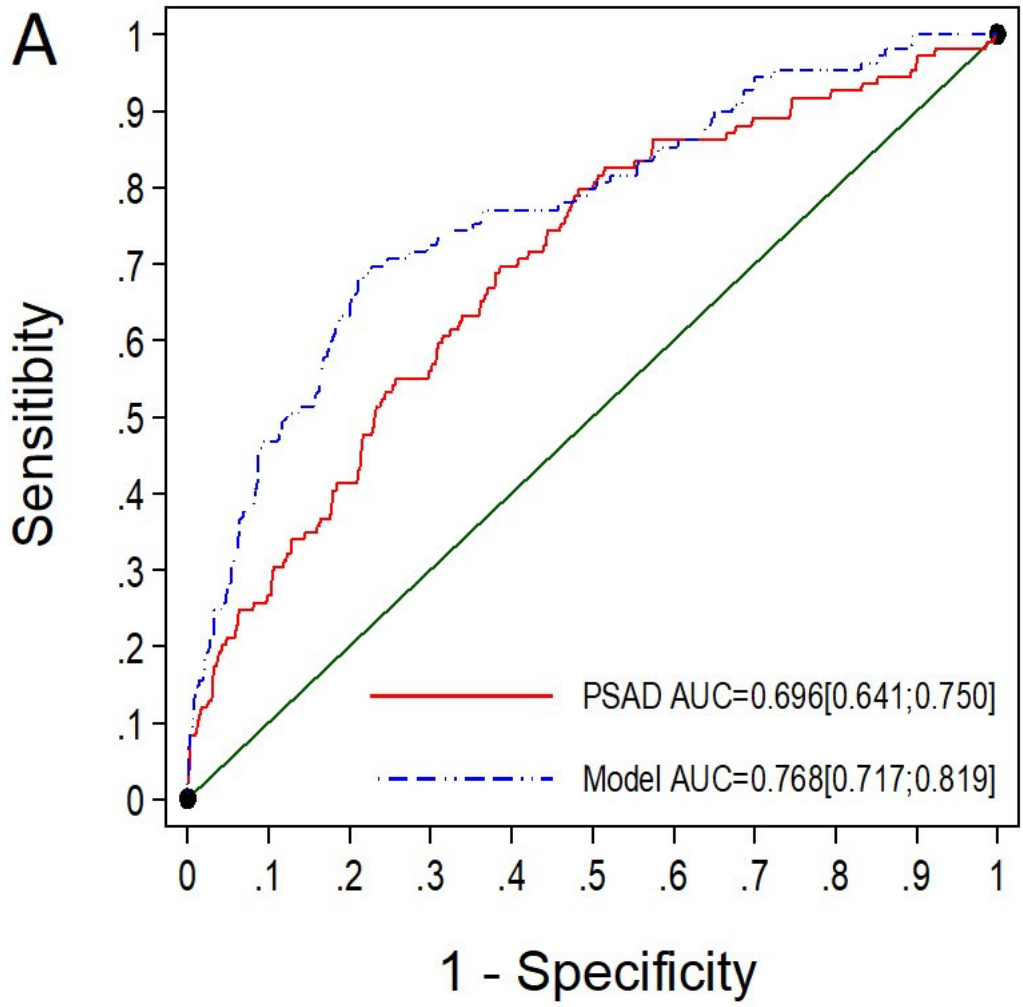

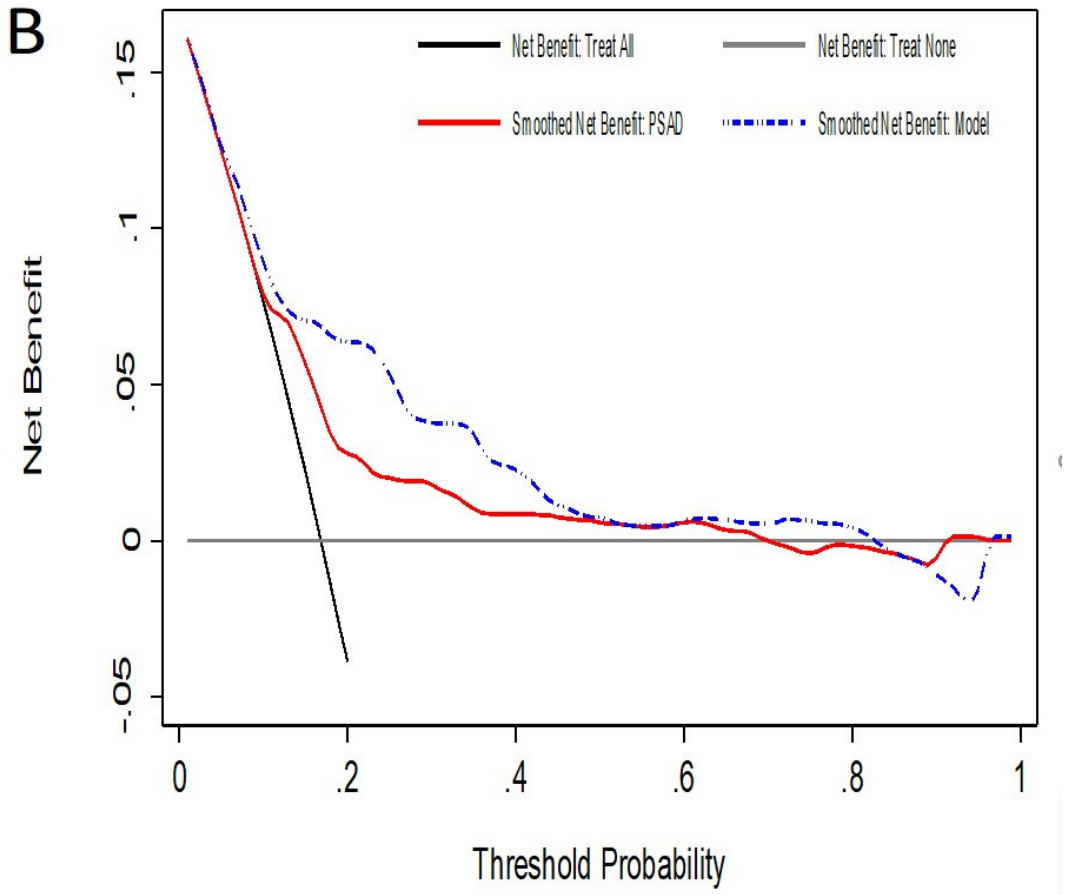

Figure 3. The ROC curves and AUCs show the efficacy of mPSAD (PSAD in the graphic) and MRI-PMbdex (model in the graphic) in detecting csPCa in men with PI-RADS 3 (**A**). The DCAs showing the net benefit of mPSAD and MRI-PMbdex over performing biopsies on all men according to the csPCa probability threshold (**B**).

The selected thresholds of MRI-PMbdex and mPSAD provided sensitivities of 78.9% and 92.7% as well as specificities of 52.1% and 20.5%, respectively, in men with PI-RADS 3. MRI-PMbdex avoided 46.8% of prostate biopsies, while mPSAD avoided 18.3%. However, the probabilities of missed csPCa were 21.7% and 7.3%, respectively. mPSAD did not detect 2.8% of PCa with ISUP-GG ≥ 3 (3/109), whereas MRI-PMbdex did not detect 10% (11/109) (Table 5).

Table 5. Performance of mPSAD and MRI-PMbdex, with respective thresholds of 0.628 ng/mL² and 13.5%, in men with PI-RADS 3.

Parameter	mPSAD	MRI-PMbdex
Sensitivity	101/109 (92.7)	86/109 (78.9)
Specificity	110/536 (20.5)	279/536 (52.1)
Negative predictive value	110/118 (93.2)	279/302 (92.4)
Positive predictive value	101/527 (19.2)	86/343 (25.1)
Accuracy	211/645 (32.5)	365/645 (56.6)
Avoided biopsies	118/645 (18.3)	302/645 (46.8)
Missed csPCa	8/109 (7.3)	23/109 (21.1)

Odds Ratio (95% CI)	3.26 (1.54–6.90)	4.06 (2.49–6.63)
p Value	<0.001	<0.001
GG 2	5	12
GG 3	2	11
GG 4	1	0
GG 5	0	0

Among the 841 men with PI-RADS 4, the MRI-PMbdex showed an AUC of 0.823 (95% CI: 0.769–0.851), while mPSAD showed an AUC of 0.742 (95% CI: 0.709–0.775), with $p < 0.001$ (Figure 4A). MRI-PMbdex showed net benefit over mPSAD in detecting csPCa from the 20% probability threshold, while mPSAD showed net benefit over performing biopsies on all men from the 35% probability threshold (Figure 4B).

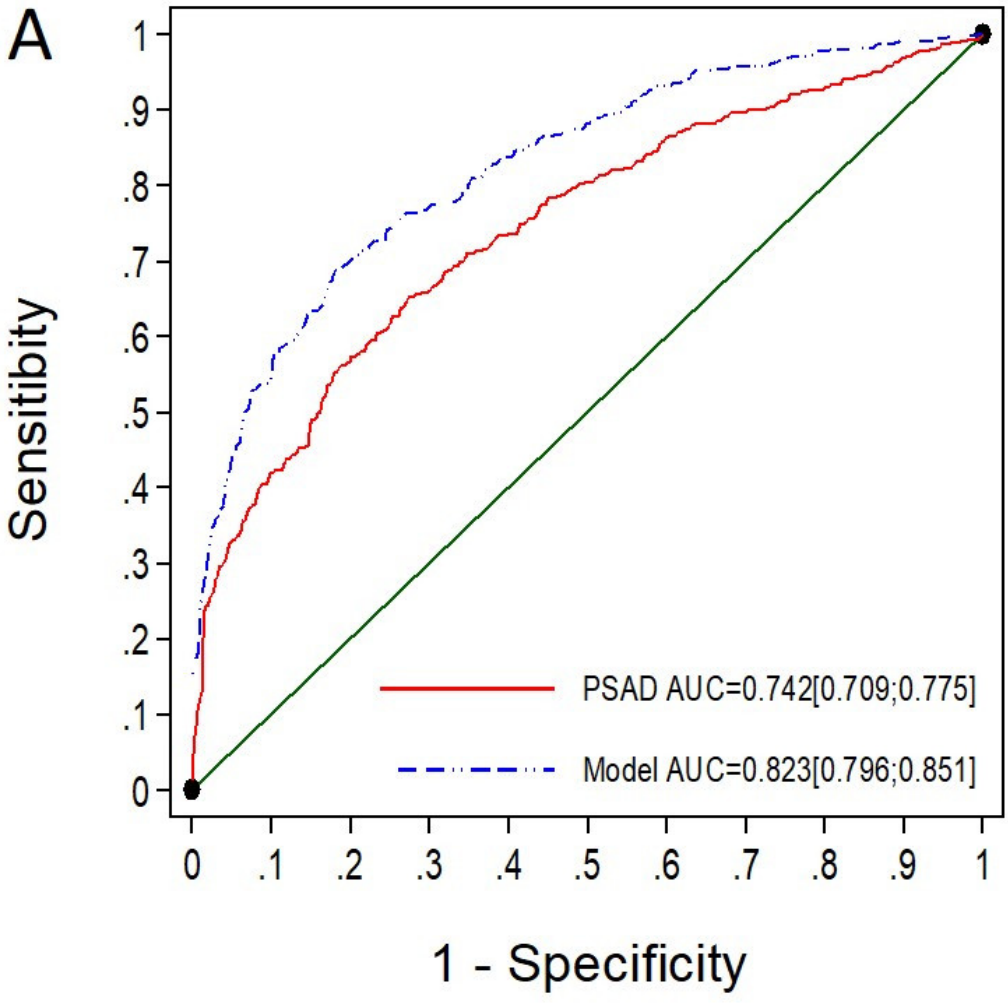

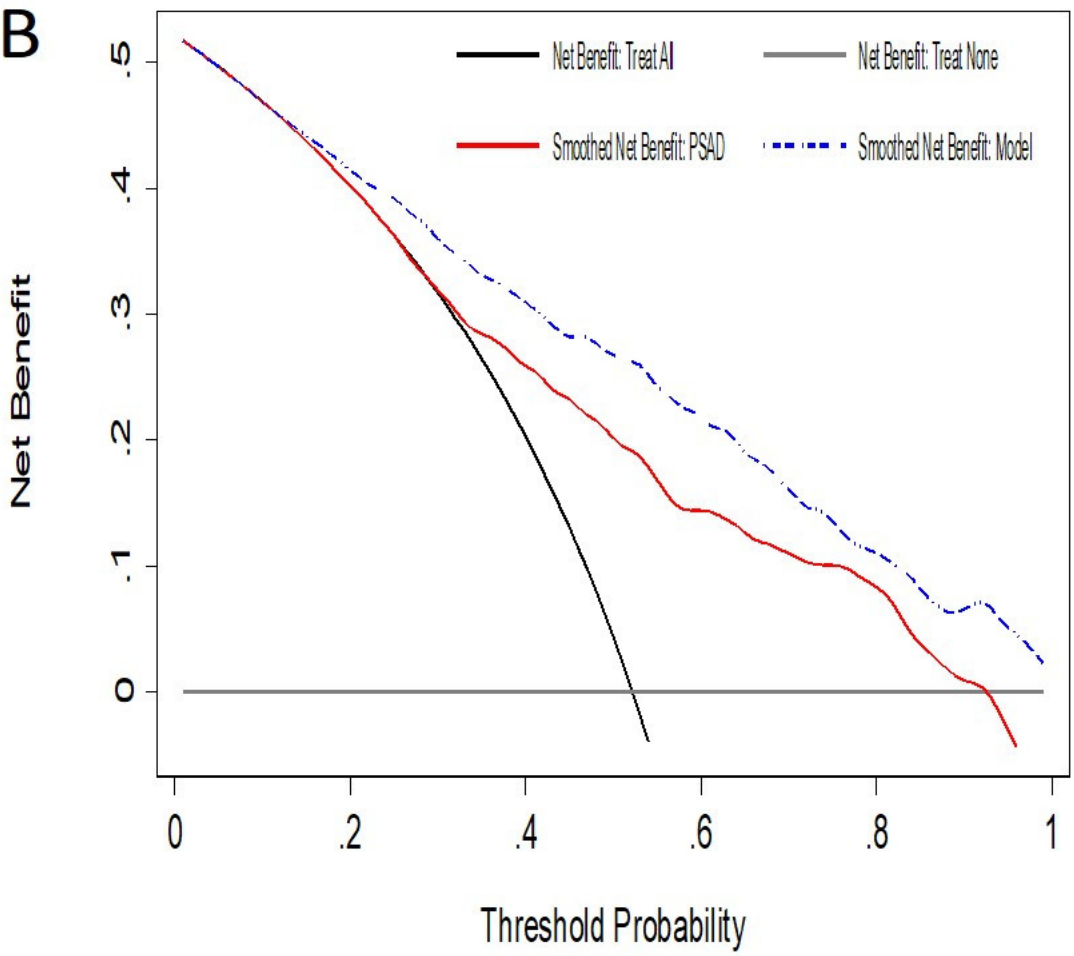

Figure 4. The ROC curves and AUCs show the efficacy of mPSAD (PSAD in the graphic) and MRI-PMbdex (model in the graphic) in detecting csPCa in men with PI-RADS 4 (**A**). The DCAs showing the net benefit of mPSAD and MRI-PMbdex over performing biopsies on all men according to the csPCa probability threshold (**B**).

The selected thresholds for MRI-PMbdex and mPSAD provided sensitivities of 98.6% and 94.3% as well as specificities of 12.2% and 16.2%, respectively, in men with PI-RADS 4. MRI-PMbdex avoided 6.5% of prostate biopsies, while mPSAD avoided 10.7%. Moreover, the rate of missed csPCa was 1.4% for MRI-PMbdex and 5.7% for mPSAD. The rate of missed PCa with ISUP-GG ≥ 4 was 0.9% (5/439) for mPSAD and 0% for MRI-PMbdex (Table 6).

Table 6. Performance of mPSAD and MRI-PMbdex, with respective thresholds of 0.628 ng/mL^2 and 13.5%, in men with PI-RADS 4.

Parameter	mPSAD	MRI-PMbdex
Sensitivity	414/439 (94.3)	433/439 (98.6)
Specificity	65/402 (16.2)	42/402 (12.2)
Negative predictive value	65/90 (72.2)	49/55 (89.1)
Positive predictive value	414/751 (55.1)	433/786 (55.1)

Accuracy	479/841 (57.0)	482/841 (57.3)
Avoided biopsies	90/841 (10.7)	55/841 (6.5)
Missed csPCa	25/439 (5.7)	6/439 (1.4)
Odds Ratio (95% CI)	3.19 (1.97–5.18)	10.02 (4.24–23.66)
p Value	<0.001	<0.001
GG 2	12	1
GG 3	8	5
GG 4	5	0
GG 5	0	0

Finally, among the 396 men with PI-RADS 5, the MRI-PMbdex showed an AUC of 0.787 (95% CI: 0.728–0.846), while mPSAD showed an AUC of 0.761 (95% CI: 0.698–0.825), with $p < 0.001$ (Figure 5A). Neither MRI-PMbdex nor mPSAD showed net benefit over performing biopsies on all men until a csPCa probability threshold of 65% was reached. In addition, from the 65% probability threshold of csPCa, both MRI-PMbdex and mPSAD showed minimal benefit over performing biopsies on all men (Figure 5B).

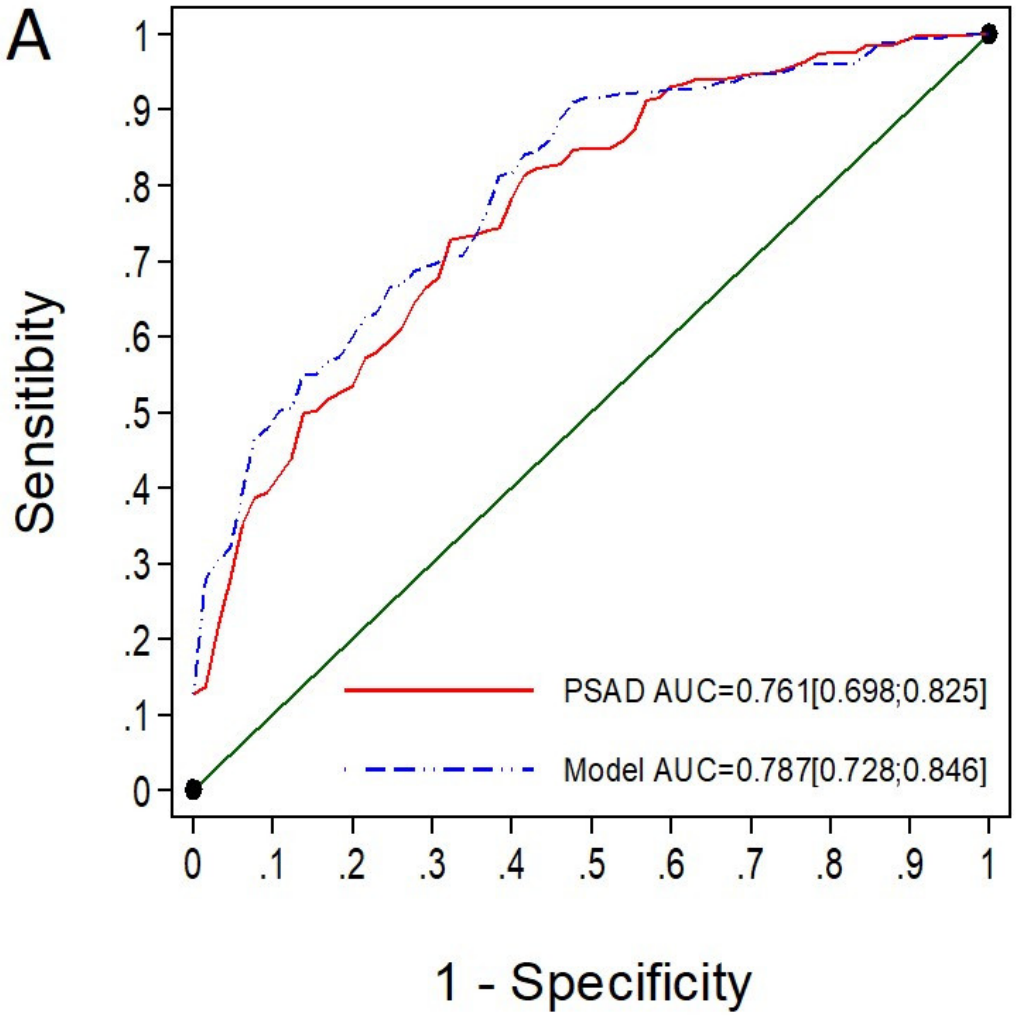
A
Sensitibity
1
.9
.8
.7
.6
.5
.4
.3
.2
.1
0
0
.1
.2
.3
.4
.5
.6
.7
.8
.9
1
PSAD AUC=0.761[0.698;0.825]
Model AUC=0.787[0.728;0.846]
1 - Specificity

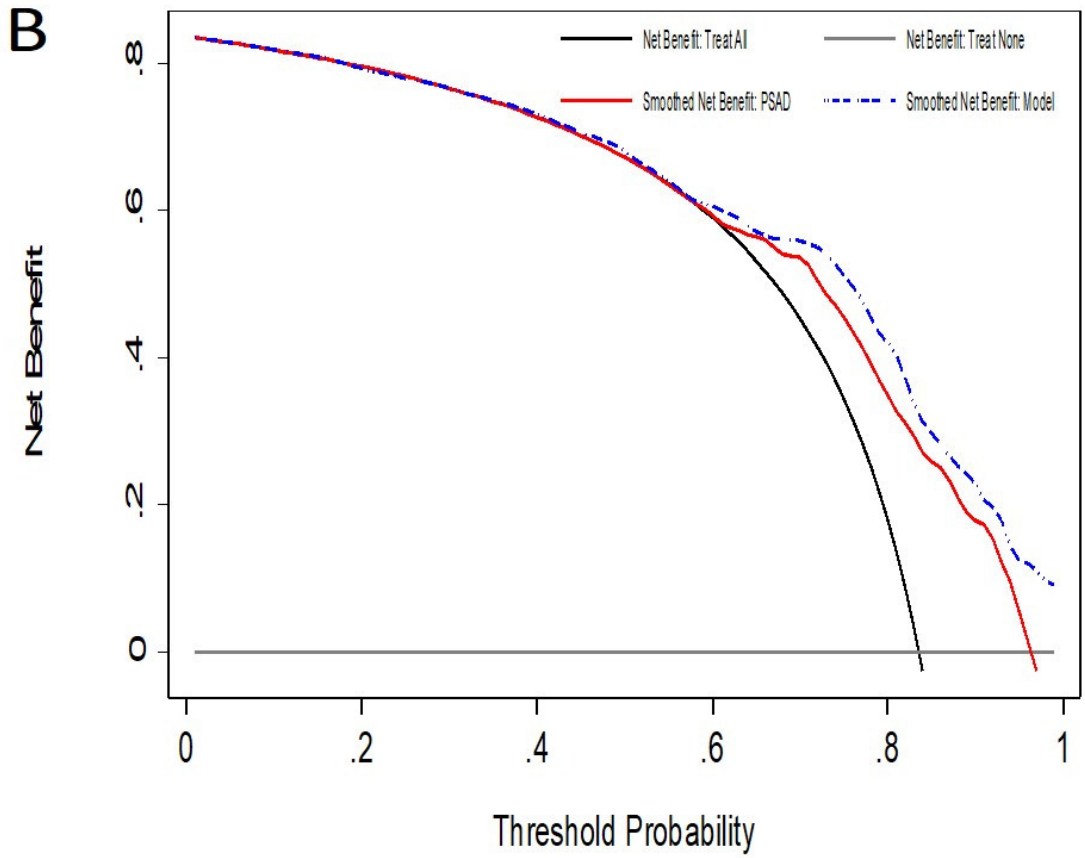

Figure 5. The ROC curves and AUCs show the efficacy of mPSAD (PSAD in the graphic) and MRI-PMbdex (model in the graphic) in detecting csPCa in men with PI-RADS 5 (**A**). The DCAs showing the net benefit of mPSAD and MRI-PMbdex over performing biopsies on all men according to the csPCa probability threshold (**B**).

The selected thresholds for MRI-PMbdex and mPSAD provided sensitivities of 100% and 97.3% as well as specificities of 4.6% and 20%, respectively, in men with PI-RADS 5. MRI-PMbdex avoided 0.8% of prostate biopsies, while mPSAD avoided 5.6%. The rate of missed csPCa was 0% for MRI-PMbdex and 2.7% for mPSAD. Moreover, mPSAD did not detect 4 PCa with ISUP-GG ≥ 4 (Table 7).

Table 7. Performance of MRI-PSAD and Barcelona MRI-predictive model in men with PI-RADS 5, from the respective thresholds of 0.628 ng/mL^2 and 13.5%.

Parameter	mPSAD	MRI-PMbdex
Sensitivity	322/331 (97.3)	331/331 (100)
Specificity	13/65 (20.0)	3/65 (4.6)
Negative predictive value	13/22 (59.1)	3/3 (100)
Positive predictive value	322/374 (86.1)	331/393 (84.2)
Accuracy	335/396 (84.6)	334/396 (84.3)
Avoided biopsies	22/396 (5.6)	3/396 (0.8)
Missed csPCa	9/331 (2.7)	0/331 (0)
Odds Ratio (95% CI)	8.94 (3.63–21.98)	-

p Value	<0.001	=0.004
GG 2	2	0
GG 3	3	0
GG 4	3	0
GG 5	1	0

4. Discussion

First, the characteristics of suspected PCa regarding PI-RADS categories are considered. The similar characteristics of men with PI-RADS 1 and PI-RADS 2, in addition to similar csPCa detection rates (9.8% vs. 10.6%) and high iPCa over detection rates (above 50%) in both subsets, justify considering these two PI-RADS categories as a negative mpMRI. The observed 90% negative predictive value of mpMRI was in the recently reported ranges (i.e., 80–95%) [10–12]. The characteristics of suspected PCa with PI-RADS 3 were closer to those with PI-RADS 2 than those with PI-RADS 4. Moreover, the csPCa detection rate with PI-RADS 3 (16.9%) was closer to that of men with PI-RADS 2 (10.8%) than that of men with PI-RADS 4 (52.2%). Therefore, PI-RADS 3 is an uncertain scenario more similar to a negative MRI than to PI-RADS 4; this justifies why some authors consider men with PI-RADS < 4 as candidates to avoid prostate biopsy [9,15]. Finally, the characteristics of those with PI-RADS 5 were notably different from those with PI-RADS 4. Furthermore, the csPCa risk increased with PI-RAD 5, reaching 83.6%. Taking these factors into account, it is clear that considering PI-RADS > 3 in the same group as the other categories is inadvisable. Hence, the data of men with PI-RADS 4 and PI-RADS 5 should be considered separately [5].

PSAD was introduced by Benson et al. in 1992 to improve the specificity of serum PSA in distinguishing men with localised PCa from those with benign prostatic enlargement [17,63]. Shortly after, it was incorporated by Catalona et al. as a tool for prostate biopsy decision-making in the early detection of PCa [64]. The inverse relationship between prostate volume and PCa risk has been recently confirmed in a systematic review of the literature from the last thirty years [65]. Transrectal ultrasonography was recommended for assessing the prostate volumetry for PSAD calculation from the beginning, as it yields a more accurate assessment than suprapubic ultrasonography [66]. Most studies analysing the clinical usefulness of PSAD have assessed the prostate volume just before TRUS systematic biopsies [67–70]. However, routine TRUS prostate volume assessment for calculating PSAD is not typically performed for prostate biopsy decision-making. The spread ERSPC (European Randomised Screening Prostate Cancer) risk calculator has incorporated the highly subjective prostate volume estimation from DRE [71,72]. The main reason for the current resurgence of PSAD may be the spread of pre-biopsy MRI [73], which provides the most accurate prostate volume assessment without additional cost; this helps avoid TRUS, which is time-consuming and cumbersome [74]. mPSAD has been directly incorporated as ng/mL^2 into some MRI-PM [23,26,32,33,75] or indirectly incorporated from serum PSA and prostate volume into other MRI-PM [28,38,76–79]. Logistical regressions performed to develop MRI-PM have shown PSAD to be the most powerful predictor of csPCa after the PI-RADS score. Recent studies analysing the clinical usefulness of mPSAD for csPCa detection according to PI-RADS categories have shown its dynamic behaviour, which suggests the need for different thresholds to obtain similar predictive values in different PI-RADS categories [21,80]. Nevertheless, the proper mPSAD thresholds for specific PI-RADS categories should be selected from each area, given the specific characteristics of cared populations of men with suspected PCa [22,81]. The most recent MRI-PMs share the latest PI-RADS versions, with direct or indirect mPSAD, and may share other independent clinical predictors, such as age, PCa family history, initial or repeat biopsy, and DRE.

Our study is the first to compare mPSAD and MRI-PM in a head-to-head manner for improving the selection of candidates for prostate biopsy in suspected PCa men after

mpMRI. The compared MRI-PMbdex shared the same predictors of csPCa as the recent Barcelona MRI-PM. MRI-PMbdex and mPSAD avoid the inconveniences of modern markers as they are free of cost, do not require sample procurement, and require very little time for the assessment. This study was carried out on a sizable, multicentre population representing a metropolitan area. In all participant institutions, the criteria for PCa suspicion and diagnostic approach adhered to the EAU PCa guidelines [7]. MRI-PMbdex outperformed mPSAD in the entire population, and it exhibited net benefit over mPSAD, which, in turn, exhibited a slight benefit over performing biopsies on all men. The behaviour of both tools regarding PI-RADS categories showed that MRI-PMbdex outperformed mPSAD in each PI-RADS ≤ 4 category, with different degrees of benefit. However, clinical benefit was found for any tool in men with PI-RADS 5. Additionally, mPSAD did not detect more aggressive tumours compared to MRI-PMbdex in men with PI-RADS ≥ 4. The different behaviour of mPSAD [21] and MRI-PMs [38] regarding PI-RADS categories is the consequence of the incidence of csPCa among them. We selected different thresholds of mPSAD to obtain similar performance in our series of PI-RADS 3 than that of Görtz et al. [22,81]. The use of appropriate thresholds in different populations has been previously described for mPSAD [19–21,82–95].

The limitations of this study include the design, which is prone to sampling and selection biases. Furthermore, no concordance analysis was performed by the pathologists, radiologists, and urologists involved in the study. In addition, the inter-variability that is inevitable among researchers involved in multicentric studies also exists. Moreover, prostate biopsies and mPSAD suffer from intrinsic limitations related to the heterogeneity of prostate cancer and prostate volume. The lack of histopathological analysis of surgical specimens is another limitation, although not every PCa patient undergoes radical prostatectomy. While the definition we adopted for csPCa is the most common one, it may not represent the true csPCa. Moreover, as the MRI-PMbdex is not the developed Barcelona MRI-PM, the results cannot be attributed to this model. Hence, further studies analysing the clinical usefulness of mPSAD and MRI-PMs according to PI-RADS categories are needed.

It will be important in the future to include the results of radiomics and radio-genomics to improve the next generation of MRI-PMs. It appears likely that we will have more powerful predictors than PI-RADS and a more refined definition of csPCa based on genomic expression in addition to the current the pathology of prostate biopsies or surgical specimens [96,97].

5. Conclusions

MRI-PMbdex, which used the same predictors as the recent Barcelona MRI-PM, outperformed mPSAD in the proper selection of candidates for prostate biopsy. MRI-PMbdex exhibited net benefit over mPSAD in men with PI-RADS ≤ 4. However, regarding men with PI-RADS 5, neither tool showed clinical benefit over biopsy. The clinical usefulness of tools that improve the selection of candidates for prostate biopsy in the entire population does not represent those observed in each PI-RADS category.

Author Contributions: Conceptualization, J.M., A.B.-F., M.T. and L.M.E.; methodology, J.M., A.B.-F. and L.M.E.; software, L.M.E. and A.B.-F.; formal analysis, J.M., A.B.-F., M.T. and L.M.E.; resources, J.M.; data curation, A.C., L.R., R.M., I.M.d.T., M.E.S., J.M.A., P.S., M.T. and J.P.; interpretation, J.M., A.B.-F. and L.M.E., A.S. and E.T.; writing—original draft preparation, J.M. and M.T.; writing—review and editing, J.M., A.B.-F., L.M.E., A.S. and E.T.; supervision, E.T.; project administration, J.M.; funding acquisition, J.M. All authors have read and agreed to the published version of the manuscript.

Funding: This research was funded by Instituto de Salut Carlos III (ESP), grant number PI20/01666.

Institutional Review Board Statement: The study was conducted in accordance with the Declaration of Helsinki and approved by the Institutional Review of Vall d´Hebron Hospital Campus (PR/AG-317/2017, approved on 28 August 2017).

Informed Consent Statement: Informed consent was obtained from all subjects involved in the study.

Data Availability Statement: The data presented in this study are available on request from the corresponding author.

Conflicts of Interest: The authors declare no conflict of interest.

Acronyms and Abbreviations

CI	confidence interval
csPCa	clinically significant PCa
DRE	digital rectal examination
GG	grade group
iPCa	insignificant PCa
IQR	interquartile range
mPSAD	MRI associated PSAD
MRI	magnetic resonance imaging
PCa	prostate cancer
PI-RADS	prostate imaging-report and data system
PSA	prostate-specific antigen
PSAD	PSA density
PM	predictive model
PMbdex	developed and externally validated Barcelona PM
RC	risk calculator
TRUS	transrectal ultrasound

References

1. Hugosson, J.; Roobol, M.J.; Månsson, M.; Tammela, T.L.J.; Zappa, M.; Nelen, V.; Kwiatkowski, M.; Lujan, M.; Carlsson, S.V.; Talala, K.M.; et al. A 16-yr Follow-up of the European Randomized study of Screening for Prostate Cancer. *Eur. Urol.* **2019**, *7*, 643–651.
2. Chou, R.; Croswell, J.M.; Dana, T.; Bougatsos, C.; Blazina, I.; Fu, R.; Gleitsmann, K.; Koenig, H.C.; Lam, C.; Maltz, A.; et al. Screening for prostate cancer: A review of the evidence for the U.S. Preventive Services Task Force. *Ann. Intern. Med.* **2011**, *155*, 762–771.
3. Drazer, M.W.; Huo, D.; Eggener, S.E. National Prostate Cancer Screening Rates After the 2012 US Preventive Services Task Force Recommendation Discouraging Prostate-Specific Antigen-Based Screening. *J. Clin. Oncol.* **2015**, *33*, 2416–2423.
4. Fenton, J.J.; Weyrich, M.S.; Durbin, S.; Liu, Y.; Bang, H.; Melnikow, J. Prostate-Specific Antigen-Based Screening for Prostate Cancer: Evidence Report and Systematic Review for the US Preventive Services Task Force. *JAMA* **2018**, *319*, 1914–1931.
5. US PSTF; Grossman, D.C.; Curry, S.J.; Owens, D.K.; Bibbins-Domingo, K.; Caughey, A.B.; Davidson, K.W.; Doubeni, C.A.; Ebell, M.; Epling, J.W.; et al. Screening for Prostate Cancer: US Preventive Services Task Force Recommendation Statement. *JAMA* **2018**, *319*, 1901–1913.
6. Van Poppel, H.; Hogenhout, R.; Albers, P.; van den Bergh, R.C.N.; Barentsz, J.O.; Roobol, M.J. A European Model for an Organised Risk-stratified Early Detection Programme for Prostate Cancer. *Eur. Urol. Oncol.* **2021**, *80*, 703–711.
7. Mottet, N.; van den Bergh, R.C.N.; Briesrs, E.; Briers, E.; Van den Broeck, T.; Cumberbatch, M.G.; De Santis, M.; Fanti, S.; Fossati, N.; Gandaglia, G.; et al. EAU-EANM-ESTRO-ESUR-SIOG Guidelines on Prostate Cancer-2020 Update. Part 1: Screening, Diagnosis, and Local Treatment with Curative Intent. *Eur. Urol.* **2021**, *79*, 243–262.
8. Schoots, I.G. MRI in early prostate cancer detection: How to manage indeterminate or equivocal PI-RADS 3 lesions. *Transl. Androl. Urol.* **2018**, *7*, 770–782.
9. Maggi, M.; Panebianco, V.; Mosca, A.; Salciccia, S.; Gentilucci, A.; Di Pierro, G.; Busetto, G.M.; Barchetti, G.; Campa, R.; Sperduti, I.; et al. Prostate Imaging Reporting and Data System 3 Category Cases at Multiparametric Magnetic Resonance for Prostate Cancer: A Systematic Review and Meta-Analysis. *Eur. Urol. Focus.* **2020**, *6*, 463–478.
10. Moldovan, P.C.; Van den Broeck, T.; Sylvester, R.; Marconi, L.; Bellmunt, J.; van den Bergh, R.C.; Bolla, M.; Briers, E.; Cumberbatch, M.G.; Fossati, N.; et al. What Is the Negative Predictive Value of Multiparametric Magnetic Resonance Imaging in Excluding Prostate Cancer at Biopsy? A Systematic Review and Meta-analysis from the European Association of Urology Prostate Cancer Guidelines Panel. *Eur. Urol.* **2017**, *71*, 618–629.
11. Sathianathen, N.J.; Omer, A.; Harriss, E.; Davies, L.; Kasivisvanathan, V.; Punwani, S.; Moore, C.M.; Kastner, C.; Barrett, T.; Van Den Bergh, R.C.; et al. Negative Predictive Value of Multiparametric Magnetic Resonance Imaging in the Detection of Clinically Significant Prostate Cancer in the Prostate Imaging Reporting and Data System Era: A Systematic Review and Meta-Analysis. *Eur Urol.* **2020**, *78*, 402–414.

12. Wagaskar, V.G.; Levy, M.; Ratnani, P.; Moody, K.; Garcia, M.; Pedraza, A.M.; Parekh, S.; Pandav, K.; Shukla, B.; Prasad, S.; et al. Clinical Utility of Negative Multiparametric Magnetic Resonance Imaging in the Diagnosis of Prostate Cancer and Clinically Significant Prostate Cancer. *Eur. Urol. Open Sci.* **2021**, *28*, 9–16.
13. Kasivisvanathan, V.; Stabile, A.; Neves, J.; Giganti, F.; Valerio, M.; Shanmugabavan, Y.; Clement, K.; Sarkar, D.; Philippou, Y.; Thurtle, D.; et al. Magnetic Resonance Imaging-targeted Biopsy Versus Systematic Biopsy in the Detection of Prostate Cancer: A Systematic Review and Meta-analysis. *Eur. Urol.* **2019**, *76*, 284–303.
14. Drost, F.H.; Osses, D.; Nieboer, D.; Bangma, C.H.; Steyerberg, E.W.; Roobol, M.J.; Schoots, I.G. Prostate Magnetic Resonance Imaging, with or without Magnetic Resonance Imaging-Targeted Biopsy, and Systematic Biopsy for Detecting Prostate Cancer: A Cochrane Systematic Review and Meta-Analysis. *Eur. Urol.* **2020**, *77*, 78–94.
15. Mazzone, E.; Stabile, A.; Pellegrino, F.; Basile, G.; Cignoli, D.; Cirulli, G.O.; Sorce, G.; Barletta, F.; Scuderi, S.; Bravi, C.A.; et al. Positive Predictive Value of Prostate Imaging Reporting and Data System Version 2 for the Detection of Clinically Significant Prostate Cancer: A Systematic Review and Meta-Analysis. *Eur. Urol. Oncol.* **2021**, *4*, 697–713.
16. Osses, D.F.; Roobol, M.J.; Schoots, I.G. Prediction Medicine: Biomarkers, Risk Calculators and Magnetic Resonance Imaging as Risk Stratification Tools in Prostate Cancer Diagnosis. *Int. J. Mol. Sci.* **2020**, *20*, 1637.
17. Benson, M.C.; Whang, I.S.; Pantuck, A.; Ring, K.; Kaplan, S.A.; Olsson, C.A.; Cooner, W.H. Prostate specific antigen density: A means of distinguishing benign prostatic hypertrophy and prostate cancer. *J. Urol.* **1992**, *147*, 815–816.
18. Dianat, S.S.; Rancier, R.R.M.; Bonekamp, D.; Carter, H.B.; Macura, K.J. Prostate volumetric assessment by magnetic resonance imaging and transrectal ultrasound: Impact of variation in calculated prostate-specific antigen density on patient eligibility for active surveillance program. *J. Comput. Assist. Tomogr.* **2013**, *37*, 589–595.
19. Boesen, L.; Nørgaard, N.; Løgager, V.; Balslev, I.; Bisbjerg, R.; Thestrup, K.C.; Jakobsen, H.; Thomsen, H.S. Prebiopsy Biparametric Magnetic Resonance Imaging Combined with Prostate-specific Antigen Density in Detecting and Ruling out Gleason 7–10 Prostate Cancer in Biopsy-naïve Men. *Eur. Urol. Oncol.* **2019**, *2*, 311–319.
20. Morote, J.; Celma, A.; Planas, J. Re: Lars Boesen, Nis Nørgaard, Vibeke Løgager, et al. Prebiopsy Biparametric Magnetic Resonance Imaging Combined with Prostate-specific Antigen Density in Detecting and Ruling out Gleason 7–10 Prostate Cancer in Biopsy-naïve Men. *Eur. Urol. Oncol.* **2020**, 3, 392–393.
21. Morote, J.; Celma, A.; Diaz, F.; Regis, L.; Roche, S.; Mast, R.; Semidey, M.E.; de Torres, I.M.; Planas, J.; Trilla, E. Prostatic-specific antigen density behavior according to multiparametric magnetic resonance imaging result. *Urol. Oncol.* **2020**, *38*, 410–417.
22. Görtz, M.; Radtke, J.P.; Hatiboglu, G.; Schütz, V.; Tosev, G.; Güttlein, M.; Leichsenring, J.; Stenzinger, A.; Bonekamp, D.; Schlemmer, H.P.; et al. The Value of Prostate-specific Antigen Density for Prostate Imaging-Reporting and Data System 3 Lesions on Multiparametric Magnetic Resonance Imaging: A Strategy to Avoid Unnecessary Prostate Biopsies. *Eur. Urol. Focus.* **2021**, *7*, 325–331.
23. Niu, X.K.; Li, J.; Das, S.K.; Xiong, Y.; Yang, C.B.; Peng, T. Developing a nomogram based on multiparametric magnetic resonance imaging for forecasting high-grade prostate cancer to reduce unnecessary biopsies within the prostate-specific antigen gray zone. *BMC Med. Imaging* **2017**, *17*, 11.
24. Kim, E.H.; Weaver, J.K.; Shetty, A.S.; Vetter, J.M.; Andriole, G.L.; Strope, S.A. Magnetic Resonance Imaging Provides Added Value to the Prostate Cancer Prevention Trial Risk Calculator for Patients with Estimated Risk of High-Grade Prostate Cancer Less Than or Equal to 10. *Urology* **2017**, *102*, 183–189.
25. Lee, S.M.; Liyanage, S.H.; Wulaningsih, W.; Wolfe, K.; Carr, T.; Younis, C.; Van Hemelrijck, M.; Popert, R.; Acher, P. Toward an MRI-based nomogram for the prediction of transperineal prostate biopsy outcome: A physician and patient decision tool. *Urol. Oncol.* **2017**, *35*, 664–668.
26. Mehralivand, S.; Shih, J.H.; Rais-Bahrami, S.; Oto, A.; Bednarova, S.; Nix, J.W.; Thomas, J.V.; Gordetsky, J.B.; Gaur, S.; Harmon, S.A.; et al. A Magnetic Resonance Imaging-Based Prediction Model for Prostate Biopsy Risk Stratification. *JAMA Oncol.* **2018**, *4*, 678–685.
27. Truong, M.; Wang, B.; Gordetsky, J.B.; Nix, J.W.; Frye, T.P.; Messing, E.M.; Thomas, J.V.; Feng, C.; Rais-Bahrami, S. Multi-institutional nomogram predicting benign prostate pathology on magnetic resonance/ultrasound fusion biopsy in men with a prior negative 12-core systematic biopsy. *Cancer* **2018**, *124*, 278–285.
28. Huang, C.; Song, G.; Wang, H.; Li, J.; Chen, Y.; Fan, Y.; Fang, D.; Xiong, G.; Xin, Z.; Zhou, L. MultiParametric Magnetic Resonance Imaging-Based Nomogram for Predicting Prostate Cancer and Clinically Significant Prostate Cancer in Men Undergoing Repeat Prostate Biopsy. *Biomed. Res. Int.* **2018**, *2018*, 6368309.
29. Bjurlin, M.A.; Rosenkrantz, A.B.; Sarkar, S.; Lepor, H.; Huang, W.C.; Huang, R.; Venkataraman, R.; Taneja, S.S. Prediction of Prostate Cancer Risk Among Men Undergoing Combined MRI-targeted and Systematic Biopsy Using Novel Pre-biopsy Nomograms That Incorporate MRI Findings. *Urology* **2018**, *112*, 112–120.
30. Grönberg, H.; Eklund, M.; Picker, W.; Aly, M.; Jäderling, F.; Adolfsson, J.; Landquist, M.; Haug, E.S.; Ström, P.; Carlsson, S.; et al. Prostate Cancer Diagnostics Using a Combination of the Stockholm3 Blood Test and Multiparametric Magnetic Resonance Imaging. *Eur. Urol.* **2018,** *74*, 722–778.
31. Liu, C.; Liu, S.L.; Wang, Z.X.; Yu, K.; Feng, C.X.; Ke, Z.; Wang, L.; Zeng, X.Y. Using the prostate imaging reporting and data system version 2 (PI-RIDS v2) to detect prostate cancer can prevent unnecessary biopsies and invasive treatment. *Asian J. Androl.* **2018**, *20*, 459–464.

32. Borque-Fernando, A.; Esteban, L.M.; Celma, A.; Roche, S.; Planas, J.; Regis, L.; de Torres, I.; Semidey, M.E.; Trilla, E.; Morote, J. How to implement magnetic resonance imaging before prostate biopsy in clinical practice: Nomograms for saving biopsies. *World J. Urol.* **2019**, *38*, 1481–1491.
33. Bjurlin, M.A.; Renson, A.; Rais-Bahrami, S.; Truong, M.; Rosenkrantz, A.B.; Huang, R.; Taneja, S.S. Predicting Benign Prostate Pathology on Magnetic Resonance Imaging/Ultrasound Fusion Biopsy in Men with a Prior Negative 12-core Systematic Biopsy: External Validation of a Prognostic Nomogram. *Eur. Urol. Focus.* **2019**, *5*, 815–822.
34. Alberts, A.R.; Roobol, M.J.; Verbeek, J.F.M.; Schoots, I.G.; Chiu, P.K.; Osses, D.F.; Tijsterman, J.D.; Beerlage, H.P.; Mannaerts, C.K.; ScAhimmöller, L.; et al. Prediction of High-grade Prostate Cancer Following Multiparametric Magnetic Resonance Imaging: Improving the Rotterdam European Randomized Study of Screening for Prostate Cancer Risk Calculators. *Eur. Urol.* **2019**, *75*, 310–318.
35. He, B.M.; Shi, Z.K.; Li, H.S.; Lin, H.Z.; Yang, Q.S.; Lu, J.P.; Sun, Y.H.; Wang, H.F. A Novel Prediction Tool Based on Multiparametric Magnetic Resonance Imaging to Determine the Biopsy Strategy for Clinically Significant Prostate Cancer in Patients with PSA Levels Less than 50 ng/mL. *Ann. Surg. Oncol.* **2020**, 27, 1284–1295.
36. Noh, T.I.; Hyun, C.W.; Kang, H.E.; Jin, H.J.; Tae, J.H.; Shim, J.S.; Kang, S.G.; Sung, D.J.; Cheon, J.; Lee, J.G.; et al. A Predictive Model Based on Bi-parametric Magnetic Resonance Imaging and Clinical Parameters for Clinically Significant Prostate Cancer in the Korean Population. *Cancer Res. Treat.* **2021**, *53*, 1148–1855.
37. Schoots, I.G.; Roobol, M.J. Multivariate risk prediction tools including MRI for individualized biopsy decision in prostate cancer diagnosis: Current status and future directions. *World J. Urol.* **2020**, *38*, 517–529.
38. Morote, J.; Borque-Fernando, A.; Triquell, M.; Celma, A.; Regis, L.; Abascal, J.M.; Sola, C.; Servian, P.; Escobar, M.; Mast, R.; et al. The Barcelona Predictive Model of Clinically Significant Prostate Cancer. *Cancers* **2022**, *14*, 1589.
39. Remmers, S.; Kasivisvanathan, V.; Verbeek, J.F.M.; Moore, C.M.; Roobol, M.J. ERSPC RSGPRECISIONIG. Reducing Biopsies and Magnetic Resonance Imaging Scans during the Diagnostic Pathway of Prostate Cancer: Applying the Rotterdam Prostate Cancer Risk Calculator to the PRECISION Trial Data. *Eur. Urol. Open Sci.* **2022**, *36*, 1–8.
40. Vickers, A.J.; Russo, G.; Lilja, H.; Evans, C.; Schalken, J.A.; Klein, E.; Eggener, S. How Should Molecular Markers and Magnetic Resonance Imaging Be Used in the Early Detection of Prostate Cancer. *Eur. Urol. Oncol.* **2021**, 5, 135–137. https://doi.org/10.1016/j.euo.2021.01.010.
41. Punnen, S.; Freedland, S.J.; Polascik, T.J.; Loeb, S.; Risk, M.C.; Savage, S.; Mathur, S.C.; Uchio, E.; Dong, Y.; Silberstein, J.L. A Multi-Institutional Prospective Trial Confirms Noninvasive Blood Test Maintains Predictive Value in African American Men. *J. Urol.* **2018**, *199*, 1459–1463.
42. Punnen, S.; Nahar, B.; Soodana-Prakash, N.; Koru-Sengui, T.; Stoyanova, R.; Pollack, A.; Gonzalgo, M.L.; Ritch, C.R.; Parekh, J. Optimizing patient's selection for prostate biopsy: A single institution experience with multi-parametric MRI and the 4Kscore test for the detection of aggressive prostate cance. *PLoS ONE* **2018**, *13*, e0201384.
43. Marzouk, K.; Ehdaie, B.; Vertosick, E.; Zappala, S.; Vickers, A. Developing an effective strategy to improve the detection of significant prostate cancer by combining the 4Kscore and multiparametric MRI. *Urol. Oncol.* **2019**, *37*, 672–677.
44. Falagario, U.G.; Martini, A.; Wajswol, E.; Treacy, P.J.; Ratnani, P.; Jambor, I.; Anastos, H.; Lewis, S.; Haines, K.; Cormio, L.; et al. Avoiding Unnecessary Magnetic Resonance Imaging (MRI) and Biopsies: Negative and Positive Predictive Value of MRI According to Prostate-specific Antigen Density, 4Kscore and Risk Calculators. *Eur. Urol. Oncol.* **2020**, *3*, 700–704.
45. Wagaskar, V.G.; Sobotka, S.; Ratnani, P.; Young, J.; Lantz, A.; Pareckh, S.; Falagario, U.G.; Li, L.; Lewis, S.; Punnen, S.; et al. A 4K score/MRI-based nomogram for predicting prostate cancer, clinically significant prostate cancer, and unfavorable prostate cancer. *Cancer Rep*. **2021**, *4*, e1357.
46. Porpiglia, F.; Russo, F.; Manfredi, M.; Mele, F.; Fiori, C.; Bollito, E.; Papotti, M.; Molineris, I.; Passera, R.; Regge, D. The roles of multiparametric MRI, PCA3 and PHI: Which is the best predictor of prostate cancer after a negative biopsy? Results of a prospective study. *J. Urol.* **2014**, *192*, 60–66.
47. Gnanapragasam, V.J.; Burling, K.; George, A.; Stearn, S.; Warren, A.; Barrett, T.; Koo, B.; Gallagher, F.A.; Doble, A.; Kastner, C.; et al. The Prostate Health Index adds predictive value to multi-parametric MRI in detecting significant prostate cancers in a repeat biopsy population. *Sci. Rep.* **2016**, *6*, 35364.
48. Fan, Y.H.; Pan, P.H.; Cheng, W.M.; Wang, H.K.; Shen, S.H.; Liu, H.T.; Cheng, H.M.; Chen, W.R.; Huang, T.H.; Wei, T.C.; et al. The Prostate Health Index aids multi-parametric MRI in diagnosing significant prostate cancer. *Sci. Rep.* **2021**, *11*, 1286.
49. Hendriks, R.J.; van der Leest, M.M.G.; Dijkstra, S.; Barentsz, J.O.; Van Criekinge, W.; Hulsbergen-van de Kaa, C.A.; Schalken, J.A.; Mulders, P.F.A.; van Oort, I.M. A urinary biomarker-based risk score correlates with multiparametric MRI for prostate cancer detection. *Prostate* **2017**, *77*, 1401–1407.
50. Hendriks, R.J.; van der Leest, M.M.G.; Israël, B.; Hannink, G.; YantiSetiasti, A.; Cornel, E.B.; Hulsbergen-van de Kaa, C.A.; Klaver, O.S.; Sedelaar, J.P.M.; Van Criekinge, W.; et al. Clinical use of the SelectMDx urinary-biomarker test with or without mpMRI in prostate cancer diagnosis: A prospective, multicenter study in biopsy-naïve men. *Prostate Cancer Prostatic Dis.* **2021**, *24*, 1110–1119.
51. Maggi, M.; Del Giudice, F.; Falagario, U.G.; Cocci, A.; Russo, G.I.; Di Mauro, M.; Sepe, G.S.; Galasso, F.; Leonardi, R.; Iacona, A.; et al. SelectMDx and Multiparametric Magnetic Resonance Imaging of the Prostate for Men Undergoing Primary Prostate Biopsy: A Prospective Assessment in a Multi-Institutional Study. *Cancers* **2021,** *13*, 2047.

52. Morote, J.; Campistol, M.; Regis, L.; Celma, A.; de Torres, I.; Semidey, M.E.; Roche, S.; Mast, R.; Santamaria, A.; Planas, J.; et al. Who with suspected prostate cancer can benefit from Proclarix after multiparametric magnetic resonance imaging. *Int. J. Biol. Markers* **2022**, 3936155221081537. https://doi.org/10.1177/03936155221081537.
53. Morote, J.; Campistol, M.; Celma, A.; Regis, L.; de Torres, I.; Semidey, M.E.; Roche, S.; Mast, R.; Santamaría, A.; Planas, J.; et al. The Efficacy of Proclarix to Select Appropriate Candidates for Magnetic Resonance Imaging and Derived Prostate Biopsies in Men with Suspected Prostate Cancer. *World J. Mens Health* **2022**, *40*, 270–279.
54. Barentsz, J.O.; Richenberg, J.; Clements, R.; Choyke, P.; Verma, S.; Villeirs, G.; Rouviere, O.; Logager, V.; Futterer, J.J. ESUR prostate MR guidelines 2012. *Eur. Radiol.* **2012**, *22*, 746–757.
55. Weinreb, J.C.; Barentsz, J.O.; Choyke, P.L.; Choyke, P.L.; Cornud, F.; Haider, M.A.; Macura, K.J.; Margolis, D.; Schnall, M.D.; Shtern, F.; et al. PI-RADS Prostate Imaging—Reporting and Data System: 2015, Version 2. *Eur. Urol.* **2016**, *69*, 16–40.
56. Schoots, I.G.; Roobol, M.J.; Nieboer, D.; Bangma, C.H.; Steyerberg, E.W.; Hunink, M.G. Magnetic resonance imaging-targeted biopsy may enhance the diagnostic accuracy of significant prostate cancer detection compared to standard transrectal ultrasound-guided biopsy: A systematic review and meta-analysis. *Eur. Urol.* **2015**, *68*, 438–450.
57. Epstein, J.I.; Egevad, L.; Amin, M.B.; Delahunt, B.; Srigley, J.R.; Humphrey, P.A.; Grading, C. The 2014 International Society of Urological Pathology (ISUP) Consensus Conference on Gleason Grading of Prostatic Carcinoma: Definition of Grading Patterns and Proposal for a New Grading System. *Am. J. Surg. Pathol.* **2016**, *40*, 244–252.
58. McShane, L.M.; Altman, D.G.; Sauerbrei, W.; Taube, S.E.; Gion, M.; Clark, G.M. Statistics SOTNCI-EORTCWGOCD. REporting recommendations for tumour MARKer prognostic studies (REMARK). *Br. J. Cancer* **2005**, *93*, 387–391.
59. Bossuyt, P.M.; Reitsma, J.B.; Bruns, D.E.; Korevaar, D.A. STARD 2015: An updated list of essential items for reporting diagnostic accuracy studies. *BMJ* **2015**, *351*, h5527.
60. Creelman, C.D.; Donaldson, W. ROC curves for discrimination of linear extent. *J. Exp. Psychol.* **1968**, *77*, 514–516.
61. DeLong, E.R.; DeLong DMClarke-Pearson, D.L. Comparing the areas under two or more correlated receiver operating characteristic curves: A nonparametric approach. *Biometrics* **1988**, *44*, 837–845.
62. Vickers, A.J.; Elkin, E.B. Decision curve analysis: A novel method for evaluating prediction models. *Med. Decis. Mak.* **2006**, *26*, 565–574.
63. Benson, M.C.; Whang, I.S.; Olsson, C.A.; McMahon, D.J.; Cooner, W.H. The use of prostate specific antigen density to enhance the predictive value of intermediate levels of serum prostate specific antigen. *J. Urol.* **1992**, *147*, 817–821.
64. Catalona, W.J.; Richie, J.P.; deKernion, J.B.; Ahmann, F.R.; Ratliff, T.L.; Dalkin, B.L.; Kavoussi, L.R.; MacFarlane, M.T.; Southwick, P.C. Comparison of prostate specific antigen concentration versus prostate specific antigen density in the early detection of prostate cancer: Receiver operating characteristic curves. *J. Urol.* **1994**, *152*, 2031–2036.
65. Yamashiro, J.R.; de Riese, W.T.W. Any Correlation Between Prostate Volume and Incidence of Prostate Cancer: A Review of Reported Data for the Last Thirty Years. *Res. Rep. Urol.* **2021**, *13*, 749–757.
66. Bangma, C.H.; Niemer, A.Q.; Grobbee, D.E.; Schröder, F.H. Transrectal ultrasonic volumetry of the prostate: In vivo comparison of different methods. *Prostate* **1996**, *28*, 107–110.
67. Thon, W.F.; Gadban, F.; Truss, M.C.; Kuczyk, M.; Hartmann, U.; Jonas, U. Prostate-specific antigen density a reliable parameter for the detection of prostate cancer. *World J. Urol.* **1996**, *14*, 53–58.
68. Keetch, D.W.; McMurtry, J.M.; Smith, D.S.; Andriole, G.L.; Catalona, W.J. Prostate specific antigen density versus prostate specific antigen slope as predictors of prostate cancer in men with initially negative prostatic biopsies. *J. Urol.* **1996**, *156*, 428–431.
69. Morote, J.; Raventós, C.X.; Lorente, J.A.; Lopez-Pacios, M.A.; Encabo, G.; de Torres, I.; Andreu, J. Comparison of percent free prostate specific antigen and prostate specific antigen density as methods to enhance prostate specific antigen specificity in early prostate cancer detection in men with normal rectal examination and prostate specific antigen between 4.1 and 10 ng/mL. *J. Urol.* **1997**, *158*, 502–504.
70. Loeb, S.; Roehl, K.A.; Thaxton, C.S.; Catalona, W.J. Combined prostate-specific antigen density and biopsy features to predict "clinically insignificant" prostate cancer. *Urology* **2008**, *72*, 143–147.
71. Roobol, M.J.; Schröder, F.H.; Hugosson, J.; Jones, J.S.; Kattan, M.W.; Klein, E.A.; Hamdy, F.; Neal, D.; Donovan, J.; Parekh, D.J.; et al. Importance of prostate volume in the European Randomised Study of Screening for Prostate Cancer (ERSPC) risk calculators: Results from the prostate biopsy collaborative group. *World J. Urol.* **2012**, *30*, 149–155.
72. Roobol, M.J.; van Vugt, H.A.; Loeb, S.; Zhu, X.; Bul, M.; Bangma, C.H.; van Leenders, A.G.; Steyerberg, E.W.; Schröder, F.H. Prediction of prostate cancer risk: The role of prostate volume and digital rectal examination in the ERSPC risk calculators. *Eur. Urol.* **2012**, *61*, 577–583.
73. Christie, D.R.H.; Sharpley, C.F. How Accurately Can Prostate Gland Imaging Measure the Prostate Gland Volume? Results of a Systematic Review. *Prostate Cancer* **2019**, *2019*, 6932572.
74. Jeong, C.W.; Park, H.K.; Hong, S.K.; Byun, S.S.; Lee, H.J.; Lee, S.E. Comparison of prostate volume measured by transrectal ultrasonography and MRI with the actual prostate volume measured after radical prostatectomy. *Urol. Int.* **2008**, *81*, 179–185.
75. Boesen, L.; Thomsen, F.B.; Nørgaard, N.; Løgager, V.; Balslev, I.; Bisbjerg, R.; Thomsen, H.S.; Jakobsen, H. A predictive model based on biparametric magnetic resonance imaging and clinical parameters for improved risk assessment and selection of biopsy-naïve men for prostate biopsies. *Prostate Cancer Prostatic Dis.* **2019**, *2*, 311–319.
76. Fang, D.; Zhao, C.; Ren, D.; Yu, W.; Wang, R.; Wang, H.; Li, X.; Yin, W.; Yu, X.; Yang, K.; et al. Could Magnetic Resonance Imaging Help to Identify the Presence of Prostate Cancer Before Initial Biopsy? The Development of Nomogram Predicting the Outcomes of Prostate Biopsy in the Chinese Population. *Ann. Surg. Oncol.* **2016**, *23*, 4284–4292.

77. Radtke, J.P.; Wiesenfarth, M.; Kesch, C.; Freitag, M.T.; Alt, C.D.; Celik, K.; Distler, F.; Roth, W.; Wieczorek, K.; Stock, C.; et al. Combined Clinical Parameters and Multiparametric Magnetic Resonance Imaging for Advanced Risk Modeling of Prostate Cancer-Patient-tailored Risk Stratification Can Reduce Unnecessary Biopsies. *Eur. Urol.* **2017**, *72*, 888–896.
78. Van Leeuwen, P.J.; Hayen, A.; Thompson, J.E.; James, E.; Moses, D.; Shnier, R.; Böhm, M.; Abuodha, M.; Haynes, A.M.; Ting, F.; et al. A multiparametric magnetic resonance imaging-based risk model to determine the risk of significant prostate cancer prior to biopsy. *BJU Int.* **2017**, *120*, 774–781.
79. Chen, R.; Verbeek, J.F.M.; Yang, Y.; Song, Z.; Sun, Y.; Roobol, M.J. Comparing the prediction of prostate biopsy outcome using the Chinese Prostate Cancer Consortium (CPCC) Risk Calculator and the Asian adapted Rotterdam European Randomized Study of Screening for Prostate Cancer (ERSPC) Risk Calculator in Chinese and European men. *World J. Urol.* **2021**, *39*, 73–80.
80. Schoots, I.G.; Padhani, A.R.; Rouvière, O.; Barentsz, J.O.; Richenberg, J. Risk-adapted biopsy decision based on prostate magnetic resonance imaging and prostate-specific antigen density for enhanced biopsy avoidance in first prostate cancer diagnostic evaluation. *BJU Int.* **2021**, *127*, 175–178.
81. Gortz, M.; Radtke, J.P.; Hatiboglu, G.; Schutz, V.; Tosev, G.; Guttlein, M.; Leichsenring, J.; Stenzinger, A.; Bonekamp, D.; Schlemmer, H.-P.; et al. The Value of Prostate-specific Antigen Density for Prostate Imaging-Reporting and Data System 3 Lesions on Multiparametric Magnetic Resonance Imaging: A Strategy to Avoid Unnecessary Prostate Biopsies. *Eur. Urol. Focus* **2021**, *7*, 325–331. https://doi.org/10.1016/j.euf.2019.11.012.
82. Washino, S.; Okochi, T.; Saito, K.; Konishi, T.; Hirai, M.; Kobayashi, Y.; Miyagawa, T. Combination of prostate imaging reporting and data system (PI-RADS) score and prostate-specific antigen (PSA) density predicts biopsy outcome in prostate biopsy naïve patients. *BJU Int.* **2017**, *119*, 225–233.
83. Jue, J.S.; Barboza, M.P.; Prakash, N.S.; Venkatramani, V.; Sinha, V.R.; Pavan, N.; Nahar, B.; Kanabur, P.; Ahdoot, M.; Dong, Y.; et al. Re-examining Prostate-specific Antigen (PSA) Density: Defining the Optimal PSA Range and Patients for Using PSA Density to Predict Prostate Cancer Using Extended Template Biopsy. *Urology* **2017**, *105*, 123–128.
84. Hansen, N.L.; Barrett, T.; Koo, B.; Doble, A.; Gnanapragasam, V.; Warren, A.; Kastner, C.; Bratt, O. The influence of prostate-specific antigen density on positive and negative predictive values of multiparametric magnetic resonance imaging to detect Gleason score 7-10 prostate cancer in a repeat biopsy setting. *BJU Int.* **2017**, *119*, 724–730.
85. Distler, F.A.; Radtke, J.P.; Bonekamp, D.; Kesch, C.; Schlemmer, H.-P.; Wieczorek, K.; Kirchner, M.; Pahernik, S.; Hohenfellner, M.; Hadaschik, B.A. The Value of PSA Density in Combination with PI-RADS™ for the Accuracy of Prostate Cancer Prediction. *J. Urol.* **2017**, *198*, 575–582.
86. Kotb, A.F.; Spaner, S.; Crump, T.; Hyndman, M.E. The role of mpMRI and PSA density in patients with an initial negative prostatic biopsy. *World J. Urol.* **2018**, *36*, 2021–2025.
87. Stevens, E.; Truong, M.; Bullen, J.A.; Ward, R.D.; Purysko ASKlein, E.A. Clinical utility of PSAD combined with PI-RADS category for the detection of clinically significant prostate cancer. *Urol. Oncol.* **2020**, *38*, 846–849.
88. Ryoo, H.; Kang, M.Y.; Sung, H.H.; Chang Jeong, B.; Seo, S.I.; Jeon, S.S.; Lee, H.M.; Jeon, H.G. Detection of prostate cancer using prostate imaging reporting and data system score and prostate-specific antigen density in biopsy-naive and prior biopsy-negative patients. *Prostate Int.* **2020**, *8*, 25–29.
89. Yusim, I.; Krenawi, M.; Mazor, E.; Novack, V.; Mabjeesh, N.J. The use of prostate specific antigen density to predict clinically significant prostate cancer. *Sci. Rep.* **2020**, *10*, 20015.
90. Yu, J.; Boo, Y.; Kang, M.; Sung, H.H.; Jeong, B.C.; Seo, S.; Jeon, S.S.; Lee, H.; Jeon, H.G. Can Prostate-Specific Antigen Density Be an Index to Distinguish Patients Who Can Omit Repeat Prostate Biopsy in Patients with Negative Magnetic Resonance Imaging. *Cancer Manag. Res.* **2021**, *13*, 5467–5475.
91. Falagario, U.G.; Jambor, I.; Lantz, A.; Ettala, O.; Stabile, A.; Taimen, P.; Aronen, H.J.; Knaapila, J.; Perez, I.M.; Gandaglia, G.; et al. Combined Use of Prostate-specific Antigen Density and Magnetic Resonance Imaging for Prostate Biopsy Decision Planning: A Retrospective Multi-institutional Study Using the Prostate Magnetic Resonance Imaging Outcome Database (PROMOD). *Eur. Urol. Oncol.* **2021**, *4*, 971–979.
92. Girometti, R.; Giannarini, G.; Panebianco, V.; Maresca, S.; Cereser, L.; De Martino, M.; Pizzolitto, S.; Pecoraro, M.; Ficarra, V.; Zuiani, C.; et al. Comparison of different thresholds of PSA density for risk stratification of PI-RADSv2.1 categories on prostate MRI. *Br. J. Radiol.* **2021,** *95*, 20210886.
93. Tafuri, A.; Iwata, A.; Shakir, A.; Iwata, T.; Gupta, C.; Sali, A.; Sugano, D.; Mahdi, A.S.; Cacciamani, G.E.; Kaneko, M.; et al. Systematic Biopsy of the Prostate can Be Omitted in Men with PI-RADS™ 5 and Prostate Specific Antigen Density Greater than 15. *J. Urol.* **2021**, *206*, 289–297.
94. Wang, Z.B.; Wei, C.G.; Zhang, Y.Y.; Pan, P.; Dai, G.C.; Tu, J.; Shen, J.K. The Role of PSA Density among PI-RADS v2.1 Categories to Avoid an Unnecessary Transition Zone Biopsy in Patients with PSA 4–20 ng/mL. *Biomed. Res. Int.* **2021**, 2021, 3995789.
95. Haroon, M.; Sathiadoss, P.; Breau, R.H.; Cagiannos, I.; Flood, T.; Lavallee, L.T.; Morash, C.; Shieda, N. Proportion of clinically significant prostate cancer diagnosed by systematic template biopsy after negative pre-biopsy multiparametric magnetic resonance imaging and predictive value of prostate-specific antigen density. *Can. Urol. Assoc. J.* **2022**, *16*, 178–180.
96. Woźnicki, P.; Westhoff, N.; Huber, T.; Riffel, P.; Froelich, M.F.; Gresser, E.; von Hardenberg, J.; Mühlberg, A.; Michel, M.S.; Schoenberg, S.O.; et al. Multiparametric MRI for Prostate Cancer Characterization: Combined Use of Radiomics Model with PI-RADS and Clinical Parameters. *Cancers* **2020**, *12*, 1767.
97. Ferro, M.; de Cobelli, O.; Vartolomei, M.D.; Lucarelli, G.; Crocetto, F.; Barone, B.; Sciarra, A.; Del Giudice, F.; Muto, M.; Maggi, M.; et al. Prostate Cancer Radiogenomics—From Imaging to Molecular Characterization. *Int. J. Mol. Sci.* **2021**, *22*, 9971.

5.4. PUBLICACIÓN 4

Título: Comparison of Rotterdam and Barcelona Magnetic Resonance Imaging Risk Calculators for Predicting Clinically Significant Prostate Cancer

Revista: European Urology Open Science

Año de publicación: 2023

Volumen: 53

Páginas: 46 – 54

DOI: https://doi.org/10.1016/j.euros.2023.03.013

Autores: Juan Morote, Ángel Borque-Fernando, Marina Triquell, Miriam Campistol, Pol Servian, Jose M. Abascal, Jacques Planas, Olga Méndez, Luis M. Esteban y Enrique Trilla

Factor de impacto: 3.2 (2023)

Cuartil: Q1 (Urología)

EUROPEAN UROLOGY OPEN SCIENCE 53 (2023) 46–54

available at www.sciencedirect.com
journal homepage: www.eu-openscience.europeanurology.com

European Association of Urology

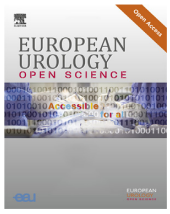

Prostatic Disease

Comparison of Rotterdam and Barcelona Magnetic Resonance Imaging Risk Calculators for Predicting Clinically Significant Prostate Cancer

Juan Morote[a,b,†,*], *Ángel Borque-Fernando*[c,†], *Marina Triquell*[a,b], *Miriam Campistol*[a,b], *Pol Servian*[d], *José M. Abascal*[e,f], *Jacques Planas*[a,b], *Olga Méndez*[g], *Luis M. Esteban*[h,‡], *Enrique Trilla*[a,b,‡]

[a] *Department of Urology, Vall d'Hebron Hospital, Barcelona, Spain;* [b] *Department of Surgery, Universitat Autònoma de Barcelona, Bellaterra, Spain;* [c] *Department of Urology, Hospital Miguel Servet, IIS-Aragon, Zaragoza, Spain;* [d] *Department of Urology, Hospital Germans Trias I Pujol, Badalona, Spain;* [e] *Department of Urology, Parc de Salut Mar, Barcelona, Spain;* [f] *Department of Surgery, Universitat Pompeu Fabra, Badalona, Spain;* [g] *Biomedical Research in Urology Unit, Vall d'Hebron Research Institute, Barcelona, Spain;* [h] *Department of Applied Mathematics, Escuela Universitaria Politécnica La Almunia, Universidad de Zaragoza, Zaragoza, Spain*

Article info

Article history:
Accepted March 19, 2023

Associate Editor:
Guillaume Ploussard

Keywords:
Prostate cancer
Clinically significant
Early detection
Magnetic resonance imaging
Predictive model
Risk calculator

Abstract

Background: Magnetic resonance imaging (MRI)-based risk calculators (MRI-RCs) individualise the likelihood of clinically significant prostate cancer (csPCa) and improve candidate selection for prostate biopsy beyond the Prostate Imaging Reporting and Data System (PI-RADS).
Objective: To compare the Barcelona (BCN) and Rotterdam (ROT) MRI-RCs in an entire population and according to the PI-RADS categories.
Design, setting, and participants: A prospective comparison of BCN- and ROT-RC in 946 men with suspected prostate cancer in whom systematic biopsy was performed, as well as target biopsies of PI-RADS $\geq$3 lesions.
Outcome measurements and statistical analysis: Saved biopsies and undetected csPCa (grade group $\geq$2) were determined.
Results and limitations: The csPCa detection was 40.8%. The median risks of csPCa from BCN- and ROT-RC were, respectively, 67.1% and 25% in men with csPCa, whereas 10.5% and 3% in those without csPCa ($p < 0.001$). The areas under the curve were 0.856 and 0.844, respectively ($p = 0.116$). BCN-RC showed a higher net benefit and clinical utility over ROT-RC. Using appropriate thresholds, respectively, 75% and 80% of biopsies were needed to identify 50% of csPCa detected in men with PI-RADS <3, whereas 35% and 21% of biopsies were saved, missing 10% of csPCa detected in men with PI-RADS 3. BCN-RC saved 15% of biopsies, missing 2% of csPCa in men with PI-RADS 4, whereas ROT-RC saved 10%, missing 6%. No RC saved biopsies without missing csPCa in men with PI-RADS 5.

† These authors contributed equally as co-first authors.
‡ These authors contributed equally as co-last authors.
* Corresponding author. Department of Urology, Vall d'Hebron Hospital, Po Vall d'Hebron 119-129, 08035 Barcelona, Spain. Tel. +34 2746100; Fax: +34 2746028.
E-mail address: juan.morote@vallhebron.cat (J. Morote).

https://doi.org/10.1016/j.euros.2023.03.013

Conclusions: ROT-RC provided a lower and narrower range of csPCa probabilities than BCN-RC. BCN-RC showed a net benefit over ROT-RC in the entire population. However, BCN-RC was useful in men with PI-RADS 3 and 4, whereas ROT-RC was useful only in those with PI-RADS 3. No RC seemed to be helpful in men with negative MRI and PI-RADS 5.

Patient summary: Barcelona risk calculator was more helpful than Rotterdam risk calculator to select candidates for prostate biopsy.

1. Introduction

The early detection of prostate cancer (PCa) has evolved towards clinically significant PCa (csPCa), avoiding unnecessary prostate biopsies and overdetection of insignificant tumours. However, PCa suspicion remains based on serum prostate-specific antigen (PSA) elevation and abnormal digital rectal examination (DRE) [1–3]. This paradigm shift has resulted from the spread of prebiopsy multiparametric magnetic resonance imaging (mpMRI), which grades the likelihood of csPCa through Prostate Imaging Reporting and Data System (PI-RADS) [4]. The negative predictive value of mpMRI reaches 95%, which makes it possible to avoid prostate biopsies for PI-RADS <3 [5,6]. Target biopsies of suspicious lesions (PI-RADS ≥3) increase the csPCa sensitivity of systematic-biopsies. However, csPCa detection does not exceed 20% in men with PI-RADS 3, is approximately 50% in men with PI-RADS 4, and reaches 90% in men with PI-RADS 5 [7].

MRI-predictive models individualise the likelihood of csPCa and improve candidate selection for prostate biopsy, although available risk calculators (RCs) and external validations are essential [8]. Among the 18 MRI-predictive models developed in the last 5 yr, seven have been validated externally and only two RCs are available [9]. Rotterdam (ROT) RC was initially designed from the Rotterdam population of the European Randomised Screening Prostate Cancer (ERSPC) trial [10,11]. ROT MRI-RC has resulted from an adjustment of the previous RCs 3 and 4 to predict PCa and high-grade PCa likelihoods in biopsy-naïve men and those with previous negative prostate biopsy, in 961 men with serum PSA ≥3.0 ng/ml and/or abnormal DRE, in whom systematic biopsy was always performed as a target biopsy to PI-RADSv.1 ≥3 lesions. PI-RADSv.1 score (1–5), age (50–75 yr), biopsy status (initial vs repeat), serum PSA (0.4–50 ng/ml), DRE (normal vs abnormal), and prostate volume (10–110 ml) were included as predictors [12]. ROT MRI-RC has been validated in some populations, although recalibrations and risk threshold adjustments have been needed to assure accurate predictions [13–16]. Barcelona (BCN) MRI-RC was recently designed among 1486 men with PSA ≥3.0 ng/ml and/or abnormal DRE, in whom systematic biopsies were always performed as target biopsies to PI-RADSv.2 ≥3 lesions. BCN MRI-RC has been validated externally and includes the same predictors as ROT MRI-RC without range limitation, PI-RADSv.2, and PCa family history (first degree vs no). The csPCa was defined as the International Society of Urologic Pathology (ISUP) grade group ≥2. BCN MRI-RC has been the first predictive model analysed according to the PI-RADS categories, showing that the efficacy in the entire population does not represents that in each PI-RADS category. In addition, the BCN MRI-RC has the possibility to select the appropriate threshold for adjustments in validation studies and according to the PI-RADS categories [17].

Owing to differences between ROT and BCN MRI-RCs, we hypothesise different behaviour for improving candidate selection for prostate biopsy. We aim to compare the clinical usefulness of ROT and BCN MRI-RCs in a whole population of suspected PCa men and according to each PI-RADS category.

2. Patients and methods

2.1. Design, setting, and participants

A prospective head-to-head comparison of ROT- and BCN-RC in 946 men with serum PSA ≥3.0 ng/ml and/or abnormal DRE, recruited in two academic centres from the Barcelona metropolitan area (PSM and GTiP), between 2018 and 2021 was performed. Prebiopsy 3-Tesla mpMRI and 12-core transrectal ultrasound (TRUS) systematic biopsy were always performed, and two- to four-core TRUS visual target biopsies were added to PI-RADSv.2 ≥3 lesions. Men undergoing 5-ARIs who had previous PCa, atypical small acinar proliferation, or high-grade prostatic intraepithelial neoplasia with atypia were excluded. The project was approved by the ethical committee of VHH (PR/AG-317/2017).

2.2. Intervention

The likelihoods of csPCa from ROT-RC (www.prostatecancer-riskcalculator.com) [12] and BCN-RC (https://mripcaprediction.shinyapps.io/MRIPCaPrediction/, second tab *'BCN2RC: MRI-based model'*) [17] were assessed. PI-RADSv.2 was introduced in both RCs as the closest value of serum PSA, prostate volume, and age when out of the accepted range in ROT-RC.

2.3. Clinically significant PCa definition

ROT-RC predicts high-grade PCa likelihood, defined as a Gleason score of ≥3 + 4, although the current RC shows this as csPCa [13]. BCN-RC predicts csPCa risk defined as an ISUP grade group of ≥2 [18].

2.4. Endpoint variables

Saved prostate biopsies and missed csPCa were determined.

2.5. Statistical analysis

Quantitative variables were expressed as median and 25–75 percentiles (interquartile range [IQR]), and qualitative variables in rates. Mann-Witney U test and chi-square test were used to compare medians and proportions [19,20]. The discrimination ability of csPCa was analysed with receiver operating characteristic (ROC) curves [21]; areas under the curve (AUCs) were compared with the test of DeLong et al [22]. Calibration curves analysed the correspondence between predictive probabilities and observed occurrence of csPCa. The net benefit of RCs over biopsying all men or none was analysed using a decision curve analysis (DCA) [23]. Specificities corresponding to 85%, 90%, and 95% sensitivities were assessed as their 95% confidence intervals (CIs). Clinical utility curves (CUCs) exploring potential rates of avoided biopsies and missed csPCa according to continuous probability of csPCa were generated [24]. Tests with two-sided $p < 0.05$ were considered statistically significant. Statistical analyses were computed using R programming language v.4.0.3 (The R Foundation for Statistical Computing, Vienna, Austria) and SPSS v.25 (Statistical Package for Social Sciences; IBM, San Francisco, CA, USA).

3. Results

3.1. Population characteristics

The characteristics of participants are summarised in Table 1. In 386 men (40.8%), csPCa was detected—17.9% in men with PI-RADS <3, 20.4% for PI-RADS 3, 51.9% for PI-RADS 4, and 84% for PI-RADS 5. A subset of 209 men (22.1%) had age (129), serum PSA (18), or prostate volume (68) out of the accepted range of ROT-RC.

Table 1 – Population characteristics

Characteristic	Measurement
Number of men	946
Age (yr), median (IQR)	67 (61–72)
Total PSA (ng/ml), median (IQR)	7.4 (5.5–10.9)
Abnormal DRE, *n* (%)	307 (32.5)
Prostate volume (ml), median (IQR)	55 (40–79)
Prior negative prostate biopsy, *n* (%)	293 (31.0)
Family history of PCa, *n* (%)	34 (3.6%)
PI-RADS, *n* (%)	
1–2	235 (24.8)
3	201 (21.2)
4	391 (41.3)
5	119 (12.6)
PCa detection, *n* (%)	521 (55.1)
csPCa detection, *n* (%)	386 (40.8)
csPCa detection by PI-RADS category, *n* (%)	
<3	42 (17.9)
3	41 (20.4)
4	203 (51.9)
5	100 (84.0)

csPCa = clinically significant PCa; DRE = digital rectal examination; IQR = interquartile range; *n* = number; PCa = prostate cancer; PI-RADS = Prostate Imaging Reporting and Data System; PSA = prostate-specific antigen.

3.2. Behaviour of ROT- and BCN-RC in the whole population

The median csPCa likelihood of ROT-RC was 3% (IQR: 2–10) in men without csPCa and 25% (9–46) in men with csPCa ($p < 0.001$), whereas those of BCN-RC were 10.5% (3.6–27.2) and 67.1% (39.3–85.6), respectively ($p < 0.001$; Fig. 1).

The calibration curves of both RCs showed certain underestimation of csPCa (Fig. 2A and 2B). BCN-RC showed a slight underestimation with a calibration in the large of 0.25 showing a minimum difference between the mean observed and the mean predicted values, with a difference of 1.96 for ROT-RC. The slopes were 0.81 and 1.04 for ROT- and BCN-RC, respectively. BCN-RC showed values near the ideal value of 1.

The discrimination ability of ROT- and BCN-RC for csPCa is presented by ROC curves in Figure 3A. The AUCs were 0.856 (95% CI: 0.831–0.881) and 0.844 (0.819–0.869) respectively ($p = 0.116$). BCN-RC showed a net benefit over biopsying all men from a 15% probability threshold; ROT MRI-RC showed the benefit from a 32% probability threshold (Fig. 3B). CUCs showed a larger clinical utility area for BCN-RC (Fig. 3C); additionally, the morphology and positioning of CUCs were different between the two RCs, shifted up and to the left of ROT-RC with respect to BCN-RC. The number of missed csPCa cases and avoided biopsies in each threshold from 1% to 100% are presented in Supplementary Table 1. The specificities corresponding to 85%, 90%, and 95% sensitivities of csPCa provided by both RCs are presented in Table 2. There were similar specificities at 85% and 90% sensitivities, with 42.1% (95% CI: 38.0–46.3) for ROT-RC and 31.8% (28.0–35.8) for BCN-RC ($p < 0.001$) at 95% sensitivity.

3.3. Behaviour of ROT- and BCN-RC according to the PI-RADS categories

Violin plots of csPCa likelihoods in men with and without csPCa, assessed with both RCs according to PI-RADSv.2 categories, show lower values and a narrow range of ROT-RC predictions (Fig. 4A) than those from BCN-RC (Fig. 4B), although significant differences existed between the medians of both subsets in all PI-RADS categories.

The AUC of ROT-RC in men with PI-RADS <3 was 0.776 (95% CI: 0.661–0.832), whereas the AUC of BCN-RC was 0.774 (0.697–0.850, $p = 0.529$; Fig. 5A). The AUCs were, respectively, 0.836 (0.756–0.916) and 0.838 (0.761–0.914) in men with PI-RADS 3 ($p = 0.954$; Fig. 5D), 0.829 (0.789–0.869) and 0.737 (0.677–0.787) in men with PI-RADS 4 ($p < 0.001$; Fig. 5G), and 0.866 (0.785–0.948) and 0.822 (0.723–0.920) in men with PI-RADS 5 ($p = 0.323$; Fig. 5J).

A small benefit over no-biopsy men with PI-RADS <3 was observed in both RCs (Fig. 5B). A clear net benefit of BCN-RC was observed over biopsying all men with PI-RADS 3 from a 10% csPCa probability, with the benefit of ROT-RC being lower (Fig. 5E). In men with PI-RADS 4, BCN-RC showed a net benefit over biopsying all men from a 17% csPCa probability; however, ROT-RC showed a small benefit between 50% and 75% csPCa probability (Fig. 5H). In men with PI-RADS 5, BCN-RC showed a benefit over biopsy-all men from 38% probability of csPCa; ROT-RC exhibited a minimal benefit from the 83% csPCa probability (Fig. 5K).

CUCs showed a striking behaviour of both RCs. ROT-RC started in PI-RADS <3 with curves displaced up and to the left, evolving with the increase of the PI-RADS category towards the graph diagonal line; BCN-RC run through the entire area of the graph, evolving from the top left to the bottom right with an increase in the PI-RADS category. CUCs of BCN-RC showed clear clinical utility in PI-RADS 3 and 4. The number of missed csPCa cases and saved biopsies in

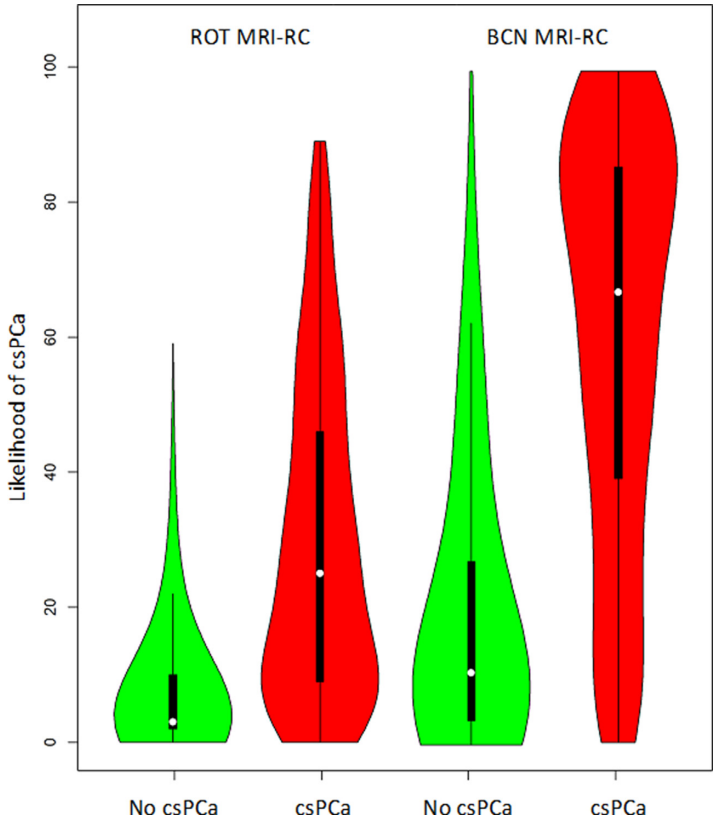

Fig. 1 – Violin plots of csPCa likelihoods of men without and with csPCa estimated with ROT MRI-RC and BCN MRI-RC. BCN = Barcelona; csPCa = clinically significant prostate cancer; MRI-RC = magnetic resonance imaging–based risk calculator; ROT = Rotterdam.

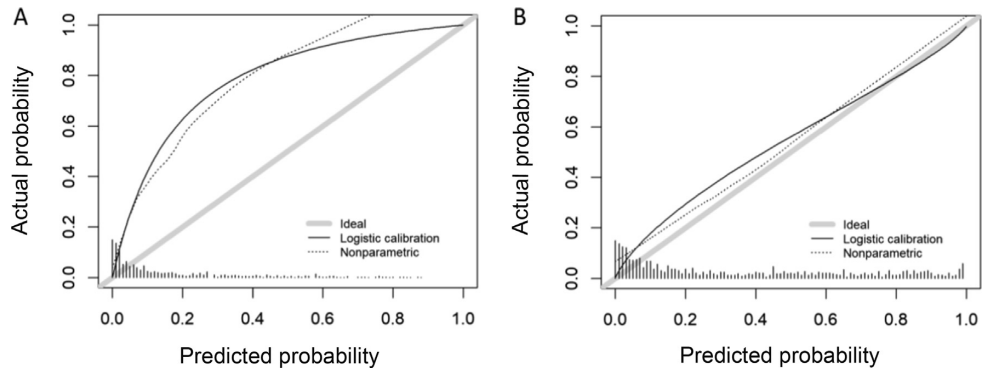

Fig. 2 – Calibration curves of (A) ROT MRI-RC and (B) BCN MRI-RC. BCN = Barcelona; MRI-RC = magnetic resonance imaging–based risk calculator; ROT = Rotterdam.

each PI-RADS category of ROT- and BCN-RC are presented in Supplementary Tables 2–5. The specificities of both RCs from 85%, 90%, and 95% sensitivities in each PI-RADS category are presented in Table 3.

As the decision of prostate biopsy is made after mpMRI, it is appropriate to define the acceptable percentages of missed csPCa according to each PI-RADS category [17]. CUCs show how no RC appeared clinically helpful for PI-RADS <3 because, to identify 50% of 42 csPCa detected (5% of all csPCa detected), 75% of men needed biopsy (18.6% of all biopsies) with ROT-RC and 80% (20% of all biopsies) with BCN-RC. The rate of csPCa detection in men with PI-RADS

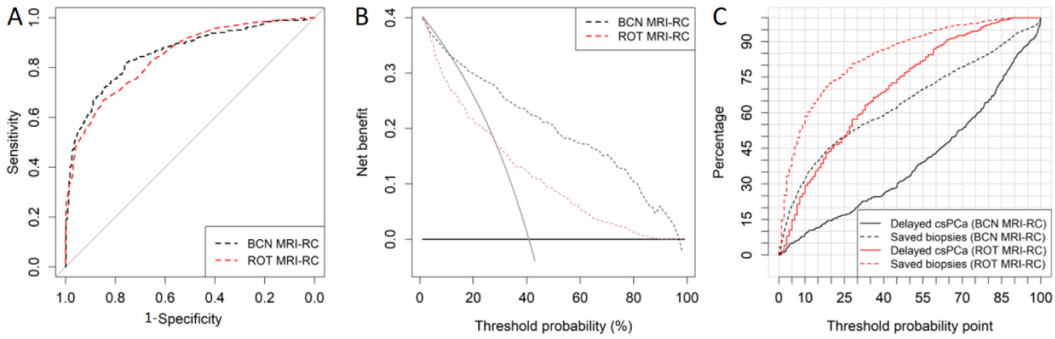

Fig. 3 – (A) Discrimination ability of csPCa of BCN MRI-RC and ROT MRI-RC presented with ROC curves, (B) net benefit of BCN MRI-RC and ROT MRI-RC over biopsying all men presented by DCAs, and (C) clinical utility of BCN MRI-RC and ROT MRI-RC showing the percentage of avoided biopsies and missed csPCa according to the threshold probability of csPCa by CUCs. BCN = Barcelona; csPCa = clinically significant prostate cancer; CUC = clinical utility curve; DCA = decision curve analysis; MRI-RC = magnetic resonance imaging–based risk calculator; ROT = Rotterdam.

Table 2 – Specificities of BCN MRI-RC and ROT MRI-RC corresponding to 85%, 90%, and 95% sensitivities for csPCa

Risk calculator	Specificity (95% CI) for sensitivities of					
	85%	*p* value	90%	*p* value	95%	*p* value
BCN MRI-RC (%)	67.3 (63.2–71.1)	0.055	52.0 (47.7–56.2)	0.392	31.8 (28.0–35.8)	<0.001
ROT MRI-RC (%)	61.7 (57.5–65.7)		54.7 (50.5–58.9)		42.1 (38.0–46.3)	

BCN = Barcelona; CI = confidence interval; MRI-RC = magnetic resonance imaging–based risk calculator; ROT = Rotterdam.

3 was 20.4%, and it was acceptable to miss up to 10% of these csPCa (5.2% of all csPCa) cases. ROT-RC saved 21% of biopsies, whereas BCN-RC saved 35%. In men with PI-RADS 4, BCN-RC saved 15% of biopsies (6% of all biopsies), missing 2% of csPCa (1% of all csPCa), whereas ROT-RC saved 10% of biopsies, with 6% of csPCa remaining undetected, which seems clinically unacceptable. Finally, in PI-RADS 5 where only 16% of biopsies were unnecessary, no RC assured to avoid any biopsy without missing csPCa.

4. Discussion

We were surprised at how far from the ideal was the calibration curve of ROT MRI-RC compared with that of BCN MRI-RC. The most probable cause was the low and narrow csPCa risk prediction range generated by ROT-RC mainly located at low predicted probabilities. We also noted that 22.1% of analysed suspected PCa men showed age, serum PSA, or prostate volume out of the accepted range of ROT MRI-RC. This drawback, not reported until now, can be a consequence of the strict inclusion criteria of the ERSPC trial in which RCs 3 and 4 were initially developed [10,11]. These limited ranges were not observed in the population of suspected PCa men in whom the ROT MRI-RC was adjusted [12], which had similar characteristics as our population study [17].

The discrimination ability of csPCa of ROT and BCN MRI-RCs was similar in the entire population; however, DCAs showed a net benefit of BCN MRI-RC over ROT MRI-RC. Since three-quarters of csPCa likelihoods predicted by ROT MRI-RC were below 24%, there was no benefit over biopsying all men from a threshold of >20%, and misclassification of csPCa > 60% remained within these thresholds that are not in the utility range [23]. In contrast, BCN MRI-RC showed a net benefit over biopsying all men above the 15% threshold. This threshold avoided 40% of prostate biopsies, missing 10% of csPCa. To know the true clinical value of MRI-RCs is essential to assess their behaviour according to the PI-RADS categories, because the discrimination ability in the whole population does not represent that of each PI-RADS [25]. ROT MRI-RC showed no benefit in men with PI-RADS <3, 4, and 5, as did BCN MRI-RC in PI-RADS <3 and 5. BCN MRI-RC showed a net benefit in men with PI-RADS 4, saving between 6% and 23% of prostate biopsies and missing between 1% and 5% of csPCa detected for risk thresholds between 13% and 28%. In men with PI-RADS 3, ROT MRI-RC with thresholds between 1% and 3% missed between 0% and 12% of csPCa, saving 0.5–45% of biopsies. BCN MRI-RC at thresholds between 1% and 11% missed between 0% and 12% csPCa, saving between 5% and 47% of biopsies.

The possible drawback of comparing both MRI-RCs in a population from the same metropolitan area where the BCN MRI-RC was developed, we note that csPCa detection rate in the cohort of suspected PCa men in whom ROT MRI-RC was adjusted was 35.8%, very close to that of 36.9% observed in the BCN MRI-RC development cohort [13,17]. The characteristics of participants of this head-to-head comparison were different from those of both the development and the adjustment cohorts of BCN and ROT MRI-RCs in terms of age, serum PSA, DRE, and csPCa detection rate of 40.8%. The close origin of this population to that of BCN MRI-RC development did not influence the results. Rather, we believe that the differences between BCN and

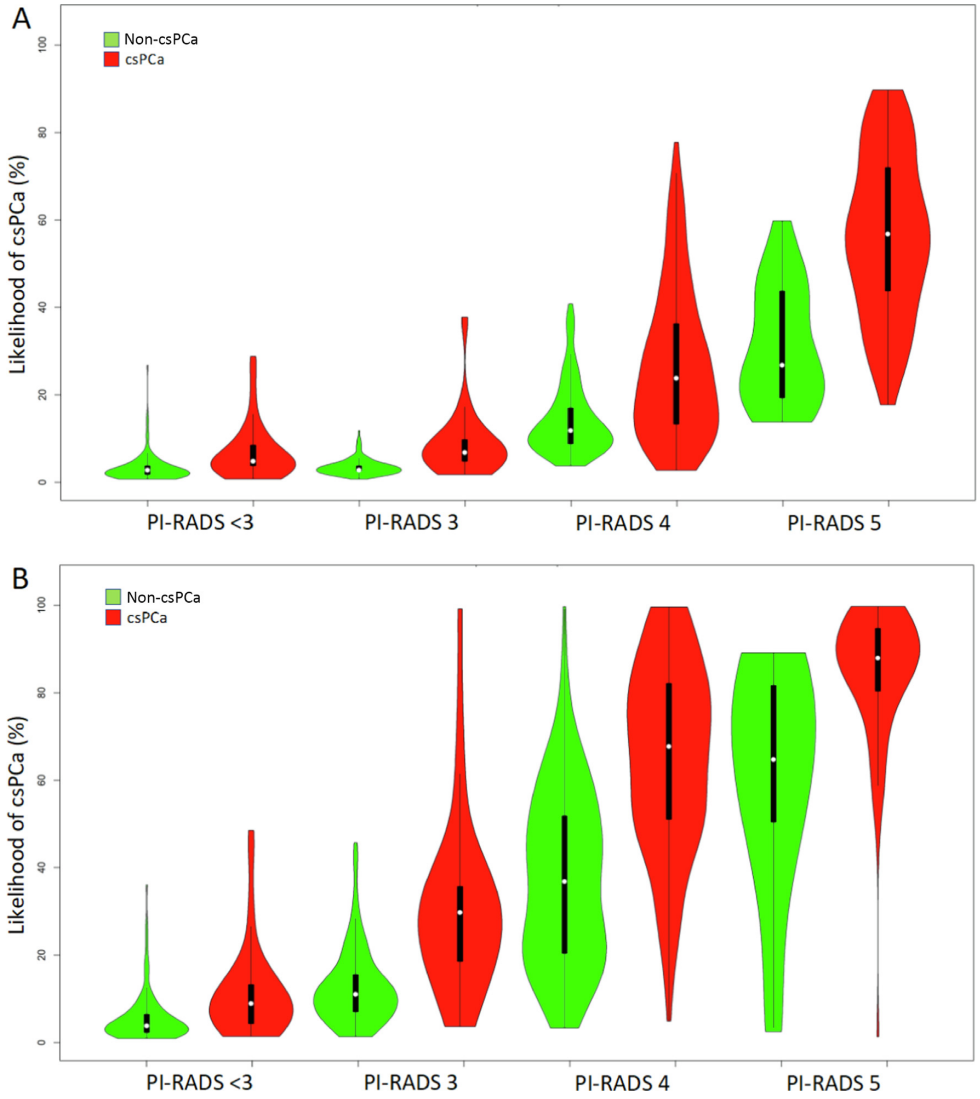

Fig. 4 – Violin plots of csPCa likelihoods, estimated from (A) ROT MRI-RC and (B) BCN MRI-RC, in men without and with csPCa according to the PI-RADS categories. BCN = Barcelona; csPCa = clinically significant prostate cancer; MRI-RC = magnetic resonance imaging–based risk calculator; PI-RADS = Prostate Imaging Reporting and Data System; ROT = Rotterdam.

ROT MRI-RCs justify their different usefulness. BCN MRI-RC predicted the likelihood of csPCa defined as grade group ≥2, while ROT MRI-RC defined as Gleason ≥3 + 4; the age, serum PSA, and prostate volume ranges were limited in ROT MRI-RC and PI-RADSv.1 was used in its adjustment cohort, whereas PI-RADSv.2 was used in the BCN MRI-RC development cohort. The expression of csPCa likelihoods without and with decimals in ROT and BCN MRI-RCs, respectively, may represent any bias. A limitation of both MRI-RCs and the present study may be that a transperineal approach is currently recommended for prostate biopsy, whereas a transrectal approach was used in the present ROT MRI-RC adjustment and BCN MRI-RC development comparative cohorts [1], which appears to improve the overall detection of csPCa [26].

There are specific limitations of predictive models. A developed predictive model reflects the probability of a condition based on the characteristics at that time. However, changes arising in the same population and those from the validation cohorts justify the need of recalibrations of the models and adjustment of risk thresholds to ensure accurate predictions [27,28]. BCN MRI-RC reports the novelty of selecting the risk threshold that can be useful in external validations and selecting appropriate thresholds

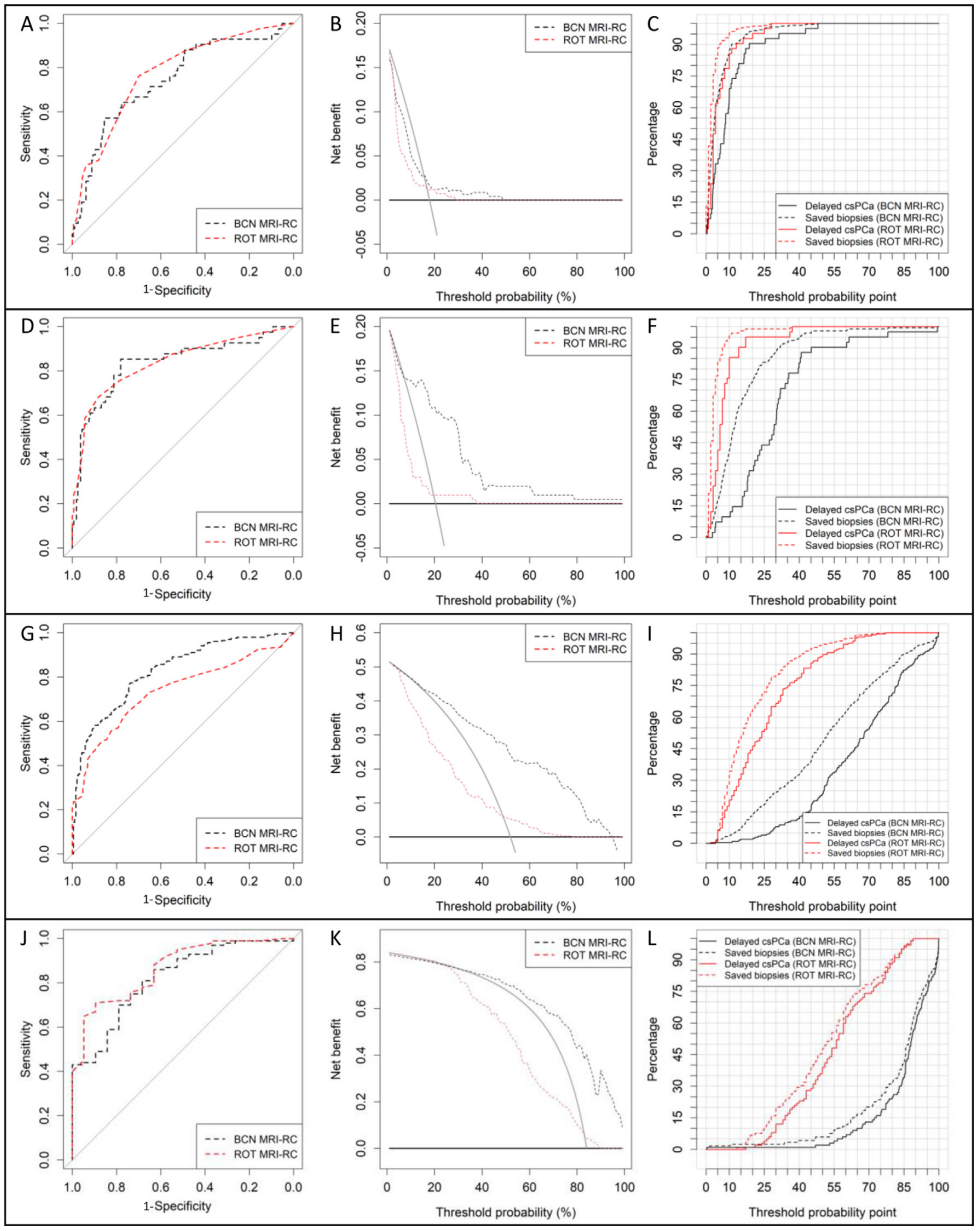

Fig. 5 – Discrimination ability presented by ROC curves, net benefit presented by DCAs, and clinical utility presented by CUCs, of BCN MRI-RC and ROT MRI-RC according to the PI-RADS categories: (A–C) PI-RADS <3, (D–F) PI-RADS 3, (G–I) PI-RADS 4, and (J–L) PI-RADS 5. BCN = Barcelona; csPCa = clinically significant prostate cancer; CUC = clinical utility curve; MRI-RC = magnetic resonance imaging–based risk calculator; PI-RADS = Prostate Imaging Reporting and Data System; ROT = Rotterdam.

for each PI-RADS category [17]. Real-time updating is a great challenge for future RCs [29]. Continuous feedback of new cases, big data integration, appropriate machine learning algorithms, and federated networking can lead to future RCs validated in each site and ensuring accurate and long-lasting predictions in many places [30].

5. Conclusions

BCN and ROT MRI-RCs showed different behaviour in this head-to-head comparative analysis. ROT MRI-RC reported a lower and narrower range of csPCa likelihoods than BCN MRI-RC. BCN MRI-RC presented a net benefit over ROT

Table 3 – Specificities of BCN MRI-RC and ROT MRI-RC corresponding to 85%, 90%, and 95% sensitivities for csPCa according to the PI-RADSv.2 category

Risk calculator	Specificity (95% CI) for sensitivities of					
	85%	*p* value	90%	*p* value	95%	*p* value
			PI-RADS <3			
BCN MRI-RC (%)	49.7 (45.5–54.0)	0.188	44.0 (39.9–48.3)	0.456	9.8 (7.6–12.7)	<0.001
ROT MRI-RC (%)	53.8 (49.6–58.0)		41.7 (37.6–45.9)		24.5 (21.1–28.3)	
			PI-RADS 3			
BCN MRI-RC (%)	78.1 (74.4–81.4)	<0.001	50.6 (46.4–54.8)	0.102	15.6 (12.8–19–0)	<0.001
ROT MRI-RC (%)	60.0 (55.8–64.0)		45.6 (41.4–49.8)		25.5 (22.0–29.4)	
			PI-RADS 4			
BCN MRI-RC (%)	62.2 (58.1–66.2)	<0.001	49.5 (45.3–53.7)	<0.001	39.9 (32.9–41.0)	<0.001
ROT MRI-RC (%)	29.7 (26.0–33.7)		20.2 (17.0–23.8)		4.6 (3.1–6.8	
			PI-RADS 5			
BCN MRI-RC (%)	63.2 (59.0–67.1)	1.000	52.6 (48.4–56.8)	0.456	36.8 (32.9–41.0)	<0.001
ROT MRI-RC (%)	63.2 (59.0–67.1)		60.5 (56.3–64.6)		52.6 (48.4–56.8)	

BCN = Barcelona; CI =confidence interval; MRI-RC = magnetic resonance imaging–based risk calculator; PI-RADS = Prostate Imaging Reporting and Data System; ROT = Rotterdam.

MRI-RC and grater clinical utility in the entire population. According to the PI-RADS category, BCN MRI-RC was helpful in men with PI-RADS 3 and 4, whereas ROT MRI-RC was helpful only in men with PI-RADS 3. No MRI-RC was helpful in men with PI-RADS <3 and 5.

Author contributions: Juan Morote had full access to all the data in the study and takes responsibility for the integrity of the data and the accuracy of the data analysis.

Study concept and design: Morote, Borque-Fernando, Esteban.
Acquisition of data: Triquell, Campistol, Servian, Abascal, Mendez, Planas.
Analysis and interpretation of data: Morote, Borque-Fernando, Esteban.
Drafting of the manuscript: Morote.
Critical revision of the manuscript for important intellectual content: Borque-Fernando, Esteban, Planas, Mendez, Trilla.
Statistical analysis: Esteban, Borque-Fernando, Morote.
Obtaining funding: Morote.
Administrative, technical, or material support: Morote.
Supervision: Morote, Trilla.
Other: None.

***Financial disclosures*:** Juan Morote certifies that all conflicts of interest, including specific financial interests and relationships and affiliations relevant to the subject matter or materials discussed in the manuscript (eg, employment/affiliation, grants or funding, consultancies, honoraria, stock ownership or options, expert testimony, royalties, or patents filed, received, or pending), are the following: None.

***Funding/Support and role of the sponsor*:** This study was supported by the Instituto Carlos III (SP) and the European Union (project ref: PI20/01666).

Appendix A. Supplementary data

Supplementary data to this article can be found online at https://doi.org/10.1016/j.euros.2023.03.013.

References

[1] Mottet N, van den Bergh RCN, Briers E, et al. EAU-EANM-ESTRO-ESUR-SIOG guidelines on prostate cancer—2020 update. Part 1: screening, diagnosis, and local treatment with curative intent. Eur Urol 2021;79:243–62.
[2] Van Poppel H, Roobol MJ, Chapple CR, et al. Prostate-specific antigen testing as part of a risk-adapted early detection strategy for prostate cancer: European Association of Urology position and recommendations for 2021. Eur Urol 2021;80:703–11.
[3] Van Poppel H, Hogenhout R, Albers P, van den Bergh RCN, Barentsz JO, Roobol MJ. European model for an organised risk-stratified early detection programme for prostate cancer. Eur Urol Oncol 2021;10:731–9.
[4] Schoots IG, Padhani AR, Rouvière O, Barentsz JO, Richenberg J. Analysis of magnetic resonance imaging-directed biopsy strategies for changing the paradigm of prostate cancer diagnosis. Eur Urol Oncol 2020;3:32–41.
[5] Sathianathen NJ, Omer A, Harriss E, et al. Negative predictive value of multiparametric magnetic resonance imaging in the detection of clinically significant prostate cancer in the prostate imaging reporting and data system era: a systematic review and meta-analysis. Eur Urol 2020;78:402–14.
[6] Wagaskar VG, Levy M, Ratnani P, et al. Clinical utility of negative multiparametric magnetic resonance imaging in the diagnosis of prostate cancer and clinically significant prostate cancer. Eur Urol Open Sci 2021;28:9–16.
[7] Mazzone E, Stabile A, Pellegrino F, et al. Positive predictive value of Prostate Imaging Reporting and Data System version 2 for the detection of clinically significant prostate cancer: a systematic review and meta-analysis. Eur Urol Oncol 2020;4:697–713.
[8] Osses DF, Roobol MJ, Schoots IG. Prediction medicine: biomarkers, risk calculators and magnetic resonance imaging as risk stratification tools in prostate cancer diagnosis. Int J Mol Sci 2020;20:1637.
[9] Triquell M, Campistol M, Celma A, et al. Magnetic resonance imaging-based predictive models for clinically significant prostate cancer: a systematic review. Cancers (Basel) 2022;14:4747.
[10] Steyberg R, Roobol-Bouts MJ, Kranse M, Schroder FH. Data storage device and method for determining the dependency of the risk for prostate cancer, device and method for indicating a risk for a disease in an individual. U.S. Patent Office, 8,087,576.
[11] Roobol MJ, Steyerberg EW, Kranse R, et al. A risk-based strategy improves prostate-specific antigen-driven detection of prostate cancer. Eur Urol 2010;57:79–85.
[12] Alberts AR, Roobol MJ, Verbeek JFM, et al. Prediction of high-grade prostate cancer following multiparametric magnetic resonance imaging: improving the Rotterdam European Randomized Study of Screening for Prostate Cancer risk calculators. Eur Urol 2019;75:310–8.
[13] Püllen L, Radtke JP, Wiesenfarth M, et al. External validation of novel magnetic resonance imaging-based models for prostate cancer prediction. BJU Int 2020;125:407–16.
[14] Chen R, Verbeek JFM, Yang Y, Song Z, Sun Y, Roobol MJ. Comparing the prediction of prostate biopsy outcome using the Chinese Prostate Cancer Consortium (CPCC) risk calculator and the Asian adapted Rotterdam European Randomized Study of Screening for Prostate Cancer (ERSPC) risk calculator in Chinese and European men. World J Urol 2021;39:73–80.

[15] Petersmann AL, Remmers S, Klein T, et al. External validation of two MRI-based risk calculators in prostate cancer diagnosis. World J Urol 2021;39:4109–16.
[16] De Nunzio C, Lombardo R, Baldassarri V, et al. Rotterdam mobile phone app including MRI data for the prediction of prostate cancer: a multicenter external validation. Eur J Surg Oncol 2021;47:2640–5.
[17] Morote J, Borque-Fernando A, Triquell M, et al. The Barcelona predictive model of clinically significant prostate cancer. Cancers (Basel) 2022;14:1589.
[18] Epstein JI, Zelefsky MJ, Sjoberg DD, et al. A contemporary prostate cancer grading system: a validated alternative to the Gleason score. Eur Urol 2016;69:428–35.
[19] Whitney J. Testing for differences with the nonparametric Mann-Whitney U test. J. Wound Ostomy Continence Nurs 1997;24:12.
[20] Plackett RL. Karl Pearson and the chi-squared test. Int Stat Rev 1983;51:59–72.
[21] Creelman CD, Donaldson W. ROC curves for discrimination of linear extent. J Exp Psychol 1968;77:514–6.
[22] DeLong ER, DeLong DM, Clarke-Pearson DL. Comparing the areas under two or more correlated receiver operating characteristic curves: a nonparametric approach. Biometrics 1988;44:837–45.
[23] Vickers AJ, Elkin EB. Decision curve analysis: a novel method for evaluating prediction models. Med Decis Making 2006;26:565–74.
[24] Borque Á, Rubio-Briones J, Esteban LM, et al. Implementing the use of nomograms by choosing threshold points in predictive models: 2012 updated Partin tables vs a European predictive nomogram for organ-confined disease in prostate cancer. BJU Int 2014;113:878–86.
[25] Moonesingh SR, Bashford T, Wagstaff D. Implementing risk calculators: time for the Trojan horse? Anesth Analg 2018;121:1192–6.
[26] Zattoni F, Marra G, Kasivisvanathan V, et al. The detection of prostate cancer with magnetic resonance imaging-targeted prostate biopsies is superior with the transperineal vs the transrectal approach. A European Association of Urology-Young Academic Urologists Prostate Cancer Working Group multi-institutional study. J Urol 2022;208:830–7.
[27] Morote J, Borque-Fernando Á, Triquell M, Esteban LM, Trilla E. The true utility of predictive models based on magnetic resonance imaging in selecting candidates for prostate biopsy. Eur Urol Open Sci 2022;42:40–1.
[28] Diniz MA. Statistical methods for validation of predictive models. J Nucl Cardiol 2022;29:3248–55.
[29] Strobl AN, Vickers AJ, Van Calster B, et al. Improving patient prostate cancer risk assessment: moving from static, globally-applied to dynamic, practice-specific risk calculators. J Biomed Inform 2015;56:87–93.
[30] Nandi A, Xhafa F. A federated learning method for real-time emotion state classification from multi modal streaming. Methods 2022;204:340–4.

Supplementary Table 1 - Missed csPCa and avoided biopsies according to the thresholds from 1 to 100% of BCN and ROT MRI-RCs in all men of study population.

Threshold (%)	BCN MRI-RC		ROT MRI-RC	
	Missed csPCa	Avoided biopsies	Missed csPCa	Avoided biopsies
1	4	48	1	32
2	5	92	7	140
3	11	132	16	238
4	17	171	31	316
5	19	195	41	354
6	21	218	57	400
7	24	242	66	432
8	27	268	83	468
9	30	282	95	497
10	34	304	100	519
11	37	326	113	553
12	40	338	118	571
13	41	356	123	586
14	43	366	128	603
15	45	374	137	618
16	47	390	142	630
17	50	402	149	643
18	54	414	157	657
19	56	424	166	672
20	56	430	169	683
21	59	442	174	690
22	60	448	179	697
23	63	461	180	701
24	65	468	183	707
25	65	472	190	719
26	67	480	194	726
27	67	485	201	739
28	71	495	209	747
29	74	501	221	763
30	78	505	221	763
31	83	513	228	771
32	88	521	230	773
33	88	525	236	780
34	90	529	244	788
35	91	533	247	792
36	94	539	250	798
37	95	542	256	805
38	95	546	258	810
39	96	552	261	813
40	99	557	264	817
41	103	565	266	820
42	106	572	270	824
43	108	579	276	831
44	108	581	280	835
45	110	585	280	836
46	119	600	286	844
47	120	606	290	848
48	122	612	292	850
49	127	621	297	856
50	129	627	299	858
51	136	634	304	863
52	140	640	306	865
53	145	648	310	869
54	148	652	311	870
55	151	661	315	874
56	153	665	317	876
57	157	672	322	881
58	159	676	326	885
59	164	684	326	885
60	167	691	335	895
61	171	698	338	898
62	175	705	340	900
63	178	711	342	902
64	182	716	346	906
65	185	720	350	910
66	192	731	352	912
67	193	733	353	913
68	200	740	354	914
69	203	745	357	917
70	204	748	357	917
71	208	753	357	917
72	214	760	359	919
73	218	764	361	921
74	224	770	363	923
75	226	773	364	924
76	232	782	364	924
77	234	784	366	926
78	239	789	370	930
79	248	799	372	932
80	252	803	374	934
81	255	807	375	935
82	260	812	377	937
83	269	821	377	937
84	278	831	379	939
85	283	836	381	941
86	292	846	382	942
87	297	852	383	943
88	305	860	383	943
89	312	869	385	945
90	320	879	386	946
91	327	886	386	946
92	330	889	386	946
93	335	894	386	946
94	339	898	386	946
95	342	901	386	946
96	349	908	386	946
97	352	911	386	946
98	356	915	386	946
99	368	927	386	946
100	386	946	386	946

Supplementary Table 2 - Missed csPCa and avoided biopsies according to the thresholds from 1 to 100% of BCN and ROT MRI-RCs in men with PI-RADS <3.

Threshold (%)	BCN MRI-RC		ROT MRI-RC	
	Missed csPCa	Avoided biopsies	Missed csPCa	Avoided biopsies
1	3	41	1	31
2	4	80	5	98
3	9	111	10	145
4	13	139	20	178
5	14	151	26	196
6	16	167	27	208
7	18	178	29	213
8	21	188	31	216
9	24	194	33	219
10	28	204	33	219
11	30	211	36	225
12	31	212	37	226
13	32	213	37	226
14	33	214	38	229
15	34	217	38	229
16	34	219	38	230
17	36	222	39	231
18	37	225	39	231
19	38	226	39	231
20	38	226	39	231
21	38	227	40	232
22	38	227	40	232
23	38	228	40	232
24	38	228	40	232
25	38	229	40	232
26	39	230	41	233
27	39	231	41	234
28	39	231	41	234
29	39	231	42	235
30	39	231	42	235
31	39	231	42	235
32	40	232	42	235
33	40	232	42	235
34	40	232	42	235
35	40	232	42	235
36	40	233	42	235
37	40	233	42	235
38	40	233	42	235
39	40	233	42	235
40	40	233	42	235
41	40	233	42	235
42	40	233	42	235
43	41	234	42	235
44	41	234	42	235
45	41	234	42	235
46	41	234	42	235
47	41	234	42	235
48	41	234	42	235
49	42	235	42	235
50	42	235	42	235
51	42	235	42	235
52	42	235	42	235
53	42	235	42	235
54	42	235	42	235
55	42	235	42	235
56	42	235	42	235
57	42	235	42	235
58	42	235	42	235
59	42	235	42	235
60	42	235	42	235
61	42	235	42	235
62	42	235	42	235
63	42	235	42	235
64	42	235	42	235
65	42	235	42	235
66	42	235	42	235
67	42	235	42	235
68	42	235	42	235
69	42	235	42	235
70	42	235	42	235
71	42	235	42	235
72	42	235	42	235
73	42	235	42	235
74	42	235	42	235
75	42	235	42	235
76	42	235	42	235
77	42	235	42	235
78	42	235	42	235
79	42	235	42	235
80	42	235	42	235
81	42	235	42	235
82	42	235	42	235
83	42	235	42	235
84	42	235	42	235
85	42	235	42	235
86	42	235	42	235
87	42	235	42	235
88	42	235	42	235
89	42	235	42	235
90	42	235	42	235
91	42	235	42	235
92	42	235	42	235
93	42	235	42	235
94	42	235	42	235
95	42	235	42	235
96	42	235	42	235
97	42	235	42	235
98	42	235	42	235
99	42	235	42	235
100	42	235	42	235

Supplementary Table 3 - Missed csPCa and avoided biopsies according to the thresholds from 1 to 100% of BCN and ROT MRI-RCs in men with PI-RADS 3.

Threshold (%)	BCN MRI-RC		ROT MRI-RC	
	Missed csPCa	Avoided biopsies	Missed csPCa	Avoided biopsies
1	0	6	0	1
2	0	10	2	42
3	1	17	5	92
4	2	25	10	136
5	3	35	13	154
6	3	42	17	168
7	4	54	22	174
8	4	66	27	182
9	4	73	30	187
10	4	83	31	190
11	5	95	35	194
12	6	104	35	195
13	6	116	35	195
14	6	124	35	195
15	6	126	37	197
16	8	133	37	197
17	9	137	37	197
18	12	142	39	199
19	13	146	39	199
20	13	149	39	199
21	15	154	39	199
22	15	157	39	199
23	17	164	39	199
24	18	167	39	199
25	18	167	39	199
26	18	167	39	199
27	18	169	39	199
28	19	172	39	199
29	20	174	39	199
30	22	176	39	199
31	27	181	39	199
32	29	183	39	199
33	29	185	39	199
34	29	185	39	199
35	30	186	39	199
36	32	188	39	199
37	32	188	40	200
38	32	188	41	201
39	32	189	41	201
40	34	191	41	201
41	36	193	41	201
42	36	194	41	201
43	36	195	41	201
44	36	195	41	201
45	36	195	41	201
46	37	197	41	201
47	37	197	41	201
48	37	197	41	201
49	37	197	41	201
50	37	197	41	201
51	37	197	41	201
52	37	197	41	201
53	37	197	41	201
54	37	197	41	201
55	37	197	41	201
56	37	197	41	201
57	37	197	41	201
58	37	197	41	201
59	37	197	41	201
60	37	197	41	201
61	38	198	41	201
62	39	199	41	201
63	39	199	41	201
64	39	199	41	201
65	39	199	41	201
66	39	199	41	201
67	39	199	41	201
68	39	199	41	201
69	39	199	41	201
70	39	199	41	201
71	39	199	41	201
72	39	199	41	201
73	39	199	41	201
74	39	199	41	201
75	39	199	41	201
76	39	199	41	201
77	39	199	41	201
78	39	199	41	201
79	40	200	41	201
80	40	200	41	201
81	40	200	41	201
82	40	200	41	201
83	40	200	41	201
84	40	200	41	201
85	40	200	41	201
86	40	200	41	201
87	40	200	41	201
88	40	200	41	201
89	40	200	41	201
90	40	200	41	201
91	40	200	41	201
92	40	200	41	201
93	40	200	41	201
94	40	200	41	201
95	40	200	41	201
96	40	200	41	201
97	40	200	41	201
98	40	200	41	201
99	40	200	41	201
100	41	201	41	201

Supplementary Table 4 - Missed csPCa and avoided biopsies according to the thresholds from 1 to 100% of BCN and ROT MRI-RCs in men with PI-RADS 4.

Threshold (%)	BCN MRI-RC		ROT MRI-RC	
	Missed csPCa	Avoided biopsies	Missed csPCa	Avoided biopsies
1	0	0	0	0
2	0	0	0	0
3	0	2	1	1
4	1	5	1	2
5	1	7	2	4
6	1	7	13	24
7	1	8	15	45
8	1	12	25	70
9	1	13	32	91
10	1	15	36	110
11	1	17	42	134
12	2	19	46	150
13	2	24	51	165
14	3	25	55	178
15	4	28	62	191
16	4	35	67	202
17	4	40	73	214
18	4	44	78	223
19	4	49	87	236
20	4	52	90	245
21	5	58	94	251
22	6	61	98	257
23	7	66	99	261
24	8	70	102	267
25	8	73	108	277
26	9	80	110	281
27	9	82	116	291
28	12	89	123	298
29	14	93	132	310
30	16	95	132	310
31	16	98	135	313
32	18	103	137	315
33	18	105	143	322
34	20	108	149	328
35	20	111	150	330
36	21	114	152	335
37	22	117	155	339
38	22	121	155	342
39	23	126	157	344
40	24	128	159	346
41	26	134	160	348
42	29	140	164	352
43	30	145	169	357
44	30	147	169	357
45	32	151	169	357
46	40	164	174	362
47	41	169	176	364
48	42	174	176	364
49	46	182	179	367
50	48	188	180	368
51	55	195	182	370
52	59	201	182	370
53	64	208	184	372
54	66	211	184	372
55	68	218	184	372
56	70	222	186	374
57	73	228	187	375
58	75	232	188	376
59	79	239	188	376
60	82	246	192	380
61	84	250	192	380
62	87	256	193	381
63	88	259	193	381
64	92	264	195	383
65	94	266	198	386
66	101	277	199	387
67	101	278	199	387
68	107	284	199	387
69	109	287	200	388
70	110	290	200	388
71	114	295	200	388
72	119	300	201	389
73	122	303	201	389
74	127	308	202	390
75	129	311	202	390
76	132	316	202	390
77	134	318	202	390
78	136	320	203	391
79	142	327	203	391
80	145	330	203	391
81	147	332	203	391
82	152	337	203	391
83	157	342	203	391
84	165	350	203	391
85	167	352	203	391
86	168	353	203	391
87	170	356	203	391
88	172	358	203	391
89	174	361	203	391
90	178	365	203	391
91	181	368	203	391
92	182	369	203	391
93	182	369	203	391
94	184	371	203	391
95	185	372	203	391
96	187	374	203	391
97	188	375	203	391
98	191	378	203	391
99	197	384	203	391
100	203	391	203	391

Supplementary Table 5 - Missed csPCa and avoided biopsies according to the thresholds from 1 to 100% of BCN and ROT MRI-RCs in men with PI-RADS 5.

Threshold (%)	BCN MRI-RC		ROT MRI-RC	
	Missed csPCa	Avoided biopsies	Missed csPCa	Avoided biopsies
1	1	1	0	0
2	1	2	0	0
3	1	2	0	0
4	1	2	0	0
5	1	2	0	0
6	1	2	0	0
7	1	2	0	0
8	1	2	0	0
9	1	2	0	0
10	1	2	0	0
11	1	3	0	0
12	1	3	0	0
13	1	3	0	0
14	1	3	0	1
15	1	3	0	1
16	1	3	0	1
17	1	3	0	1
18	1	3	1	4
19	1	3	1	6
20	1	3	1	8
21	1	3	1	8
22	1	3	2	9
23	1	3	2	9
24	1	3	2	9
25	1	3	3	11
26	1	3	4	13
27	1	3	5	15
28	1	3	6	16
29	1	3	8	19
30	1	3	8	19
31	1	3	12	24
32	1	3	12	24
33	1	3	12	24
34	1	4	14	26
35	1	4	16	28
36	1	4	17	29
37	1	4	19	31
38	1	4	20	32
39	1	4	21	33
40	1	5	22	35
41	1	5	23	36
42	1	5	23	36
43	1	5	24	38
44	1	5	28	42
45	1	5	28	43
46	1	5	29	46
47	1	6	31	48
48	2	7	33	50
49	2	7	35	53
50	2	7	36	54
51	2	7	39	57
52	2	7	41	59
53	2	8	43	61
54	3	9	44	62
55	4	11	48	66
56	4	11	48	66
57	5	12	52	70
58	5	12	55	73
59	6	13	55	73
60	6	13	60	79
61	7	15	63	82
62	7	15	64	83
63	9	18	66	85
64	9	18	68	87
65	10	20	69	88
66	10	20	70	89
67	11	21	71	90
68	12	22	72	91
69	13	24	74	93
70	13	24	74	93
71	13	24	74	93
72	14	26	75	94
73	15	27	77	96
74	16	28	78	97
75	16	28	79	98
76	19	32	79	98
77	19	32	81	100
78	22	35	84	103
79	24	37	86	105
80	25	38	88	107
81	26	40	89	108
82	26	40	91	110
83	30	44	91	110
84	31	46	93	112
85	34	49	95	114
86	42	58	96	115
87	45	61	97	116
88	51	67	97	116
89	56	73	99	118
90	60	79	100	119
91	64	83	100	119
92	66	85	100	119
93	71	90	100	119
94	73	92	100	119
95	75	94	100	119
96	80	99	100	119
97	82	101	100	119
98	83	102	100	119
99	89	108	100	119
100	100	119	100	119

5.5. PUBLICACIÓN 5

Título: A Clinically Significant Prostate Cancer Predictive Model Using Digital Rectal Examination Prostate Volume Category to Stratify Initial Prostate Cancer Suspicion and Reduce Magnetic Resonance Imaging Demand

Revista: Cancers

Año de publicación: 2022

Volumen: 14

Páginas: 5100

DOI: https://doi.org/10.3390/cancers14205100

Autores: Juan Morote, Ángel Borque-Fernando , Marina Triquell, Miriam Campistol, Anna Celma, Lucas Regis, José M. Abascal, Pol Servian, Jacques Planas, Olga Mendez, Luis M. Esteban y Enrique Trilla

Factor de impacto: 4.5 (2023)

Cuartil: Q1 (Oncología)

cancers

MDPI

Article

A Clinically Significant Prostate Cancer Predictive Model Using Digital Rectal Examination Prostate Volume Category to Stratify Initial Prostate Cancer Suspicion and Reduce Magnetic Resonance Imaging Demand

Juan Morote [1,*,†], Ángel Borque-Fernando [2,†], Marina Triquell [1], Miriam Campistol [1], Anna Celma [1], Lucas Regis [1], José M. Abascal [3], Pol Servian [4], Jacques Planas [1], Olga Mendez [5], Luis M. Esteban [6,‡] and Enrique Trilla [1,‡]

[1] Department of Urology and Surgery, Vall d'Hebron Hospital and Universitat Autònoma de Barcelona, 08035 Barcelona, Spain
[2] Department of Urology, Hospital Miguel Servet, IIS-Aragon, 50009 Zaragoza, Spain
[3] Departments of Urology and Surgery, Parc de Salut Mar and Universitat Pompeu Fabra, 08003 Barcelona, Spain
[4] Department of Urology, Hospital Germans Trias I Pujol, 08916 Badalona, Spain
[5] Urology Biomedical Research Unit, Vall d´Hebron Research Institute, 08035 Barcelona, Spain
[6] Department of Applied Mathematics, Escuela Universitaria Politécnica La Almunia, Universidad de Zaragoza, 50100 Zaragoza, Spain
* Correspondence: juan.morote@vallhebron.cat
† These authors contributed equally to this work.
‡ These authors contributed equally to this work.

check for updates

Citation: Morote, J.; Borque-Fernando, Á.; Triquell, M.; Campistol, M.; Celma, A.; Regis, L.; Abascal, J.M.; Servian, P.; Planas, J.; Mendez, O.; et al. A Clinically Significant Prostate Cancer Predictive Model Using Digital Rectal Examination Prostate Volume Category to Stratify Initial Prostate Cancer Suspicion and Reduce Magnetic Resonance Imaging Demand. *Cancers* **2022**, *14*, 5100. https://doi.org/10.3390/cancers14205100

Academic Editor: Grace Lu-Yao

Received: 20 September 2022
Accepted: 14 October 2022
Published: 18 October 2022

Publisher's Note: MDPI stays neutral with regard to jurisdictional claims in published maps and institutional affiliations.

Simple Summary: Early detection of PCa (PCa) has evolved towards clinically significant PCa (csPCa) after the spread of pre-biopsy multiparametric magnetic resonance imaging (mpMRI). However, PCa suspicion remains based on prostate-specific antigen (PSA) elevation and/or abnormal digital rectal examination (DRE). This change of paradigm and approach has reduced unnecessary prostate biopsies and overdetection of insignificant PCa, while the demand for mpMRI has skyrocketed despite its implementation not being allowed at all sites. The European Association of Urology (EAU) proposes risk-organized models for early detection of csPCa stratifying the initial PCa suspicion to reduce MRI scans and then prostate biopsies after mpMRI. Risk calculators are efficient tools for individualizing the risk of csPCa, especially when prostate volume is included in the predictive models. After the development and external validation of the Barcelona MRI risk calculator (BCN-RC 2) for the selection of candidates for prostate biopsy, we have now developed and externally validated BCN-RC 1 with the aim of reduce mpMRI demand. Both BCN-RC 1 and RC 2 are ready to be integrated in a risk-organized model for early detection of csPCa.

Abstract: A predictive model including age, PCa family history, biopsy status (initial vs repeat), DRE (normal vs abnormal), serum prostate-specific antigen (PSA), and DRE prostate volume ca-tegory was developed to stratify initial PCa suspicion in 1486 men with PSA > 3 ng/mL and/or abnormal DRE, in whom mpMRI followed; 2- to 4-core TRUS-guided biopsies where Prostate Imaging Report and Data System (PI-RADS) > 3 lesions and/or 12-core TRUS systematic biopsies were performed in one academic institution between 1 January 2016–31 December 2019. The csPCa detection rate, defined as International Society of Uro-Pathology grade group 2 or higher, was 36.9%. An external validation of designed BCN-RC 1 was carried out on 946 men from two other institutions in the same metropolitan area, using the same criteria of PCa suspicion and diagnostic approach, yielded a csPCa detection rate of 40.8%. The areas under the receiver operating characteristic curves of BCN-RC 1 were 0.823 (95% CI: 0.800–0.846) in the development cohort and 0.837 (95% CI: 0.811–0.863) in the validation cohort (p = 0.447). In both cohorts, BCN-RC 1 exhibited net benefit over performing mpMRI in all men from 8 and 12% risk thresholds, respectively. At 0.95 sensitivity of csPCa, the specificities of BCN-RC 1 were 0.24 (95% CI: 0.22–0.26) in the development cohort and 0.34 (95% CI:

0.31–0.37) in the validation cohort ($p < 0.001$). The percentages of avoided mpMRI scans were 17.2% in the development cohort and 22.3% in the validation cohort, missing between 1.8% and 2% of csPCa among men at risk of PCa. In summary, BCN-RC 1 can stratify initial PCa suspicion, reducing the demand of mpMRI, with an acceptable loss of csPCa.

Keywords: prostate cancer; suspicion; clinically significant; predictive model; risk calculator; external validation; magnetic resonance imaging; development; external validation

1. Introduction

The European Randomised Screening Prostate Cancer (ERSPC) trial continues to show that early detection of clinically significant prostate cancer (csPCa) decreases PCa mortality beyond twenty years of follow-up [1]. After the stated position of the US Preventive Services Task Force against PCa screening with prostate-specific antigen (PSA), due to the high percentage of unnecessary prostate biopsies and overdetection of insignificant PCa (iPCa) [2], early detection of PCa has evolved towards csPCa due to the spread of pre-biopsy multiparametric magnetic resonance imaging (mpMRI) [3]. However, PCa suspicion remains based on serum PSA elevation and/or abnormal digital rectal examination [4,5]. Currently, mpMRI exhibits a high enough negative predictive value to allow for the avoidance of prostate biopsies when the Prostate Imaging Report and Data System (PI-RADS) score is less than 3 [6]. In addition, mpMRI also allows targeted biopsies on suspicious lesions, improving the sensitivity for csPCa of classic systematic prostate biopsies [7,8]. Therefore, the current approach of csPCa requires pre-biopsy mpMRI after serum PSA > 3.0 ng/mL and/or abnormal DRE and targeted biopsies to Prostate Imaging Report and Data System (PI-RADS) lesions ≥ 3, complemented with systematic prostate biopsies [4]. This paradigm change in the early detection of PCa has triggered the demand for mpMRI scans, which are not allowed at some sites [9]. In experienced centers, mpMRI has been replaced with biparametric MRI (bpMRI), reducing the MRI scan time fourfold while maintaining the quality and reproducibility of PI-RADS [10]. Further, PSA density, modern markers, and predictive models have been proposed to improve the selection of candidates for prostate biopsy after MRI in uncertain scenarios where a high percentage of unnecessary biopsies or overdetection of iPCa remain [11]. However, any increase in the current cost of early detection of csPCa is generally rejected [12]. The European Association of Urology (EAU) proposes risk-organized models of early detection of csPCa based on stratifying the initial PCa suspicion to reduce unnecessary MRI scans and, after that, a new stratification for reducing unnecessary prostate biopsies [9,13].

Prostate volume is a valuable predictor of csPCa, its inverse relationship with csPCa risk having recently been confirmed in a systematic review of studies carried out over the last thirty years [14]. An accurate prostate volume is essential for PSA density calculation, requiring measurement by transrectal ultrasonography (TRUS) since its introduction [15]. Today, MRI provides the most accurate prostate volume measurement [16]; TRUS is mainly used to perform prostate biopsies but infrequently to assess prostate volume alone [17]. However, prostate volume is needed for PSA density calculation and for some new markers assessment [18] to improve the efficacy of predictive models to stratify the initial suspicion of PCa [9]. Roobol et al. showed how the Rotterdam risk calculator´s prostate volume estimated with DRE can replace TRUS prostate volume [19,20]. Classically, urologists have performed a complete DRE, with great efficiency, detecting abnormalities in the posterior prostate gland surface and categorizing the prostate volume [21]. Regrettably, the use of DRE is limited even among physicians who diagnose and treat prostate cancer [22].

After developing and externally validating the Barcelona MRI predictive model and designing the risk calculator, now named BCN-RC 2, for selecting proper candidates for prostate biopsy after mpMRI [23], we aim to develop a new predictive model of csPCa to stratify the initial suspicion of PCa, including the DRE prostate volume category, for

avoiding unnecessary MRI scans. External validation of designed web BCN-RC 1 in the Barcelona metropolitan area was also performed. Our second objective is to propose a risk-organized model for the early detection of csPCa by sequencing both BCN-RC 1 and RC 2.

2. Materials and Methods

This predictive model was developed and externally validated from the same cohorts in which BCN-RC 2 was developed and externally validated.

2.1. Development Cohort

A group of 1486 men with serum PSA > 3 ng/mL and/or abnormal DRE were recruited from 1 January 2016–31 December 2019 in an academic institution of the metropolitan area of Barcelona (Vall d´Hebron Hospital), Spain. Pre-biopsy 3 Tesla mpMRI was performed followed by 2- to 4-core transrectal TRUS visual-guided biopsies for all PI-RADS v.2 >3 lesions and 12-core TRUS systematic biopsy and 12-core TRUS systematic biopsy in men with PI-RADS v.2 < 3. The dataset was recruited prospectively according to the standards of reporting for MRI-targeted biopsy studies (START) [24]. Men under 5-α reductase inhibitors and prior PCa detected were excluded, as well as those with prior atypical small acinar proliferation or high-grade prostate intraepithelial neoplasia with atypia.

2.2. Validation Cohort

The validation was formed with 946 men with the same criteria of PCa suspicion as those of the development cohort, retrospectively recruited in two academic institutions (Parc de Salut Mar and Germans Trias i Pujol Hospital) of the Barcelona metropolitan area, Spain. The diagnostic approach of csPCa was also the same as that of the development cohort.

2.3. MpMRI Characteristics

MpMRI was acquired with 3-Tesla scanners and surface phased-array coil. T2-weighted imaging (T2W), diffusion-weighted imaging (DWI), and dynamic-contrast-enhanced (DCE) imaging were analyzed according to the guidelines of European Society of Urogenital Radiology [25]. An expert radiologist with more than three years' experience and more than 300 reports per year reported mpMRI scans with the PI-RADS v.2.0 [26]. All reports of mpMRI included the prostate volume.

2.4. DRE-Prostate Volume Category Assessment

The prostate volume categories assessable with DRE were defined as category I when MRI prostate volume was less than 30 mL, category II when it was between 30 and 59 mL, and category III when MRI prostate volume was 60 mL or higher [19,20].

2.5. CsPCa Definition

All cores were separately submitted to the pathology departments. Expert pathologists analyzed material and csPCa was defined by the International Society of Uro-Pathology (ISUP) grade group 2 or higher [27].

2.6. Predictive Model Development

Age (years), ethnicity (Caucasian vs non-Caucasian), serum PSA level (ng/mL), DRE (normal vs abnormal), PCa family history (no vs first-degree), biopsy status (biopsy-naïve vs prior negative biopsy), and DRE prostate volume category (I to III) were explored as predictive variables of csPCa.

2.7. Endpoint Measurements

Avoided mpMRI scans and missed csPCa.

2.8. Statistical Analysis

Reporting tumour marker prognostic studies recommendations were followed (REMARK) [28], as well as update standards for reporting diagnostic accuracy studies (STARD 2015) [24]. Comparison between proportions and medians were made with the chi-squared test and Mann–Whitney U tests. A binary logistic regression of csPCa candidate predictors was used to generate the predictive model. Continuous variables were modeled as linear or nonlinear predictors using restricted cubic splines. Calibration of the predictive model was assessed in developed and validation cohorts. Discrimination ability was assessed from receiver operating characteristic (ROC) curves [29], and areas under the curve (AUC) were compared with the DeLong test [30]. The net benefit of stratifying PCa suspicion with the predictive model and perform mpMRI to all men was analyzed with decision curve analysis (DCA) [31]. Clinical utility was assessed via clinical utility curve (CUC), exploring potential rates of missed csPCa and avoided mpMRI scans [32]. Specificities for the 80, 85, 90, and 95% sensitivity of csPCa of the predictive model in development and external validation cohorts were compared with chi-squared test. Sensitivity, specificity, and positive and negative predictive value were analyzed, and the rates of avoidable MRI exams and potentially undetected csPCa were analyzed. Odds ratios (OR) and 95% confidence intervals (CI) were calculated. For external validation, transparent reporting of the multivariable prediction model for individual prognosis or diagnosis (TRIPOD) statements followed. Statistical analysis was conducted with the R programming language v.4.0.3 (R Foundation for Statistical Computing, Vienna, Austria) and SPSS v.25 (IBM, statistical package for social sciences, San Francisco, CA, USA).

3. Results

3.1. Characteristics of the Development and Validation Cohorts

Characteristics of the development and validation cohorts are summarized in Table 1. We note significance in younger men with higher serum PSA in the external validation cohort ($p < 0.001$). We also note a higher percentage of abnormal DRE and repeat prostate biopsies in the validation cohort, compared with a lower percentage of men with PCa family history ($p < 0.001$). Prostate volume was similar in both cohorts ($p = 0.559$). Caucasian ethnicity was predominant in both cohorts ($p = 0.738$). A similar distribution of DRE prostate volume categories was observed in both cohorts ($p = 0.675$). There was a different case-mix of PI-RADS categories in both cohorts ($p < 0.001$). An increased trend of csPCa and a significant increase of iPCa ($p < 0.001$) was found in the validation cohort ($p = 0.058$). The distribution of csPCa according to the PI-RADS categories was similar in both cohorts when they were > 3, and a higher percentage of csPCa existed in men with PI-RADS < 3 in the validation cohort ($p < 0.001$).

Table 1. Characteristics of men making up the development and validation cohort.

Variable	Development Cohort	Validation Cohort	*p*-Value
Number of men	1,486	946	-
Caucasian ethnicity, n (%)	1.465 (98.6)	931 (98.4)	0.738
Median age at biopsy (IQR), years	69 (62–74)	67 (61–72)	<0.001
Median serum PSA (IQR), ng/mL	6.0 (4.4–9.2)	7.4 (5.5–10.9)	<0.001
Abnormal DRE, *n* (%)	329 (22.1)	283 (29.9)	<0.001
PCa family history, *n* (%)	127 (8.5)	34 (3.6)	<0.001
Prior negative prostate biopsy, *n* (%)	388 (26.1)	293 (31.0)	=0.010
Median prostate volume (IQR), mL	55 (40–76)	55 (40–78)	=0.559
DRE-prostate volume category, *n* (%)			=0.675
I	140 (9.4)	96 (10.2)	
II	681 (45.8)	417 (44.2)	
III	665 (44.8)	431 (45.7)	

Table 1. *Cont.*

Variable	Development Cohort	Validation Cohort	*p*-Value
PI-RADS v.2.0, *n* (%)			<0.001
1	242 (16.3)	185 (19.6)	
2	73 (4.9)	50 (5.3)	
3	444 (29.9)	201 (21.2)	
4	450 (30.3)	391 (41.3)	
5	277 (18.6)	119 (12.6)	
PCa detection, *n* (%)	693 (46.6)	521 (55.1)	<0.001
csPCa detection, *n* (%)	548 (36.9)	386 (40.8)	=0.058
iPCa detection, *n* (%)	145 (9.8)	135 (14.3)	<0.001
csPCa detection according to PI-RADS			<0.001
<3	13 (4.1)	42 (17.9)	
3	68 (15.3)	41 (20.4)	
4	236 (52.4)	203 (51.9)	
5	231 (83.4)	100 (84.0)	

IQR = interquartile range; *n* = number; PSA = prostatic specific antigen; DRE = digital rectal examination; PI-RADS = Prostate Imaging Reporting and Data System; PCa = prostate cancer; csPCa = clinically significant PCa; iPCa = insignificant PCa; I = up to 30 mL; II = between 30 and 59 mL; III = 60 mL or above.

3.2. Development of the Predictive Model and Its Calibration in the Development and Validation Cohorts

Independent predictors of csPCa were selected to generate the predictive model; ORs with 95% CIs in univariate and multivariate analysis are presented in Table 2. We note that the DRE prostate volume category was an independent predictor of csPCa. The non-linear dependence of PSA analysed by restricted cubic splines was adjusted by a logarithmic transformation. The developed nomogram is presented in Figure 1. Calibration curves of the developed model in the development and validation cohorts are presented in Figure 2. We note a good agreement between predictions and real outcomes in both development (A) and validation (B) cohorts. In the validation cohort, a slight underestimation of csPCa incidence was observed with a calibration of approximately 0.118, showing a minimum difference between the mean observed and the mean predicted and an almost perfect slope of 1.013.

Table 2. Odds ratios and 95% confidence intervals for csPCa of independent predictive values in univariate and multivariate analysis.

Predictive Variable	Univariate OR (95% CI)	*p*-Value	Multivariate OR (95% CI)	*p*-Value
Age at biopsy, years	1.08 (1.06-1.09)	<0.001	1.08 (1.06–1.10)	<0.001
Median log serum PSA, ng/mL	8.03 (5.31-12.14)	<0.001	12.96 (7.69–21.84)	<0.001
Abnormal DRE, yes vs no	4.51 (3.48-5.84)	<0.001	3.19 (2.34–4.34)	<0.001
PCa family history, yes vs no	1.77 (1.23-2.56)	=0.002	1.69 (1.06–2.68)	=0.026
Prior negative prostate biopsy, yes vs no	0.68 (0.53-0.87)	=0.002	0.63 (046–0.85)	=0.003
DRE-prostate volume category, II vs I	0.37 (0.25-0.55)	<0.001	0.35 (0.22–0.55)	<0.001
DRE-prostate volume category, III vs I	0.11 (0.07-0.16)	<0.001	0.07 (0.04–0.12)	<0.001

O.R. = odd ratio; C.I. = confidence interval; PCa =prostate cancer; DRE =digital rectal examination; PSA =prostate-specific antigen; I = < 30 mL; II = 30–59 mL; III = > 60 mL.

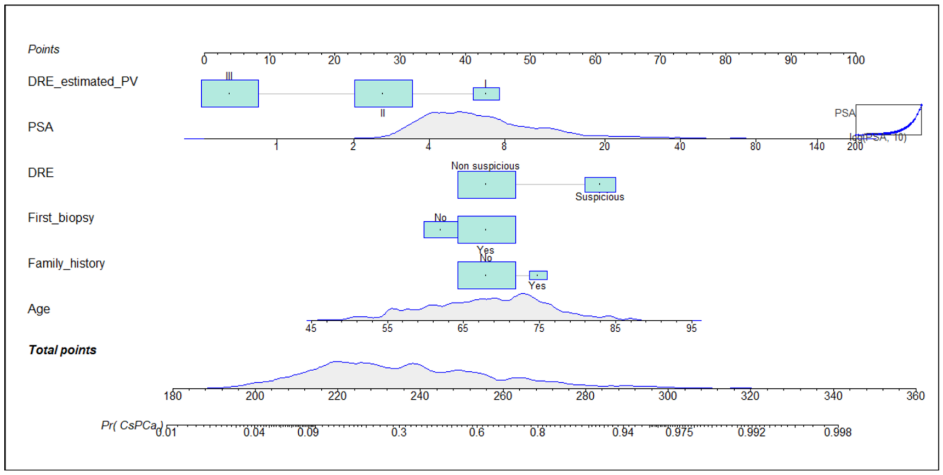

Figure 1. Nomogram of development model. DRE_estimated_PV = digital rectal examination prostate volume category; PSA = prostate-specific antigen; *Pr* = probability.

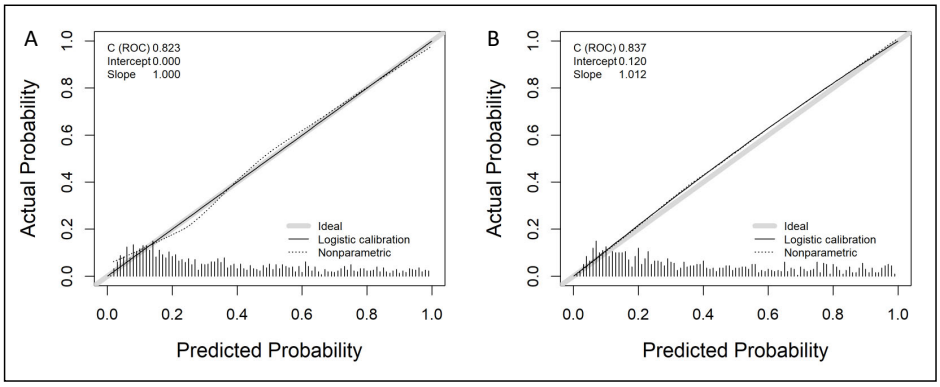

Figure 2. Calibration curves of predictive model in development cohort (**A**) and validation cohort (**B**).

3.3. Discrimination Ability of BCN-RC 1 for csPCa, Net Benefit over Performing mpMRI in All Men, Clinical Utility and Performance in the Development and Validation Cohorts

A web app for BCN-RC 1 was designed and is freely available with the BCN-RC 2 at https://mripcaprediction.shinyapps.io/MRIPCaPrediction/ (accessed on 16 October 2022). The discrimination ability for csPCa of BCN-RC 1 in the development and validation cohorts, analysed through ROC curves, are presented in Figure 3. The AUC of BCN-RC 1 was 0.823 (95% CI: 0.800–0.846) in the development cohort and 0.837 (95% CI: 0.810–0.863) in the validation cohort ($p = 0.447$).

BCN-RC 1 showed net benefit, analysed with DCAs, over performing mpMRI in all men in the development cohort from 12% threshold probability (A) and from 8% threshold probability in the validation cohort (B), Figure 4.

Finally, the clinical utility of BCN-RC 1 in the development and validated cohorts is reported through CUCs in Figure 5. Percentages of avoided mpMRI and missed csPCa are presented for a continuous expression of csPCa risk threshold.

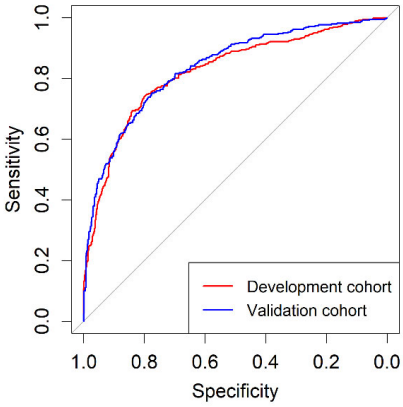

Figure 3. Discrimination ability represented by receiver operating characteristic curves of BCN-RC 1 in the development cohort and validation cohort.

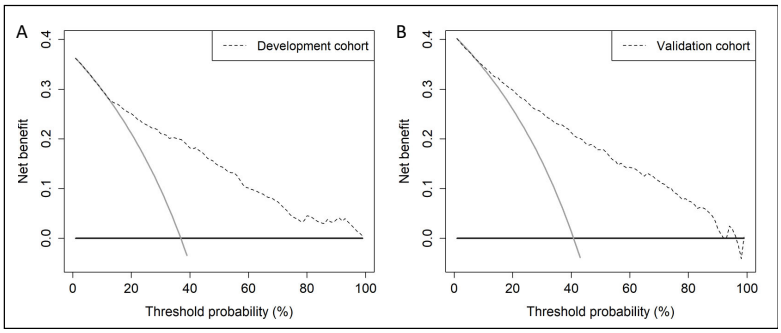

Figure 4. Net benefit of BCN-RC 1 over performing MRI scans represented through decision curve analysis in all men in the development cohort (**A**) and the validation cohort (**B**).

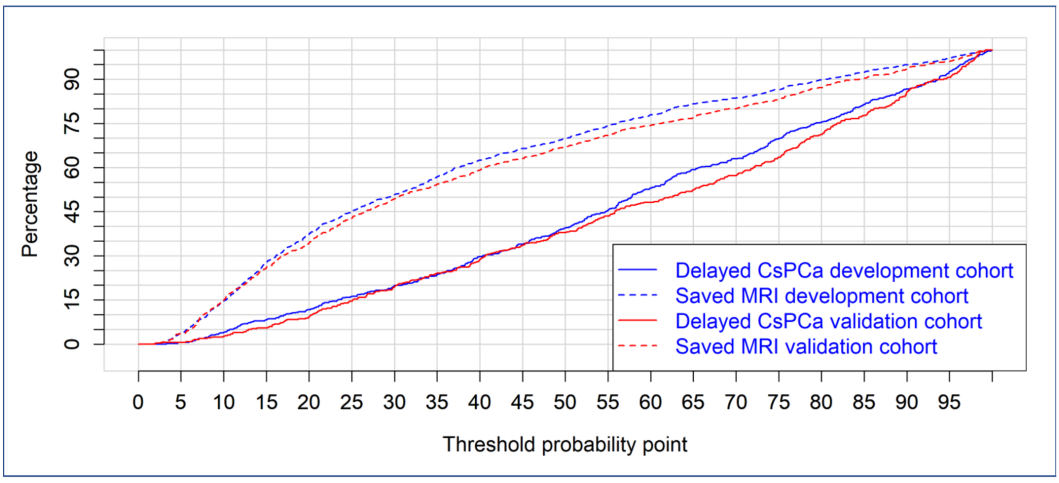

Figure 5. Saved mpMRI scans and missed csPCa for a continuous risk threshold of csPCa, represented through clinical utility curves.

Specificities obtained with the probability thresholds at 0.80 to 0.95% sensitivities for csPCa are presented in Table 3. We note that at 11.1% and 13.3%, which were the 0.95 sensitivity thresholds, that specificity in the development cohort was 0.24 (95% CI: 0.22–0.26), compared with 0.34 (95% CI: 0.31–0.37) in the validation cohort ($p < 0.001$), Table 3. At 0.80 and 0.85 sensitivities, the specificities were similar in both development and validation cohorts, while at 0.90 and 0.95 sensitivities, the specificities in the validation cohort were significantly higher than those observed in the development cohort.

Table 3. Specificities of developed predictive model corresponding to sensitivities of 0.80, 0.85, 0.90, and 0.95 in the development and validation cohorts.

Sensitivity	Development Cohort		Validation Cohort		*p* Value
	Specificy (95% CI)	Threshold (%)	Specificy (95% CI)	Threshold (%)	
0.80	0.70 (0.68–0.72)	30.8	0.70 (0.67–0.73)	30.3	0.927
0.85	0.59 (0.56–0.61)	23.4	0.63 (0.59–0.66)	25.1	0.187
0.90	0.45 (0.43–0.48)	17.2	0.53 (0.49–0.56)	30.3	<0.001
0.95	0.24 (0.22–0.26)	11.1	0.34 (0.31–0.37)	13.3	<0.001

CI = confidence interval.

We found that, using the probability threshold of missing 5% of all detected csPCa, which represents 1.8% and 2% of missed csPCa among the men at risk of PCa in the development and validation cohorts, respectively, the percentage of saved mpMRI scans was 17.2% in the development cohort but reached up to 22.3% in the validation cohort ($p < 0.001$) (Table 4, Figure 5). Performance parameters of BCN-RC 1 at 0.95 sensitivity threshold (11.1%) in the development cohort and validation cohort (13.3%) are presented in Table 4.

Table 4. Performance of developed predictive model of csPCa in development and validation cohorts from the 95% sensitivity threshold of csPCa of the development cohort.

Parameter	Development Cohort	Validation Cohort
Sensitivity, number (%)	520/548 (95.0)	367/386 (95.0)
Specificity, number (%)	228/938 (24.3)	192/560 34.3)
Positive predictive value, number (%)	520/1230 (42.3)	367/737 (49.8)
Negative predictive value, number (%)	228/256 (89.1)	192/209 (91.9)
Accuracy, number (%)	748/1486 (50.3)	559/946 (59.1)
Avoided mpMRI exams, number (%)	256/1486 (17.2)	211/946 (22.3)
Missed csPCa, number (%)	28/548 (5.0)	19/386 (5.0)
Odds ratio (95% confidence interval)	6.19 (4.06-9.43)	9.92 (6.06-16.24)

MpMRI = multiparametric magnetic resonance imaging.

Finally, Table 5 describes the number of missed csPCa and saved mpMRI scans in a hypothetical 1000 men with PCa suspicion in the development and validation cohorts according to threshold probabilities of csPCa from 1 to 100%.

Table 5. Number of missing csPCa and mpMRI scans saved for different thresholds in a hypothetical 1000 cases of PCa suspicion in development and validation cohorts.

Threshold Probability	Development Cohort		Validation Cohort	
	Missed csPCa	Saved mpMRI	Missed csPCa	Saved mpMRI
1	0	0	0	0
2	0	1	1	2
3	0	7	2	6
4	1	20	2	17
5	2	38	2	35

Table 5. *Cont.*

Threshold Probability	Development Cohort		Validation Cohort	
	Missed csPCa	Saved mpMRI	Missed csPCa	Saved mpMRI
6	3	55	3	49
7	7	81	6	74
8	8	97	7	106
9	11	124	10	127
10	15	146	11	150
11	19	170	14	177
12	24	197	16	195
13	27	224	20	217
14	29	247	22	238
15	30	278	22	259
16	32	295	27	280
17	36	318	31	302
18	39	336	34	317
19	40	353	35	326
20	43	374	38	344
21	46	392	44	369
22	52	410	49	379
23	54	424	52	395
24	58	439	56	418
25	60	451	59	428
26	63	466	64	442
27	65	476	70	456
28	67	491	73	468
29	68	497	74	478
30	73	507	79	494
35	87	569	98	543
40	110	625	117	592
45	125	664	137	631
50	145	699	154	670
55	168	742	178	709
60	196	779	197	743
65	219	817	214	768
70	232	836	234	800
75	257	865	259	832
80	278	898	291	872
85	300	925	317	904
90	320	950	350	938
95	342	973	370	961
100	369	1000	408	1000

mpMRI = multiparametric magnetic resonance imaging; csPCa = clinically significant prostate cancer.

4. Discussion

The designed BCN-RC 1 model, based on a new developed predictive model using the DRE prostate volume category, was validated in the Barcelona metropolitan area with the aim of stratifying initial suspicion of PCa to avoid unnecessary mpMRI scans. Since pre-biopsy mpMRI and guided biopsies were performed on all suspicious lesions, BCN-RC1 predicts csPCa risk even in the anterior prostate gland. The new BCN-RC 1 and BCN-RC 2, designed for selecting men for prostate biopsy after mpMRI [23], could be sequenced to establish a risk-organized model for early detection of csPCa in the Barcelona metropolitan area, where both risk calculators were validated. This risk-organized model can be especially useful in sites where access to mpMRI is limited [9,13].

The prestigious Rotterdam risk calculator was designed from the predictive models developed among the participants of the Rotterdam section of the ERSPC trial. The Rotterdam RC 3 and RC 4 calculators were designed before the spread of mpMRI to individualize the risk of PCa and high-grade PCa in biopsy-naïve men and those with prior negative prostate

biopsy, respectively [33]. After the recommendation of pre-biopsy mpMRI, both risk calculators have been validated for selecting candidates for MRI [34,35]. Both Rotterdam RC 3 and RC 4 initially included the serum PSA, DRE (normal vs abnormal), hypoechoic areas in TRUS (presence vs absence), and prostate volume assessed from TRUS as predictive variables [34]. However, since 2012, it has been possible to introduce the estimated prostate volume with DRE. This modification was motivated by TRUS prostate volume usually not being available at initial PCa suspicion [19–21]. DRE categories were established from the TRUS prostate volume intervals of less than 30 mL, 30 to 59 mL, and 60 mL or above [34,35]. Under these conditions, Alberts et al. analysed Rotterdam RC 4 in 122 men with suspected PCa and prior negative prostate biopsy, in 26% of whom csPCa was detected. Using a 3% risk threshold for csPCa, Rotterdam RC 4 avoided 51% of mpMRI scans missing 9.7% of detected csPCa [34]. Similarly, Manners et al. analysed Rotterdam RC 3 in 200 biopsy-naïve suspected PCa men in 33.5% of whom csPCa was detected. After adjusting the risk threshold to 4%, 36.5% of mpMRI scans were avoided, missing 6% of detected csPCa [35]. Remmers et al., in a recent analysis of the current Rotterdam risk calculator without MRI, among the 206 men of the PRECISION trial MRI arm, in whom 70 csPCa were diagnosed, observed after recalibration of the model and adjustment of the risk threshold, there was 13.1% reduction in MRI scans, missing 7.1% of detected csPCa [36].

The new BCN-RC 1 includes the same clinical predictive variables as BCN-RC 2, except those derived from mpMRI. Age (years), PCa family history (yes vs no), biopsy status (naïve vs repeat), serum PSA (ng/mL), DRE (normal vs abnormal), and DRE prostate volume category (which substituted the MRI prostate volume), were found to be independent clinical predictors of csPCa in logistic regression analysis. The calibration curves showed a good agreement between predictions and the real outcome in both development and validation cohorts. The discrimination ability of csPCa was similar in both development and validation cohorts, despite their four-percentage-point difference in csPCa detection. The observed AUCs were like those reported by Alberts et al. in men with previous negative prostate biopsy [34]. Manners et al. [35] and Remmers et al. [36] did not report the discrimination ability of Rotterdam RC in their studies. In both development and validation cohorts, we observed net benefit of BCN-RC 1 over performing mpMRI for all men when from a risk threshold of csPCa between 8 to 12%. We estimated the performance of BCN-RC 1 with different sensitivities; however, with the 0.95 sensitivity of csPCa, which is in our opinion appropriate at initial PCa suspicion, the specificities in the development and validation cohort were 0.24 and 0.34, respectively, which allowed avoidance of 17.2% and 22.3% of mpMRI scans, respectively. These percentages of saved mpMRI scans were below the 51% reported with Rotterdam RC 4 and the 36.5% reported with Rotterdam RC 3, although the reported missed high-grade PCa percentages were 6% and 9.7%, respectively, compared with the up to 5% fixed for BCN-RC 1 [34,35]. In the recent Rotterdam RC 3 analysis, carried out in the PRECISION trial MRI arm, the percentage of avoided mpMRI decreased to 13.1% compared to the 36.5% reported by Manners et al., with percentages of missed csPCa of 7.1% and 6%, respectively [35,36]. We also have analysed the behaviour of BCN-RC 1 in a hypothetical 1000 men with PCa suspicion, observing that while missing 5% of detected csPCa, 410 mpMRI would be saved in the development cohort, compared to 382 in the validation cohort. Comparisons between Rotterdam RC 3 and RC 4 with BCN-RC 1 are difficult because it was developed to stratify the initial PCa suspicion of any men, whether biopsy-naïve or with previous negative prostate biopsy. The validation studies of Rotterdam RC 3 and RC 4 were performed with the based TRUS prostate volume, whereas we used the DRE prostate volume category estimated from the MRI prostate volume [19,20]. Regrettably, DRE is not routinely performed to suspect PCa [22], which is why we report the routine and complete achievement of DRE at initial PCa suspicion, assessing the prostate volume category beyond the abnormalities in the posterior prostate gland surface [20].

The web app of BCN-RC 1 was designed from a predictive model developed and externally validated in sizable cohorts of consecutive men of the same metropolitan area, with the same criteria of PCa suspicion and following the same diagnostic approach of csPCa, without limitations in age, serum PSA, or prostate volume as exist in the Rotterdam RCs. Even so, we found a 4% difference between the csPCa detection observed in development and validation cohorts, which was a stressful scenario for the predictive model. Despite this difference, the discrimination ability of the developed predictive model remained, and the rate of avoided mpMRI even increased somewhat in the validation cohort. Our study is limited by the fact that we assumed DRE accurately classifies the prostate volume category assessed from MRI. Roobol et al. made the same assumption regarding TRUS reported prostate volume due to previous evidence [19,20]. Recently, Massanova et al. confirmed a good correlation between the DRE estimated prostate volume with that assessed from MRI [37]. However, we believe that prospective analysis to define accurate MRI prostate volume intervals assessed by DRE categories is needed. Additionally, the current study takes on the limitations of predictive models that provide the specific risk of csPCa based on the landscapes in which they are developed [33]. The essential web or smartphone risk calculators need validation in each population where they will be conducted. Usually, external validations are carried out in populations with different characteristics and landscapes than those of a development cohort, and recalibrations and adjustments of csPCa risk thresholds are usually needed to obtain accurate predictions [38]. Because characteristics of populations, PCa incidence, and diagnostic approaches frequently change, making accurate real-time predictions adapted to the continuous evolution is challenging [39]. Continuous updating of risk calculators from the feedback of new cases, integrating the generation of big data, appropriate machine-learning algorithm design [40,41], and federated networks will provide the opportunity to develop future predictive models and risk calculators guaranteeing accurate and enduring overall and specific predictions [42].

Finally, we note that sequencing predictive tools are recommended for risk-orga-nised models of early detection of csPCa, first stratifying the initial PCa suspicion to reduce MRI demand and after MRI to reduce unnecessary prostate biopsies [9]. Remmers et al., after reducing 13.1% of mpMRI requests in a first stratification, observed how in a second stratification with the Rotterdam RC, MRI decreased up to 20.9% of prostate biopsies, whereas the percentage of missed csPCa increased from 7% to 8.6% [36]. Recently, the initial PCa suspicion of 2881 men has been stratified to avoid MRI scans first from the subset of men with serum PSA > 10 ng/mL and abnormal DRE [43], and thereafter with the PSA density calculated from the prostate volume estimated with DRE, resulting in a 20.3% reduction of MRI scans with 3.8% missing csPCa [21]. New combinations of appropriate tools available before and after MRI for risk-organized models of early detection of csPCa must be explored.

5. Conclusions

Currently, the EAU recommends risk-organized models for early detection of csPCa, stratifying the initial suspicion of PCa for avoiding MRI scans, and then stratifying men after MRI to avoid prostate biopsies. We have designed and validated BCN-RC 1 to stratify the initial PCa suspicion to reduce mpMRI demand. BCN-RC 1 includes the same clinical predictors as BCN-RC 2, except those derived from mpMRI, having substituted the MRI derived prostate volume with the DRE prostate volume category. The new BCN-RC 1 avoided between 17.2% and 22.3% mpMRI scans while missing 5% of detected csPCa, which represented 1.8% of men at risk in the development cohort and 2% in the validation cohort. We report efficient accomplishment of DRE in the early detection of csPCa for an appropriate selection for mpMRI. BCN-RC 1 is ready to be sequenced with BCN-RC 2 in a risk-organized model of csPCa.

Author Contributions: Conceptualization, J.M., Á.B.-F. and L.M.E.; methodology, J.M., Á.B.-F. and L.M.E.; formal analysis, J.M., Á.B.-F. and L.M.E.; resources, Á.B.-F., L.M.E.; data curation, M.T., M.C., A.C., O.M., J.P., J.M.A., P.S., L.R., E.T.; writing—original draft preparation, J.M.; writing—review and editing, J.M., Á.B.-F. and L.M.E.; supervision, J.M., E.T.; project administration, J.M.; funding acquisition, J.M. All authors have read and agreed to the published version of the manuscript.

Funding: This research was funded by Instituto de Salut Carlos III (SP) and European Union, grant number PI20/01666.

Institutional Review Board Statement: The study was conducted in accordance with the Declaration of Helsinki and approved by the Institutional Ethics Committee of Vall d'Hebron Hospital (PR/AG-317/2017 approved on 28 August 2017).

Informed Consent Statement: Informed consent was obtained from all subjects involved in the study.

Data Availability Statement: The data presented in this study are available on request from the corresponding author.

Conflicts of Interest: The authors declare no conflict of interest.

References

1. Frånlund, M.; Månsson, M.; Godtman, R.A.; Aus, G.; Holmberg, E.; Kollberg, K.S.; Lodding, P.; Pihl, C.G.; Stranne, J.; Lilja, H.; et al. Results from 22 years of Followup in the Göteborg Randomized Population-Based Prostate Cancer Screening Trial. *J. Urol.* **2022**, *208*, 292–300. [CrossRef] [PubMed]
2. Chou, R.; Croswell, J.M.; Dana, T.; Bougatsos, C.; Blazina, I.; Fu, R.; Gleitsmann, K.; Koenig, H.C.; Lam, C.; Maltz, A.; et al. Screening for prostate cancer: A review of the evidence for the U.S. Preventive Services Task Force. *Ann. Intern. Med.* **2011**, *155*, 762–771. [CrossRef] [PubMed]
3. Schoots, I.G.; Padhani, A.R.; Rouvière, O.; Barentsz, J.O.; Richenberg, J. Analysis of Magnetic Resonance Imaging-directed Biopsy Strategies for Changing the Paradigm of Prostate Cancer Diagnosis. *Eur. Urol. Oncol.* **2020**, *3*, 32–41. [CrossRef]
4. Mottet, N.; van den Bergh, R.C.N.; Briesrs, E.; Briers, E.; Van den Broeck, T.; Cumberbatch, M.G.; De Santis, M.; Fanti, S.; Fossati, N.; Gandaglia, G.; et al. EAU-EANM-ESTRO-ESUR-SIOG Guidelines on Prostate Cancer-2020 Update. Part 1: Screening, Diagnosis, and Local Treatment with Curative Intent. *Eur. Urol.* **2021**, *79*, 243–262. [CrossRef]
5. Van Poppel, H.; Roobol, M.J.; Chapple, C.R.; Catto, J.W.F.; N'Dow, J.; Sønksen, J.; Stenzl, A.; Wirth, M. Prostate-specific Antigen Testing as Part of a Risk-Adapted Early Detection Strategy for Prostate Cancer: European Association of Urology Position and Recommendations for 2021. *Eur. Urol.* **2021**, *80*, 703–711. [CrossRef]
6. Sathianathen, N.J.; Omer, A.; Harris, S.; Davies, L.; Kasivisvanathan, V.; Punwani, S.; Moore, C.M.; Kastner, C.; Barrett, T.; Van Den Bergh, R.C.; et al. Negative Predictive Value of Multiparametric Magnetic Resonance Imaging in the Detection of Clinically Significant Prostate Cancer in the Prostate Imaging Reporting and Data System Era: A Systematic Review and Meta-analysis. *Eur. Urol.* **2020**, *78*, 402–414. [CrossRef] [PubMed]
7. Drost, F.H.; Osses, D.; Nieboer, D.; Bangma, C.H.; Steyerberg, E.W.; Roobol, M.J.; Schoots, I.G. Prostate Magnetic Resonance Imaging, with or Without Magnetic Resonance Imaging-targeted Biopsy, and Systematic Biopsy for Detecting Prostate Cancer: A Cochrane Systematic Review and Meta-analysis. *Eur. Urol.* **2020**, *77*, 78–94. [CrossRef] [PubMed]
8. Mazzone, E.; Stabile, A.; Pellegrino, F.; Basile, G.; Cignoli, D.; Cirulli, G.O.; Sorce, G.; Barletta, F.; Scuderi, S.; Bravi, C.A.; et al. Positive Predictive Value of Prostate Imaging Reporting and DataSystem Version 2 for the Detection of Clinically Significant Prostate Cancer: A Systematic Review and Meta-analysis. *Eur. Urol. Oncol.* **2020**, *4*, 697–713. [CrossRef] [PubMed]
9. Van Poppel, H.; Hogenhout, R.; Albers, P.; van den Bergh, R.C.N.; Barentsz, J.O.; Roobol, M.J. A European Model for an Organised Risk-stratified Early Detection Programme for Prostate Cancer. *Eur. Urol. Oncol.* **2021**, *4*, 731–739. [CrossRef]
10. Belue, M.J.; Yilmaz, E.C.; Daryanani, A.; Turkbey, B. Current Status of Biparametric MRI in Prostate Cancer Diagnosis: Literature Analysis. *Life* **2022**, *12*, 804. [CrossRef]
11. Osses, D.F.; Roobol, M.J.; Schoots, I.G. Prediction Medicine: Biomarkers, Risk Calculators and Magnetic Resonance Imaging as Risk Stratification Tools in Prostate Cancer Diagnosis. *Int. J. Mol. Sci.* **2020**, *20*, 1637. [CrossRef]
12. Govers, T.M.; Hesses, D.; Vlaeminck-Guillem, V.; Schmitz-Dräger, B.J.; Stief, C.G.; Martinez-Ballesteros, C.; Ferro, M.; Borque-Fernando, A.; Rubio-Briones, J.; Sedelaar, J.P.M.; et al. Cost-effectiveness of SelectMDx for prostate cancer in four European countries: A comparative modeling study. *Prostate Cancer Prostatic Dis.* **2018**, *22*, 101–109. [CrossRef]
13. Vickers, A.J.; Russo, G.; Lilja, H.; Evans, C.; Schalken, J.A.; Klein, E.; Eggener, S. How Should Molecular Markers and Magnetic Resonance Imaging Be Used in the Early Detection of Prostate Cancer. *Eur. Urol. Oncol.* **2022**, *5*, 135–137. [CrossRef]
14. Yamashiro, J.R.; de Riese, W.T.W. Any Correlation Between Prostate Volume and Incidence of Prostate Cancer: A Review of Reported Data for the Last Thirty Years. *Res. Rep. Urol.* **2021**, *13*, 749–757. [CrossRef]
15. Benson, M.C.; Whang, I.S.; Pantuck, A.; Ring, K.; Kaplan, S.A.; Olsson, C.A.; Cooner, W.H. Prostate specific antigen density: A means of distinguishing benign prostatic hypertrophy and prostate cancer. *J. Urol.* **1992**, *147*, 815–816. [CrossRef]

16. Dianat, S.S.; Rancier Ruiz, R.M.; Bonekamp, D.; Carter, H.B.; Macura, K.J. Prostate volumetric assessment by magnetic resonance imaging and transrectal ultrasound: Impact of variation in calculated prostate-specific antigen density on patient eligibility for active surveillance program. *J. Comput. Assist. Tomogr.* **2013**, *37*, 589–595. [CrossRef]
17. Morote, J.; Celma, A.; Diaz, F.; Regis, L.; Roche, S.; Mast, R.; Semidey, M.E.; de Torres, I.M.; Planas, J.; Trilla, E. Prostatic-specific antigen density behavior according to multiparametric magnetic resonance imaging result. *Urol. Oncol.* **2020**, *38*, 410–417. [CrossRef]
18. Morote, J.; Díaz, F.; Celma, A.; Planas, J.; Trilla, E. Behavior of SelectMDx and Prostate-specific Antigen Density in the Challenging Scenario of Prostate Imaging-Reporting and Data System Category 3 Lesions. *Eur. Urol.* **2022**, *81*, 124–125. [CrossRef]
19. Roobol, M.J.; van Vugt, H.A.; Loeb, S.; Zhu, X.; Bul, M.; Bangma, C.H.; van Leenders, A.G.; Steyerberg, E.W.; Schröder, F.H. Prediction of prostate cancer risk: The role of prostate volume and digital rectal examination in the ERSPC risk calculators. *Eur. Urol.* **2012**, *61*, 577–583. [CrossRef]
20. Roobol, M.J.; Schröder, F.H.; Hugosson, J.; Jones, J.S.; Kattan, M.W.; Klein, E.A.; Hamdy, F.; Neal, D.; Donovan, J.; Parekh, D.J.; et al. Importance of prostate volume in the European Randomised Study of Screening for Prostate Cancer (ERSPC) risk calculators: Results from the prostate biopsy collaborative group. *World J. Urol.* **2012**, *30*, 149–155. [CrossRef]
21. Roehrborn, C.G.; Girman, C.J.; Rhodes, T.; Hanson, K.A.; Collins, G.N.; Sech, S.M.; Jacobsen, S.J.; Garraway, W.M.; Lieber, M.M. Correlation between prostate size estimated by digital rectal examination and measured by transrectal ultrasound. *Urology* **1997**, *49*, 548–557. [CrossRef]
22. Naji, L.; Randhawa, H.; Sohani, Z.; Dennis, B.; Lautenbach, D.; Kavanagh, O.; Bawor, M.; Banfield, L.; Profetto, J. Digital Rectal Examination for Prostate Cancer Screening in Primary Care: A Systematic Review and Meta-Analysis. *Ann. Fam. Med.* **2018**, *16*, 149–154. [CrossRef] [PubMed]
23. Morote, J.; Borque-Fernando, A.; Triquell, M.; Celma, A.; Regis, L.; Abascal, J.M.; Sola, C.; Servian, P.; Escobar, M.; Mast, R.; et al. The Barcelona Predictive Model of Clinically Significant Prostate Cancer. *Cancers* **2022**, *14*, 1589. [CrossRef] [PubMed]
24. Bossuyt, P.M.; Reitsma, J.B.; Bruns, D.E.; Korevaar, D.A. STARD 2015: An updated list of essential items for reporting diagnostic accuracy studies. *BMJ* **2015**, *351*, h5527. [CrossRef] [PubMed]
25. Barentsz, J.O.; Richenberg, J.; Clements, R.; Choyke, P.; Verma, S.; Villeirs, G.; Rouviere, O.; Logager, V.; Futterer, J.J. ESUR prostate MR guidelines 2012. *Eur. Radiol.* **2012**, *22*, 746–757. [CrossRef] [PubMed]
26. Weinreb, J.C.; Barentsz, J.O.; Choyke, P.L.; Cornud, F.; Haider, M.A.; Macura, K.J.; Margolis, D.; Schnall, M.D.; Shtern, F.; Tempany, C.M.; et al. PI-RADS Prostate Imaging—Reporting and Data System: 2015, Version 2. *Eur. Urol.* **2016**, *69*, 16–40. [CrossRef]
27. Epstein, J.I.; Egevad, L.; Amin, M.B.; Delahunt, B.; Srigley, J.R.; Humphrey, P.A.; Grading, C. The 2014 International Society of Urological Pathology (ISUP) Consensus Conference on Gleason Grading of Prostatic Carcinoma: Definition of Grading Patterns and Proposal for a New Grading System. *Am. J. Surg. Pathol.* **2016**, *40*, 244–252. [CrossRef]
28. McShane, L.M.; Altman, D.G.; Sauerbrei, W.; Taube, S.E.; Gion, M.; Clark, G.M. Statistics SOTNCI-EORTCWGOCD. Reporting recommendations for tumour MARKer prognostic studies (REMARK). *Br. J. Cancer.* **2005**, *93*, 387–391. [CrossRef]
29. Creelman, C.D.; Donaldson, W. ROC curves for discrimination of linear extent. *J. Exp. Psychol.* **1968**, *77*, 514–516. [CrossRef]
30. DeLong, E.R.; DeLong DMClarke-Pearson, D.L. Comparing the areas under two or more correlated receiver operating characteristic curves: A nonparametric approach. *Biometrics* **1988**, *44*, 837–845. [CrossRef]
31. Vickers, A.J.; Elkin, E.B. Decision curve analysis: A novel method for evaluating prediction models. *Med. Decis. Mak.* **2006**, *26*, 565–574. [CrossRef] [PubMed]
32. Borque, A.; Rubio-Briones, J.; Esteban, L.M.; Sanz, G.; Dominguez-Escrig, J.; Ramirez-Backhaus, M.; Calatrava, A.; Solsona, E. Implementing the use of nomograms by choosing threshold points in predictive models: 2012 updated Partin Tables vs a European predictive nomogram for organ-confined disease in prostate cancer. *B.J.U Int.* **2014**, *113*, 878–886. [CrossRef] [PubMed]
33. Roobol, M.J.; Steyerberg, E.W.; Kranse, R.; Wolters, T.; van den Bergh, R.C.; Bangma, C.H.; Schroder, F.H. A risk-based strategy improves prostate-specific antigen-driven detection of prostate cancer. *Eur. Urol.* **2010**, *57*, 79–85. [CrossRef] [PubMed]
34. Aberts, A.R.; Schoots, I.G.; Bokhorst, L.P.; van Leenders, G.J.; Bangma, C.H.; Roobol, M.J. Risk-based Patient Selection for Magnetic Resonance Imaging-targeted Prostate Biopsy after Negative Transrectal Ultrasound-guided Random Biopsy Avoids Unnecessary Magnetic Resonance Imaging Scans. *Eur. Urol.* **2016**, *69*, 1129–1134. [CrossRef]
35. Mannaerts, C.K.; Gayet, M.; Verbeek, J.F.; Engelbrecht, M.R.W.; Savci-Heijink, C.D.; Jager, G.J.; Gielens, M.P.M.; van der Linden, H.; Beerlage, H.P.; de Reijke, T.M.; et al. Prostate Cancer Risk Assessment in Biopsy-naïve Patients: The Rotterdam Prostate Cancer Risk Calculator in Multiparametric Magnetic Resonance Imaging-Transrectal Ultrasound (TRUS) Fusion Biopsy and Systematic TRUS Biopsy. *Eur. Urol. Oncol.* **2018**, *1*, 109–117. [CrossRef]
36. Remmers, S.; Kasivisvanathan, V.; Verbeek, J.F.M.; Moore, C.M.; Roobol, M.J. ERSPC RSGPRECISIONIG. Reducing Biopsies and Magnetic Resonance Imaging Scans During the Diagnostic Pathway of Prostate Cancer: Applying the Rotterdam Prostate Cancer Risk Calculator to the PRECISION Trial Data. *Eur. Urol. Open. Sci.* **2022**, *36*, 1–8. [CrossRef]
37. Massanova, M.; Robertson, S.; Barone, B.; Dutto, L.; Caputo, V.F.; Bhatt, J.R.; Ahmad, I.; Bada, M.; Obeidallah, A.; Crocetto, F. The Comparison of Imaging and Clinical Methods to Estimate Prostate Volume: A Single-Centre Retrospective Study. *Urol. Int.* **2021**, *105*, 804–810. [CrossRef]
38. Diniz, M.A. Statistical methods for validation of predictive models. *J. Nucl. Cardiol.* **2022**, 1–18. [CrossRef]

39. Strobl, A.N.; Vickers, A.J.; Van Calster, B.; Steyerberg, E.; Leach, R.J.; Thompson, I.M.; Ankerst, D.P. Improving patient prostate cancer risk assessment: Moving from static, globally-applied to dynamic, practice-specific risk calculators. *J. Biomed. Inform.* **2015**, *56*, 87–93. [CrossRef]
40. Checcucci, E.; De Cillis, S.; Granato, S.; Chang, P.; Afyouni, A.S.; Okhunov, Z.; Uro-technology and SoMe Working Group of the Young Academic Urologists Working Party of the European Association of Urology. Applications of neural networks in urology: A systematic review. *Curr. Opin. Urol.* **2020**, *30*, 788–807. [CrossRef]
41. Checcucci, E.; Rosati, S.; De Cillis, S.; Vagni, M.; Giordano, N.; Piana, A.; Granato, S.; Amparore, D.; De Luca, S.; Fiori, C.; et al. Artificial intelligence for target prostate biopsy outcomes prediction the potential application of fuzzy logic. *Prostate Cancer Prostatic Dis.* **2022**, *25*, 359–362. [CrossRef] [PubMed]
42. Nandi, A.; Xhafa, F. A federated learning method for real-time emotion state classification from multi modal streaming. *Methods* **2022**, *204*, 340–344. [CrossRef] [PubMed]
43. Morote, J.; Celma, A.; Roche, S.; de Torres, I.M.; Mast, R.; Semedey, M.E.; Regis, L.; Planas, J. Who Benefits from Multiparametric Magnetic Resonance Imaging After Suspicion of Prostate Cancer. *Eur. Urol. Oncol.* **2019**, *2*, 664–669. [CrossRef]

6. RESUMEN GLOBAL DE LOS RESULTADOS

En el momento en que se realizó la revisión sistemática, marzo de 2022, se encontraron en la literatura 17 modelos predictivos de *csPCa* desarrollados a partir de la *MRI* y variables clínicas (*MRI-PMs*) (164–180). Los datos clínicos utilizados incluidos en estos *MRI-PMs* fueron la edad, el *DRE*, los antecedentes familiares de *PCa*, el tipo de biopsia (inicial o repetida), la etnia, el *PSA* sérico, la *PSAD* y el volumen prostático. Los hallazgos de la *MRI* se informaron principalmente a través de la versión más actualizada de *PI-RADS* (versión 2) aunque los modelos desarrollados más antiguos utilizaron la versión 1 (164–167,169,170,172).

Los *MRI-PMs* mejoraron la capacidad de discriminación del *csPCa* en comparación con los modelos desarrollados a partir de datos clínicos (a los que denominamos modelos de base) o en comparación con la *MRI*. En todos los modelos se evaluó su capacidad discriminatoria de *csPCa* a través de curvas *ROC* y en algunos casos se analizaron curvas de decisión para evaluar su beneficio neto comparado con biopsiar a todos los varones con sospecha de *PCa*. Los *MRI-PMs* siempre mostraron mayor beneficio neto que los modelos de base (164,169–173,175,176,178,179). En un estudio, la eficacia diagnóstica se representó gráficamente a partir de curvas de utilidad clínica (*CUCs)* (176). Los *MRI-PMs* mostraron su capacidad para reducir biopsias de próstata innecesarias e identificar el *csPCa* con mayor precisión. Algunos *MRI-PMs* se desarrollaron en cohortes específicas de hombres con biopsias previas negativas (166,169,171–173), o sometidos a biopsias iniciales (164,166,168,169,172,175,179). Se identificaron sólo algunos *MRI-PMs* con validaciones externas (170–172,174,177,178). Ningún modelo analizó su eficacia clínica según la categoría *PI-RADS.* Los modelos predictivos generalmente se han representado a través de nomogramas; sin embargo, su uso lento e incómodo ha hecho esencial el diseño de calculadoras de riesgo como aplicaciones web o para *smartphones,* para facilitar el uso ágil en la clínica diaria. De los *MRI-PMs* analizados en nuestra

revisión tan solo se encontraron dos calculadoras de riesgo (176,180), y solamente una *online* (176). Después de analizar las limitaciones de los *MRI-PMs* disponibles decidimos iniciar el desarrollo un nuevo modelo predictivo basado en la *mpMRI* el cual se incluyó posteriormente en nuestra revisión sistemática.

Se diseñó una nueva calculadora de riesgo *online* para evaluar la probabilidad de *csPCa*, basada en un *MRI-PM* desarrollado en el Hospital Universitario Vall d'Hebron y validado externamente en el área metropolitana de Barcelona. No se observaron diferencias significativas entre las tasas de detección de *csPCa* entre las cohortes de desarrollo y validación externa ($p = 0.054$), aunque se detectó un incremento en la tasa de detección de *iPCa* ($p < 0.001$). La tasa de detección de *csPCa* fue del 36.9% en la cohorte de desarrollo. El 21.2% de los participantes tenía *PI-RADS* < 3, el 29.9% tenía *PI-RADS* 3, el 30.3% tenía *PI-RADS* 4 y el 18.6% tenía *PI-RADS* 5. La tasa de detección de *csPCa* fue del 40.8% en la cohorte de validación, y el 24.9% de los hombres tenía *PI-RADS* < 3, el 21.2% tenía *PI-RADS* 3, el 41.3% tenía *PI-RADS* 4 y el 12.6% tenía *PI-RADS* 5.

Se realizó un análisis de regresión logística en el que se identificaron la edad, el *PSA* sérico, el *DRE*, el volumen de la próstata, la historia familiar de *PCa*, el tipo de biopsia (inicial o repetida) y el *PI-RADS* v2.0 como predictores independientes de *csPCa*, **Tabla 2 (art. 2.).** El *forest plot* representando la razón de probabilidades de cada predictor se muestra en la **Figura suplementaria 1 (art. 2.).** Se desarrolló el nomograma del modelo, **Figura 3 (art. 2.)** y se realizó su calibración (**Figura suplementaria 2A, art. 2.**). Se observó que el *AUC* de la *mpMRI* sola aumentó significativamente cuando se utilizó junto a variables clínicas en el *MRI-PM* (**Figura 2A, art. 2.**) siendo la primera de 0.842 (95% *CI*: 0.822-0.861) y la segunda de 0.897 (95% *CI*: 0.880-0.914), ($p < 0.011$). También se observó que el *MRI-PM* proporcionó un beneficio neto respecto a la realización de biopsias en todos los varones con sospecha de *PCa* y respecto a la *mpMRI* desde el umbral de

probabilidad de *csPCa* del 2% (**Figura 2B, art. 2.**). Las *CUCs* mostraron la tasa de biopsias potencialmente evitables y su correspondiente porcentaje de *csPCa* no detectado en función del umbral continuo de probabilidades de *csPCa* (**Figura 4, art. 2.**). Se seleccionó como más apropiado el umbral del 15% debido a su sensibilidad del 95% para detectar *csPCa* y su capacidad para evitar el 40% de las biopsias innecesarias. La tasa de las biopsias evitables y el riesgo correspondiente de no detectar *csPCa*, en relación al umbral de probabilidad para una cohorte de desarrollo de 1000 hombres con sospecha de *PCa,* se muestran en valores absolutos en la **Tabla suplementaria 1 (art. 2.)** y en valores relativos en la **Tabla suplementaria 2 (art. 2.)**

La validación externa del *MRI-PM* se realizó en 946 varones con sospecha de *PCa* de dos hospitales del área metropolitana de Barcelona, Parc Salut Mar (Barcelona) y Hospital Germans Trias i Pujol (Badalona). Para una probabilidad de *csPCa* del 20%, la incidencia real fue aproximadamente del 25%, lo que significa que el modelo subestimó ligeramente la incidencia real de *csPCa* en esta cohorte de validación. Esto se debe probablemente a una incidencia de *csPCa* un 4% más alta (40.8% *vs*. 36.9%) en la cohorte de validación respecto a la de desarrollo (**Figura suplementaria 2B, art. 2.**). Las curvas *ROC* del *MRI-PM* en la cohorte de validación externa y la cohorte de desarrollo (**Figura 5A, art. 2.**), mostraron su elevada capacidad discriminatoria de *csPCa*. El *AUC* de la *mpMRI* en la cohorte de validación externa fue de 0.743 (95% *CI*: 0.711-0.776) en comparación con 0.842 (95% *CI*: 0.822-0.861) en la cohorte de desarrollo ($p < 0.001$). El *AUC* del *MRI-PM* en la cohorte de validación externa fue de 0.858 (95% *CI*: 0.833-0.883) mientras que en la cohorte de desarrollo fue de 0.897 (95% *CI*: 0.880-0.914) ($p = 0.009$). En resumen, la eficacia del *MRI-PM* fue mayor que la de la *mpMRI* sola en diferentes niveles de sensibilidad (85%, 90% y 95%) tanto en la cohorte de desarrollo como en la de validación **(Tabla 3, art. 2.).**

Seleccionando el umbral del 15%, se analizó la capacidad de discriminación del *MRI-PM* para el *csPCa* en las categorías de *PI-RADS* en la cohorte de desarrollo y de validación **(Tabla 4, art. 2.).** Las biopsias evitables fueron del 4% en *PI-RADS* 4 y del 0,5% en *PI-RADS* 5 en la cohorte de desarrollo, y del 7,3% y del 2,4%, respectivamente, en la cohorte de validación externa. En varones con *PI-RADS* 3, se podrían haber evitado el 61,9% y el 63,2% de las biopsias de próstata en las cohortes de desarrollo y validación externa, respectivamente, mientras que el 28,2% y el 14% de los *csPCa* existentes no se llegaron a detectar. Finalmente, en varones con *mpMRI* normal (*PI-RADS* < 3), se podría evitar el 95.7% y un 93.5% de biopsias, detectando el 33,3% y el 18,2% de los *csPCa* existentes, respectivamente. La capacidad de discriminación del *MRI-PM* en las diferentes categorías *PI-RADS* a través de las curvas *ROC* y los beneficios netos a través del análisis de curvas de decisión se muestra en las **Figura suplementarias 4A (art. 2.).** para la cohorte de desarrollo y **4B** para la cohorte de validación.

La calculadora de riesgo diseñada, que incorpora la novedad de poder seleccionar el umbral de probabilidad de *csPCa,* se encuentra disponible de forma gratuita en el repositorio de la dirección *web* https://mripcaprediction.shinyapps.io/MRIPCaPrediction/. Debido a haberse desarrollado y validado en Barcelona, al *MRI-PM* y la herramienta *web* se les ha dado el nombre de *BCN MRI-PM* y *BCN MRI-RC*, respectivamente.

Se comparó el *BCN MRI-PM* con la *PSAD*. Las características de los 2432 participantes se resumen en la **Tabla 1 (art. 3.).** Se diagnosticó *PCa* en 1214 hombres (49.9%), *csPCa* en 934 hombres (38.4%) e *iPCa* en 280 hombres (11.5%). Las características de los participantes según las categorías *PI-RADS*, así como las comparaciones entre cada par de categorías *PI-RADS* contiguas se presentan en la **Tabla 2 (art. 3.).** El rendimiento de la *PSAD* y *BCN MRI-PM* fue evaluada mediante distintas estrategias. La eficacia del *BCN MRI-PM* en la detección del

csPCa fue mayor que la de la *PSAD* siendo el *AUC* de 0.893 (95% *CI:* 0.880-0.906) para *BCN MRI-PM* y de 0.764 (95% *CI*: 0.744-0.783) para la *PSAD* ($p < 0.001$) **(Figura 1A, art. 3.).** El *BCN MRI-PM* mostró un beneficio neto sobre la *PSAD* y sobre biopsiar a toda la cohorte a partir de un umbral de probabilidad de *csPCa* del 2%, mientras que la *PSAD* mostró un beneficio neto desde un umbral de probabilidad de *csPCa* del 18% **(Figura 1B, art. 3.).** Los umbrales seleccionados para el *BCN MRI-PM* y la *PSAD* con una sensibilidad del 95% para *csPCa* fueron 13.5% y 0.628 ng/mL^2, respectivamente, con sus correspondientes especificidades del 51.1% y 19.6% ($p < 0.001$) **(Tabla 3, art. 3.).** El *BCN MRI-PM* y la *PSAD* permitieron evitar el 33.4% y el 14.0% de las biopsias de próstata, respectivamente, y dejaron ambos de detectar el 5% de *csPCa*. En cuanto a la agresividad del *csPCa* no detectado, tanto la *PSAD* como el *BCN MRI-PM* no detectaron el 2.4% de los de tumores con $GG \geq 3$. Respecto a los tumores de mayor agresividad, la *PSAD* no detectó el 1% de *csPCa* con $GG \geq 4$, mientras que el *BCN MRI-PM* no dejó de detectar ningún tumor de esa categoría.

El rendimiento diagnóstico de la *PSAD* y del *BCN MRI-PM* se evaluó según las categorías *PI-RADS*. Entre los hombres con *mpMRI* negativa (*PI-RADS* < 3) el *BCN MRI-PM* mostró un *AUC* de 0.824 (95% *CI*: 0.756-0.892), mientras que la *PSAD* mostró un *AUC* de 0.685 (95% *CI*: 0.610-0.761) ($p < 0.001$) **(Figura 2A, art. 3.).** En dicho grupo de hombres, el *BCN MRI-PM* mostró un beneficio neto sobre la *PSAD* en la detección del *csPCa* **(Figura 2B, art. 3.).** Entre los hombres con *PI-RADS* 3, el *BCN MRI-PM* exhibió un *AUC* de 0.768 (95% *CI:* 0.717-0.819), mientras que la *PSAD* presentó un *AUC* de 0.696 (95% *CI*: 0.641-0.750) ($p < 0.001$) **(Figura 3A, art. 3.).** El *BCN MRI-PM* mostró un beneficio neto sobre la *PSAD* desde un umbral de probabilidad de *csPCa* del 18% (**Figura 3B, art. 3.).** Entre los hombres con *PI-RADS* 4, el *BCN MRI-PM* mostró un *AUC* de 0.823 (95% *CI*: 0.769-0.851), mientras que *PSAD* tuvo un *AUC* de 0.742 (95% *CI*: 0.709-0.775) ($p < 0.001$) **(Figura 4A, art. 3.)**. El *BCN MRI-PM* mostró un beneficio neto sobre la *PSAD*

desde un umbral de probabilidad de *csPCa* del 20% respecto al 35% de la *PSAD* **(Figura 4B, art. 3.).** Finalmente, entre los hombres con *PI-RADS* 5, el *BCN MRI-PM* mostró un *AUC* de 0.787 (95% *CI*: 0.728-0.846), mientras que *PSAD* tuvo un *AUC* de 0.761 (95% *CI*: 0.698-0.825) ($p < 0.001$) (**Figura 5A, art. 3.**) Entre los hombres con *PI-RADS* 5, tanto el *BCN MRI-PM* como la *PSAD* mostraron un beneficio mínimo con respecto a biopsiar a todos los hombres desde un umbral de probabilidad de *csPCa* del 65% (**Figura 5B, art. 3.**). En resumen, estos resultados sugieren que el *BCN MRI-PM* es mejor predictor del *csPCa* que la *PSAD* en todas las categorías de *PI-RADS,* aunque el beneficio fue mínimo en *PI-RADS* 5.

Se llevó a cabo una comparación directa entre la Rotterdam *MRI-RC* y la *BCN MRI-RC* en la cohorte de validación en el área metropolitana de Barcelona. Entre los 946 participantes se detectaron 386 *csPCa* (40.8%), que suponían el 17.9% en varones con *MRI* negativa, 20.4% con lesiones *PI-RADS* 3, 51.9% *PI-RADS* 4 y 84% en *PI-RADS* 5. La Rotterdam *MRI-RC* utiliza entre sus factores predictores el *PI-RADS*v1 (rango de 1 a 5), edad (rango entre 50 y 75 años), estado de la biopsia (inicial *vs.* repetida), *PSA* sérico (rango entre 0.4 y 50 ng/ml), *DRE* (normal *vs.* patológico), y volumen prostático (rango entre 10 y 110 ml). Hasta 209 hombres de la cohorte (22.1%) tenían valores fuera del rango aceptado por la Rotterdam *MRI-RC*. En global, la probabilidad mediana de *csPCa* generada a partir de la Rotterdam *MRI-RC* fue del 3% (rango intercuartílico 2-10) en hombres sin *csPCa* y del 25% (9-46) en hombres con *csPCa* ($p < 0.001$), mientras que *BCN MRI-RC* tuvo probabilidades del 10.5% (3.6-27.2) y del 67.1% (39.3-85.6), respectivamente ($p < 0.001$; **Figura 1, art. 4.**). Las curvas de calibración de ambos *RCs* mostraron subestimación del *csPCa,* aunque la *BCN MRI-RC* presentó una curva casi perfecta con una mínima diferencia entre probabilidades reales y predichas (**Figura 2A y 2B, art. 4.**). En global, las *AUC* para la detección de *csPCa* de la *BCN MRI-RC* y la Rotterdam *MRI-RC* y la se presentan en la **Tabla 3A, art.**

4. Estas fueron de 0.856 (95% *CI*: 0.831-0.881) y de 0.844 (95% *CI:* 0.819-0.869) respectivamente (p = 0.116) (**Figura 3A, art. 4.**) La *BCN MRI-RC* mostró beneficio frente a biopsiar a todos los hombres a partir de un umbral de probabilidad del 15%, en cambio, la Rotterdam *MRI-RC* a partir de un 32% (**Figura 3B, art. 4.**).

En las diferentes categorías *PI-RADS*, se observó que la Rotterdam *MRI-RC* mostró valores de probabilidad de *csPCa* más bajos y un rango estrecho de predicciones **(Figura 4A, art. 4.)** en comparación con *BCN MRI-RC* (**Figura 4B, art. 4.**). Las *AUC* en función de las categorías *PI-RADS* fueron similares para ambos modelos, sin embargo, sí se vieron diferencias entre la utilidad clínica de las calculadoras según la categoría *PI-RADS*. Ninguna de las dos calculadoras fue útil en *PI-RADS* < 3 puesto que, para identificar el 50% de los 42 casos de *csPCa* en *MRI* negativa (un 5% del total de *csPCa* detectado) se necesitaría biospiar a un 75% de los hombres en caso de usar la Rotterdam *MRI-RC* y un 80% en caso de la *BCN MRI-RC* (**Figura 5C, art. 4.**). Sin embargo, en *PI-RADS* 3, la *BCN MRI-RC* proporciona un claro beneficio sobre biopsiar a todos los hombres a partir de un umbral de riesgo de 10%, siendo el beneficio de la Rotterdam *MRI-RC* menor (**Figura 5E, art. 4.**). En adición, en hombres con *PI-RADS* 4, la *BCN MRI-RC* mostró un beneficio neto sobre la realización de biopsias en un umbral del 17% de probabilidad de *csPCa,* mientras que Rotterdam *MRI-RC* mostró un pequeño beneficio entre el 50% y el 75% de probabilidad de *csPCa (***Figura 5H, art. 4***).* En hombres con *PI-RADS* 5, la *BCN MRI-RC* mostró un beneficio a partir del 38% de probabilidad de *csPCa,* mientras que Rotterdam *MRI-RC* exhibió un beneficio mínimo a partir del 83% de probabilidad de *csPCa* (**Figura 5K, art. 4.**) En *PI-RADS* 5, donde solo un 16% de las biopsias eran innecesarias, ninguna de las dos calculadoras aseguró ahorrar biopsias innecesarias sin dejar de detectar *csPCa*. En resumen, se observó un comportamiento diferencial entre la Rotterdam *MRI-RC* y la *BCN MRI-RC* en función de las categorías *PI-RADS*. La *BCN MRI-*

RC mostró un rendimiento superior en *PI-RADS* ≥ 3 pero ninguna mostró utilidad en *MRI* negativa y en *PI-RADS* 5.

Por último, después del desarrollo de la *BCN MRI-RC*, a la que a partir de este momento la denominaremos Barcelona *Risk Calculator* 2 (*BCN RC-2*), su validación externa y comparación con la *PSAD* y la Rotterdam *MRI-RC*, se ha desarrollado y validado externamente la Barcelona *Risk Calculator* 1 (*BCN RC-1*) con objetivo de reducir la demanda de *mpMRI* (**art. 5.**). Los números 1 y 2 tienen razón en el orden en los que se podrían utilizar en un modelo de riesgo organizado para la estratificación del riesgo *csPCa*. Las características de las cohortes de desarrollo y validación se resumen en la **Tabla 1** (**art. 5.**). El nuevo modelo predictivo incluyó variables clínicas predictivas similares al *BCN PM-2*, excluyendo obviamente las derivadas de *mpMRI*. Dichas variables fueron edad (años), antecedentes familiares de *PCa* (sí *vs.* no), estado de biopsia (primera vez *vs*. repetida), *PSA* sérico (ng/mL), *DRE* (normal *vs.* anormal) y categoría de volumen prostático por *DRE* (sustituyendo al volumen prostático calculado por *MRI*) resultaron ser predictores clínicos independientes de *csPCa* en el análisis de regresión logística. La capacidad de discriminación de *csPCa* fue similar en ambas cohortes, a pesar de su diferencia del cuatro por ciento en la incidencia del *csPCa*. El nomograma desarrollado se presenta en la **Figura 1 (art. 5.)**. Las curvas de calibración mostraron una buena concordancia entre las predicciones y los resultados reales tanto en la cohorte de desarrollo como en la cohorte de validación **Figura 2 (art. 5.).** En el grupo de validación, se observó una ligera subestimación de la incidencia de *csPCa* con una calibración de aproximadamente 0.118, lo que muestra una diferencia mínima entre la media observada y la media predicha y una pendiente (*slope*) casi perfecta de 1.013. Se desarrolló la aplicación *web* del *BCN RC-1*, que está disponible de forma gratuita en el repositorio *web* https://mripcaprediction.shinyapps.io/MRIPCaPrediction/.

La capacidad de discriminación de la *BCN RC-1* para identificar el *csPCa* en los grupos de desarrollo y validación se evaluó a través de curvas *ROC* (**Figura 3, art. 5.**). El *AUC* de la *BCN RC-1* fue de 0.823 (95% *CI*: 0.800-0.846) en el grupo de desarrollo y de 0.837 (95% *CI*: 0.810-0.863) en el grupo de validación (p = 0.447). *BCN RC-1* demostró un beneficio neto en comparación con la realización de *mpMRI* en todos los hombres en el grupo de desarrollo a partir de un umbral de probabilidad del 12% (**Figura 4A, art. 5.**) y a partir del 8% en el grupo de validación (**Figura 4B, art. 5.**). Finalmente, la utilidad clínica de *BCN RC-1* en los grupos de desarrollo y validación a través de las *CUCs* se muestra en la **Figura 5 (art. 5.)**. El umbral de riesgo para una sensibilidad del 0.95 fue del 11.1% en el grupo de desarrollo y del 13.3% en el grupo de validación, siendo la especificidad de 0.24 en el primer grupo (95% *CI:* 0.22–0.26) y 0.34 (95% *CI*: 0.31–0.37) en el segundo (p < 0.001), **Tabla 3 (art. 5.).** Seleccionando el umbral de riesgo del 5%, las *MRIs* evitadas fueron del 17.2% en la cohorte de desarrollo y del 22.3% en la cohorte de validación, dejando de detectar el 1.8% y el 2% de *csPCa*, respectivamente (**Tabla 5, art. 5.**).

7. RESUMEN GLOBAL DE LA DISCUSIÓN

Los modelos predictivos de *csPCa* son herramientas que proporcionan el riesgo individualizado de *csPCa* en varones con sospecha de *PCa,* a través de variables predictoras independientes que ayudan al clínico a mejorar la selección de candidatos a ser biopsiados. Estos modelos han evolucionado y actualmente incluyen los hallazgos de la *MRI* reportados a través del *PI-RADS score*. Esta estrategia puede reducir un buen número de biopsias de próstata innecesarias, perdiendo la detección de una tasa aceptable de *csPCa*. Las características de la *MRI* son importantes ya que es el mayor predictor del *csPCa* (47). Según la síntesis de la evidencia de nuestra revisión sistemática, la versión 2.0 del sistema *PI-RADS* se utilizó en 11 de los 17 modelos predictivos revisados (168,169,173–180). En un reciente metanálisis se observó que el *PI-RADSv2.0* tiene una sensibilidad agrupada más alta que el *PI-RADSv1* y una especificidad agrupada similar (181). En una validación externa del modelo de Radtke *et al*., basado en *PI-RADSv1*, se observó un mejor rendimiento al reemplazar el *PI-RADSv1* por el *PI-RADSv2.0* (182). Sin embargo, faltan datos consistentes que analicen la influencia de la versión del *PI-RADS* en el rendimiento de los *MRI-PMs*. En general, en la *MRI* en la que se basan los *MRI-PMs* se han utilizado intensidades de campo magnético de 1,5 y 3 Tesla con un protocolo de adquisición que incluye imágenes ponderadas en T2, *DWI* y *DCE* (183). Cabe mencionar la aparición de los modelos que proponen utilizar *bpMRI*, ya que evita la administración de contraste siendo una alternativa más económica y rápida que puede mantener una buena precisión diagnóstica en centros con amplia experiencia (184–186).

Las variables predictoras independientes incorporadas en los *MRI-PMs* para predecir *csPCa* en los análisis de regresión logística han sido *PI-RADS*, edad, *DRE*, antecedentes familiares de *PCa*, estado de la biopsia, etnia, *PSA, PSAD* o volumen prostático. La mayor edad está relacionada con una mayor incidencia y agresividad del *PCa* (187). Aunque el *PSA* tiene limitaciones conocidas, sigue siendo fundamental para establecer la sospecha de *PCa*, y todos los modelos lo

incluyen como predictor solo o en combinación con el volumen prostático expresado como *PSAD* (188). La *PSAD* ha resultado ser la variable que más fuertemente se relaciona con el *csPCa* después de la puntuación *PI-RADS* (110). El uso de la *PSAD* se ha incrementado desde el uso generalizado de la *MRI* ya que esta última permite la evaluación del volumen prostático sin coste adicional y evita la *TRUS* para su medición (47). Además, el volumen prostático estimado a partir de la *MRI* es más preciso que el proporcionado por la *TRUS* y el *DRE* (188). Por su parte, el *DRE* ha sido cuestionado debido al modesto aumento en la detección de *csPCa* en hombres con *PSA* sérico bajo (189). Aun así, un *DRE* anormal se asocia con el diagnóstico de tumores de mayor grado y localmente avanzados, por lo que sigue teniendo un papel relevante en la detección del *PCa* (190). La etnia se incluyó como predictor en solamente tres estudios debido a la homogeneidad racial de la mayoría de las poblaciones de estudio (165,174,180). El antecedente de biopsia de próstata previa negativa es un escenario común en la práctica clínica a pesar de que algunos modelos se han desarrollado exclusivamente en varones *naïve* para biopsia (164,166,168,169,172,175,179). Los modelos basados solamente en un estado de biopsia dificultan su uso generalizado. El protocolo de biopsia prostática influye en la detección del *csPCa* y es heterogéneo entre los *MRI-PMs* analizados. Es conocido que las biopsias dirigidas a las lesiones sospechosas aumentan la sensibilidad de la biopsia de próstata para detectar *csPCa* (50). Se ha observado que la tasa de detección de *csPCa* en las biopsias sistemáticas puede aumentar alrededor de un 20% en el caso de biopsias iniciales y hasta en un 40% en caso de biopsias de repetición. Omitir las biopsias sistemáticas puede condicionar la pérdida de detección del 16% de *csPCa* en caso de hombres sometidos a su primera biopsia y del 10% en el caso de biopsias de repetición (56). En algunos modelos se han utilizado biopsias sistemáticas entre 8 y 14 cilindros junto a 1-4 biopsias dirigidas, a cada lesión sospechosa, mientras que otros no proporcionan esta información (164,165,172). Otros estudios utilizan esquemas con biopsias por mapeo entre 24

y 40 cilindros y 2-4 biopsias dirigidas (167,169,170,178). La mayoría de las biopsias en los modelos de nuestra revisión se realizaron por vía transrectal, excepto aquellas que utilizaron mapeo por vía transperineal (167,169,170,178). A partir de 2021, la guías de *PCa* de la *European Association of Urology* recomiendan realizar las biopsias de próstata a través de la vía transperineal para reducir las complicaciones infecciosas (80). Por lo tanto, los *MRI-PMs* desarrollados con esquemas de biopsia transrectal es necesario que se adapten a este cambio en las recomendaciones y deben ser validados en series que utilicen esquemas transperineales. Algunos estudios utilizaron exclusivamente biopsias guiadas cognitivamente (167,168,174,175,178–180), mientras otros utilizaron biopsias guiadas por software de fusión de imágenes (166,169,171,174), y algunos utilizaron ambos tipos (165,170,172). Anecdóticamente también analizamos un estudio que utilizó biopsias guiadas *in-bore* con la *MRI* (172). Según la evidencia actual, no se ha demostrado claramente un beneficio de las biopsias guiadas con software sobre las guiadas cognitivamente, especialmente cuando son realizadas por profesionales experimentados (76,77). La definición de *csPCa* más utilizada ha sido el *GS* igual o mayor a 3+4 o *GG* de *ISUP* igual o mayor a 2 (164–166,168,169,171–177,180). Tres *MRI-PMs* utilizaron una definición más estricta de *csPCa* incluyendo *PCa* Gleason 3+4 con una extensión tumoral de cilindro afectado mayor a 6 mm (167,170,179). Todos los *MRI-PMs* incluidos utilizan como estándar de referencia los hallazgos histopatológicos de *csPCa* en las biopsias de próstata. Liu *et al.* desarrollaron un modelo en el que los hallazgos histopatológicos se obtuvieron no solo en la biopsia de próstata, sino que también estaban disponibles los de toda la glándula prostática, incluyendo la resección transuretral de la próstata, la enucleación transuretral de la próstata y la prostatectomía radical (191). Un modelo basado en una cohorte de varones cuyas muestras patológicas se obtengan solamente mediante la extracción quirúrgica de la próstata también tiene sus limitaciones, puesto que excluye estadios que implican tratamiento radioterápico, vigilancia activa o pacientes metastásicos. A

pesar de esto, puesto que la biopsia prostática puede subestimar el grado verdadero de tumor, la fortaleza de estos estudios reside en un diagnóstico y gradación certera del *PCa* (192).

La validación externa en una cohorte independiente es crucial para el uso de todos los modelos predictivos, aunque no se ha realizado en la mayoría de los modelos desarrollados (170–172,174,177,178). Los modelos predictivos sobrestimarán la probabilidad de *csPCa* cuando la incidencia disminuye y la subestimarán cuando la incidencia aumente (193,194). Es posible que se requiera una selección ajustada del umbral de probabilidad de *csPCa* para superar esta limitación (194). Por ejemplo, Mehralivand *et al.*, en la validación de su *MRI-PM* observaron similar capacidad discriminativa con una diferencia del 10% en la incidencia de *csPCa* (174). En otro estudio, Pullen *et al*. validaron tres *MRI-PMs* en una cohorte externa de 307 hombres. Las *AUC* de los tres modelos fueron similares; sin embargo, después de ajustar el umbral de riesgo, se observó una mejor calibración y beneficio neto del modelo de Rotterdam comparado con el resto (195). Finalmente, Saba *et al.* llevaron a cabo la validación y comparación de tres *MRI-PMs* en 468 hombres con sospecha de *PCa*. Los autores concluyeron que los *MRI-PMs* superaron a los modelos que no incluían *MRI*. Sin embargo, el beneficio clínico neto sólo se observó cuando el umbral de riesgo no era mayor al 15% (196). Las calculadoras de riesgo son esenciales para el uso rutinario de los *MRI-PMs* y solamente dos modelos estudiados disponían de una calculadora disponible en *web* o *app* móvil (176,180). La calculadora de riesgo de Rotterdam, basada en el más ampliamente validado de los *MRI-PMs* desarrollado por Alberts *et al.*, fue incorporada posteriormente (142,172). A una categoría *PI-RADS* mayor se le relaciona una probabilidad de *csPCa* y grado de agresividad del *PCa* también mayor (54). En el momento de nuestra revisión no existía ningún *MRI-PM* que hubiera analizado su utilidad en cada categoría *PI-RADS*. Los déficits

encontrados en la mayoría de los *MRI-PMs* fue el motivo por el que iniciamos nuestro proyecto de desarrollo del *BCN MRI-PM* y su calculadora de riesgo.

Nuestro *MRI-PM,* actualmente denominado *BCN PM*-2, fue desarrollado a partir de una regresión logística binaria en la que se incorporaron las variables independientes *PIRADS v2*.0 (1-5), edad (años), historia familiar de *PCa* (no *vs*. sí), *DRE* (normal *vs*. sospechoso), tipo de biopsia (inicial *vs*. repetida), PSA sérico (ng/ml), y volumen prostático derivado de la *MRI (*ml*).* Como hemos mencionado anteriormente, la validación externa de un modelo predictivo es un punto clave para asegurar la aplicabilidad del modelo (193). A pesar de utilizar los mismos criterios de sospecha de *PCa* y el mismo enfoque diagnóstico para *csPCa* en la cohorte de desarrollo y validación se observó una diferencia de casi cuatro puntos porcentuales en la incidencia de *csPCa* que ascendió del 36.9% de la cohorte de desarrollo al 40.8% en la cohorte de validación. Esta situación representó un factor estresante para nuestro modelo, aunque su capacidad de discriminación del *csPCa* siguió siendo buena con una subestimación mínima en su calibración.

Para la aplicación de los modelos predictivos en la práctica clínica diaria son necesarias calculadoras de riesgo accesibles para evitar el engorroso y lento uso de los nomogramas (176,180). Una novedad de nuestra calculadora de riesgo es la opción de seleccionar el umbral de probabilidad de *csPCa* para la población en general. El umbral puede adaptarse a la incidencia general de *csPCa* de las poblaciones de validación externa. Además, la selección del umbral también puede mejorar la utilidad del modelo en categorías específicas de *PI-RADS*. Hasta la publicación de nuestro proyecto, la utilidad clínica y el beneficio neto de los *MRI-PMs* desarrollados nunca se había analizado en función del *PI-RADS*. La eficacia del *BCN MRI-PM* fue limitada en hombres con *PI-RADS* 4, y especialmente con *PI-RADS* 5, en quienes la biopsia es obligada. En cambio, el

rendimiento diagnóstico y el beneficio neto en varones con *PI-RADS* < 3 fueron mejores. Las categorías de *PI-RADS* altas exhiben tasas más elevadas de *csPCa* además de que este presenta mayor agresividad; por lo tanto, perder pequeñas tasas de *csPCa*, puede llegar a ser una situación peligrosa (106,162,197).

En nuestra publicación número 3 comparamos la *PSAD* derivada del cálculo del volumen prostático por *MRI* con el *BCN MRI-PM*. Las distintas tasas de detección de *csPCa* según la categoría *PI-RADS* puso de manifiesto las diferencias entre sus eficacias en cada categoría *PI-RADS*. Las tasas de detección de *csPCa* fueron similarmente bajas entre *PI-RADS* 1 y 2 siendo elevada la sobre-detección *iPCa*, justificándose considerar estas categorías como *mpMRI* negativa. El patrón de detección de *PCa* en hombres con *PI-RADS* 3 fue más cercana a la de *PI-RADS* 2 que a la de *PI-RADS* 4, justificándose considerar el *PI-RADS* 3 como un escenario incierto, más similar a una *MRI* negativa. Las características de los varones con *PI-RADS* 5 son notablemente diferentes de las de *PI-RADS* 4, con un aumento notable en el riesgo de *csPCa*. Por lo tanto, consideramos por separado a los hombres con *PI-RADS* 4 y especialmente con *PI-RADS* 5, ya que el riesgo de *csPCa* es muy superior al de las otras categorías. La *PSAD* fue introducida en 1992 por Benson *et al*. para mejorar la especificidad del *PSA* sérico en la distinción entre hombres con *PCa* localizado y aquellos con hiperplasia prostática benigna (107). Posteriormente, Catalona *et al*. la incorporaron como una herramienta para la toma de decisiones en biopsias de próstata por su relación directamente proporcional al *csPCa* (198). Yamashiro *et al*. llegó a la conclusión de que la relación entre volumen prostático y el riesgo de *PCa* es inversa (199). Antes del uso generalizado de la *MRI* para el diagnóstico del cs*PCa*, la *TRUS* era la herramienta usada para la evaluación del volumen prostático justo antes de la biopsia (200–202). Actualmente, debido a la generalización de la *MRI* antes de la biopsia que facilita la medición del volumen prostático, la *PSAD* ha recobrado un papel relevante en la predicción del *csPCa* (116). Aun así, la elevada demanda de

MRI y la falta de disponibilidad de esta herramienta en todos los centros ha obligado a estudiar cual es el papel actual de la estimación subjetiva del volumen prostático estimado por *DRE* con objetivo de evitar resonancias, y así lo ha incorporado recientemente la calculadora de riesgo de Rotterdam (142). Se ha descrito que un umbral de *PSAD* superior a 0.20 o 0.15 ng/dl/cc está relacionado con el *csPCa* (87). Estudios recientes sugieren un comportamiento dinámico de la *PSAD* y ponen de manifiesto la necesidad de utilizar distintos umbrales para obtener valores predictivos similares en diferentes *PI-RADS* (115,116). Destacamos la importancia de seleccionar umbrales apropiados de *PSAD* para las distintas categorías *PI-RADS* y las características específicas en cada población de hombres con sospecha de *PCa* (203). Ambas herramientas, el *BCN MRI-PM* y la *PSAD*, son no invasivas y no tienen coste adicional. Según nuestros resultados, en general el *BCN MRI-PM* superó la eficacia de la *PSAD* en toda la población mostrando además mayor beneficio neto. Al analizar las categorías *PI-RADS* independientemente se observó que el *BCN MRI-PM* superó a la *PSAD* en las categorías *PI-RADS* ≤ 4, con diferentes grados de beneficio. Sin embargo, tanto el *BCN MRI-PM* como la *PSAD* mostraron un beneficio neto mínimo en varones con *PI-RADS* 5.

Puesto que el Rotterdam *MRI-PM* junto con su *RC* es el más prestigioso y validado de los modelos que incluyen *MRI*, decidimos comparar la *BCN MRI-RC* con la Rotterdam *MRI-RC* en la cohorte de 946 varones correspondiente a nuestra serie de validación en el área metropolitana de Barcelona, trabajo recogido en el artículo número 4. Alberts *et al*. ajustó el modelo de Rotterdam en 961 hombres con sospecha de *PCa* reclutados en Düsseldorf y cuatro ciudades holandesas, que se sometieron a biopsias sistemáticas y biopsias guiadas por *MRI* en caso de lesiones *PI-RADS* ≥ 3. Se detectó *csPCa* de alto grado (*GS* 3+4) en el 35,9% (172). La validación externa del Rotterdam *MRI-PM* en la población del ensayo *PRECISION* requirió recalibración y adaptación del umbral de riesgo para lograr

predicciones adecuadas (204). El *BCN MRI-PM* utiliza los mismos predictores que el Rotterdam *MRI-PM*, además de la historia familiar de *PCa* y el *PI-RADS v.2*. En nuestro trabajo, la *BCN MRI-RC* mostró un beneficio neto sobre la Rotterdam *MRI-RC* para hombres con lesiones *PI-RADS* 3 o 4; sin embargo, ninguno de los dos modelos mostró utilidad clínica para hombres con *MRI* negativa o una lesión *PI-RADS* 5. La Rotterdam *MRI-RC* presentó una curva de calibración lejos de la ideal en comparación con la *BCN MRI-RC*. La causa principal pudo ser el rango estrecho y bajo de predicción de riesgo de *csPCa* generado por la Rotterdam *MRI-RC* observado en las curvas de calibración. Un porcentaje significativo (22.1%) de la población mostró valores de edad, *PSA* en suero y volumen prostático fuera del rango aceptado por la Rotterdam *MRI-RC*. Esto podría ser en consecuencia de los criterios estrictos de inclusión de la población del ensayo *ERSPC* sobre el que se desarrollaron las calculadoras de riesgo de Rotterdam (21). La capacidad discriminatoria del *csPCa* entre la Rotterdam *MRI-RC* y la *BCN MRI-RC* fue similar en la población general, pero las curvas de utilidad clínica demostraron que la *BCN MRI-RC* presentó ventajas sobre la Rotterdam *MRI-RC* en la reducción de biopsias y la detección de *csPCa* en diferentes rangos de riesgo, especialmente en *PI-RADS* 4, siendo similar en *PI-RADS 3*. Destacamos de nuevo la importancia del análisis de los valores predictivos de los *MRI-PMs* según las categorías *PI-RADS*, ya que la capacidad de discriminación en la población global no representa la eficacia en cada categoría *PI-RADS*.

A pesar de sus limitaciones, la introducción de la *mpMRI* en el algoritmo diagnóstico del *PCa* ha conseguido mejorar la selección de candidatos a biopsia prostática. Aun así, el alta demanda de *MRI* en los centros de referencia ha llevado a la *European Association of Urology* a aconsejar usar modelos predictivos de riesgo de *csPCa* para reducir la demanda de *MRIs* (154). En la publicación número 5 reportamos el desarrollo y validación de un modelo predictivo de

csPCa complementario a la *BCN MRI-PM*, el *BCN PM-1*, y su calculadora de riesgo, la *BCN RC*-1. Este nuevo modelo predictivo podría ser utilizado en el momento inicial de sospecha de *CaP* y ser útil para reducir la demanda de *MRIs.* Las variables incluidas en este modelo fueron la edad (años), *PSA* sérico (ng/ml), historia familiar de *PCa* (no *vs.* sí), tipo de biopsia (inicial *vs.* repetición) y categoría de volumen prostático derivada del *DRE* (pequeña, mediana, grande). La calculadora de riesgo de Rotterdam fue diseñada a partir de modelos predictivos desarrollados entre los participantes de la sección de Rotterdam del ensayo *ERSPC*. Las calculadoras de Rotterdam denominadas 3 y 4 fueron diseñadas antes del uso de la *mpMRI* para individualizar el riesgo de *PCa* y *PCa* de alto grado en varones sin biopsia previa y con biopsia previa negativa, respectivamente (141). Después de la recomendación de realizar *mpMRI* previa a la biopsia, ambas calculadoras han sido validadas para seleccionar candidatos a *MRI* (205,206). Tanto la Rotterdam *RC*-3 como *RC*-4 inicialmente incluían el *PSA* sérico, *DRE* (normal *vs.* anormal), áreas hipoecoicas en *TRUS* (presencia *vs.* ausencia) y volumen prostático evaluado por *TRUS* como variables predictivas (206). Sin embargo, desde 2012, se introdujo la estimación del volumen prostático a partir del *DRE*. Esta modificación se produjo debido a la falta de información del volumen prostático hasta la *TRUS* que se realiza en el momento de la biopsia (207). Las categorías de *DRE* (pequeña, mediana y grande) se equipararon a volúmenes prostáticos analizados por *TRUS* de menos de 30 ml, entre 30 a 59 ml y mayores a 60 ml o más (205,206). Bajo estas condiciones, Alberts *et al.* analizaron la Rotterdam *RC*-4 en 122 hombres con sospecha de *PCa*. Utilizando un umbral del 3%, la Rotterdam *RC*-4 evitó el 51% de las *mpMRI*, perdiendo un 9.7% de *csPCa* (206). De manera similar, Mannaerts *et al.* analizaron la Rotterdam *RC*-3 en 200 hombres con sospecha de *PCa* y después de ajustar el umbral de riesgo al 4%, se evitaron el 36.5% de las *mpMRI*, perdiendo el 6% de *csPCa* (205). Remmers *et al*. testaron la actual calculadora de riesgo de Rotterdam para selección de candidatos a *MRI* entre los 206 hombres del brazo *MRI* del ensayo *PRECISION*.

Después de la recalibración del modelo con ajustes del umbral de riesgo, la reducción de la demanda de *MRIs* fue de un 13.1% perdiendo el 7.1% de *csPCa* (204). Las *AUC* de la *BCN PM-1* fueron similares a las reportadas por Alberts *et al.* en varones con biopsia previa negativa (206). Mannaerts *et al.* (205) y Remmers *et al.* (204) no informaron la capacidad de discriminación de la Rotterdam *RC* en sus estudios. En ambas cohortes de nuestro estudio, se observó un beneficio neto de la *BCN PM-1* sobre la demanda de *mpMRI* con umbrales de riesgo de *csPCa* entre el 8 y 12%. El rendimiento de la *BCN PM-1* con una sensibilidad para *csPCa* del 0.95 presentó especificidades en las cohortes de desarrollo y validación del 0.24 y 0.34, respectivamente, lo que habría permitido evitar el 17.2 y 22.3% de *mpMRI*, respectivamente. Estos porcentajes de reducción de *mpMRI* estuvieron por debajo del 51% reportado por la Rotterdam *RC*-4 y del 36.5% reportado con Rotterdam *RC*-3, aunque los porcentajes de *csPCa* de alto grado perdidos fueron del 6% y del 9.7%, respectivamente (205,206). En el análisis reciente de la Rotterdam *RC*-3, llevado a cabo en el brazo de *MRI* del ensayo *PRECISION*, el porcentaje de *mpMRI* evitadas disminuyó al 13.1% en comparación con el 36.5% reportado por Mannaerts *et al*., con porcentajes de *csPCa* perdidos del 7.1% y 6%, respectivamente (204,205). Los estudios de validación de las Rotterdam *RCs* se realizaron con el volumen prostático medido por *TRUS*, mientras que en nuestro estudio utilizamos la categoría de volumen prostático por *DRE* (117,156). Cabe destacar que la medida del volumen prostático por *DRE* podría resultar inexacta en facultativos inexpertos (43). El *BCN PM*-1 está limitado por el hecho de que asumimos que el *DRE* clasifica con precisión la categoría de volumen prostático evaluada por *MRI*. Roobol *et al.* realizaron la misma apreciación con respecto al volumen prostático informado por ecografía transrectal (117,156). Recientemente, Massanova *et al*. han encontrado una buena correlación entre el volumen prostático estimado por *DRE* y el evaluado por *MRI* en un estudio retrospectivo (188). Sin embargo, creemos que se necesita un análisis prospectivo

para definir la correlación entre intervalos de volumen estimados por *DRE* y calculados por *MRI* para obtener una mayor evidencia.

Los modelos predictivos tienen limitaciones intrínsecas que son generales en todos ellos. Un modelo predictivo refleja la probabilidad de una condición o riesgo basada en las características de la población en el momento de su desarrollo (141). Por lo tanto, el *BCN PM*-1 y *PM*-2 proporcionan los resultados en función de la incidencia o riesgo de *csPCa* de la población en la que se desarrolló. En un escenario real, existen cambios constantes tanto en la misma población como en las cohortes de validación (162). Para eludir este inconveniente, es necesario recalibrar y ajustar estos modelos predictivos para mantener su precisión aun con los cambios en la población y condiciones de evaluación (208).

En cuanto a las limitaciones específicas de nuestros modelos desarrollados, observamos que la predicción de *csPCa* se basó en biopsias prostáticas, las cuales no representan la verdadera patología de la glándula prostática entera (209). Destacamos también la falta de un análisis de concordancia entre los clínicos que participan en el proceso de diagnóstico precoz del *csPCa* (urólogos, radiólogos y patólogos). La presencia de *csPCa* en la biopsia se definió como *PCa* con grupo de grado de *ISUP* 2 o superior, aunque existen otras definiciones también aceptadas y con mayor correlación con el resultado en la glándula entera (87). Remarcamos que desde el año 2021 la biopsia prostática vía transperineal es la recomendada con el objetivo de reducir las complicaciones infecciosas de la vía transrectal (80). En consecuencia, nuestros modelos desarrollados con la biopsia prostática realizada por vía transrectal no son generalizables para la biopsia transperineal y deberían ser testados. Otro inconveniente es el empleo de la versión 2.0 de *PI-RADS* para el informe de la *mpMRI* cuando actualmente existe una versión más actualizada, la *PI-RADSv2.1* (52). Por último, cabe destacar que

nuestro modelo no se puede implementar en poblaciones donde la etnia predominante no es la caucásica.

Para finalizar, destacamos que los modelos predictivos de Barcelona y sus calculadoras de riesgo están desarrollados para su uso en dos estadios de la detección de *csPCa,* en el momento inicial de sospecha de *PCa* antes de la *MRI* y posterior a la realización *MRI.* Esta capacidad podría ser utilizada para construir modelos de riesgo organizado para mejorar la detección del *csPCa*.

8. CONCLUSIONES

1. Los modelos predictivos de *PCa* basados en *MRI* y variables clínicas son el mejor método para seleccionar candidatos a biopsia prostática. Las *RC*s y la validación externa en la población en la que van a ser utilizadas son esenciales para la aplicación de los modelos predictivos en la práctica clínica diaria. En el momento de nuestra revisión sistemática de la literatura, el modelo Rotterdam-*MRI,* desarrollado con la versión *PI-RADS* 1.0, disponía de una *RC* accesible y ninguno de los publicados se había evaluado según la categoría *PI-RADS.* Estos resultados condujeron a desarrollar una nueva *RC*.

2. El *BCN MRI-PM*, actualmente denominado *BCN PM-2*, consiguió evitar biopsias innecesarias con una tasa aceptable de *csPCa* no detectado. Por primera vez en la literatura se demostró que la utilidad clínica de los modelos predictivos varía en función de la categoría *PI-RADS*. Su validación externa mostró una buena calibración y la *RC* diseñada permite la selección del umbral de probabilidad de *csPCa,* novedad que facilitará la validación del modelo en otras poblaciones o en diferentes *PI-RADS.*

3. El *BCN PM-2* fue más preciso y presentó mayor beneficio neto que la *PSAD* para seleccionar candidatos para biopsia prostática en global y para todos los *PI-RADS*, con la excepción de varones con *PI-RADS* 5, que deben ser siempre sometidos a biopsia. El *BCN PM-2* mostró mayor beneficio neto para seleccionar candidatos a biopsia prostática que el Rotterdam *MRI-PM* globalmente, aunque ninguno de ellos fue útil para seleccionar individuos con *MRI* negativa o *PI-RADS* 5.

4. El *BCN PM-1,* desarrollado a partir de las variables clínicas disponibles en el momento de la sospecha de *PCa* y la categorización del volumen

prostático a partir del *DRE*, consiguió reducir la demanda de *MRI* con una tasa aceptable de *csPCa* no detectado. Su validación externa mostró una buena calibración y la *RC* diseñada permite la selección del umbral de probabilidad de *csPCa.*

5. Finalmente, en relación a nuestro objetivo principal, concluimos que los modelos predictivos de Barcelona y su *RC* permitieron mejorar el diagnóstico precoz del *csPCa*, optimizando la selección de candidatos a *MRI* y a biopsia prostática.

9. LÍNEAS DE FUTURO

Recientemente, nuestro grupo ha publicado la integración de los dos modelos predictivos desarrollados en esta tesis doctoral en el modelo organizado de riesgo (*ROM*) de Barcelona. Este pudo evitar el 30.8% de los exámenes de *mpMRI* e incrementar el porcentaje de biopsias evitadas desde el 24.8% observado con el enfoque estándar hasta el 28.2%. El porcentaje de *csPCa* no detectados disminuyó de 10.9 a 6.7%, respectivamente. Por lo tanto, el *BCN-ROM* permitió mejorar la detección precoz de *csPCa* reduciendo la demanda de exámenes de *mpMRI* y biopsias prostáticas, incrementando la detección de *csPCa* (210).

Por otro lado, el análisis radiómico de las imágenes de *mpMRI* pueden mejorar la predicción de la probabilidad de *csPCa* basada en el *PI-RADS*. Nuestro grupo de investigación está desarrollando el proyecto financiado por ISCIII (PI2001666) titulado "Aplicación de la radiogenómica en el diagnóstico precoz del *csPCa*". Este proyecto pretende desarrollar algoritmos basados en técnicas de inteligencia artificial "*deep learning*" y "*machine learning*" que mejoren la predicción semi-cuantitativa del *PI-RADS* y del *BCN MRI-PM*. Además añade la aportación de la genómica, que puede permitir realizar una caracterización biológica del *csPCa,* hasta ahora basada en la antigua, pero no superada, clasificación de Gleason.

Nuestro proyecto ha tenido como objetivo principal mejorar el diagnóstico precoz del *csPCa* a través del desarrollo de dos modelos predictivos confeccionados a partir de variables clínicas antes de la realización de la *mpMRI* y variables clínicas una vez realizada la *mpMRI.* Se abren, pues, nuevas vías de investigación basadas en superar las limitaciones que surgen en el desarrollo y aplicación de los modelos predictivos en poblaciones externas. Frente a las limitaciones propias de los modelos predictivos desarrollados a través de regresión logística, que no tienen capacidad de aprendizaje, los algoritmos

basados en técnicas de inteligencia artificial tienen la capacidad de mejorar sus predicciones a través de la retroalimentación de nuevos datos. De esta manera, un algoritmo común desarrollado y utilizado en redes federadas con distintos participantes clínicos puede retroalimentarse constantemente con la incorporación de nuevos casos que representen la variabilidad de las condiciones específicas de cada población y los cambios que se vayan produciendo en la metodología diagnóstica del *csPCa,* llegándose a obtener una utilidad creciente pero adaptada a cada entorno de los nodos de la red federada. Actualmente, nuestro grupo coordina dos proyectos multicéntricos que tienen como objetivo implementar redes federadas para desarrollar algoritmos predictivos en distintas áreas del diagnóstico del *csPCa*, predicción de datos clínicos e imágenes de *mpMRI* y de anatomía patológica. En el proyecto nacional "TARTAGLIA" (Red Federada Para Acelerar La Aplicación De La Inteligencia Artificial En El Sistema Sanitario Español), financiado por el Ministerio de Asuntos Económicos y Transformación Digital (MIA.2021.M02.0005) se van a desarrollar varios algoritmos de *machine learning* con la pretensión de mejorar la capacidad discriminatoria de los *BCN PMs* 1 y 2. En el proyecto "FLUTE" (*Federated Learning and mUlti-party computation Techniques for prostatE cancer*), HORIZON-HLTH-2022-IND-13 (101095382), se pretenden desarrollar algoritmos radiómicos, basados en *deep learning* y *machine learning* a partir de las imágenes de *mpMRI* de tres centros clínicos europeos y una empresa multinacional de la imagen de resonancia. Las técnicas de *deep learning* para el análisis radiómico precisan de un número de casos muy elevado y exportan imágenes de los centros hospitalarios en Europa, siendo tremendamente complejas en términos de seguridad y confidencialidad de los pacientes. Mediante ciertos algoritmos de inteligencia artificial hoy en día es posible generar datos e imágenes sintéticas adecuadamente etiquetadas que pueden almacenarse en las plataformas de la red federada y utilizarse para desarrollar los algoritmos de predicción. La generación de datos sintéticos es la tercera vía de investigación aplicada al diagnóstico precoz del *csPCa*, que está

siendo aplicada en los dos proyectos citados anteriormente, a través de la participación del *Barcelona Super Computing Center* en el proyecto TARTAGLIA y de la Universidad Politécnica de Catalunya en el proyecto FLUTE.

Para concluir este apartado final de nuestra memoria, podemos afirmar que nuestro proyecto ha sido el embrión de un abanico de vías de investigación nuevas aplicadas al diagnóstico precoz del *csPCa* que permitirán mejorar su predicción e implementación de los programas de *screening* y metodología diagnóstica de forma más eficiente.

10. Bibliografía

1. Sung H, Ferlay J, Siegel RL, Laversanne M, Soerjomataram I, Jemal A, et al. Global Cancer Statistics 2020: GLOBOCAN Estimates of Incidence and Mortality Worldwide for 36 Cancers in 185 Countries. CA Cancer J Clin. 2021;71:209–249.
2. Haas GP, Delongchamps N, Brawley OW, Wang CY, de la Roza G. The Worldwide Epidemiology of Prostate Cancer: Perspectives from Autopsy Studies. Can J Urol. 2008;15:3866.
3. Center MM, Jemal A, Lortet-Tieulent J, Ward E, Ferlay J, Brawley O, et al. International variation in prostate cancer incidence and mortality rates. Eur Urol. 2012;61:1079-1092.
4. Culp MBB, Soerjomataram I, Efstathiou JA, Bray F, Jemal A. Recent Global Patterns in Prostate Cancer Incidence and Mortality Rates. Eur Urol. 2020;77:38–52.
5. Rawla P. Epidemiology of Prostate Cancer. World J Oncol. 2019;10:63–89.
6. SEOM: Sociedad Española de Oncología Médica. El cáncer en cifras 2023.
7. Bell KJL, del Mar C, Wright G, Dickinson J, Glasziou P. Prevalence of incidental prostate cancer: A systematic review of autopsy studies. Int J Cancer. 2015;137:1749–1757.
8. Hemminki K. Familial risk and familial survival in prostate cancer. World J Urol. 2012;30:143-148.
9. Beebe-Dimmer JL, Kapron AL, Fraser AM, Smith KR, Cooney KA. Risk of Prostate Cancer Associated With Familial and Hereditary Cancer Syndromes. J Clin Oncol. 2020;38:1807-1813.
10. al Olama AA, Dadaev T, Hazelett DJ, Li Q, Leongamornlert D, Saunders EJ, et al. Multiple novel prostate cancer susceptibility signals identified by fine-mapping of known risk loci among Europeans. Hum Mol Genet. 2015;24:5589–5602.

11. Pritchard CC, Mateo J, Walsh MF, de Sarkar N, Abida W, Beltran H, et al. Inherited DNA-Repair Gene Mutations in Men with Metastatic Prostate Cancer. NEJM. 2016;375:443-453.
12. Giri VN, Hegarty SE, Hyatt C, O'Leary E, Garcia J, Knudsen KE, et al. Germline genetic testing for inherited prostate cancer in practice: Implications for genetic testing, precision therapy, and cascade testing. Prostate. 2019;79:333–339.
13. Andriole GL, Bostwick DG, Brawley OW, Gomella LG, Marberger M, Montorsi F, et al. Effect of Dutasteride on the Risk of Prostate Cancer. NEJM. 2010;362:1192–1202.
14. Thompson IM, Goodman PJ, Tangen CM, Lucia MS, Miller GJ, Ford LG, et al. The influence of finasteride on the development of prostate cancer. NEJM. 2003;349:215–224.
15. Hu X, Wang YH, Yang ZQ, Shao YX, Yang WX, Li X. Association of 5-alpha-reductase inhibitor and prostate cancer incidence and mortality: a meta-analysis. Transl Androl Urol. 2020;9:2519–2532.
16. Knijnik PG, Brum PW, Cachoeira ET, Paludo A de O, Gorgen ARH, Burttet LM, et al. The impact of 5-alpha-reductase inhibitors on mortality in a prostate cancer chemoprevention setting: a meta-analysis. World J Urol. 2021;39:365–376.
17. Haider A, Zitzmann M, Doros G, Isbarn H, Hammerer P, Yassin A. Incidence of prostate cancer in hypogonadal men receiving testosterone therapy: observations from 5-year median followup of 3 registries. J Urol. 2015;193:80–86.
18. Watts EL, Appleby PN, Perez-Cornago A, Bueno-de-Mesquita HB, Chan JM, Chen C, et al. Low Free Testosterone and Prostate Cancer Risk: A Collaborative Analysis of 20 Prospective Studies. Eur Urol. 2018;74:585–594.

19. Carthon B, Sibold HC, Blee S, D. Pentz R. Prostate Cancer: Community Education and Disparities in Diagnosis and Treatment. Oncologist. 2021;26:537–548.
20. Leitzmann MF, Rohrmann S. Risk factors for the onset of prostatic cancer: age, location, and behavioral correlates. Clin Epidemiol. 2012;4:1-11.
21. Hugosson J, Roobol MJ, Månsson M, Tammela TLJ, Zappa M, Nelen V, et al. A 16-yr Follow-up of the European Randomized study of Screening for Prostate Cancer. Eur Urol. 2019;76:43–51.
22. Cornford P, van den Bergh RCN, Briers E, Van den Broeck T, Cumberbatch MG, De Santis M, et al. EAU-EANM-ESTRO-ESUR-SIOG Guidelines on Prostate Cancer. Part II-2020 Update: Treatment of Relapsing and Metastatic Prostate Cancer. Eur Urol. 2021;79:263–282.
23. Hara M, Koyanagi Y, Inoue T, Fukuyama T. Some physico-chemical characteristics of " -seminoprotein", an antigenic component specific for human seminal plasma. Forensic immunological study of body fluids and secretion. VII. Nihon Hoigaku Zasshi. 1971;25:322–324.
24. Yousef GM, Diamandis EP. The new human tissue kallikrein gene family: structure, function, and association to disease. Endocr Rev. 2001;22:184-204.
25. Digby M, Zhang XY, Richards RI. Human prostate specific antigen (PSA) gene: structure and linkage to the kallikrein-like gene, hGK-1. Nucleic Acids Res. 1989;17:2137.
26. Henttu P, Liao SS, Vihko P. Androgens up-regulate the human prostate-specific antigen messenger ribonucleic acid (mRNA), but down-regulate the prostatic acid phosphatase mRNA in the LNCaP cell line. Endocrinology. 1992;130:766-72.
27. Wang MC, Papsidero LD, Kuriyama M, Valenzuela LA, Murphy GP, Chu TM. Prostate antigen: a new potential marker for prostatic cancer. Prostate. 1981;2:89-96.

28. Stamey TA, Yang N, Hay AR, McNeal JE, Freiha FS, Redwine E. Prostate-Specific Antigen as a Serum Marker for Adenocarcinoma of the Prostate. NEJM. 1987;317:909–916.

29. Semonjow A, Brandt B, Oberpenning F, Roth S, Hertle L. Discordance of assay methods creates pitfalls for the interpretation of prostate-specific antigen values. Discordance of assay methods creates pitfalls for the interpretation of prostate-specific antigen values. Prostate Suppl. 1996;16:7–3.

30. Thompson IM, Pauler DK, Goodman PJ, Tangen CM, Lucia MS, Parnes HL, et al. Prevalence of Prostate Cancer among Men with a Prostate-Specific Antigen Level ≤4.0 ng per Milliliter. NEJM. 2004;350:2239–2246.

31. Carter HB, Albertsen PC, Barry MJ, Etzioni R, Freedland SJ, Greene KL, et al. Early detection of prostate cancer: AUA guideline. J Urol. 2013;190:419–426.

32. Vickers AJ, Ulmert D, Sjoberg DD, Bennette CJ, Bjork T, Gerdtsson A, et al. Strategy for detection of prostate cancer based on relation between prostate specific antigen at age 40-55 and long term risk of metastasis: case-control study. BMJ. 2013;346:f2023–f2023.

33. Gelfond J, Choate K, Ankerst DP, Hernandez J, Leach RJ, Thompson IM. Intermediate-Term Risk of Prostate Cancer is Directly Related to Baseline Prostate Specific Antigen: Implications for Reducing the Burden of Prostate Specific Antigen Screening. J Urol. 2015;194:46–51.

34. Stephan C, Lein M, Jung K, Schnorr D, Loening SA. The influence of prostate volume on the ratio of free to total prostate specific antigen in serum of patients with prostate carcinoma and benign prostate hyperplasia. Cancer. 1997;79:104–109.

35. Huang Y, Li ZZ, Huang YL, Song HJ, Wang YJ. Value of free/total prostate-specific antigen (f/t PSA) ratios for prostate cancer detection in patients

with total serum prostate-specific antigen between 4 and 10ng/mL. Medicine. 2018;97:e0249.

36. Morote J, Campistol M, Triquell M, Celma A, Regis L, de Torres I, et al. Improving the Early Detection of Clinically Significant Prostate Cancer in Men in the Challenging Prostate Imaging-Reporting and Data System 3 Category. Eur Urol Open Sci. 2022;37:38–44.
37. Moyer VA; U.S. Preventive Services Task Force. Screening for prostate cancer: U.S. Preventive Services Task Force recommendation statement. Ann Intern Med. 2012;157:120-134.
38. Kelly SP, Anderson WF, Rosenberg PS, Cook MB. Past, Current, and Future Incidence Rates and Burden of Metastatic Prostate Cancer in the United States. Eur Urol Focus. 2018;4:121–127.
39. Siegel RL, Miller KD, Jemal A. Cancer statistics, 2019. CA Cancer J Clin. 2019;69:7–34.
40. Grossman DC, Curry SJ, Owens DK, Bibbins-Domingo K, Caughey AB, Davidson KW, et al. Screening for Prostate Cancer: US Preventive Services Task Force Recommendation Statement. JAMA. 2018;319:1901-1913.
41. Májek O, Babjuk M, Roobol MJ, Bratt O, Van Poppel H, Zachoval R, et al. How to follow the new EU Council recommendation and improve prostate cancer early detection: the Prostaforum 2022 declaration. Eur Urol Open Sci. 2023;53:106–108.
42. Richie JP, Catalona WJ, Ahmann FR, Hudson MA, Scardino PT, Flanigan RC, et al. Effect of patient age on early detection of prostate cancer with serum prostate-specific antigen and digital rectal examination. Urology. 1993;42:365–374.
43. Naji L, Randhawa H, Sohani Z, Dennis B, Lautenbach D, Kavanagh O, et al. Digital Rectal Examination for Prostate Cancer Screening in Primary Care: A Systematic Review and Meta-Analysis. The Annals of Family Medicine. 2018;16:149–154.

44. Gosselaar C, Roobol MJ, Roemeling S, Schröder FH. The Role of the Digital Rectal Examination in Subsequent Screening Visits in the European Randomized Study of Screening for Prostate Cancer (ERSPC), Rotterdam. Eur Urol. 2008;54:581–588.

45. Prebay ZJ, Medairos R, Doolittle J, Langenstroer P, Jacobsohn K, See WA, et al. The prognostic value of digital rectal exam for the existence of advanced pathologic features after prostatectomy. Prostate. 2021;81:1064–1070.

46. Berlin A, Brierley J, Cornford P, Chung P, Giannopoulos E, Mason M, et al. TNM Staging of Prostate Cancer: Challenges in Securing a Globally Applicable Classification. Eur Urol. 2022;82:e52–53.

47. Ahmed HU, El-Shater Bosaily A, Brown LC, Gabe R, Kaplan R, Parmar MK, et al. Diagnostic accuracy of multi-parametric MRI and TRUS biopsy in prostate cancer (PROMIS): a paired validating confirmatory study. The Lancet. 2017;389:815–822.

48. Smeenge M, Barentsz J, Cosgrove D, de la Rosette J, de Reijke T, Eggener S, et al. Role of transrectal ultrasonography (TRUS) in focal therapy of prostate cancer: report from a Consensus Panel. BJU Int. 2012;110:942–948.

49. Bratan F, Niaf E, Melodelima C, Chesnais AL, Souchon R, Mège-Lechevallier F, et al. Influence of imaging and histological factors on prostate cancer detection and localisation on multiparametric MRI: a prospective study. Eur Radiol. 2013;23:2019–2029.

50. Drost FJH, Osses DF, Nieboer D, Steyerberg EW, Bangma CH, Roobol MJ, et al. Prostate MRI, with or without MRI-targeted biopsy, and systematic biopsy for detecting prostate cancer. Cochrane Database of Systematic Reviews. 2019;4.

51. Weinreb JC, Barentsz JO, Choyke PL, Cornud F, Haider MA, Macura KJ, et al. PI-RADS Prostate Imaging – Reporting and Data System: 2015, Version 2. Eur Urol. 2016;69:16–40.

52. Turkbey B, Rosenkrantz AB, Haider MA, Padhani AR, Villeirs G, Macura KJ, et al. Prostate Imaging Reporting and Data System Version 2.1: 2019 Update of Prostate Imaging Reporting and Data System Version 2. Eur Urol. 2019;76:340–351.

53. Dickinson L, Ahmed HU, Allen C, Barentsz JO, Carey B, Futterer JJ, et al. Magnetic Resonance Imaging for the Detection, Localisation, and Characterisation of Prostate Cancer: Recommendations from a European Consensus Meeting. Eur Urol. 2011;59:477–494.

54. Padhani AR, Barentsz J, Villeirs G, Rosenkrantz AB, Margolis DJ, Turkbey B, et al. PI-RADS Steering Committee: The PI-RADS Multiparametric MRI and MRI-directed Biopsy Pathway. Radiology. 2019;292:464–474.

55. Goldberg H, Ahmad AE, Chandrasekar T, Klotz L, Emberton M, Haider MA, et al. Comparison of Magnetic Resonance Imaging and Transrectal Ultrasound Informed Prostate Biopsy for Prostate Cancer Diagnosis in Biopsy Naïve Men: A Systematic Review and Meta-Analysis. J Urol. 2020;203:1085–1093.

56. Rouvière O, Puech P, Renard-Penna R, Claudon M, Roy C, Mège-Lechevallier F, et al. Use of prostate systematic and targeted biopsy on the basis of multiparametric MRI in biopsy-naive patients (MRI-FIRST): a prospective, multicentre, paired diagnostic study. Lancet Oncol. 2019;20:100–109.

57. van der Leest M, Cornel E, Israël B, Hendriks R, Padhani AR, Hoogenboom M, et al. Head-to-head Comparison of Transrectal Ultrasound-guided Prostate Biopsy Versus Multiparametric Prostate Resonance Imaging with Subsequent Magnetic Resonance-guided Biopsy in Biopsy-naïve Men with Elevated Prostate-specific Antigen: A Large Prospective Multicenter Clinical Study. Eur Urol. 2019;75:570–578.

58. Kasivisvanathan V, Rannikko AS, Borghi M, Panebianco V, Mynderse LA, Vaarala MH, et al. MRI-Targeted or Standard Biopsy for Prostate-Cancer Diagnosis. NEJM. 2018;378:1767–1777.

59. Panebianco V, Barchetti G, Simone G, Del Monte M, Ciardi A, Grompone MD, et al. Negative Multiparametric Magnetic Resonance Imaging for Prostate Cancer: What's Next? Eur Urol. 2018;74:48–54.

60. Mottet N, van den Bergh RCN, Briers E, Van den Broeck T, Cumberbatch MG, De Santis M, et al. EAU-EANM-ESTRO-ESUR-SIOG Guidelines on Prostate Cancer—2020 Update. Part 1: Screening, Diagnosis, and Local Treatment with Curative Intent. Eur Urol. 2021;79:243–262.

61. Porter KK, King A, Galgano SJ, Sherrer RL, Gordetsky JB, Rais-Bahrami S. Financial implications of biparametric prostate MRI. Prostate Cancer Prostatic Dis. 2020;23:88–93.

62. Haghighi M, Shah S, Taneja SS, Rosenkrantz AB. Prostate Cancer. J Comput Assist Tomogr. 2013;37:980–988.

63. Tan CH, Hobbs BP, Wei W, Kundra V. Dynamic contrast-enhanced MRI for the detection of prostate cancer: meta-analysis. AJR. 2015;204:W439-448.

64. Greer MD, Shih JH, Lay N, Barrett T, Kayat Bittencourt L, Borofsky S, et al. Validation of the Dominant Sequence Paradigm and Role of Dynamic Contrast-enhanced Imaging in PI-RADS Version 2. Radiology. 2017;285:859–869.

65. Kang Z, Min X, Weinreb J, Li Q, Feng Z, Wang L. Abbreviated Biparametric Versus Standard Multiparametric MRI for Diagnosis of Prostate Cancer: A Systematic Review and Meta-Analysis. AJR. 2019;212:357-365.

66. Gleason DF, Mellinger GT, Veterans Administration Cooperative Urological Research Group. Prediction of prognosis for prostatic adenocarcinoma by combined histological grading and clinical staging. 1974. J Urol. 2002;167:953–959.

67. Epstein JI, Allsbrook WC Jr, Amin MB, Egevad LL; ISUP Grading Committee. The 2005 International Society of Urological Pathology (ISUP) Consensus Conference on Gleason Grading of Prostatic Carcinoma. Am J Surg Pathol. 2005;29:1228-1242.

68. Harnden P, Shelley MD, Coles B, Staffurth J, Mason MD. Should the Gleason grading system for prostate cancer be modified to account for high-grade tertiary components? A systematic review and meta-analysis. Lancet Oncol. 2007;8:411–419.

69. Saeter T, Vlatkovic L, Waaler G, Servoll E, Nesland JM, Axcrona K, et al. Intraductal Carcinoma of the Prostate on Diagnostic Needle Biopsy Predicts Prostate Cancer Mortality: A Population-Based Study. Prostate. 2017;77:859–865.

70. Van der Kwast T, Bubendorf L, Mazerolles C, Raspollini MR, Van Leenders GJ, Pihl CG, et al. Guidelines on processing and reporting of prostate biopsies: the 2013 update of the pathology committee of the European Randomized Study of Screening for Prostate Cancer (ERSPC). Virchows Archiv. 2013;463:367–377.

71. Epstein JI, Egevad L, Amin MB, Delahunt B, Srigley JR, Humphrey PA; Grading Committee. The 2014 International Society of Urological Pathology (ISUP) Consensus Conference on Gleason Grading of Prostatic Carcinoma: Definition of Grading Patterns and Proposal for a New Grading System. Am J Surg Pathol. 2016;40:244-252.

72. van Leenders GJLH, van der Kwast TH, Grignon DJ, Evans AJ, Kristiansen G, Kweldam CF, et al. The 2019 International Society of Urological Pathology (ISUP) Consensus Conference on Grading of Prostatic Carcinoma. Am J Surg Pathol. 2020;44:87–99.

73. Eichler K, Hempel S, Wilby J, Myers L, Bachmann LM, Kleijnen J. Diagnostic Value of Systematic Biopsy Methods in the Investigation of Prostate Cancer: A Systematic Review. J Urol. 2006;175:1605–1612.

74. Kenigsberg AP, Renson A, Rosenkrantz AB, Huang R, Wysock JS, Taneja SS, et al. Optimizing the Number of Cores Targeted During Prostate Magnetic Resonance Imaging Fusion Target Biopsy. Eur Urol Oncol. 2018;1:418–425.

75. Arsov C, Rabenalt R, Blondin D, Quentin M, Hiester A, Godehardt E, et al. Prospective Randomized Trial Comparing Magnetic Resonance Imaging (MRI)-guided In-bore Biopsy to MRI-ultrasound Fusion and Transrectal Ultrasound-guided Prostate Biopsy in Patients with Prior Negative Biopsies. Eur Urol. 2015;68:713–720.

76. Watts KL, Frechette L, Muller B, Ilinksy D, Kovac E, Sankin A, Aboumohamed A. Systematic review and meta-analysis comparing cognitive vs. image-guided fusion prostate biopsy for the detection of prostate cancer. Urol Oncol. 2020;38:734.e19-734.e25.

77. Wegelin O, van Melick HHE, Hooft L, Bosch JLHR, Reitsma HB, Barentsz JO, et al. Comparing Three Different Techniques for Magnetic Resonance Imaging-targeted Prostate Biopsies: A Systematic Review of In-bore versus Magnetic Resonance Imaging-transrectal Ultrasound fusion versus Cognitive Registration. Is There a Preferred Technique? Eur Urol. 2017;71:517–531.

78. Tu X, Liu Z, Chang T, Qiu S, Xu H, Bao Y, et al. Transperineal Magnetic Resonance Imaging–Targeted Biopsy May Perform Better Than Transrectal Route in the Detection of Clinically Significant Prostate Cancer: Systematic Review and Meta-analysis. Clin Genitourin Cancer. 2019;17:e860–870.

79. Pradere B, Veeratterapillay R, Dimitropoulos K, Yuan Y, Omar MI, MacLennan S, et al. Nonantibiotic Strategies for the Prevention of Infectious Complications following Prostate Biopsy: A Systematic Review and Meta-Analysis. J Urol. 2021;205:653–563.

80. Bennett H, Roberts MJ, Doi S, Gardiner R. The global burden of major infectious complications following prostate biopsy. Epidemiol Infect. 2016;144:1784–1791.

81. Pilatz A, Dimitropoulos K, Veeratterapillay R, Yuan Y, Omar MI, MacLennan S, et al. Antibiotic Prophylaxis for the Prevention of Infectious Complications following Prostate Biopsy: A Systematic Review and Meta-Analysis. J Urol. 2020;204:224–230.

82. Franks LM. Latent carcinoma of the prostate. J Pathol Bacteriol. 1954;68:603–616.

83. Ross HM, Kryvenko ON, Cowan JE, Simko JP, Wheeler TM, Epstein JI. Do adenocarcinomas of the prostate with Gleason score (GS) ≤6 have the potential to metastasize to lymph nodes? Am J Surg Pathol. 2012;36:1346–1352.

84. Anderson BB, Oberlin DT, Razmaria AA, Choy B, Zagaja GP, Shalhav AL, et al. Extraprostatic Extension Is Extremely Rare for Contemporary Gleason Score 6 Prostate Cancer. Eur Urol. 2017;72:455–460.

85. Sauter G, Clauditz T, Steurer S, Wittmer C, Büscheck F, Krech T, et al. Integrating Tertiary Gleason 5 Patterns into Quantitative Gleason Grading in Prostate Biopsies and Prostatectomy Specimens. Eur Urol. 2018;73:674–683.

86. Ahmed HU, Hu Y, Carter T, Arumainayagam N, Lecornet E, Freeman A, et al. Characterizing Clinically Significant Prostate Cancer Using Template Prostate Mapping Biopsy. J Urol. 2011;186:458–464.

87. Matoso A, Epstein JI. Defining clinically significant prostate cancer on the basis of pathological findings. Histopathology. 2019;74:135–145.

88. Mohler JL, Antonarakis ES, Armstrong AJ, D'Amico AV, Davis BJ, Dorff T, et al. Prostate Cancer, Version 2.2019, NCCN Clinical Practice Guidelines in Oncology. J Natl Compr Canc Netw. 2019;17:479-505.

89. Jo JK, Hong SK, Byun SS, Lee SE, Lee S, Oh JJ. Prognostic Significance of the Disparity Between Biopsy and Pathologic Gleason Score After Radical Prostatectomy in Clinical Candidates for Active Surveillance According to the Royal Marsden Criteria. Clin Genitourin Cancer. 2016;14:e329-333.
90. Loeb S, Vonesh EF, Metter EJ, Carter HB, Gann PH, Catalona WJ. What Is the True Number Needed to Screen and Treat to Save a Life With Prostate-Specific Antigen Testing? J Clin Oncol. 2011;29:464–467.
91. Klotz L. Active surveillance for prostate cancer: for whom? J Clin Oncol. 2005;23:8165–8169.
92. Bruinsma SM, Roobol MJ, Carroll PR, Klotz L, Pickles T, Moore CM, et al. Expert consensus document: Semantics in active surveillance for men with localized prostate cancer - results of a modified Delphi consensus procedure. Nat Rev Urol. 2017;14:312–322.
93. Albertson PC. Editorial comment on: Insignificant prostate cancer and active surveillance: from definition to clinical implications. Eur Urol. 2009;55:1331–1332.
94. Selvadurai ED, Singhera M, Thomas K, Mohammed K, Woode-Amissah R, Horwich A, et al. Medium-term Outcomes of Active Surveillance for Localised Prostate Cancer. Eur Urol. 2013;64:981–987.
95. Musunuru HB, Yamamoto T, Klotz L, Ghanem G, Mamedov A, Sethukavalan P, et al. Active Surveillance for Intermediate Risk Prostate Cancer: Survival Outcomes in the Sunnybrook Experience. J Urol. 2016;196:1651–1658.
96. Dall'Era MA, Konety BR, Cowan JE, Shinohara K, Stauf F, Cooperberg MR, et al. Active surveillance for the management of prostate cancer in a contemporary cohort. Cancer. 2008;112:2664–2670.
97. Komisarenko M, Martin LJ, Finelli A. Active surveillance review: contemporary selection criteria, follow-up, compliance and outcomes. Transl Androl Urol. 2018;7:243–255.

98. Bul M, Zhu X, Valdagni R, Pickles T, Kakehi Y, Rannikko A, et al. Active Surveillance for Low-Risk Prostate Cancer Worldwide: The PRIAS Study. Eur Urol. 2013;63:597–603.

99. Soloway MS, Soloway CT, Williams S, Ayyathurai R, Kava B, Manoharan M. Active surveillance; a reasonable management alternative for patients with prostate cancer: the Miami experience. BJU Int. 2008;101:165-169.

100. Tosoian JJ, Mamawala M, Epstein JI, Landis P, Wolf S, Trock BJ, et al. Intermediate and Longer-Term Outcomes From a Prospective Active-Surveillance Program for Favorable-Risk Prostate Cancer. J Clin Oncol. 2015;33:3379–3385.

101. Adamy A, Yee DS, Matsushita K, Maschino A, Cronin A, Vickers A, et al. Role of Prostate Specific Antigen and Immediate Confirmatory Biopsy in Predicting Progression During Active Surveillance for Low Risk Prostate Cancer. J Urol. 2011;185:477–482.

102. Lam TBL, MacLennan S, Willemse PPM, Mason MD, Plass K, Shepherd R, et al. EAU-EANM-ESTRO-ESUR-SIOG Prostate Cancer Guideline Panel Consensus Statements for Deferred Treatment with Curative Intent for Localised Prostate Cancer from an International Collaborative Study (DETECTIVE Study). Eur Urol. 2019;76:790–813.

103. Bill-Axelson A, Holmberg L, Garmo H, Taari K, Busch C, Nordling S, et al. Radical Prostatectomy or Watchful Waiting in Prostate Cancer - 29-Year Follow-up. NEJM. 2018;379:2319–2329.

104. Hamdy FC, Donovan JL, Lane JA, Mason M, Metcalfe C, Holding P, et al. 10-Year Outcomes after Monitoring, Surgery, or Radiotherapy for Localized Prostate Cancer. NEJM. 2016;375:1415–1424.

105. Bryant RJ, Oxley J, Young GJ, Lane JA, Metcalfe C, Davis M, et al. The ProtecT trial: analysis of the patient cohort, baseline risk stratification and disease progression. BJU Int. 2020;125:506–514.

106. Mazzone E, Stabile A, Pellegrino F, Basile G, Cignoli D, Cirulli GO, et al. Positive Predictive Value of Prostate Imaging Reporting and Data System Version 2 for the Detection of Clinically Significant Prostate Cancer: A Systematic Review and Meta-analysis. Eur Urol Oncol. 2021;4:697–713.
107. Benson MC, Whang IS, Pantuck A, Ring K, Kaplan SA, Olsson CA, et al. Prostate specific antigen density: a means of distinguishing benign prostatic hypertrophy and prostate cancer. J Urol. 1992;147:815–816.
108. Lujan M, Paez A, Llanes L, Miravalles E, Berenguer A. Prostate specific antigen density. Is there a role for this parameter when screening for prostate cancer? Prostate Cancer Prostatic Dis. 2001;4:146–149.
109. Omri N, Kamil M, Alexander K, Alexander K, Edmond S, Ariel Z, et al. Association between PSA density and pathologically significant prostate cancer: The impact of prostate volume. Prostate. 2020;80:1444–1449.
110. Nordström T, Akre O, Aly M, Grönberg H, Eklund M. Prostate-specific antigen (PSA) density in the diagnostic algorithm of prostate cancer. Prostate Cancer Prostatic Dis. 2018;21:57–63.
111. Yusim I, Krenawi M, Mazor E, Novack V, Mabjeesh NJ. The use of prostate specific antigen density to predict clinically significant prostate cancer. Sci Rep. 2020;10:20015.
112. Hansen NL, Barrett T, Koo B, Doble A, Gnanapragasam V, Warren A, et al. The influence of prostate-specific antigen density on positive and negative predictive values of multiparametric magnetic resonance imaging to detect Gleason score 7-10 prostate cancer in a repeat biopsy setting. BJU Int. 2017;119:724–730.
113. Washino S, Okochi T, Saito K, Konishi T, Hirai M, Kobayashi Y, et al. Combination of prostate imaging reporting and data system (PI-RADS) score and prostate-specific antigen (PSA) density predicts biopsy outcome in prostate biopsy naïve patients. BJU Int. 2017;119:225–233.

114. Pagniez MA, Kasivisvanathan V, Puech P, Drumez E, Villers A, Olivier J. Predictive Factors of Missed Clinically Significant Prostate Cancers in Men with Negative Magnetic Resonance Imaging: A Systematic Review and Meta-Analysis. J Urol. 2020;204:24–32.
115. Morote J, Celma A, Diaz F, Regis L, Roche S, Mast R, et al. Prostatic-specific antigen density behavior according to multiparametric magnetic resonance imaging result. Urol Oncol. 2020;38:410–417.
116. Schoots IG, Padhani AR. Risk-adapted biopsy decision based on prostate magnetic resonance imaging and prostate-specific antigen density for enhanced biopsy avoidance in first prostate cancer diagnostic evaluation. BJU Int. 2021;127:175–178.
117. Roobol MJ, Schröder FH, Hugosson J, Jones JS, Kattan MW, Klein EA, et al. Importance of prostate volume in the European Randomised Study of Screening for Prostate Cancer (ERSPC) risk calculators: results from the prostate biopsy collaborative group. World J Urol. 2012;30:149–155.
118. Morote J, Triquell M, Campistol M, Abascal JM, Servian P, Trilla E. Stratifying the initial prostate cancer suspicion to avoid magnetic resonance exams by sequencing men according to serum prostate-specific antigen, digital rectal examination and the prostate-specific antigen density based on digital rectal prostate volume category. BJUI Compass. 2023;4:266–268.
119. Schoots IG, Roobol MJ. Multivariate risk prediction tools including MRI for individualized biopsy decision in prostate cancer diagnosis: current status and future directions. World J Urol. 2020;38:517–529.
120. de la Calle C, Patil D, Wei JT, Scherr DS, Sokoll L, Chan DW, et al. Multicenter Evaluation of the Prostate Health Index to Detect Aggressive Prostate Cancer in Biopsy Naïve Men. J Urol. 2015;194:65–72.
121. Zappala SM, Scardino PT, Okrongly D, Linder V, Dong Y. Clinical performance of the 4Kscore Test to predict high-grade prostate cancer at

biopsy: A meta-analysis of us and European clinical validation study results. Rev Urol. 2017;19:149–155.

122. Catalona WJ, Partin AW, Sanda MG, Wei JT, Klee GG, Bangma CH, et al. A Multicenter Study of [-2]Pro-Prostate Specific Antigen Combined With Prostate Specific Antigen and Free Prostate Specific Antigen for Prostate Cancer Detection in the 2.0 to 10.0 ng/ml Prostate Specific Antigen Range. J Urol. 2011;185:1650–1655.
123. Nordström T, Vickers A, Assel M, Lilja H, Grönberg H, Eklund M. Comparison Between the Four-kallikrein Panel and Prostate Health Index for Predicting Prostate Cancer. Eur Urol. 2015;68:139–146.
124. Campistol M, Triquell M, Regis L, Celma A, Trilla E, Morote J et al. Relationship between Proclarix and the Aggressiveness of Prostate Cancer. Mol Diagn Ther. 2023;27:487-498.
125. Durand X, Moutereau S, Xylinas E, de la Taille A. Progensa™ PCA3 test for prostate cancer. Expert Rev Mol Diagn. 2011;11:137–44.
126. Gittelman MC, Hertzman B, Bailen J, Williams T, Koziol I, Henderson RJ, et al. PCA3 Molecular Urine Test as a Predictor of Repeat Prostate Biopsy Outcome in Men with Previous Negative Biopsies: A Prospective Multicenter Clinical Study. J Urol. 2013;190:64–69.
127. Haese A, de la Taille A, van Poppel H, Marberger M, Stenzl A, Mulders PFA, et al. Clinical Utility of the PCA3 Urine Assay in European Men Scheduled for Repeat Biopsy. Eur Urol. 2008;54:1081–1088.
128. Van Neste L, Hendriks RJ, Dijkstra S, Trooskens G, Cornel EB, Jannink SA, et al. Detection of High-grade Prostate Cancer Using a Urinary Molecular Biomarker–Based Risk Score. Eur Urol. 2016;70:740–748.
129. Hendriks RJ, van der Leest MMG, Israël B, Hannink G, YantiSetiasti A, Cornel EB, et al. Clinical use of the SelectMDx urinary-biomarker test with or without mpMRI in prostate cancer diagnosis: a prospective, multicenter

study in biopsy-naïve men. Prostate Cancer Prostatic Dis. 2021;24:1110–1119.

130. Tomlins SA, Aubin SMJ, Siddiqui J, Lonigro RJ, Sefton-Miller L, Miick S, et al. Urine TMPRSS2:ERG fusion transcript stratifies prostate cancer risk in men with elevated serum PSA. Sci Transl Med. 2011;3:94ra72.
131. Hessels D, Smit FP, Verhaegh GW, Witjes JA, Cornel EB, Schalken JA. Detection of TMPRSS2-ERG Fusion Transcripts and Prostate Cancer Antigen 3 in Urinary Sediments May Improve Diagnosis of Prostate Cancer. Clin Can Res. 2007;13:5103–5108.
132. Roumiguié M, Ploussard G, Nogueira L, Bruguière E, Meyrignac O, Lesourd M, et al. Independent Evaluation of the Respective Predictive Values for High-Grade Prostate Cancer of Clinical Information and RNA Biomarkers after Upfront MRI and Image-Guided Biopsies. Cancers (Basel). 2020;12:285.
133. James G, Witten D, Hastie T, Tibshirani R. An Introduction to Statistical Learning. Springer New York. 2013.
134. Hosmer DW, Lemeshow S, Sturdivant RX. Applied Logistic Regression. Wiley. 2013.
135. Hastie T, Tibshirani R, Friedman J. The Elements of Statistical Learning. Springer New York. 2009.
136. Adam A, Hellig JC, Perera M, Bolton D, Lawrentschuk N. "Prostate Cancer Risk Calculator" mobile applications (Apps): a systematic review and scoring using the validated user version of the Mobile Application Rating Scale (uMARS). World J Urol. 2018;36:565–573.
137. Vickers AJ, Cronin AM, Aus G, Pihl CG, Becker C, Pettersson K, et al. A panel of kallikrein markers can reduce unnecessary biopsy for prostate cancer: Data from the European Randomized Study of Prostate Cancer Screening in Göteborg, Sweden. BMC Med. 2008;6:1–10.
138. Cestari A. Predictive Models in Urology. Urologia. 2013;80:42–45.

139. Roobol MJ, Kerkhof M, Schröder FH, Cuzick J, Sasieni P, Hakama M, et al. Prostate Cancer Mortality Reduction by Prostate-Specific Antigen–Based Screening Adjusted for Nonattendance and Contamination in the European Randomised Study of Screening for Prostate Cancer (ERSPC). Eur Urol. 2009;56:584–591.

140. van Leeuwen PJ, Connolly D, Gavin A, Roobol MJ, Black A, Bangma CH, et al. Prostate cancer mortality in screen and clinically detected prostate cancer: Estimating the screening benefit. Eur J Cancer. 2010;46:377–383.

141. Roobol MJ, Steyerberg EW, Kranse R, Wolters T, van den Bergh RCN, Bangma CH, et al. A Risk-Based Strategy Improves Prostate-Specific Antigen–Driven Detection of Prostate Cancer. Eur Urol. 2010;57:79–85.

142. https://www.prostatecancer-riskcalculator.com/.

143. Thompson IM, Ankerst DP, Chi C, Goodman PJ, Tangen CM, Lucia MS, et al. Assessing prostate cancer risk: results from the Prostate Cancer Prevention Trial. J Natl Cancer Inst. 2006;98:529–534.

144. Virtanen A, Gomari M, Kranse R, Stenman UH. Estimation of prostate cancer probability by logistic regression: free and total prostate-specific antigen, digital rectal examination, and heredity are significant variables. Clin Chem. 1999;45:987–994.

145. Karakiewicz PI, Benayoun S, Kattan MW, Perrotte P, Valiquette L, Scardino PT, et al. Development and validation of a nomogram predicting the outcome of prostate biopsy based on patient age, digital rectal examination and serum prostate specific antigen. J Urol. 2005;173:1930–1934.

146. Garzotto M, Hudson RG, Peters L, Hsieh YC, Barrera E, Mori M, et al. Predictive modeling for the presence of prostate carcinoma using clinical, laboratory, and ultrasound parameters in patients with prostate specific antigen levels < or = 10 ng/mL. Cancer. 2003;98:1417–1422.

147. Ankerst DP, Thompson IM. Merging digital rectal exam, family history, age and prostate-specific antigen to create a decision-making tool. Arch Ital Urol Androl. 2006;78:143–146.

148. Grönberg H, Eklund M, Picker W, Aly M, Jäderling F, Adolfsson J, et al. Prostate Cancer Diagnostics Using a Combination of the Stockholm3 Blood Test and Multiparametric Magnetic Resonance Imaging. Eur Urol. 2018;74:722–728.

149. Ruffion A, Devonec M, Champetier D, Decaussin-Petrucci M, Rodriguez-Lafrasse C, Paparel P, et al. PCA3 and PCA3-based nomograms improve diagnostic accuracy in patients undergoing first prostate biopsy. Int J Mol Sci. 2013;14:17767–17780.

150. Verbeek JFM, Bangma CH, Kweldam CF, van der Kwast TH, Kümmerlin IP, van Leenders GJLH, et al. Reducing unnecessary biopsies while detecting clinically significant prostate cancer including cribriform growth with the ERSPC Rotterdam risk calculator and 4Kscore. Urol Oncol. 2019;37:138–144.

151. Roobol MJ, Vedder MM, Nieboer D, Houlgatte A, Vincendeau S, Lazzeri M, et al. Comparison of Two Prostate Cancer Risk Calculators that Include the Prostate Health Index. Eur Urol Focus. 2015;1:185–190.

152. Schoots IG, Padhani AR. Personalizing prostate cancer diagnosis with multivariate risk prediction tools: how should prostate MRI be incorporated? World J Urol. 2020;38:531-545.

153. Van Poppel H, Albreht T, Basu P, Hogenhout R, Collen S, Roobol M. Serum PSA-based early detection of prostate cancer in Europe and globally: past, present and future. Nat Rev Urol. 2022;19:562–572.

154. van Harten MJ, Roobol MJ, van Leeuwen PJ, Willemse PM, van den Bergh RCN. Evolution of European prostate cancer screening protocols and summary of ongoing trials. BJU Int. 2024;134:31-42.

155. Yamashiro JR, de Riese WTW. Any Correlation Between Prostate Volume and Incidence of Prostate Cancer: A Review of Reported Data for the Last Thirty Years. Res Rep Urol. 2021;13:749–757.

156. Roobol MJ, van Vugt HA, Loeb S, Zhu X, Bul M, Bangma CH, et al. Prediction of prostate cancer risk: the role of prostate volume and digital rectal examination in the ERSPC risk calculators. Eur Urol. 2012;61:577–583.

157. Hoffman RM. Clinical practice. Screening for prostate cancer. NEJM. 2011;365:2013–2019.

158. Auvinen A, Moss SM, Tammela TLJ, Taari K, Roobol MJ, Schröder FH, et al. Absolute Effect of Prostate Cancer Screening: Balance of Benefits and Harms by Center within the European Randomized Study of Prostate Cancer Screening. Clin Can Res. 2016;22:243–249.

159. Polanec SH, Bickel H, Wengert GJ, Arnoldner M, Clauser P, Susani M, et al. Can the addition of clinical information improve the accuracy of PI-RADS version 2 for the diagnosis of clinically significant prostate cancer in positive MRI? Clin Radiol. 2020;75:157.e1-157.e7.

160. Sathianathen NJ, Omer A, Harriss E, Davies L, Kasivisvanathan V, Punwani S, et al. Negative Predictive Value of Multiparametric Magnetic Resonance Imaging in the Detection of Clinically Significant Prostate Cancer in the Prostate Imaging Reporting and Data System Era: A Systematic Review and Meta-analysis. Eur Urol. 2020;78:402–414.

161. Morote J, Celma A, Roche S, de Torres IM, Mast R, Semidey ME, et al. Who Benefits from Multiparametric Magnetic Resonance Imaging After Suspicion of Prostate Cancer? Eur Urol Oncol. 2019;2:664–669.

162. Osses DF, Roobol MJ, Schoots IG. Prediction medicine: Biomarkers, risk calculators and magnetic resonance imaging as risk stratification tools in prostate cancer diagnosis. Int J Mol Sci. 2019;20:1637.

163. Cohen JF, Korevaar DA, Altman DG, Bruns DE, Gatsonis CA, Hooft L, et al. STARD 2015 guidelines for reporting diagnostic accuracy studies: explanation and elaboration. BMJ Open. 2016;6:e012799.

164. Fang D, Zhao C, Ren D, Yu W, Wang R, Wang H, et al. Could Magnetic Resonance Imaging Help to Identify the Presence of Prostate Cancer Before Initial Biopsy? The Development of Nomogram Predicting the Outcomes of Prostate Biopsy in the Chinese Population. Ann Surg Oncol. 2016;23:4284–4292.

165. Kim EH, Weaver JK, Shetty AS, Vetter JM, Andriole GL, Strope SA. Magnetic Resonance Imaging Provides Added Value to the Prostate Cancer Prevention Trial Risk Calculator for Patients With Estimated Risk of High-grade Prostate Cancer Less Than or Equal to 10%. Urology. 2017;102:183–189.

166. Bjurlin MA, Rosenkrantz AB, Sarkar S, Lepor H, Huang WC, Huang R, et al. Prediction of Prostate Cancer Risk Among Men Undergoing Combined MRI-targeted and Systematic Biopsy Using Novel Pre-biopsy Nomograms That Incorporate MRI Findings. Urology. 2018;112:112–120.

167. Lee SM, Liyanage SH, Wulaningsih W, Wolfe K, Carr T, Younis C, et al. Toward an MRI-based nomogram for the prediction of transperineal prostate biopsy outcome: A physician and patient decision tool. Urol Onc. 2017;35:664.e11-664.e18.

168. Niu X ke, Li J, Das SK, Xiong Y, Yang C bing, Peng T. Developing a nomogram based on multiparametric magnetic resonance imaging for forecasting high-grade prostate cancer to reduce unnecessary biopsies within the prostate-specific antigen gray zone. BMC Med Imaging. 2017;17:1–9.

169. Radtke JP, Wiesenfarth M, Kesch C, Freitag MT, Alt CD, Celik K, et al. Combined Clinical Parameters and Multiparametric Magnetic Resonance Imaging for Advanced Risk Modeling of Prostate Cancer—Patient-tailored

Risk Stratification Can Reduce Unnecessary Biopsies. Eur Urol. 2017;72:888–896.

170. van Leeuwen PJ, Hayen A, Thompson JE, Moses D, Shnier R, Böhm M, et al. A multiparametric magnetic resonance imaging-based risk model to determine the risk of significant prostate cancer prior to biopsy. BJU Int. 2017;120:774–781.
171. Truong M, Wang B, Gordetsky JB, Nix JW, Frye TP, Messing EM, et al. Multi-institutional nomogram predicting benign prostate pathology on magnetic resonance/ultrasound fusion biopsy in men with a prior negative 12-core systematic biopsy. Cancer. 2018;124:278–285.
172. Alberts AR, Roobol MJ, Verbeek JFM, Schoots IG, Chiu PK, Osses DF, et al. Prediction of High-grade Prostate Cancer Following Multiparametric Magnetic Resonance Imaging: Improving the Rotterdam European Randomized Study of Screening for Prostate Cancer Risk Calculators. Eur Urol. 2019;75:310–318.
173. Huang C, Song G, Wang H, Ji G, Li J, Chen Y, et al. MultiParametric Magnetic Resonance Imaging-Based Nomogram for Predicting Prostate Cancer and Clinically Significant Prostate Cancer in Men Undergoing Repeat Prostate Biopsy. Biomed Res Int. 2018;2018:6368309.
174. Mehralivand S, Shih JH, Rais-Bahrami S, Oto A, Bednarova S, Nix JW, et al. A magnetic resonance imaging–based prediction model for prostate biopsy risk stratification. JAMA Oncol. 2018;4:678–685.
175. Boesen L, Thomsen FB, Nørgaard N, Løgager V, Balslev I, Bisbjerg R, et al. A predictive model based on biparametric magnetic resonance imaging and clinical parameters for improved risk assessment and selection of biopsy-naïve men for prostate biopsies. Prostate Cancer Prostatic Dis. 2019;22:609–616.
176. Borque-Fernando Á, Esteban LM, Celma A, Roche S, Planas J, Regis L, et al. How to implement magnetic resonance imaging before prostate biopsy

in clinical practice: nomograms for saving biopsies. World J Urol. 2020;38:1481–1491.

177. Chen S, Yang Y, Peng T, Yu X, Deng H, Guo Z. The prediction value of PI-RADS v2 score in high-grade prostate cancer: A multicenter retrospective study. Int J Med Sci. 2020;17:1366–1374.
178. Noh T Il, Hyun CW, Kang HE, Jin HJ, Tae JH, Shim JS, et al. A Predictive Model Based on Bi-parametric Magnetic Resonance Imaging and Clinical Parameters for Clinically Significant Prostate Cancer in the Korean Population. Cancer Res Treat. 2021;53:1148–1155.
179. Sakaguchi K, Hayashida M, Tanaka N, Oka S, Urakami S. A risk model for detecting clinically significant prostate cancer based on bi-parametric magnetic resonance imaging in a Japanese cohort. Sci Rep. 2021;11:1–8.
180. Kinnaird A, Brisbane W, Kwan L, Priester A, Chuang R, Barsa DE, et al. A prostate cancer risk calculator (PCRC-MRI): Use of clinical and magnetic resonance imaging data to predict biopsy outcome in North American men. Can Urol A J. 2021;16:161–166.
181. Woo S, Suh CH, Kim SY, Cho JY, Kim SH. Diagnostic Performance of Prostate Imaging Reporting and Data System Version 2 for Detection of Prostate Cancer: A Systematic Review and Diagnostic Meta-analysis. Eur Urol. 2017;72:177–188.
182. Radtke JP, Giganti F, Wiesenfarth M, Stabile A, Marenco J, Orczyk C, et al. Prediction of significant prostate cancer in biopsy-naïve men: Validation of a novel risk model combining MRI and clinical parameters and comparison to an ERSPC risk calculator and PI-RADS. PLoS One. 2019;14:e0221350.
183. Bjurlin MA, Carroll PR, Eggener S, Fulgham PF, Margolis DJ, Pinto PA, et al. Update of the Standard Operating Procedure on the Use of Multiparametric Magnetic Resonance Imaging for the Diagnosis, Staging and Management of Prostate Cancer. J Urol. 2020;203:706–712.

184. Kuhl CK, Bruhn R, Krämer N, Nebelung S, Heidenreich A, Schrading S. Abbreviated Biparametric Prostate MR Imaging in Men with Elevated Prostate-specific Antigen. Radiology. 2017;285:493–505.

185. Tamada T, Kido A, Yamamoto A, Takeuchi M, Miyaji Y, Moriya T, et al. Comparison of Biparametric and Multiparametric MRI for Clinically Significant Prostate Cancer Detection With PI-RADS Version 2.1. J Magn Reson Imaging. 2021;53:283–291.

186. Porter KK, King A, Galgano SJ, Sherrer RL, Gordetsky JB, Rais-Bahrami S. Financial implications of biparametric prostate MRI. Prostate Cancer Prostatic Dis. 2020;23:88–93.

187. Boyle HJ, Alibhai S, Decoster L, Efstathiou E, Fizazi K, Mottet N, et al. Updated recommendations of the International Society of Geriatric Oncology on prostate cancer management in older patients. Eur J Cancer. 2019;116:116–136.

188. Massanova M, Robertson S, Barone B, Dutto L, Caputo VF, Bhatt JR, et al. The Comparison of Imaging and Clinical Methods to Estimate Prostate Volume: A Single-Centre Retrospective Study. Urol Int. 2021;105:804–810.

189. Cui T, Kovell RC, Terlecki RP. Is it time to abandon the digital rectal examination? Lessons from the PLCO Cancer Screening Trial and peer-reviewed literature. Curr Med Res Opin. 2016;32:1663–1669.

190. Okotie OT, Roehl KA, Han M, Loeb S, Gashti SN, Catalona WJ. Characteristics of prostate cancer detected by digital rectal examination only. Urology. 2007;70:1117–1120.

191. Liu C, Liu SL, Wang ZX, Yu K, Feng CX, Ke Z, et al. Using the prostate imaging reporting and data system version 2 (PI-RADS v2) to detect prostate cancer can prevent unnecessary biopsies and invasive treatment. Asian J Androl. 2018;20:459–464.

192. Andras I, Cata ED, Serban A, Kadula P, Telecan T, Buzoianu M, et al. Combined Systematic and MRI-US Fusion Prostate Biopsy Has the Highest

Grading Accuracy When Compared to Final Pathology. Medicina (Kaunas). 2021;57:519.

193. Ewout, S. Clinical Prediction Models: A Practical Approach to Development, Validation, and Updating. Springer. 2009.
194. Wynants L, van Smeden M, McLernon DJ, Timmerman D, Steyerberg EW, Van Calster B, et al. Three myths about risk thresholds for prediction models. BMC Med. 2019;17:192.
195. Püllen L, Radtke JP, Wiesenfarth M, Roobol MJ, Verbeek JFM, Wetter A, et al. External validation of novel magnetic resonance imaging-based models for prostate cancer prediction. BJU Int. 2020;125:407–416.
196. Saba K, Wettstein MS, Lieger L, Hötker AM, Donati OF, Moch H, et al. External Validation and Comparison of Prostate Cancer Risk Calculators Incorporating Multiparametric Magnetic Resonance Imaging for Prediction of Clinically Significant Prostate Cancer. J Urol. 2020;203:719–726.
197. Schoots IG. MRI in early prostate cancer detection: how to manage indeterminate or equivocal PI-RADS 3 lesions? Transl Androl Urol. 2018;7:70–82.
198. Catalona WJ, Richie JP, deKernion JB, Ahmann FR, Ratliff TL, Dalkin BL, et al. Comparison of prostate specific antigen concentration versus prostate specific antigen density in the early detection of prostate cancer: receiver operating characteristic curves. J Urol. 1994;152:2031–1036.
199. Yamashiro JR, de Riese WTW. Any Correlation Between Prostate Volume and Incidence of Prostate Cancer: A Review of Reported Data for the Last Thirty Years. Res Rep Urol. 2021;13:749–757.
200. Morote J, Raventos CX, Lorente JA, Lopez-Pacios MA, Encabo G, de Torres I, et al. Comparison of Percent Free Prostate Specific Antigen and Prostate Specific Antigen Density as Methods to Enhance Prostate Specific Antigen Specificity in Early Prostate Cancer Detection in Men With Normal Rectal

Examination and Prostate Specific Antigen Between 4.1 and 10 ng./ml. J Urol. 1997;158:502–504.

201. Keetch DW, McMurtry JM, Smith DS, Andriole GL, Catalona WJ. Prostate specific antigen density versus prostate specific antigen slope as predictors of prostate cancer in men with initially negative prostatic biopsies. J Urol. 1996;156:428–431.
202. Thon WF, Gadban F, Truss MC, Kuczyk M, Hartmann U, Jonas U. Prostate-specific antigen density--a reliable parameter for the detection of prostate cancer? World J Urol. 1996;14:53–58.
203. Görtz M, Radtke JP, Hatiboglu G, Schütz V, Tosev G, Güttlein M, et al. The Value of Prostate-specific Antigen Density for Prostate Imaging-Reporting and Data System 3 Lesions on Multiparametric Magnetic Resonance Imaging: A Strategy to Avoid Unnecessary Prostate Biopsies. Eur Urol Focus. 2021;7:325–331.
204. Remmers S, Kasivisvanathan V, Verbeek JFM, Moore CM, Roobol MJ, ERSPC Rotterdam Study Group PRECISION Investigators Group. Reducing Biopsies and Magnetic Resonance Imaging Scans During the Diagnostic Pathway of Prostate Cancer: Applying the Rotterdam Prostate Cancer Risk Calculator to the PRECISION Trial Data. Eur Urol Open Sci. 2022;36:1–8.
205. Mannaerts CK, Gayet M, Verbeek JF, Engelbrecht MRW, Savci-Heijink CD, Jager GJ, et al. Prostate Cancer Risk Assessment in Biopsy-naïve Patients: The Rotterdam Prostate Cancer Risk Calculator in Multiparametric Magnetic Resonance Imaging-Transrectal Ultrasound (TRUS) Fusion Biopsy and Systematic TRUS Biopsy. Eur Urol Oncol. 2018;1:109–117.
206. Alberts AR, Schoots IG, Bokhorst LP, van Leenders GJ, Bangma CH, Roobol MJ. Risk-based Patient Selection for Magnetic Resonance Imaging-targeted Prostate Biopsy after Negative Transrectal Ultrasound-guided

Random Biopsy Avoids Unnecessary Magnetic Resonance Imaging Scans. Eur Urol. 2016;69:1129–1134.

207. Roehrborn CG, Girman CJ, Rhodes T, Hanson KA, Collins GN, Sech SM, et al. Correlation between prostate size estimated by digital rectal examination and measured by transrectal ultrasound. Urology. 1997;49:548–557.

208. Diniz MA. Statistical methods for validation of predictive models. J Nucl Cardiol. 2022;29:3248–3255.

209. Rapisarda S, Bada M, Crocetto F, Barone B, Arcaniolo D, Polara A, et al. The role of multiparametric resonance and biopsy in prostate cancer detection: comparison with definitive histological report after laparoscopic/robotic radical prostatectomy. Abdom Radiol (NY). 2020;45:4178–4184.

210. Morote J, Borque-Fernando Á, Triquell M, Abascal JM, Servian P, Planas J, et al. A risk-organised model for clinically significant prostate cancer early detection. BJUI Compass. 2023;4:420–422.